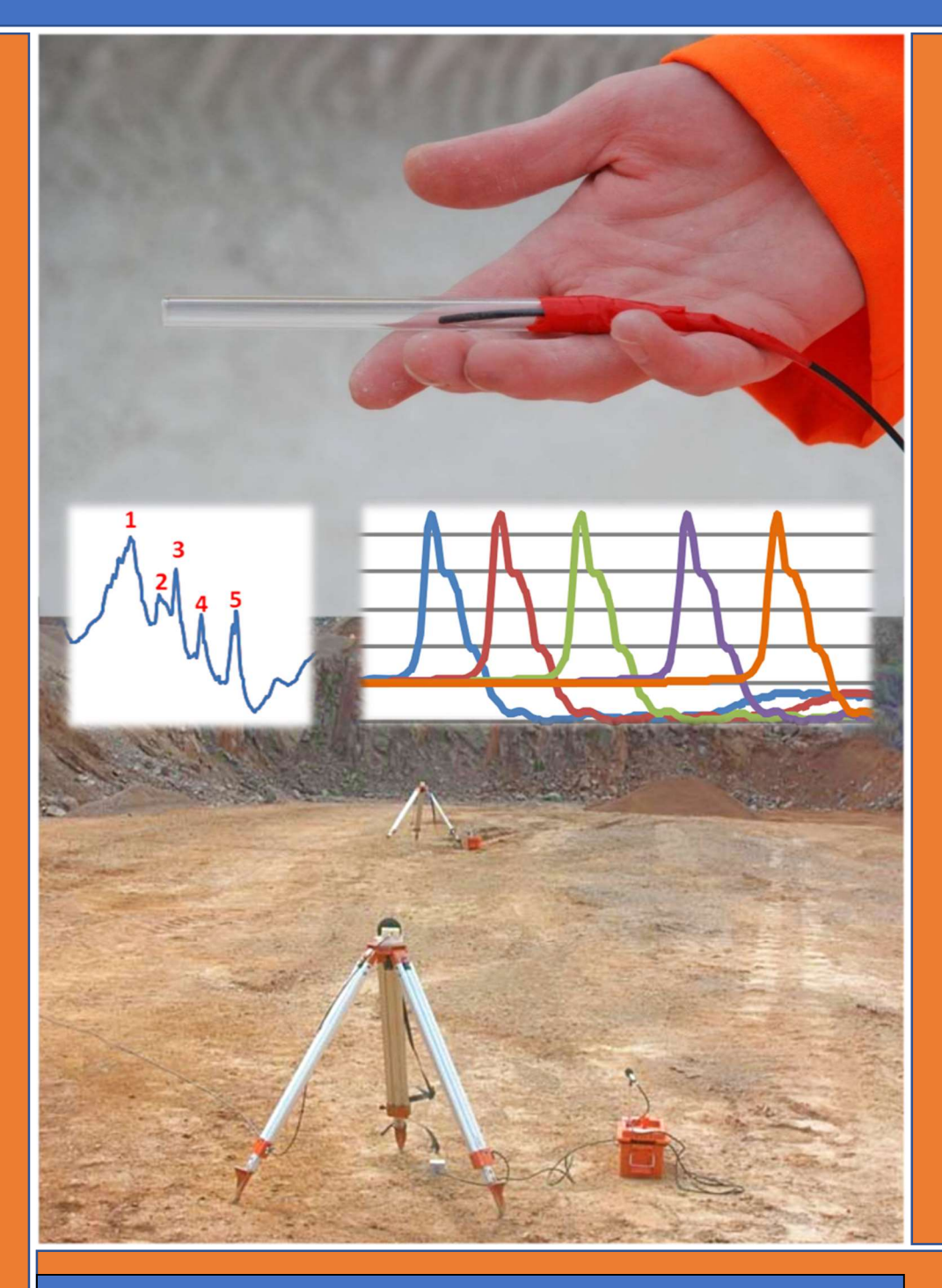
Full Scale Investigation into the Origins and Prediction of Air Overpressure from Quarry Blasting

Thematic Research Priority: Impact Mitigation and Management

Dust, Noise and Vibration



Research funded through Defra's Aggregates Levy Sustainability Fund











Full Scale Investigation into the Origins and Prediction of Air Overpressure from Quarry Blasting

Thematic Research Priority: Impact Mitigation and Management

Dust, Noise and Vibration

The University of Leeds
The Energy & Resources Research Institute
School of Process, Environmental & Materials Engineering

In conjunction with

Blast Log Ltd, EPC-UK Ltd and Terrock

Executive Summary

Full Scale Investigation into the Origins of Air Overpressure from Quarry Blasting

Final report: February 2011

Whilst this study has not definitively determined all the controlling factors and how they related to each other in giving rise to the precise magnitude of the peak air overpressure for a given quarry blast, it has laid down a foundation for other researchers to build upon. The model relationships proposed in this report need to be verified by quality data derived from monitoring many different types of quarry blasting in many different rock types.

Generic models of the type

$$AoP = C \left\lceil \frac{D}{W^{1/3}} \right\rceil^{-a}$$

provides only a very general starting point for "guestimating" the maximum air overpressure pulse from a given quarry blast. It should not be used to predict levels of air overpressure, neither should it be used regulators for enforcement purposes. The study has confirmed the findings of other researchers in that the magnitude of the air overpressure pulse in front of the quarry face being blasted will be significantly higher that the magnitude of the air overpressure pulse recorded from the same blast but monitored on the quarry bench behind the quarry face being blasted. For purposes of prediction, such results should be considered as two separate data sets.

However if a higher degree of certainty is required, then all three parameters (distance [D], charge weight [E] and burden [B]) must be known and each must be considered as independent variable with respect to the dependant variable Peak air overpressure (in Pascals). The form of the relationship being

Peak AOP =
$$C \times D^{-x} \times E^{+y} \times B^{-z}$$

This needs to be considered using a quadrivarainte statistical relationship in order to be able to specify the probability of the maximum magnitude of an air overpressure pulse from a given quarry blast.

The propagation of a shock wave through air as a result of quarry blasting consists only of one type of wave, the compression wave. This is in marked contrast to seismic waves where a number of different types of wave are generated by the one blasting event. Even so the interaction of the burn time of a single hole and the resulting air overpressure is still too complicated to be able to be accurately modelled. It is considered that the best way forward is to monitor an individual single hole to obtain a signature wave form that has resulted from this complex interaction. Once this wave form is known, the variation in geometry of a mutli hole blast and the timings of the successive detonations can be modelled to give a sufficient degree of accuracy to recreate the likely magnitude, duration and wave form of a multi hole quarry type blast. This can then be directly compared with actual air over pressure wave forms from quarry blast to verify the model.

The study has determined that if the air overpressure pulse from a blast hole has passed the equivalent distance to an adjacent blast hole before that hole is fired, then no positive interaction between the two separate pulse will occur. However, it has also been shown that the negative phase of the air overpressure pulse is usually of the order of 3 to 5 x the positive pulse and unless this portion of the air overpressure pulse has also passed the adjacent hole before it is detonated, then a negative interaction will occur. It is this interaction between successively detonated blast holes 9either positive or negative) that makes air overpressure so difficult to predict.

The research work carried out has established that the air overpressure pulse for a quarry blast from a single hole is dependent on the following parameters:

- 1. The total power of the explosive in Kilograms
- 2. The duration of the detonation
- 3. The distance from the origin of the detonation to the observation point
- 4. the burden of rock in front of the blast hole at the initial point of detonation

In addition to these parameters detailed above, for a multi hole quarry blast, the geometry of the blast with respect to the observation point must also be taken into consideration. The resulting air overpressure pulse will be depend on

- 5. The spacing of the holes (in metres)
- 6. The orientation of the blast pattern
- 7. The timing between successive detonations
- 8. The speed of sound in air at the precise time of the blast

The derived time at which the air overpressure pulse exited the blast face did not coincide with either the derived time at which the shock wave exited the face nor indeed the measured first movement of the face. The timing order indicates that the shock wave comes first, then the air overpressure pulse originates on the blast face and then the blast face moves.

Given the amount of energy and volume of gas generated in the gas pressure pulse and that by definition the gas pressure pulse cannot arrive at the blast face before the shock wave, nor can it arrive after the face has commenced to move, it is logical that this is where the next phase of the research that should be targeted.

In the interest of standardisation it recommended that all overpressure measurements should be in Pascals and reported in Pascals.

Acknowledgements

This study would not have been possible without the cooperation of many different organisations and individuals. Special thanks needs to be given to all the project partners and their staff.

Blast Log Ltd as a company and Dr Shazad Hosein and Emily Hunger.

EPC-UK as a company and Dr Robert Farnfield and Dr. Mark Pegden.

Terrock as a company and Alan Richards and Adrian Moore.

Liam Bermingham - postgraduate student at the University of Leeds.

Lafarge Aggregates as a company and Shane Tomkin, Peter Bates, Steve Sockett, John Bradshaw, Steve Carter, Keith Farley, Simon Edwards, Mick Jones, Angus Shedden and Ian Brown.

Singleton Birch as a company and Mark Sacker, Dean Kirkby, Lawrence Thompson, Alan Holt, Steve Price and David Allis.

Cemex as a company and Alan Black.

Tarmac as a company and Alan Scally and Gareth Williams.

BAM Ritchies and Glyn Barnes and David Scaife.

Miller Argent as a company and James Poyner and David Mason.

Finally to the Mineral Industry Research Organisation [MIRO] for providing the funding via ALSF and in particular to Abbie Drew, Pam Badham and Robert Fenton for their support and encouragement throughout the project.

William John Birch

Toby White

Joint Project Leaders.

Contents

Executive Summary	ii
Acknowledgements	V
Contents	vi
Figures	xii
Tables	xviii
Plates	xix
Chapter 1 Fundamentals of surface blasting	1
1.1 Introduction	1
1.2 Characteristics of explosives	1
1.2.1 Strength	1
1.2.2 Density	2
1.2.3 Velocity of Detonation (VOD)	2
1.2.4 Water resistance	2
1.2.5 Sensitivity	2
1.2.6 Sensitiveness	3
1.2.7 Stability	3
1.3 Explosive types	3
1.3.1 Nitro-glycerine based explosives	3
1.3.2 Ammonium Nitrate/Fuel Oil mixtures	3
1.3.3 Slurry explosives	4
1.3.4 Emulsion explosives	4
1.4 Detonators	4
1.4.1 Electric detonators	4
1.4.2 Delayed action detonators	5
1.4.3 Shock tube detonators	5
1.4.4 Electronic detonators	6
1.5 Single hole initiation	7
1.6 Mechanism of rock breakage	9
1.6.1 Energy considerations	9
1.6.2 Strain energy	10
1.6.3 Thrust energy	12
1.7 Blast planning for surface excavations	14

1.7.1 Factors influencing blast design	14
1.7.1.1 Thickness of the deposit to be worked	14
1.7.1.2 The hardness of the rock	14
1.7.1.3 The presence of joints and bedding planes	14
1.7.1.4 The required shape of the muck pile	14
1.7.1.5 The degree of fragmentation required	15
1.7.1.6 The type of drilling machine	15
1.7.1.7 The amount of rainfall and groundwater present	15
1.7.1.8 The proximity of environmentally sensitive structures and neighbours	16
1.7.2 Factors affecting performance	16
1.7.2.1 Loading density	16
1.7.2.2 Loading rate	16
1.7.2.3 Charge diameter	16
1.7.3 Primary blast design	17
1.7.3.1Blast geometry	17
1.7.3.2 Bench heights	18
1.7.3.3 Borehole diameter	18
1.7.3.4 Burden	19
1.7.3.5 Drill hole spacing	19
1.7.3.6 Inclination of the borehole	19
1.7.3.7 Sub-grade drilling	20
1.7.3.8 Hole depth	20
1.7.3.9 Base charge	20
1.7.3.10 Stemming	20
1.7.3.11 Column charge	21
1.7.3.12 Detonating method	21
1.7.3.13 Primer position	21
1.7.3.14 Detonating sequence	21
1.7.3.15 Choosing a detonating sequence	23
1.7.3.16 Blasting Ratio	24
1.7.3.17 Calculation of Blast Ratio	24
1.8 Environmental blast design	25
1.8.1 Alter the Drill Ratio	25
1.8.2 Split the bench	27
1.8.3 Split the charge in the blast hole	27

1.9 Conclusion	28
Chapter 2 Physics of blast vibrations through air	30
2.1 General properties of waves	30
2.2 Types of waves generated by quarry blasts	31
2.3 What is air overpressure?	31
2.3.1 Air Overpressure	32
2.4 Technical information on the various factors that affect the level of air overpressure	34
2.4.1 Charge mass and distance	34
2.4.2 Face height and orientation	35
2.4.3 Stemming height and type	36
2.4.4 Blast hole diameter to burden ratio	37
2.4.5 Topographic shielding	38
2.4.6 Wave front reinforcement - the combined effect of burden, spacing and sequential initiation timing	40
2.4.7 Meteorological conditions	41
2.5 Review of models available for the prediction of air overpressure for initial quarry blast design	42
2.5.1 Effect of Charge Mass and Distance	42
2.5.1.1 Face Height and Orientation	43
2.5.1.2 Topographic Shielding	43
2.5.1.3 Stemming Height and Type	43
2.5.1.4 Blast hole Diameter to Burden Ratio	44
2.5.1.5 Burden, Spacing, and Sequential Initiation Timing	45
2.5.1.6 Meteorological Conditions	46
2.6 Good Practice for minimising air overpressure	46
2.7 Measurement of air overpressure	47
2.8 Conclusions	48
Chapter 3 Preliminary Investigation into the relationship between air overpressure and face velocity at Newbridge Quarry	49
3.1 Introduction	49
3.2 Front Calc Software	51
3.3 Results	53
3.3.1 Relationship between Air Overpressure & Face Velocities	54
3.3.2 Recommended Protocol	62
3.4 Conclusion	64

Chapter 4 Blast air overpressure instrumentation	65
4.1 Seismographs	65
4.1.1 White Mini-Seis II seismograph	65
4.1.2 Instantel Minimate Plus Series III seismograph	67
4.2 Instrumentation used to establish the origin of air overpressure	68
4.2.1 Piezoelectric sensor	68
4.2.2 Borehole microphone	70
4.2.3 Low frequency air overpressure microphones	70
4.2.4 MREL Microtrap TM data logger	71
4.2.5 Optic fibre triggering system	73
4.3. Conclusions	73
Chapter 5 Development and application of a low cost optic fibre system to monitor blast performance	
5.1 Introduction	
5.2 Optic Fibre Instrumentation	76
5.2.1 Optical Interface Unit	76
5.2.2 Data logging	77
5.2.3 Deployment of the equipment.	78
5.3 Determinations of timing scatter in shock tube Detonators and Delay Relay Detonators.	81
5.4 Comparison of VOD Measurements	86
5.5 Conclusions	88
Chapter 6 Air overpressure data collection and analysis	90
6.1 Introduction	90
6.2 Statistical Analysis Techniques	90
6.2.1 Scaled distance regression	90
6.2.2 Standard Error	93
6.2.3 Correlation Coefficient	95
6.2.4 Criticism of the scaled distance regression method for predicting air overpressure	95
6.3 Data Collection	96
6.4 Whitwell quarry	97
6.5 Melton Ross quarry	100
6.6 Comparisons of air overpressure levels between conventional bench blasting and fully confined 'buffer' blasting	110
6.7 The influence of rock type on levels of air overpressure produced from blasting	111

	6.8 Conclusion	113
Cha	pter 7 Field investigation, with respect to orientation and distance from an explosive source, into the interaction of multiple short delay detonations in free air	
	7.1 Introduction	114
	7.2 Results	118
	7.2.1 First Test – single charge	118
	7.2.2 Second test – single charge	120
	7.2.3 Third test – 5 charges with a 25ms delay	121
	7.2.4 Fourth test – 5 charges with a 8ms delay	123
	7.2.5 Fifth test – 5 charges with a delay of 12ms & 1ms	125
	7.2.6 Sixth test – 3 rd single charge	127
	7.3 Theoretical single hole wave form modelling	128
	7.3.1 Creating a model of an unconfined blast at Melton Ross	134
	7.4 Conclusions	135
Cha	pter 8 Single hole air overpressure test blasts at Melton Ross Quarry	136
	8.1 Introduction	136
	8.2 The experiment	136
	8.3 Results of the experiment	136
	8.3.1 The value of the air overpressure wave as it decayed with distance	138
	8.3.2 The shape of the air overpressure time history trace as it decayed with distance	141
	8.3 Conclusions & Summary	142
Cha	pter 9 Application of statistical analysis in combination with a linear superposition technique using a signature acoustic wave form to create a model of the air overpressure produced from a full scale production blast at Melton Ross Quarry	143
	9.1 The Application of linear Superposition techniques to the air overpressure generated by quarry blasting	143
	9.1.1 Linear Superposition	143
	9.2 Optimisation with Linear Superposition	144
	9.3 Application of Linear Superposition Techniques to Air Overpressur	e 145
	9.4 Air overpressure monitoring at Melton Ross Quarry	148
	9.5 Statistical comparison of the original air overpressure data with the	
	derived data	
	9.5.1 Statistical comparison using a trivariate relationship	150
	9.5.2 Statistical comparison using a quadrivarainte relationship	153

9.5.2.1 Average burden	155
9.5.2.2 Median burden	155
9.5.2.3 Toe burden	156
9.5.2.4 Using the first hole in each blast	157
9.6 Conclusion	158
Chapter 10 Determination of the origins of air overpressure from blasting at Melton Ross Quarry	159
10.1 Previous research in determining the precise origin of air overpressure in surface blasting	159
10.2 Air overpressure monitoring at Melton Ross Quarry	161
10.3 Example calculation	162
10.3.1 Calculating air overpressure velocity	163
10.3.2 Determining the source of air overpressure	165
10.4 Origins of air overpressure at Melton Ross quarry	169
10.5 Conclusions	171
Chapter 11 Conclusions and further work	173
11.1 Summary of conclusions	173
11.2 Further work	177
REFERENCES	178

Figures

Figure 1.1 Electric pyrotechnic delayed action detonator	5
Figure 1.2 Non electric pyrotechnic delayed action detonator	6
Figure 1.3 Electronic detonator	7
Figure 1.4 Cross section showing the component parts of a typical blast hole charged and ready to fire	
Figure 1.5 Blast hole fires from the base upwards giving rise to a compressive shatter zone and shock wave	
Figure 1.6 Compression wave reaches the free quarry face and undergoes 18 degree phase change and is reflected as a tensile wave	
Figure 1.7 Gas produced by the explosive under high pressure penetrates the fragment rock and pushes it onto the quarry floor	
Figure 1.8 Annotated diagram of the key elements of a quarry blast design 1	. 8
Figure 1.9 Electric detonator sequence in a quarry blast	22
Figure 1.10 Interaction between detonating relays and long period detonator to create advanced initiation in a quarry blast	
Figure 1.11 Ranging diagram for a Terex RH120 face shovel	27
Figure 1.12 Double decking and double shot in a single blast hole to reduce the maximum instantaneous charge weight to ensure environmental compliance2	
Figure 2.1 Behaviour of an air over pressure pulse from a single event3	3
Figure 2.2 120 dB(lin) Contours for Different Stemming Heights on 500metre x 500 metres grid pattern	
Figure 2.3 120 dB(Lin) Contours for Different Stemming Heights and Burder	
Figure 2.4 The relationship between shielding, the effective barrier height and the incident angle	
Figure 2.5 The relationship between secondary shielding measured in decibels linear dB(Lin), barrier height, and incident angle	
Figure 2.6 resulting air overpressure wave front pattern [spacing 3 metre spacing delay 9 ms & velocity 340 m/s]	

Figure 2.7 example of air overpressure reinforcement due to atmospheric conditions
Figure 3.1 Data processed in SDA 50
Figure 3.2 Air overpressure trace plotted in Microsoft Excel
Figure 3.3 Inserting points to monitor face velocities from a particular hole 52
Figure 3.4 Tracing of points in Front Calc
Figure 3.5 Example air overpressure trace
Figure 3.6 Correlation of peak air overpressure and average face velocity of each blast hole monitored
Figure 3.7 Peak air overpressure (in front of the blast) plotted against average face velocity (1 st hole only)
Figure 3.8 Peak air overpressure (at the rear of the Blast) plotted against average face velocity (1 st hole only)
Figure 3.9 Scaled air overpressure vs. average face velocity in front of the blast
Figure 3.10 Scaled air overpressure behind the blast vs. average face velocity
Figure 4.1 An example of a recording from a piezoelectric sensor69
Figure 5.1 Output from MicrotrapTM VOD/Data Recorder81
Figure 5.2 Close up surface Delay Relay Detonator firing section of Figure 5.1
Figure 5.3 Close up In-hole Detonator firing section of Figure 5.1
Figure 5.4 Close up of Figure 8 - Flame in Twin Shock tubes passing In-hole optic sensor
Figure 5.5 Interaction between surface delay relay detonators relays and long period in hole detonators to create advanced initiation in a quarry blast
Figure 5.6 Output from Optic Fibre system showing time of 1.230 ms for 4.5 metres travel as the detonation front proceeded through the Anfo explosive86
Figure 5.7 Output from MREL Handitrap showing VoD of 3615 m/s in site mixed Anfo
Figure 5.8 Output from Optic Fibre system showing time of 2.100 ms and 2.108 ms for 4.5 metres travel as the flame front proceeded down the shock tube 88

Figure 6.1 Example of a scaled distance regression model applied to air overpressure
Figure 6.2 Example of a data set with a high standard error
Figure 6.3 Example of scaled distance regression model with a low standard
error
Figure 6.4 All air overpressure data recorded 97
Figure 6.5 Regression curve for the entire data set accumulated at Whitwell quarry
Figure 6.6 Regression model depicting the location of recorded air overpressure levels
Figure 6.7 Regression model of air overpressure levels in front of the blasts at Melton Ross quarry
Figure 6.8 Regression model of air overpressure levels recorded on the surface of the bench at Melton Ross quarry
Figure 6.9 Example of monitoring locations on bench surface in relation to directionality of a blast
Figure 6.10 Regression model showing variations in air overpressure levels due to directionality in relation to the blasting pattern and firing sequence
Figure 6.11 Air overpressure waveform on the blast bench perpendicular to blast pattern
Figure 6.12 air overpressure waveform on the blast bench in line with the blast pattern and the timing sequence between holes going away from the monitoring point
Figure 6.13 air overpressure waveform on the blast bench in line with the blast pattern and the timing sequence between holes going towards the monitoring point.
Figure 6.14 Example of the effects of wave front reinforcement - 5 single holes detonating so as to arrive at a monitoring location @ 6 milli second intervals.
Figure 6.15 Example of the effects of wave front reinforcement - Resulting Air overpressure pulse from the combine effect of the 5 separate holes
Figure 6.16 Example of the effects of wave front reinforcement - 5 single holes detonating so as to arrive at a monitoring location @ 28 milli second intervals.

overpressure pulse from the combine effect of the 5 separate holes	
Figure 6.18 Regression model of air overpressure recorded from confin	
blasts	
Figure 6.19 Regression model comparing air overpressure levels from vario	
rock types	
Figure 7.1 Plan of the monitoring locations	
Figure 7.2 Results from the first single charge test	118
Figure 7.3 Air overpressure waveform recorded from the first test	119
Figure 7.4 Air overpressure waveform recorded at 4096sps	120
Figure 7.5 results from the second single charge test	120
Figure 7.6 Air overpressure waveform recorded from the second single chatest	_
Figure 7.7 Results from the third test	121
Figure 7.8 Air overpressure traces between locations perpendicular to charges at a distance of 50m	
Figure 7.9 Air overpressure traces between locations parallel to the charges a distance of 50m with the firing sequence towards the monitoring location	
Figure 7.10 Results from the fourth test	124
Figure 7.11 Air overpressure traces between locations perpendicular to charges with 8ms delay times.	
Figure 7.12 Air overpressure traces between locations parallel to the charwith the firing sequence towards the monitoring location 8ms delay times	_
Figure 7.13 Results from the fifth test	126
Figure 7.14 Air overpressure traces between locations perpendicular to charges with detonations 1 to 4 @ 12ms & detonation 5 @ 1ms delay times	
Figure 7.15 Air overpressure traces between locations parallel to the charge with detonations 1 to 4 @ 12ms & detonation 5 @ 1ms delay times	_
Figure 7.16 Results from the sixth test	128
Figure 7.17 Use of single charge waveform to model an unconfined qua	arrv
blast	-

at Melton Ross quarry
Figure 7.19 air overpressure waveform recorded from the 2nd single hole blast at Melton Ross quarry
Figure 7.20 air overpressure recorded from a single 1m length of detonation cord being fired in "free air"
Figure 7.21 Pressure wave down sampled to 1024sps
Figure 7.22 Comparison between a confined and unconfined single hole blast
Figure 7.23 Comparison in air overpressure of a semi confined and unconfined blast at Melton Ross
Figure 8.1 location of the air overpressure monitors with respect to the two single hole blasts.
Figure 8.2 Plot of the two single hole tests
Figure 9.1 Example of a blast vibration optimisation chart for a single row blast
Figure 9.2 Air overpressure trace from individual holes firing at different designated times.
Figure 9.3 Combined effect of the traces from the individual holes into a single trace in comparison with an actual air overpressure trace from a 5 hole blast 146
Figure 9.4 Modification of the amplitude of the individual holes to match an actual air overpressure trace from a 5 hole blast
Figure 9.5 Air overpressure optimisation chart demonstrating how the initiation interval between successive holes in a multi hole blast pattern would interact.
Figure 9.6 five hole blast recorded on 12 th march 2010 at 44.5 metres from the quarry face of the blast
Figure 9.7 Model of 5 separate holes with varying magnitude and timings 149
Figure 10.1 Typical trace showing the precise firing times of the surface delay relay detonators and then the long lead time in hole detonators for a 5 hole blast at Melton Ross Quarry.
Figure 10.2 Optical fibre interface unit's output used to determine the precise time the first blast hole was fired

Figure 10.3 Air overpressure trace recorded by the first microphone at 40.17m
Figure 10.4 Air overpressure trace recorded by the second microphone at 80.17m
Figure 10.5 the recorded vibration on the vertical channel of both linked seismographs
Figure 10.7 Face profile data of the first blast hole
Figure 10.8 Output from the piezoelectric sensor in front the of face 168
Figure 10.9 The first movement detected by the piezoelectric sensor 168

Tables

Table 3.1 Measured data from each blast including the scaled air overpressure	. 60
Table 3.2 Air overpressure recorded behind each blast and the corresponding scaled	. 61
Table 5.1 Statistical analysis of detonator performance	. 85
Table 6.1 Summary for all data collected	. 96
Table 6.2 Statistical table comparing Air Overpressure levels on the top of the blast bench, behind the blast.	104
Table 8.1 The relationship between air overpressure, distance charge weight and burden for blast 1	138
Table 8.2 The relationship between air overpressure, distance charge weight and burden for blast 2	139
Table 9.1 arrival times and magnitudes used to form the prediction model in Figure 9.6	149
Table 9.2 relationship of blast parameters to maximum actual and derived air overpressure levels	150
Table 10.1 Air overpressure levels timings and associated velocities related to Burden	169
Table 10.2 Comparison of time differences between shock wave and face movement in relationship to air overpressure pulse leaving the quarry face	170

Plates

Plate 1.1 Sequence of photographs demonstrating how the quarry face reacts to the detonation of the shot holes
Plate 4.1 White Mini-Seis II seismograph deployed and ready to monitor 66
Plate 4.2 Instantel Minimate Plus Series III seismograph
Plate 4.3 Face sensor is encased in a rubber ball, positioned in front of the face
Plate 4.4 Air overpressure microphones positioned directly in front of the first blast hole
Plate 4.5 MREL Microtrap TM deployed and armed
Plate 5.1 Optical Interface Unit
Plate 5.2. MREL Microtrap TM VOD/Data Recorder
Plate 5.3 10 mm (0.4 in) diameter x 10 cm (3.9 in) length of laboratory glass tubing with Optic Fibre Cable
Plate 5.4 attaching Glass tubing with Optic fibre Cable to down hole Shock Tube
Plate 5.5. Lowering primer cartridge with Shock tube detonators and Optic fibre cable down the blast hole
Plate 5.6 Yellow shock tube to In-hole Detonators connected to red surface Delay Relay Detonators. Green shock tube links one detonating relay to the next. Black optic fibre cable connected to the Optical Interface Unit
Plate 7.1 Setup of five 1m lengths of detonation cord suspended on bamboo poles, spaced 4m apart
Plate 7.2 Close up of the electronic detonator connected to the detonator cord which in turn is strapped to the glass tube with the optic fibre cable in it

Chapter 1

Fundamentals of surface blasting

1.1 Introduction

Many techniques for surface blast design exist and these may vary both between industries and countries. However in all cases the main aim of the blasting exercise is to create a product that can be more easily moved and used. This can range from the need to simply break the rock so that it can be moved [e.g. such as in the construction of a road cutting through solid rock] up to the need to prepare a specific product that can then be processed at the lowest unit costs [e.g. blasting a hard granite to provide aggregates in an attempt to create a specific grading curve as a means to reduce the energy needed in the primary, secondary and tertiary crushers]. Clearly in all such cases, the handlability of the material is the design criteria and the need to do this to lessen the environmental impact is a secondary consideration that will inevitably entail increased cost.

1.2 Characteristics of explosives

When explosives are used in controlled blasting operations, the type of explosive selected is just as important as the way in which it is applied. It is essential that the characteristics of the explosive are suitable for the conditions under which it will be used. Every type of explosive has its own set of characteristics which will decide whether or not it will be suitable for a specific application. The characteristics of the explosive used in a quarry blast will also have a significant but secondary influence on the Environmental impact created, whether it be in the form of ground vibrations or the generation of air overpressure. These characteristics include:

1.2.1 Strength

The strength of an explosive is a measure of the ability of the explosive to do useful work. It refers to the energy content of the explosive. The "relative weight strength" of an explosive is the actual strength of a certain weight of the explosive compared with the strength of the same weight of blasting gelatine and or ANFO are expressed as %BG or %ANFO. The "relative bulk strength" of an explosive is the

actual strength of a certain volume of the explosive compared with the strength of the same volume of blasting gelatine and is expressed as %BG or %ANFO.

1.2.2 Density

The density of an explosive has a large effect on many of the other characteristics of an explosive, such as its ability to sink in water, its sensitivity and velocity of detonation. The units of density are Kg/litre.

1.2.3 Velocity of Detonation (VOD)

The velocity of detonation of an explosive is the speed of the detonation wave as it passes through the explosive and is usually connected with the shattering ability of the product. The actual velocity of detonation of an explosive depends not only on the nature of the formulation but also on the strength of the initiator, the hole diameter and the state of confinement of the explosive. Weakly initiated explosives may not achieve a steady state velocity instantly and can take a length equivalent to three diameters to build up to the appropriate Figure.

The velocity of detonation is an important characteristic when considering the choice of explosive composition for a primer. In this case the velocity must build up to a steady state high value over a very short distance along the cartridge.

1.2.4 Water resistance

Water can greatly affect sensitivity and performance. Slurries and emulsions have an excellent resistance to water since their structure is, by nature, water resistant. ANFO has no water resistance. Emulsion/ANFO blends have a resistance to water which is determined by the percentage of emulsion content in the formulation.

1.2.5 Sensitivity

Sensitivity is a measure of the ease of initiation of an explosive. Three levels are usually defined as:

- Cord sensitive (to standard cord)
- Detonator sensitive (to No 8 strength detonators)

Booster sensitive (to a cast primer such as pentolite, or RDX/TNT.) As a general rule, sensitivity decreases as the density increases.

1.2.6 Sensitiveness

This is an indication of the ability to maintain the detonation wave through the length of a column of explosive.

1.2.7 Stability

Stability is usually considered to be a measure of the safety of an explosive after a long period of storage, or it can relate to the general safety in application.

1.3 Explosive types

Many types of high explosives are now available to meet the varied requirements of the Mining, Quarrying and Construction Industries.

1.3.1 Nitro-glycerine based explosives

Nitro-glycerine was for a long time the most important sensitiser for commercial explosives. It is made by reacting a mixture of glycerine and glycol with a mixture of nitric acid, sulphuric acid and water, during which process the temperature must be very carefully controlled.

The quantity of nitro-glycerine and the way in which it is mixed with other ingredients, determines the type of explosive product.

1.3.2 Ammonium Nitrate/Fuel Oil mixtures

Ammonium Nitrate is the cheapest source of oxygen available for commercial explosives at the present time. It is a very important ingredient in the explosive industry for the production of fixed explosives where it is used with solid fuels and sensitisers such as nitro-glycerine. Absorbent grade Ammonium Nitrate is required for use in conjunction with fuel oils. The bulk density of this material is about 0.7 to 0.8 g/cc. and it can absorb 7 - 8% of fuel oil without appearing unduly wet. Diesel oil is the most suitable ingredient and it has been found that about 6% of this oil gives the maximum power on detonation producing negligible poisonous fumes.

Aluminium is often added to the mixture to give a higher temperature reaction, thus enhancing the strength characteristics. The main disadvantage of Ammonium Nitrate/Fuel Oil compositions is that they are not waterproof and also have low bulk strength.

1.3.3 Slurry explosives

Slurry explosives have developed as a result of attempts to waterproof, strengthen and sensitise Ammonium Nitrate. Ammonium Nitrate is dissolved in a sensitiser solution and more salts are added along with a gelling agent which ensures its firmness, giving it excellent waterproofing characteristics.

As technology has developed, strength, sensitivity, velocity of detonation, sensitiveness and stability have all been improved to provide a comprehensive range of explosives with acceptable fume characteristics, as the product vapour contains no atomised nitro-glycerine.

1.3.4 Emulsion explosives

Emulsion explosives are prepared in the form of water-in-oil emulsions. The internal phase (the water phase) consists of droplets of a saturated solution of the oxidising agents suspended in a matrix of the fuel phase. The physical properties of the composition are determined by the substance of the fuel phase, which can be altered by using a range of different oils or waxes. The stability is maintained by the addition of a suitable emulsifying agent. Solid fuels may be added, usually in the form of fine aluminium, to provide explosives of different strengths. Also incorporated into the emulsion is entrapped air usually in the form of hollow microscopes of glass, plastic or resin. A modern development is the inclusion of chemicals such as Sodium Nitrate and Acetic acid which on reacting within the blast hole produce bubbles of nitrogen which in turn then sensitise the explosive emulsion. In whichever way they are provided, these bubbles or microspheres act as a bulking agent and provide centres of reaction which ensure sufficient sensitivity for continuous detonation.

1.4 Detonators

1.4.1 Electric detonators

The modern commercial electric detonator consists of a thin walled tube made from copper or aluminium, closed at one end and containing a high explosive base charge, a priming charge and a fuse head. The tube is sealed with a Neoprene plug through which the leading wires of the fuse head assembly pass.

The fuse head itself consists of two metal foils separated by a layer of insulation. The leading wires are soldered to the base of the foils and a very fine

wire connects their tips. Around this wire a bead of an igniting composition is usually constructed in several layers, the innermost being readily ignited by heat. The electrical properties of this wire and the sensitivity of the fuse head chemicals determine all the firing characteristics of the detonators, such as no-fire current, all-fire current and minimum series firing current. The electrical resistance of the detonator is the sum of the fuse head resistance plus the lead wire resistance.

When an electric current of sufficient power is passed down the lead wires, the fine wire in the fuse head rapidly heats up to the point where the igniting composition flares and initiates the priming charge which, in turn, initiates the base charge.

1.4.2 Delayed action detonators

For most blasting operations, it is an advantage to have various charges initiated in a pre-determined sequence with regular time intervals between detonations. Delayed action detonators have been developed to meet this requirement.

The construction of a delayed action detonator is like that of the standard electric detonator, except that a special delay element has been introduced between the fuse head and the base charge. This delay element consists of a column of slow burning composition contained in a thick walled metal tube. The length of this column and its composition determine the amount of delay time introduced into the detonation train

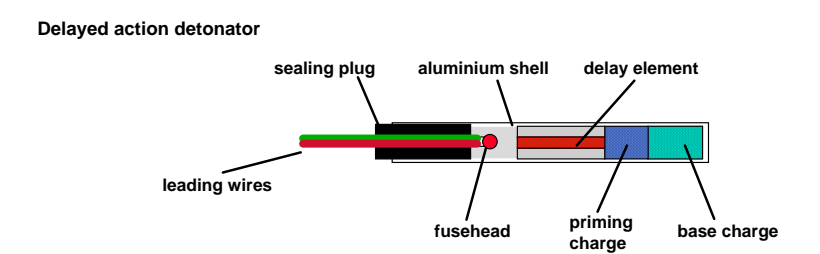


Figure 1.1 Electric pyrotechnic delayed action detonator

1.4.3 Shock tube detonators

Becoming the most popular type of detonating system, however, are the **non electric** systems of initiation based around a hollow plastic shock tube which

replaces the electrical components in conventionally constructed detonators. The inside of the plastic tubing is coated with a reactive substance which propagates a shock wave down the tube at a speed of approx. 2000 metres/sec. This shock tube has sufficient energy to initiate the primary explosive or delay element in a detonator. Since the propagating shock wave is contained in the tube, this has no blasting effect and the tubing acts merely as a signal conductor.

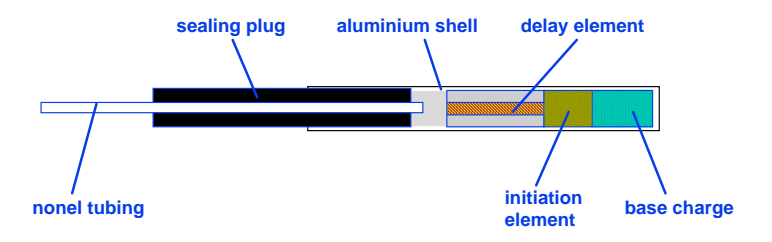


Figure 1.2 Non electric pyrotechnic delayed action detonator

1.4.4 Electronic detonators

Detonators based on pyrotechnic delay elements have an inherent significant delay scatter. To overcome this limitation, electronic detonators have been developed. In an electronic detonator the pyrotechnic delay element has been replaced with an electronic microchip giving greatly enhanced accuracy and improved safety levels. Timing accuracies of +/- 0.1 milliseconds are routinely measured.

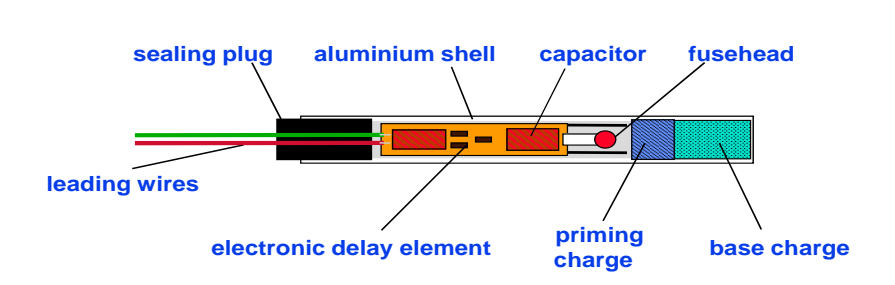


Figure 1.3 Electronic detonator

1.5 Single hole initiation

In the past it was common practice to initiate the detonation of boreholes using surface detonating cord with detonating relays. Modern practice is to detonate the explosive in the boreholes using "down hole detonators" placed directly into primer cartridges of explosives. Where column separation may be considered to be a potential problem then the explosives in the blast hole can be linked by detonating cord.

If detonating cord passes through the stemming, disruption will always occur and the degree of confinement of the charge is often significantly reduced. With respect to opencast buffer blasting where the aim is to crack and not throw the blasted material, this in the past has given rise to large volumes of dust and poor blast performance as a result of the detonating cord blowing a small diameter hole through the stemming and then the gases effectively scouring out the stemming material on occasions to leave a clear hole.

The performance of emulsions, slurries, ANFO and emulsion/ANFO blends depend a great deal on the degree of confinement, much more so than sensitive nitroglycerine based compositions and this reduction can affect the results significantly. The detonation of slurries and emulsions by side initiation is much poorer with the diameters used in the United Kingdom. A third and important factor is that the loss

of energy caused by the detonation of cords on the surface and in the upper parts of the borehole, will be transformed into both noise and air blast and will often result in complaints from neighbours.

For environmental and efficiency reasons there has been renewed interest in initiating boreholes with down hole detonators. The use of long lead electric detonators has lost favour as a result of the development of non-electric systems particularly in hazardous (electrically) situations. With any down hole detonating system, it is standard practice in the UK to use two detonators in any explosive charge.

For large diameter holes using two detonators in continuous charges, both detonators can be in the same primer near or at the bottom of the hole or preferably one detonator is placed in a primer near or at the bottom of the hole and the second detonator placed in a separate primer near the top of the explosive column. The top detonator should be of a later delay period and, as such, will only be used in the case of a failure by the bottom detonator or as a result of a discontinuity of the column. In either case, the redundant (later firing) detonator is destroyed in the explosion.

Figure 1.5 is a cross section of a typical blast hole charged with explosive. The key component parts are two detonators to initiate the blast (in this case one at the top of the hole and the other at the bottom). Each detonator is inserted into a detonator sensitive primer. This primer then initiates the base charge which is typically of a higher explosive energy per kilogram which in turn then initiates the column charge which is typically ANFO or an emulsion explosive.

TOP AND BOTTOM PRIMING WITH DOWN HOLE DETONATORS

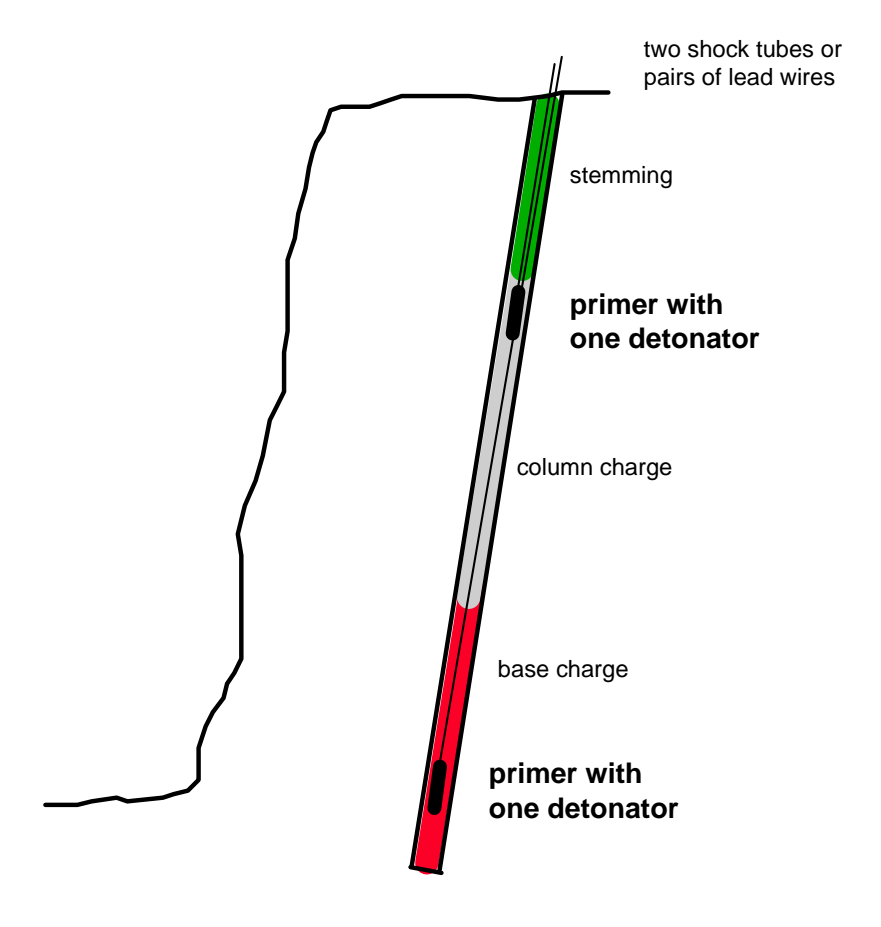


Figure 1.4 Cross section showing the component parts of a typical blast hole charged and ready to fire.

1.6 Mechanism of rock breakage

1.6.1 Energy considerations

When an explosive charge is detonated in a drill hole, there is a sudden release of the stored energy in the form of an outburst of gas at high temperature and pressure.

1.6.2 Strain energy

The effect of the sudden release of energy in a drill hole is to apply a high pressure pulse to the rock surface and to generate a compressive strain pulse in the surrounding rock. This pulse travels radially from the borehole decaying in amplitude as it travels outwards (see Figure 1.6).

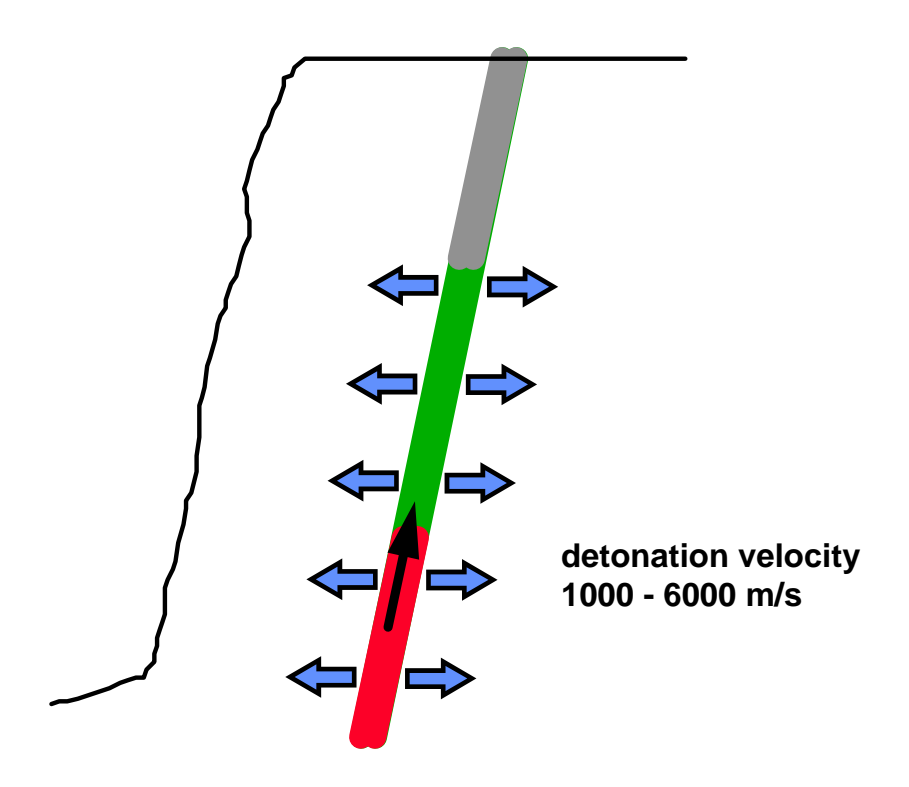
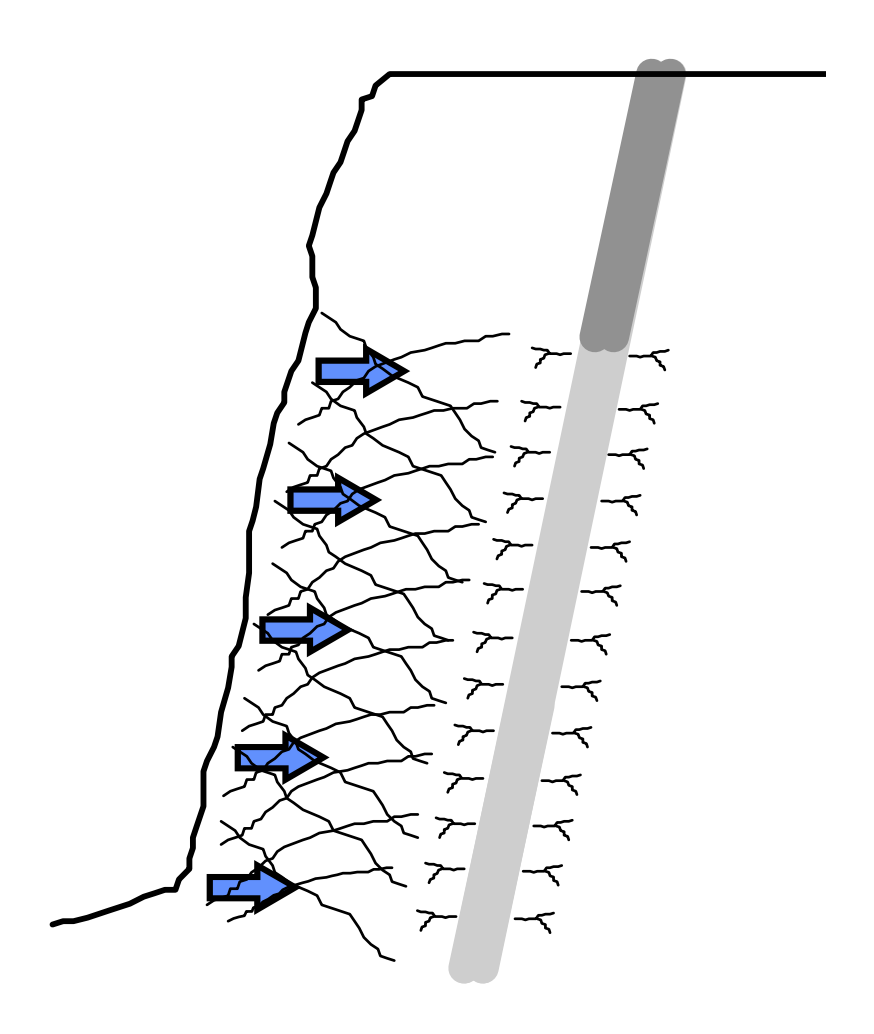


Figure 1.5 Blast hole fires from the base upwards giving rise to a compressive shatter zone and shock wave.

The effect of this is to produce crushed rock in the vicinity of the drill hole (White and Robinson 1995). As long as the amplitude of the compressive strain pulse exceeds the crushing strength of the rock, further disintegration will occur. At a point further from the borehole, where this is no longer the case, the pulse will then travel as a seismic disturbance without causing further breakage or fracture.

When the compressive wave reaches a free face (e.g. a quarry face or open joint), reflected tensile waves are produced. Since rock is weaker in tension than in compression (usually by a factor of five or more), the rock is slabbed off and is projected away from the face (see Figure 1.7).

For breakage to occur by this method, enough energy must be transmitted on detonation to account for losses in transmission through the rock, the energy of motion of the broken fragments and the potential energy of the new surface created by the breakage.



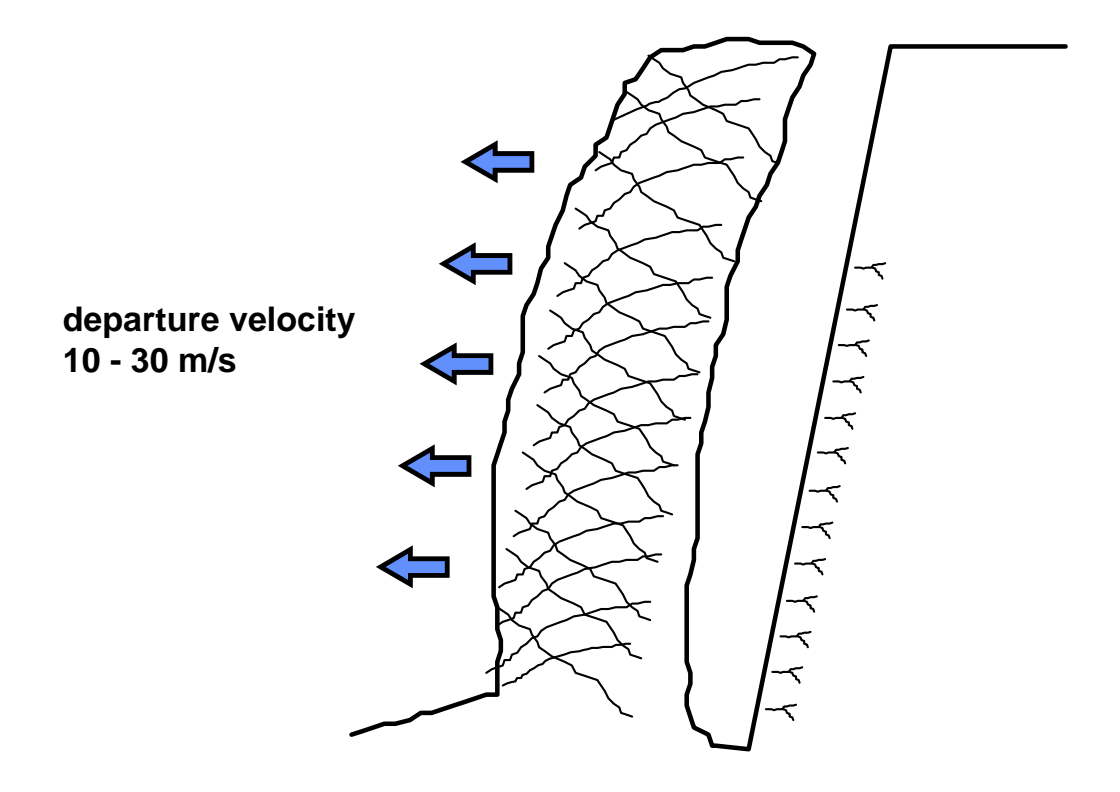
Reflection of shock waves

Figure 1.6 Compression wave reaches the free quarry face and undergoes 180 degree phase change and is reflected as a tensile wave.

Fragmentation by tensile fracture may be the only means of breaking the hardest rocks with explosives although fragmentation by compression may be important in the softer and lower density rocks.

1.6.3 Thrust energy

This term is used to describe the work done by the gases produced by a detonation, that is the heaving and churning action of the expanding gases in the borehole and the further disintegration of the rock which occurs from this powerful source of energy (see Figure 1.7).



Gas Pressure Phase

Figure 1.1 Gas produced by the explosive under high pressure penetrates the fragment rock and pushes it onto the quarry floor

The sequence of photographs in plate 1.1 illustrates how the quarry face reacts to the actual detonations of the shot holes. Picture 1 is immediately prior to the blast being detonated. Picture 2 shows the Nonel detonating relays firing on the surface (see slight "puffs of dust". Picture 3 shows the shock wave had moved out from the shot holes and then reflected at the quarry face to send a tensile wave back into the rock, thus breaking it up in tension. The Gas phase of the explosion then takes over to push the rock out in a "bow shaped" arc as per Figure 1.7 above.



Plate 1.1 Sequence of photographs demonstrating how the quarry face reacts to the detonation of the shot holes.

Picture 4 shows the broken rock mass then moving under both gravity and the gas phase. Picture 5 shows the final events of the gas phase pushing out the rock pile along the quarry floor. Picture 6 shows the completion of the process with the spent water vapour from the explosion together with some dust seeping into the atmosphere from out of the rock pile.

1.7 Blast planning for surface excavations

1.7.1 Factors influencing blast design

Much knowledge of the deposit needs to be known before a suitable blasting regime can be embarked upon and a number of factors need to be taken into consideration.

1.7.1.1 Thickness of the deposit to be worked

The thickness of the deposit influences the type of blasting operation to be carried out, in that it often limits the bench height. This is equal to the bench height or is a multiple of it, particularly so when working horizontal or near horizontal deposits of bedded rock or ore either near the surface or at depth, between other rocks with different properties or values. In thicker deposits, the bench height is often influenced by the extent of the proposed workings to accommodate haul roads and changes in surface heights.

1.7.1.2 The hardness of the rock

The hardness of the rock will influence the type of drilling operation which needs to be mounted, for example, a hard rock may need to be drilled by a drifter, whilst a softer rock may be drilled by other methods. The cost of drilling often influences the degree to which the drill holes are utilised. A hard rock quarry would consider it unacceptable to fill less than 60% of the drill hole with explosives whilst an opencast coal site with relatively soft rock and easier drilling, will often utilise less than 25% of the borehole volume, the rest being stemming.

1.7.1.3 The presence of joints and bedding planes

Joints and bedding planes affect blasting results more than any properties of the explosive to be used. Where the rock exhibits a high frequency of joints and bedding planes, satisfactory fragmentation, displacement, and muck pile looseness are usually achieved with a relatively low explosive to rock ratio. When the rock is tough and massive, a much higher explosive ratio is required.

1.7.1.4 The required shape of the muck pile

A front end loader works best on very low blast profiles where the rock is spread out a few metres high. This is best achieved from single row blasts from medium to high faces, where the explosives ratio is relatively high and the degree of fragmentation is better than most other cases. On the other hand, face shovels, either

hydraulic or rope operated, perform best on muck piles which are compact, and this can be produced from a medium low face and multi-row blasts. One must also take into consideration that some machines, for example backhoes and draglines, sit on the muck which is blasted and for this type of operation, regardless of other considerations, the muck pile must retain its shape and be compact enough to bear the weight of the machine..

1.7.1.5 The degree of fragmentation required

The degree of fragmentation required is often determined by the type of crushing machinery available. Crushing machines should be chosen for the size of their aperture as well as their output capacity, but the increase in capacity with a small increase in size of jaw is often tremendous, as also is the power requirement of the machine. Where mineral is carried to tip, fragmentation should be optimum for loading and should be suitable to achieve the degree of compaction required on the tip. The production of block stone is a very special case requiring separate consideration as the main aim will be to produce large blocks of stone and to do as little internal damage as possible to the blocks produced.

1.7.1.6 The type of drilling machine

The type of drilling machine available is not always as versatile as one would like. The smaller the bench height, the smaller the diameter of drill which would appear suitable, and indeed this is often so, but the advance of down-the-hole rock drilling equipment for use in relatively soft rocks, means that the intermediate size of the borehole, say 85 mm diameter to 130 mm diameter, is used in all but the very smallest or very largest of operations. Indeed a significant proportion of the explosive manufacturers' production is made suitable for 105 mm diameter holes.

1.7.1.7 The amount of rainfall and groundwater present

Wet conditions affect the choice of explosives, since most operations these days will consider the use of some ANFO, and this composition is not compatible with wet conditions under any circumstances. Attempts at dewatering boreholes have met with some success where rainwater has been the cause of wet boreholes, but where the "make" of groundwater is significant, waterproof explosives, which will sink, are necessary. Pumpable emulsion/ANFO blend explosives which will displace water as they are loaded into the hole can be considered.

1.7.1.8 The proximity of environmentally sensitive structures and neighbours

Environmental considerations often determine the size of the blast, the maximum instantaneous charge and the detonating sequence. The increasing awareness of disturbance to the environment and its effect on the quality of life, coupled with a better knowledge of the rights of people in this respect, has caused the blasting engineer to make vibration and air blast one of the prime considerations in blast design.

1.7.2 Factors affecting performance

1.7.2.1 Loading density

The total potential for work of an explosive may be approximated by the total heat of explosion. However, the manner in which this energy is expended depends on how the explosive is loaded into the borehole. Maximum utilisation occurs when the explosive fills the complete volume of the borehole at the explosives absolute density, that is, its coupling factor is then unity (100%).

Loading density can be expressed in terms of a coupling factor which is the ratio of the borehole cross sectional area to that covered by the explosive. Modern explosives try to achieve a loading density close to one by making use of cartridges which will "slump". Bulk explosives completely fill the cross section of the borehole.

1.7.2.2 Loading rate

This is the rate at which the explosive fills the hole and is expressed in terms of kilograms per metre. It is a measure of energy concentration. The actual loading rate of explosives depends upon the density of the explosive, its diameter, the degree of slumping and whether or not the hole contains water.

1.7.2.3 Charge diameter

The velocity of detonation of most commercial explosives increases with diameter until an optimum value is reached and, therefore, it is advantageous to fill the whole cross sectional area of the borehole.

1.7.3 Primary blast design

The important requirements for any primary blast are:

- That it is safe
- That it ensures optimum results for the existing operating conditions
- That it is simple to employ.

A balance needs to be obtained by the arrangement of the holes, their location and the correct choice of explosive types in order to utilise the explosive properties, to produce fragmentation and breakage of the materials being blasted.

1.7.3.1Blast geometry

The blast geometry is completely defined if hole depth, hole diameter, inclination, azimuth, burden, spacing and number of holes per row are specified. The first six factors are considered to be interrelated in that a change in one will affect the values of the other. Two other factors to be considered in blast geometry are the depth of stemming and the amount of sub-grade drilling (see Figure 1.8).

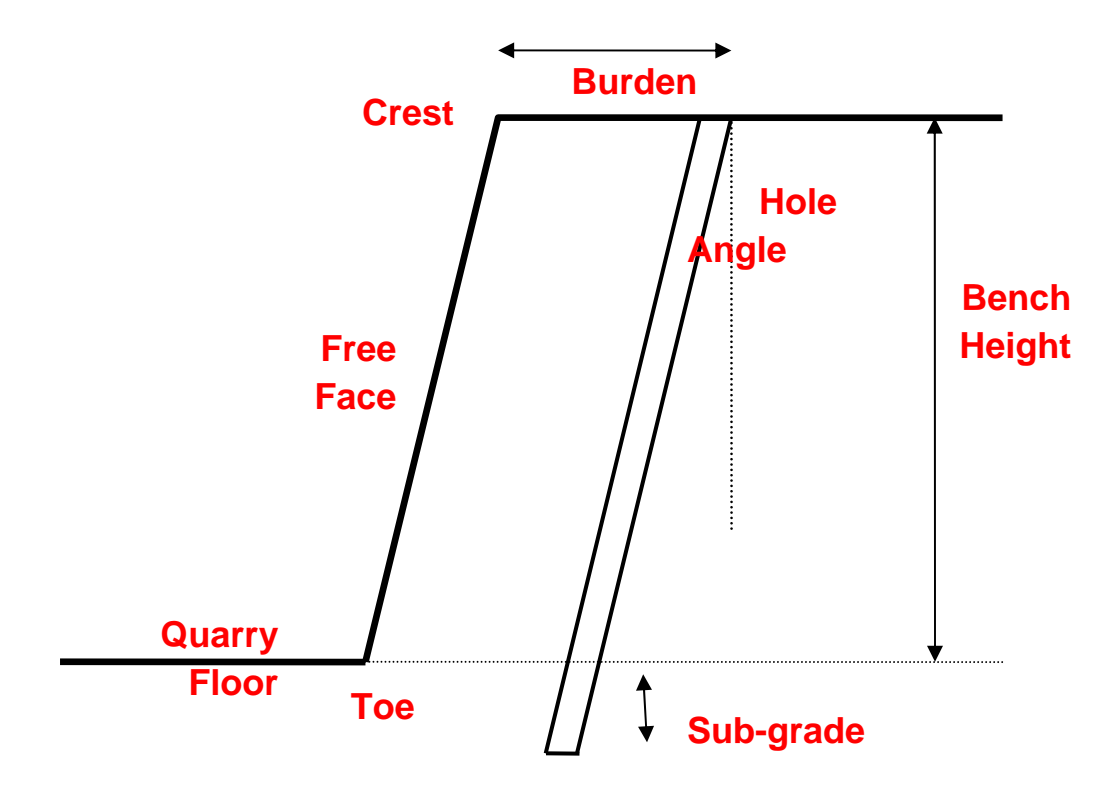


Figure 1.2 Annotated diagram of the key elements of a quarry blast design

1.7.3.2 Bench heights

Bench heights of between 10 and 20 have been considered the most economical to work and certainly the least hazardous. Bench height affects the blast result in many ways. Unless the face height is large enough, the optimum burden and spacing is not achieved, if the correct Blast Ratio [see definition in 1.7.1.15] is to be employed. For hard rock, a charge height, of at least twice the burden, is generally employed. If the holes are too shallow, the charge cannot be distributed correctly and the correct Blast Ratio cannot be achieved unless burden and spacing are reduced. High faces pose the problem of "drill bit wander" and thus drilling deviation considerations often limit the bench height. Face stability may also be a problem.

1.7.3.3 Borehole diameter

Where rock is hard, it is possible to get better distribution of the charges by using small diameter holes. When the blast hole diameter is increased for a given set of conditions, the larger blast hole pattern generally causes coarser fragmentation. To achieve finer fragmentation, then small borehole diameters and closer borehole patterns are required. In rocks which exhibit a dense network of natural fissures,

fragmentation is controlled by the structure of the rock, and a decrease in blast hole diameter will often result in a relatively small improvement in fragmentation. However, a reduction in drilling cost can be achieved by increasing the borehole diameter and also increasing the patterns. Part of the subsequent loss in fragmentation can be overcome by decreasing the Blasting Ratio. Where blasting agents, slurries and emulsion/ANFO blends are to be used, better performance of the explosive can be obtained by increasing the diameter, since the velocity of detonation of ANFO increases with the diameter of borehole up to 400 mm.

1.7.3.4 Burden

Burden is the distance back from the front face to the first row of holes or the distance between rows of holes. A useful 'rule of thumb' used in the UK surface mining industry for burden is

Burden = $(30 \text{ to } 45) \times \text{borehole diameter}$

1000

where the burden is in metres and the diameter is in millimetres. The factor which varies from 30 to 45 covers hard to soft rocks.

1.7.3.5 Drill hole spacing

In the United Kingdom, burdens and spacings are often chosen to be equal. Most blasting experts state that the spacing should be between 1 and 1.5 times the burden for best fragmentation.

Spacing = $1.25 \times Burden$

Using excessive spacings produces an uneven quarry face and the fragmentation distribution will contain both fines and oversize rocks.

1.7.3.6 Inclination of the borehole

Inclined drilling provides better charge distribution and is very effective in overcoming tough toe conditions and reducing overbreak. A given borehole

inclination is often chosen to give a stable face profile. This is usually determined by an assessment of the geotechnical conditions for a particular mine or quarry face.

1.7.3.7 Sub-grade drilling

To avoid unblasted rock above the floor level of the bench, holes are drilled a certain distance below the level up to a maximum of one third of the burden. Explosives placed above and below the floor level have an effect on the movement and fragmentation of rock at floor level, but at distances greater than one third of the burden, this effect is minimal.

Sub-grade = Burden / 3

1.7.3.8 Hole depth

The hole depth is given by the bench height plus the sub-grade drilling depth, multiplied by a factor to take account of the inclination.

Hole Depth = (face height + sub grade)/cos (inclination)

1.7.3.9 Base charge

Since explosives at the base of the borehole have, in addition to breaking out to the face of the blast, a great deal of work to do to form a new floor, it is generally agreed that about three times as much work is required to be done by explosives in that part of the blast. In practice, the weight of the base charge of heavy explosive can be increased until the explosive is so far from the base that it performs no useful work at floor level. This point is reached when the sub-grade and a distance up the column equal to the burden is filled.

Max. height of Base Charge = Sub-grade + Burden

1.7.3.10 Stemming

Normally, the height of the stemming is taken to be at least equal to the burden. If this is reduced, there is risk of flyrock from the top of the borehole or flyrock coming through the stemming. Other considerations of rock strength, type of stemming material, explosive type, or initiation methods will necessitate changes in the actual stemming depth used.

Stemming = Burden

1.7.3.11 Column charge

The column charge is the charge between the base charge and the stemming. The concentration of charge may be lower than at the base of the borehole but if the charge is not continuous, the full effect of drilling the borehole is not being achieved.

1.7.3.12 Detonating method

The method of detonating a column of explosive will affect the results significantly. Nowadays, the trend is to use methods which involve point initiation to ensure that the explosive is initiated at the optimum point only, and that low order detonations and desensitisation of explosive do not occur. Higher efficiency can be obtained by point initiation since the stemming is not disrupted nor is there any waterfall effect which will often result from top initiation.

1.7.3.13 Primer position

Rock mechanical studies have shown that the position of the primer in a borehole has a direct effect on the size and shape of the stress wave in the rock. At first sight since maximum stress occurs in the direction that the explosive is detonating it would seem therefore that for maximum fragmentation at the bottom of the borehole top initiation is best. However, in practice, factors other than stress levels must be considered in deciding between top and bottom initiation.

Bottom initiation offers the advantage that the expanding gases are confined for long and consequently work harder. Since the Velocity of Detonation (the fragmenting characteristic) is often increased substantially with greater confinement, in practice, the best place for a primer cartridge is at the floor level. This requires good loading conditions to be able to free fall a couple of cartridges into the subgrade drilling area without fear of them blocking the hole, and a knowledge of the location of the floor in relation to the bottom of the borehole (this can be obtained from the profile drawing).

1.7.3.14 Detonating sequence

Delayed action shotfiring is almost essential for environmental reasons. The maximum instantaneous charge is a factor which is derived from regression line analysis associated with vibration level predictions. If, however, consideration is not given to the creation and use of free faces then the vibration levels from any type of

blast will be significantly affected. The creation of a much more acceptable free face for subsequent parts of the blast after the first hole has been fired, together with the reduction of effective burden, increases the likelihood of achieving optimum fragmentation. With multi-row shots, hole placement and delay sequence are fundamental to producing effective breakout, resulting in better control of the blast (i.e., reduction of the chances of cut-off misfires, flyrock projections and improving fragmentation and vibration).

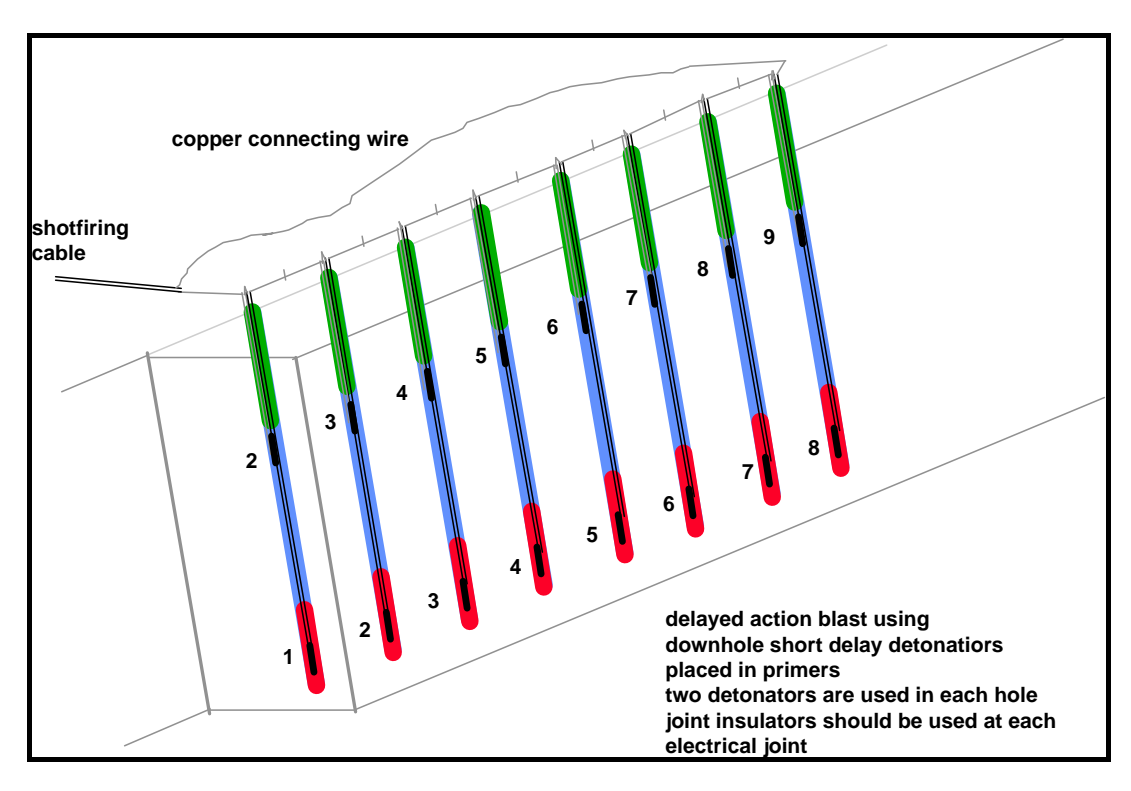


Figure 1.3 Electric detonator sequence in a quarry blast

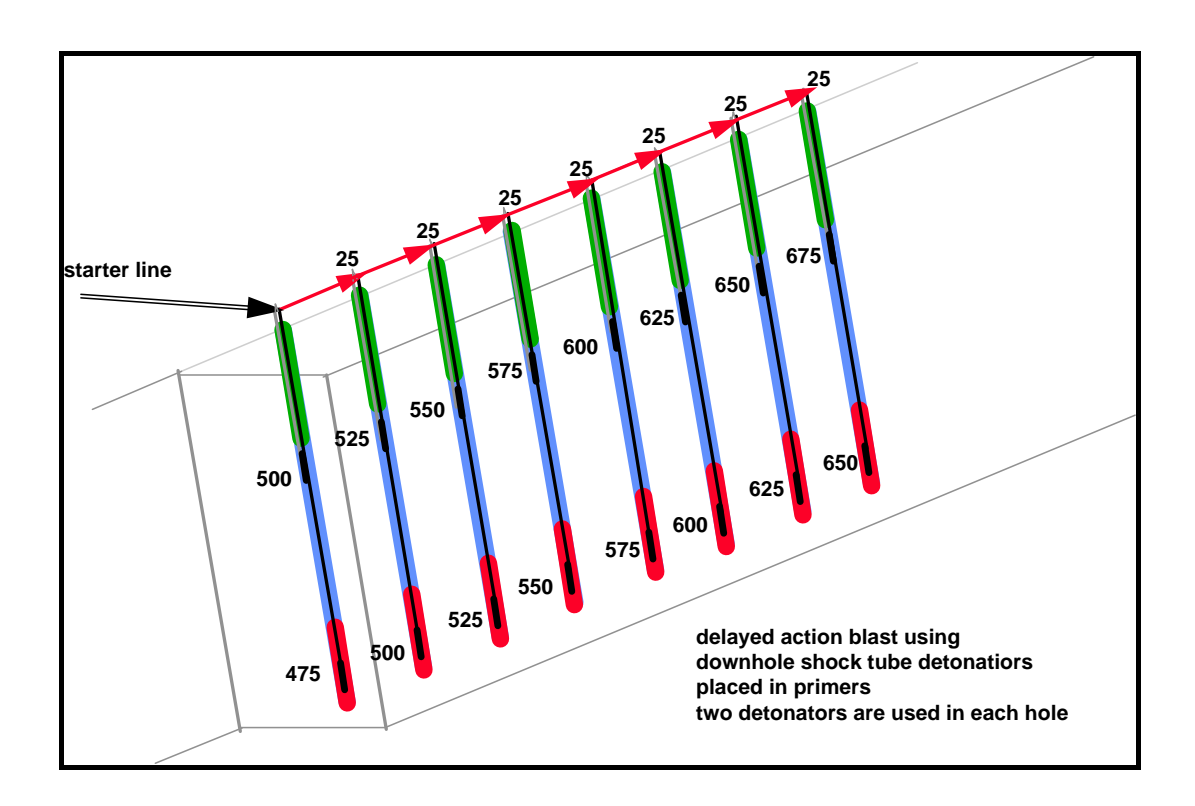


Figure 1.4 Interaction between detonating relays and long period detonators to create advanced initiation in a quarry blast.

1.7.3.15 Choosing a detonating sequence

The safety and success of any blasting operation is dependant to some extent on the order and time at which holes fire in relation to one another. A wrong choice of time delay can lead to operational difficulties caused by inadequate ground movement if times of firing are too close together or to cut off misfires or even such disastrous consequences as flyrock if times of firing between adjacent holes are too long. Optimised fragmentation is achieved with the correct choice of delay and sequence, and, as a result vibration is usually minimised.

As a starting point the time delays between adjacent holes is normally chosen

as Between Holes in a Row: 5 to 10 ms per metre of Spacing
Between Rows of Holes: 10 to 30 ms per metre of Burden

When choosing a sequence it is necessary to identify and locate all available free faces. The first hole to fire is the one with most free face available to fire towards. Thereafter other considerations apply. The timing is chosen based on the actual burdens and spacings using the Figures mentioned above. The maximum instantaneous charge sets the number of holes or fractions of holes which can be fired at any one moment. With shock tube and sequential timer initiation systems

two detonations are considered to be coincident if they occur less at less than eight milliseconds time separation.

The strength and competence of rock has to be considered. Igneous rocks require time delays at the shorter end of the range and sedimentary rocks require the longer time. Broken ground reacts faster than solid ground and thus shorter times are used in broken ground. In extreme cases it may be appropriate to use no delay between adjacent holes in the same row.

1.7.3.16 Blasting Ratio

The quality of the rock being worked and the type of operation being carried out determines the amount of explosives required to produce effective fragmentation.

There are two ways of expressing the blast ratio for any blast.

- 1. In Quarry blasting it is more usual to express the ratio as the weight of rock excavated divided by the quantity of explosive used to achieve the result. The units are therefore Tonnes/Kilogram.
- 2. In the opencast coal industry it is common to calculate the blast ratio in terms of the volume of rock blasted divided by the quantity of explosive required and the units for this are therefore cubic metres per kilogram.

Typical values are:

Granites	4.5 to 5.0 T/kg
Hard Limestone	5.5 to 6.0 T/kg
Soft Limestone	6.0 to 7.0 T/kg
Shale / Mudstone	6.5 to 7.0 T/kg
Opencast Coal	$4.0 \text{ to } 7.0 \text{ m}^3/\text{kg}$

In other countries this ratio is defined as "Powder Factor". Powder Factor is the reciprocal of Blast Ratio.

1.7.3.17 Calculation of Blast Ratio

The blast ratio when calculated for a single hole can be different to that calculated on a whole blast basis when such considerations as the presence of tight ends/free ends are taken into account.

Yield = Inclined Burden x Spacing x Face Height (cubic metres)

The weight of rock is given by the following:-

Weight of Rock = Yield x Density of Rock (Tonnes)

For a whole blast, the ratio is calculated as follows:-

Blast Ratio = Number of Spacings x Weight of rock per Hole in Tonnes

Total Weight of explosive used

1.8 Environmental blast design

As previously outlined the Blasting Ratio chosen will depend on the type of operation being undertaken. However there will be occasions when economic production requires charge weights which could produce vibration levels at or above pre determined limits. These limits might have been established on the basis so as to prevent damage, or they may be simply to reduce the nuisance effect to local residents living nearby. In either case, if they are contained within the Planning Conditions or Permit to Operate, they are statutory and to contravene such limits is to be in default, which in itself for an operator is a serious matter.

It is known from many years of monitoring and analysis of blast vibration data that primarily the vibration levels produced in terms of Peak Particle Velocity [PPV] are inversely proportional to the distance from the observation point to the blast and directly proportion to the square root of the maximum explosive charge detonated at any one time. Thus larger charge weights produce higher vibrations and the closer the blast is to the observation point, the higher the vibration. Thus any mitigation measures employed must in the first instance take these two primary factors into account. There are a number of options that can be taken to attempt to mitigate the problem.

1.8.1 Alter the Drill Ratio

The blasting ratio as defined above is the amount of tonnes or cubic metres of rock produced per Kilogramme of explosive. If this has been arrived at by an empirical method, then clearly, to radically alter this will have a direct effect on the product produced. Thus to simply to reduce the charge weight whilst keeping the burden and spacing of the drilling pattern the same will rapidly increase the blasting

ratio. The key is to reduce the drilling ratio. The drill ratio is defined as the total volume of rock in a blast divided by the total length of blast holes drilled. This will also certainly result in an increase in cost. However to make sure that all the other parameters within the blast design are kept in balance then it will be necessary to alter the borehole diameter to ensure that the reduced maximum instantaneous charge weight used is correctly distributed throughout the rock mass to be blasted. Not to do so will inevitably result in the lower portion of the rock mass being over blasted and the upper portion being under blasted. Suppose that the current practice on an opencast coal site is to blast a heavy sandstone horizon for an RH120 face shovel operation to a 10 metre face with a design blasting ratio being 4.0 cubic metres per kilogram (see Figure 1.10). If the original blasting pattern was 5 metres x 5 metres (burden and spacing) using a 127 mm diameter hole, then the resulting maximum instantaneous charge weight per hole would be approximately 62.5 kilograms. However if, on encountering environmental problems, the blast design was altered to a 4 metres x 4 metres (burden and spacing) using a 101 mm diameter hole, then the resulting maximum instantaneous charge weight per hole would be approximately 40 kilograms. This would then ensure that the original design blasting ratio could be maintained.

There is reluctance by both the opencast coal mining and the quarrying industries in the UK to implement this method of vibration control on the basis of increased cost. However in arriving at this conclusion, it is the author's opinion that not sufficient account has been taken of the fact that smaller lightweight drill rigs require less set up time, less time to drill a borehole and less time to move from borehole to borehole. Such factors rarely appear to be considered in determining the unit cost of drilling and blasting in either £ per tonne or £ per cubic metre of rock produced.

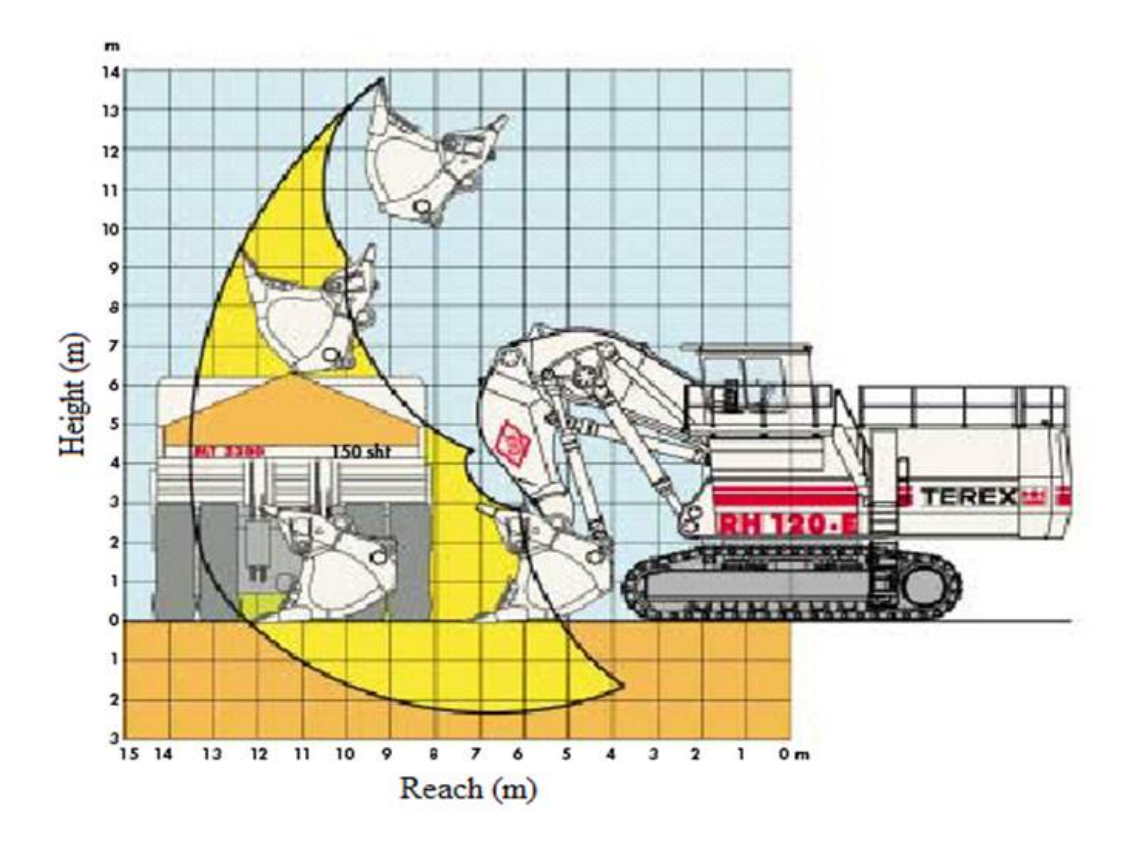


Figure 1.5 Ranging diagram for a Terex RH120 face shovel

1.8.2 Split the bench

The practice of splitting the benches, so as to ensure that the design blasting ratio can be employed, is more common in the opencast coal mining and the quarrying industries in the UK than that of altering the drill ratio. However if in the previous example the 10 metre bench had been split in to two 5 metre benches in order to continue with the same 5 metres x 5 metres (burden and spacing) using a drill rig with a 127 mm diameter hole, then as can be seen from Figure 1.11 the face would barely be up to the drivers cab level. Thus would necessitate frequent moves and more frequent assistance from wheeled bull dozers in cleaning up spillage. All of which would result in a marked reduction in output in terms of loose cubic metres per hour and thus a significant increase in the unit cost of the rock moved.

1.8.3 Split the charge in the blast hole

Deck charging is the most common practice employed in the opencast coal mining and the quarrying industries in the UK when environmental issue necessitate a reduction in the maximum instantaneous charge weight that can be used.

Figure 1.12 shows a typical double decked and double shot quarry blast. This ensures that there is sufficient time between the first shot in the borehole firing and the second so as to eliminate the possibility of the first shock wave being reinforced by the second

DECKING WITH DOWNHOLE DETONATORS

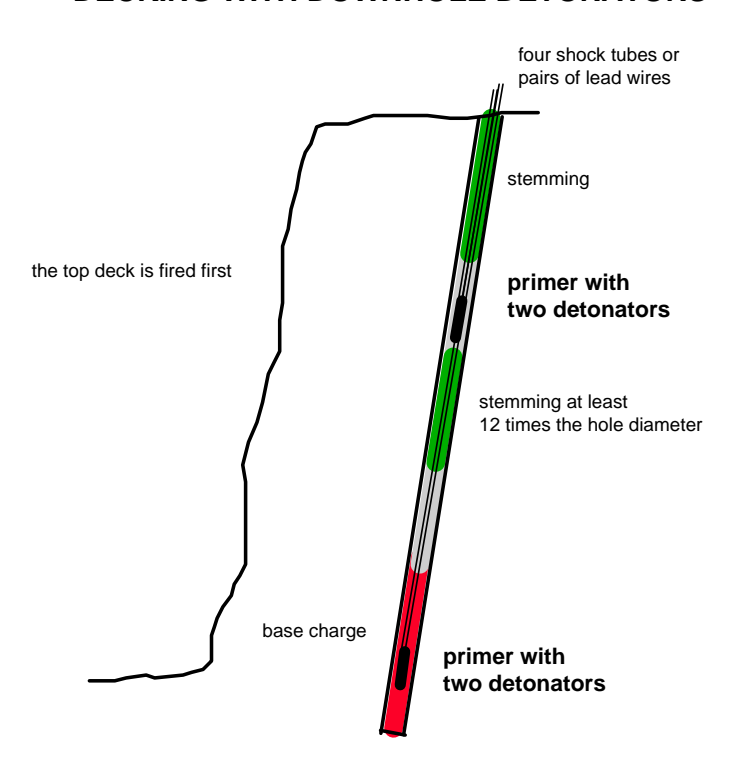


Figure 1.6 Double decking and double shot in a single blast hole to reduce the maximum instantaneous charge weight to ensure environmental compliance

The two explosive decks are separated by stemming material so as to avoid the possibility of instantaneous sympathetic detonation of the second deck in response to the detonation of the first deck. When firing decked holes it is usually better for vibration reasons and for considerations of the generation of new free faces to initiate the top deck first.

1.9 Conclusion

This section has outlined the fundamentals of blasting as employed in quarries and opencast coal sites in the UK. It is not intended as a definitive guide, but rather as a basic introduction to the key elements that need to be considered when designing a surface blast. It has explained the key ingredients that constitute an explosive and then continued on to discuss the methodology required to design an

effective blast. Finally it has defined the terms Blast Ratio and Drill Ratio. It has then outlined that in terms of environmental limitations, that there is no need for an experienced blast design engineer to compromise the intended Blast Ratio required to efficiently carry out the set task, provided that consequential impact on the Drill Ratio is fully understood.

Chapter 2

Physics of blast vibrations through air

2.1 General properties of waves

Physically, waves are a travelling disturbance and represent the transfer of energy from one point in a given medium to another other point. Thus, for a wave to exist, there must be an initial disturbance of the medium, that is, some forces must act to disturb the medium from its equilibrium position and thereby introduce new energy into the medium. The action of the forces causes the nearby portions of the medium to oscillate about their rest position much as a spring mass system. The oscillatory disturbance is transmitted from one particle to the next, then to the next and so on causing a wave motion to propagate through the medium.

There is no bulk movement or transport of matter during wave motion (Bollinger, 1980). The constituent particles of the medium oscillate and/or rotate only about space limited paths and do not travel through the medium. This fact introduces the necessity for consideration of two velocities:

- a wave velocity that describes the rate at which the disturbance propagates through the medium
- a particle velocity that describes the small oscillations that any given particle executes about its equilibrium position as wave energy excites it.

The energy introduced by the disturbance travels as kinetic energy of the particle motion and potential energy of particle displacement in the wave motion. As a wave propagates through an infinite medium, it tends to spread out and this introduces a geometrical effect on the energy concentration of the wave. Thus in a perfectly elastic medium of infinite extent; a point source in such medium would induce spherical waves. The area of these wave fronts increase as r², where r is the distance from the source, thus the energy flow per unit area would decrease as r².

In practice we do not have a perfect medium and thus there are additional losses as the wave propagates. These are absorptive losses, which attenuate wave amplitude with distance and/or time; absorptive loss is often exponential.

2.2 Types of waves generated by quarry blasts

There are two ways that blast vibrations can propagate from a quarry blast and then have an environmental impact of structures and residents living adjacent to the quarry:

Ground Vibration

Air Overpressure.

Vibrations transmitted through the ground (seismic waves) and pressure waves through the air (overpressure) shake buildings and people and may, in extreme cases, cause nuisance or damage. The effects of the two factors are difficult for even an expert to distinguish without instrumentation. However, the pressure wave through the air may arrive after the ground vibration by up to 2 seconds over a distance of 1km. The perception of both factors is likely to be stronger inside a building than outside.

As this report is specifically related to air overpressure as a result of quarry blasting, the subject area of ground vibration induced by quarry blasting is outside the scope of this report.

2.3 What is air overpressure?

Air overpressure consists of air transmitted sound pressure waves that move outwards from an exploding charge. Air overpressure can be measured in any unit which measures pressure. The commonest are Pascals (Pa), which is a linear scale, and decibels (dB), which is a logarithmic scale using the ratio of the recorded pressure to a reference pressure. Unlike noise measurements, there is no weighting applied to the value in decibels and so the unit is sometimes given as dB(Lin) although this is often abbreviated to dB. Strictly, it should also give the frequency above which it is linear (e.g. 2Hz). However, dB(Lin) should not be confused with dB(A) which is the weighting which is applied when monitoring for noise. The values obtained when measuring dB(Lin) will nearly always be higher than when

measuring for dB(A). For example the air overpressure from a blast may be around 95dB(Lin), but the noise may only be 60dB(A). Air overpressure may vibrate buildings but damage would seem to be rare. Damage in the form of broken windows is possible but extremely unlikely at 140dB. More frequently it adds to the perception of vibration and causes complaints by making windows, ornaments, etc, rattle and startling people, which is possible at 120dB. It is probably less of a problem than ground vibration especially where the use of surface detonating cord and plaster/secondary blasting are avoided

A well confined explosives charge creates pressure waves with frequencies that are predominantly less than 20 Hz, with a relatively small amount of energy having frequencies above 20 Hz. The human ear responds to frequencies above 20 Hz, but filters out frequencies below 20 Hz. Buildings respond predominantly to frequencies in the range 2 to 20 Hz. Community noise measurement for health or environmental purposes uses sound level meters that filter out frequencies below 20 Hz, and record the filtered sound level on a decibel A (or dB(A)) scale. Because air overpressure from blasting consists of frequencies that are substantially below 20 Hz, air over-pressure levels are measured with a meter that measures frequencies in the range 2 to 250 Hz on a decibel (Linear) or dB(Lin) scale.

2.3.1 Air Overpressure

Air overpressure means simply the air pressure over and above that of atmospheric pressure which is always present due to blasting (ISEE Blasters Handbook 1998). In a Quarry blast, the pressure wave that causes air overpressure is generated in part from the detonation of an explosive charge, as well as by the displacement of air as a result of the movement of the rock from the face. The detonation of an explosive charge causes the expanding gaseous reaction to compress the surrounding air and moves it outwards with a high velocity. The shock wave that is produced has a steep shock front which is closely followed by a rapidly decreasing pressure.

The detonation of explosives causes the pressure of the surrounding air to rise instantaneously from an ambient pressure to its peak value (Persson et al. 1994). Once the pressure peaks, it gradually decays back down to the original ambient pressure but then proceeds to decay to a negative pressure value. This negative phase (also known as the suction phase) lasts longer than the positive phase; whilst the

magnitude is not inversely proportional, the total energy of each phase will be equal. Figure 2.1. is an example of the pressure wave's two phases.

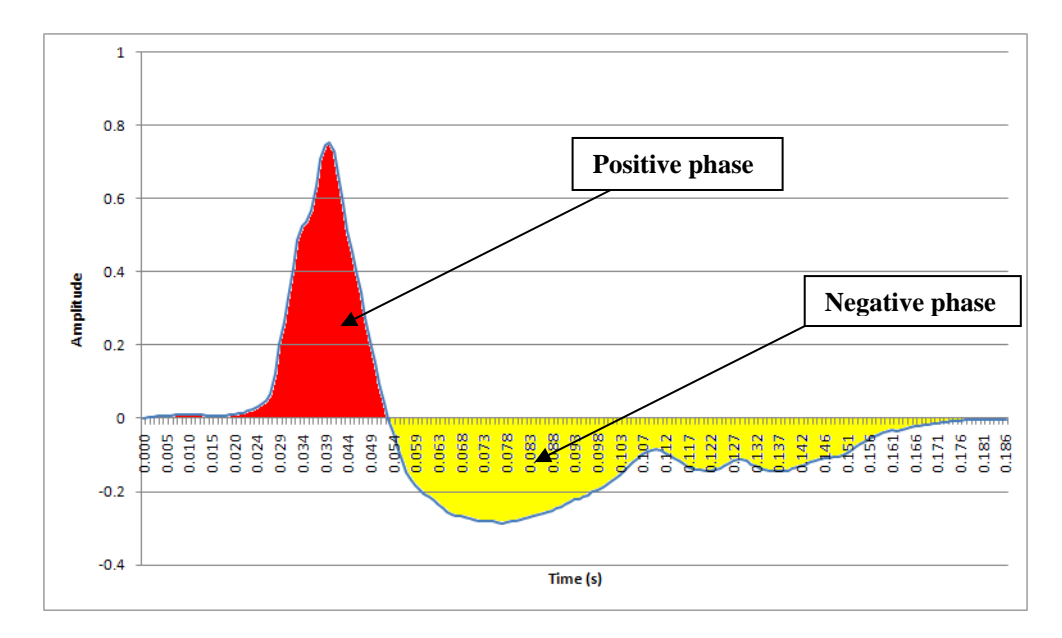


Figure 2.1 Behaviour of an air over pressure pulse from a single event

The pressure wave above was measured from a single hole blast at Newbridge Quarry. The negative phase lasts for approximately three times the duration of the positive phase.

The pressure wave then travels through the air until is eventually dissipates or its path is blocked. The pressure wave's travel is dictated by the temperature of the air, the speed and direction of wind and also the presence of any obstructions e.g. trees, buildings.

Wiss and Linehan (1978) and Siskind et al. (1980) divided the causes of an air blast into several mechanisms.

- 1. Rock pressure pulse
- 2. Air pressure pulse
- 3. Gas release pulse
- 4. Stemming release pulse

Rock pressure pulse is generated by vertical vibrations of the ground. The pulse arrives simultaneously with the ground vibration. The rock pressure pulse is

the first component of the air overpressure reading and is smaller than that of the air pressure pulse and will form the lower bound of the possible blast sound pressure.

Air pressure pulse is produced by direct rock displacement at a blast. The displacement of the rock transmits a pressure pulse into the surrounding air, thus producing an air pressure pulse. The air pressure pulse makes up the second section of the recorded air overpressure reading, after the rock pressure pulse. This is largely due to the lower medium propagation velocity and also has lower frequency content than the rock pressure pulse (Persson et al. 1994). This usually produces the largest amplitudes and so can be controlled by deeper charges or better confinement i.e. more adequate stemming.

The gas release pulse is caused by the escaping of gases from the explosion through fractured material, either inadequate stemming or fractured rock. This pressure pulse controls the height of the individual spikes within the readings. This is measured after the air pressure pulse and is the cause of most disturbances to people.

The stemming release pulse is caused by the escaping gases from the blownout stemming. This is characterised by a high frequency wave which is superimposed on the air pressure pulse.

2.4 Technical information on the various factors that affect the level of air overpressure

Important factors influencing air blast levels are:

- 1. Charge mass and distance from blast.
- 2. Face height and orientation.
- 3. Topographic shielding.
- 4. Stemming height and type.
- 5.Blast hole diameter to burden ratio.
- 6. Burden, spacing, and sequential initiation timing.
- 7. Meteorological conditions.

2.4.1 Charge mass and distance

As a general rule, if other factors are equal, air blast levels increase with increased Charge mass, and decrease as the distance from the blast site increases.

Established scaling methods have been used for many years to determine the relationship between charge mass, distance, and blast vibration levels.

Air vibration levels from quarry blasts have been commonly assessed using the following cube root scaling formula:

$$P = C \left[\frac{D}{W^{1/3}} \right]^{-a}$$

where:

P = pressure (kPa)

W = explosives charge mass per delay (kg)

D = distance from charge (m)

C = site constant

a= site exponent

For unconfined surface charges, in situations which are not affected by meteorology, a good estimate may be obtained by using a site exponent (a) of -1.45, (which corresponds to an attenuation rate of 9 dB(Lin) with doubling of distance), and a site constant (C) of 516.

For confined blast hole charges used in quarrying or construction blasting, the site constant is commonly in the range 10 to 100 (for a site exponent (a) of -1.45). This is equivalent to a site constant in the range 3.15 to 31.5 for a site exponent of -1.2. It should be noted that air vibration is proportional to the cube root of the charge mass. This limits the effectiveness of charge mass reduction as a method of reducing vibration levels; other factors are often more important, especially for confined blast hole charges.

2.4.2 Face height and orientation

When an explosive charge in a vertical hole is fired towards a free vertical face, the resulting air blast levels are greater in front of the face than behind it due to the shielding effect of the face (Moore et al, 1993). They developed an empirical computer-based model to aid in air blast assessment based on elliptical air

overpressure (AOP) contours that are "stretched" in front of the face and generally flattened behind the face.

For design purposes, the size of the elliptical AOP contours can be determined from the inputs: burden, hole diameter and charge mass. The model may also be used for the analysis of air vibration measurements and the assessment of air vibration levels at unmonitored locations.

They determined that for blasts without a vertical free face, or where the air blast emission is predominantly controlled by the stemming height, the AOP contours are circular, the size of which can be determined from the inputs: stemming height, blast hole diameter, and charge mass.

Their model produces decibel contour plans to a scale that can be overlain on aerial photographs, maps, or plans of the area surrounding the blast site.

2.4.3 Stemming height and type

From their experience, good quality crushed rock stemming with a size in the range stemming height of drill cuttings should be used. They found that if stemming height is equal to burden, then aggregate stemming is very effective. A stemming height less than burden may be satisfactory, but stemming heights of less than 0.8 x burden are unlikely to be consistently effective in urban situations. Air blast levels will increase as stemming height is reduced beyond the level necessary to effectively contain the explosive gases during detonation.

An example of the effect of reducing stemming from 3.0 m to 1.6 m is given in Figure 2.2.

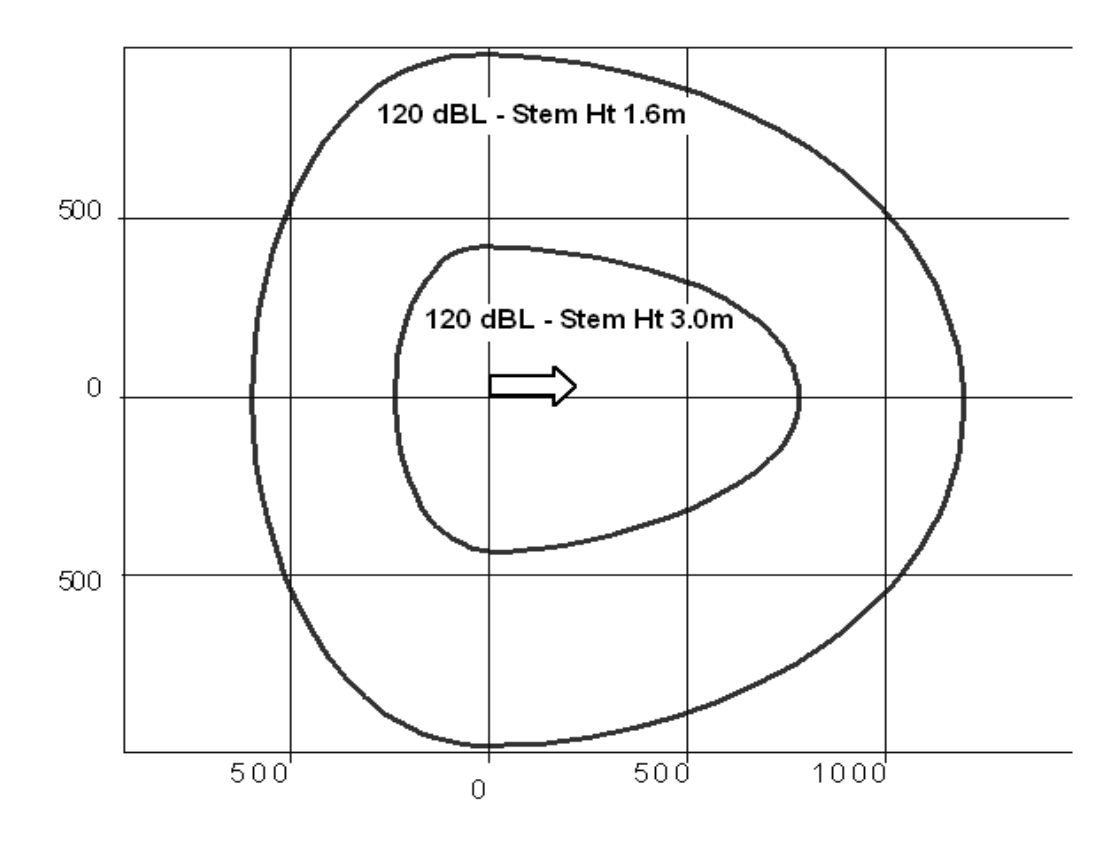


Figure 2.2 120 dB(lin) Contours for Different Stemming Heights on a 500metre x 500 metres grid pattern

2.4.4 Blast hole diameter to burden ratio

The burden of blast holes can have a significant influence on vibration levels. Too much burden may increase ground vibration levels; too little burden in front row holes may result in flyrock and will increase air vibration levels. The effect of burden reduction is illustrated in Figure 2.3, which shows the size and shape of 120 dB(lin) contours when front row burden is changed from 3.6 m to 2.8 m. Blast hole diameter remained constant at 89 mm.

The assessment contours for blasts without wave front reinforcement can be used to determine the effect of changing burden to alter rock pile profile, and to illustrate the effect of reductions in burden due to face irregularities or poor burden control. As blast hole diameter increases, the burden must be increased to prevent excessive air blast and flyrock.

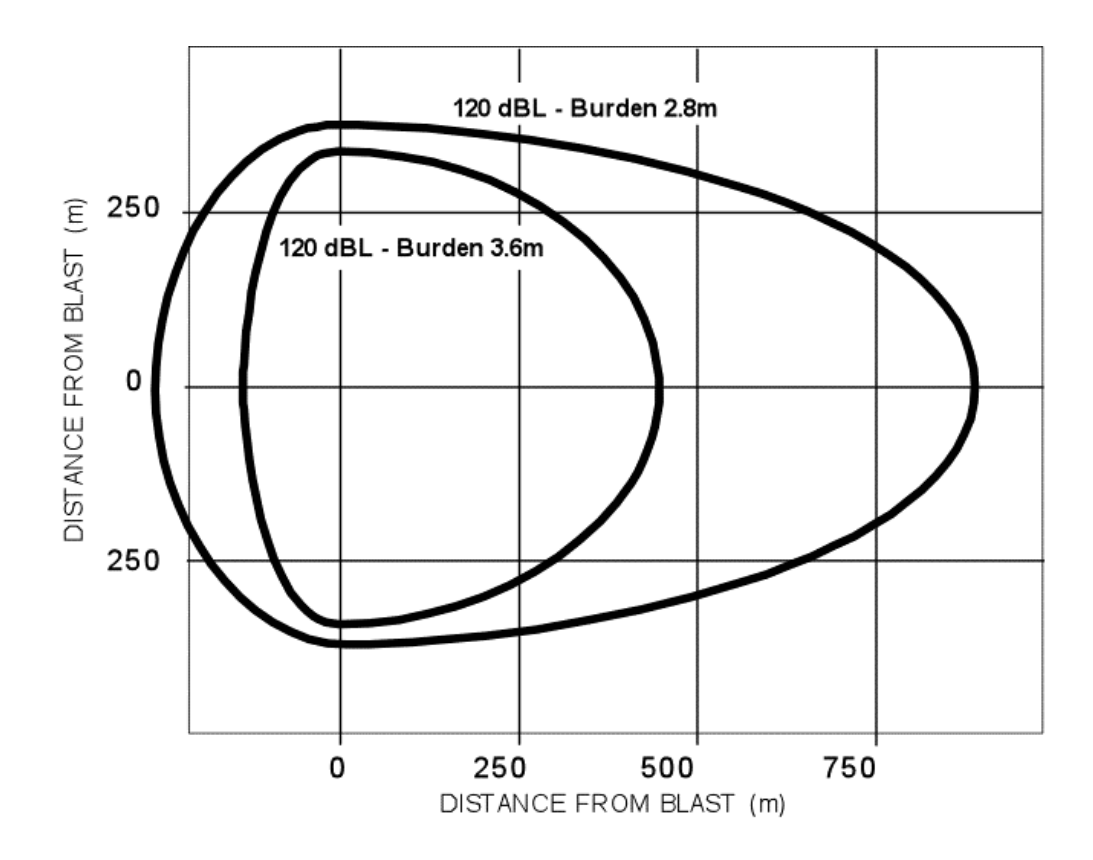


Figure 2.3 120 dB(Lin) Contours for Different Stemming Heights and Burdens

2.4.5 Topographic shielding

In hilly terrain, or deep excavations, air blast levels resulting in the surrounding area are reduced by secondary shielding (Moore et al, 1993). The relationship between shielding, the effective barrier height and the incident angle, has been investigated. These terms are illustrated below (see Figure 2.4).

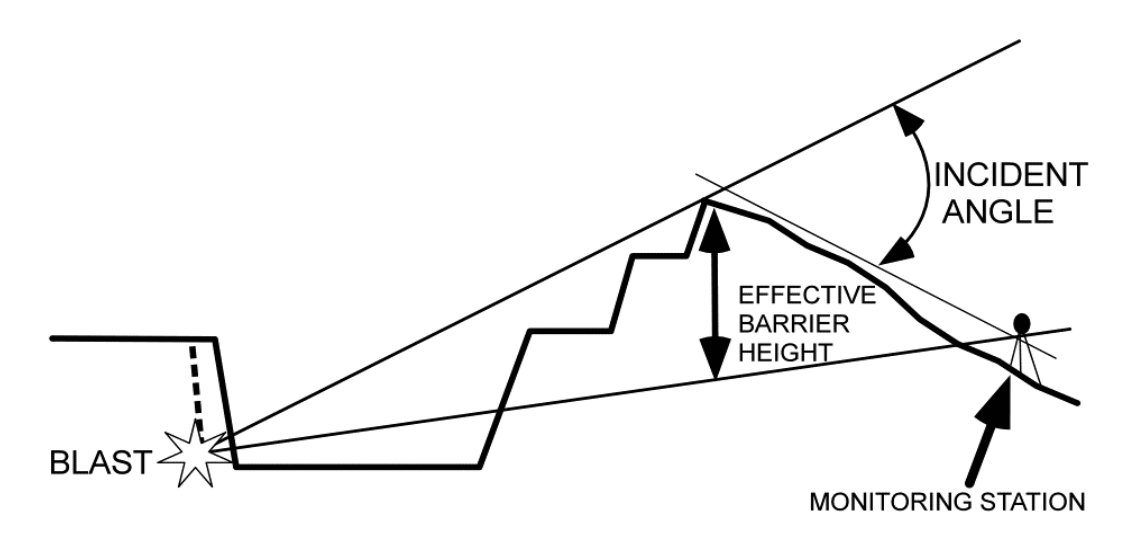


Figure 2.4 The relationship between shielding, the effective barrier height and the incident angle

Analysis of their measurements taken for various shielding situations when blasting in different rock types has permitted a relationship to be developed. The relationship between secondary shielding measured in decibels-linear dB(Lin), barrier height, and incident angle is shown in Figure 2.5 below.

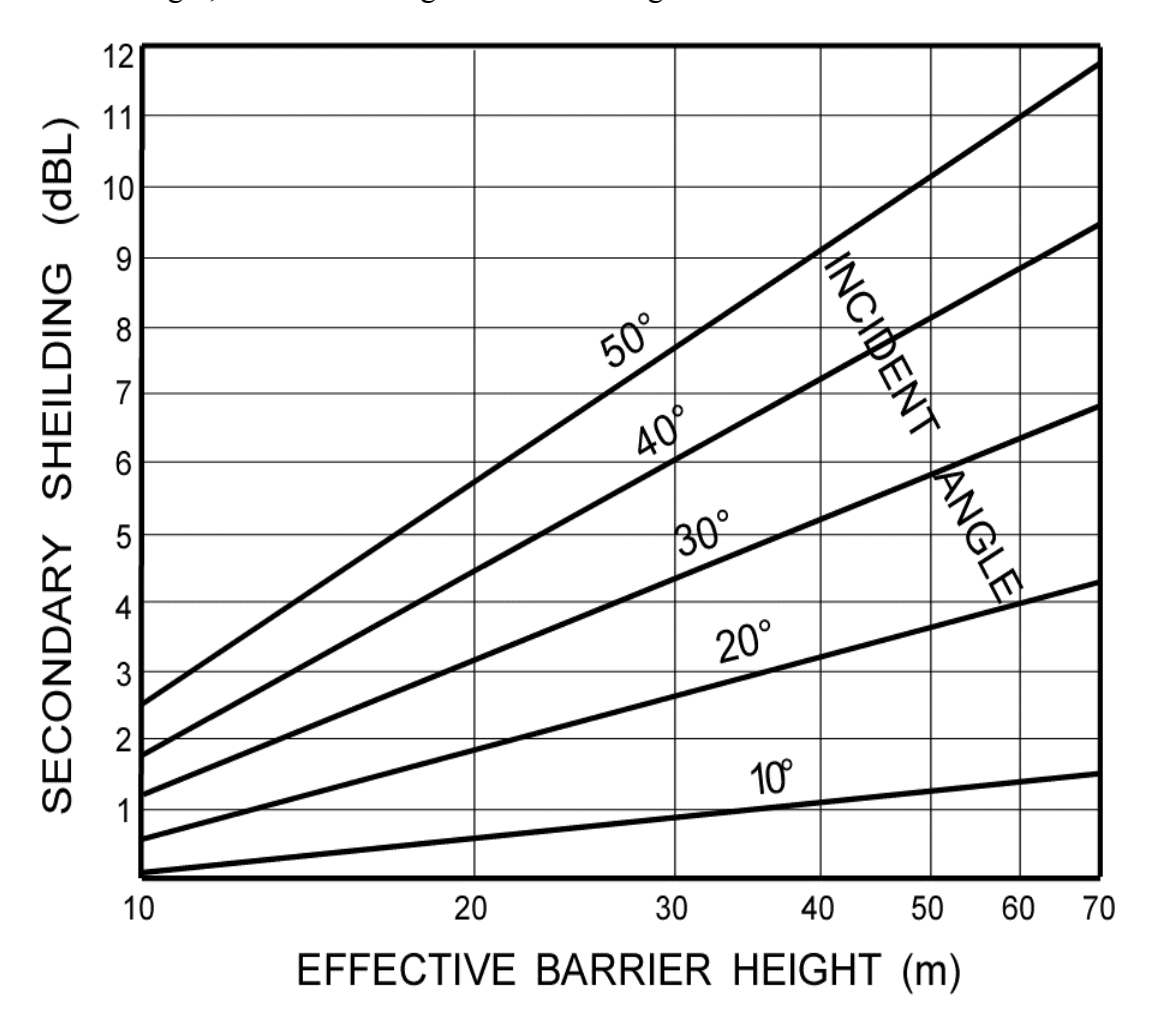


Figure 2.5 The relationship between secondary shielding measured in decibels-linear dB(Lin), barrier height, and incident angle

This relationship permits adjustments to be made to the sound pressure (dB(Lin)) levels determined using the basic air blast contour model to increase its accuracy. In practice, it has been found that the elliptical air blast model works satisfactorily without the need for shielding adjustments when the incident angle between the blast face and the measurement station does not exceed 15 degrees or the effective barrier height is less than 20 m. Topographic shielding can be important in deep excavations or in hilly country.

2.4.6 Wave front reinforcement - the combined effect of burden, spacing and sequential initiation timing

When a single blast hole is fired, a vibration wave front is created which spreads uniformly in all directions at the propagation speed (e.g. 340 m/sec for sound waves). At any period of time after firing, the wave front will have travelled a distance from the blast hole which is proportional to time.

If the distance between blast holes coincides with the distance the wave front has travelled, then reinforcement will occur. For example, if a row of blast holes 3 m apart are fired with a 9 ms delay between them, the resulting wave front diagram is shown in Figure 2.6. This pattern will result in a dramatic increase in air vibration in the direction of initiation. (Richards & Moore, 1995).

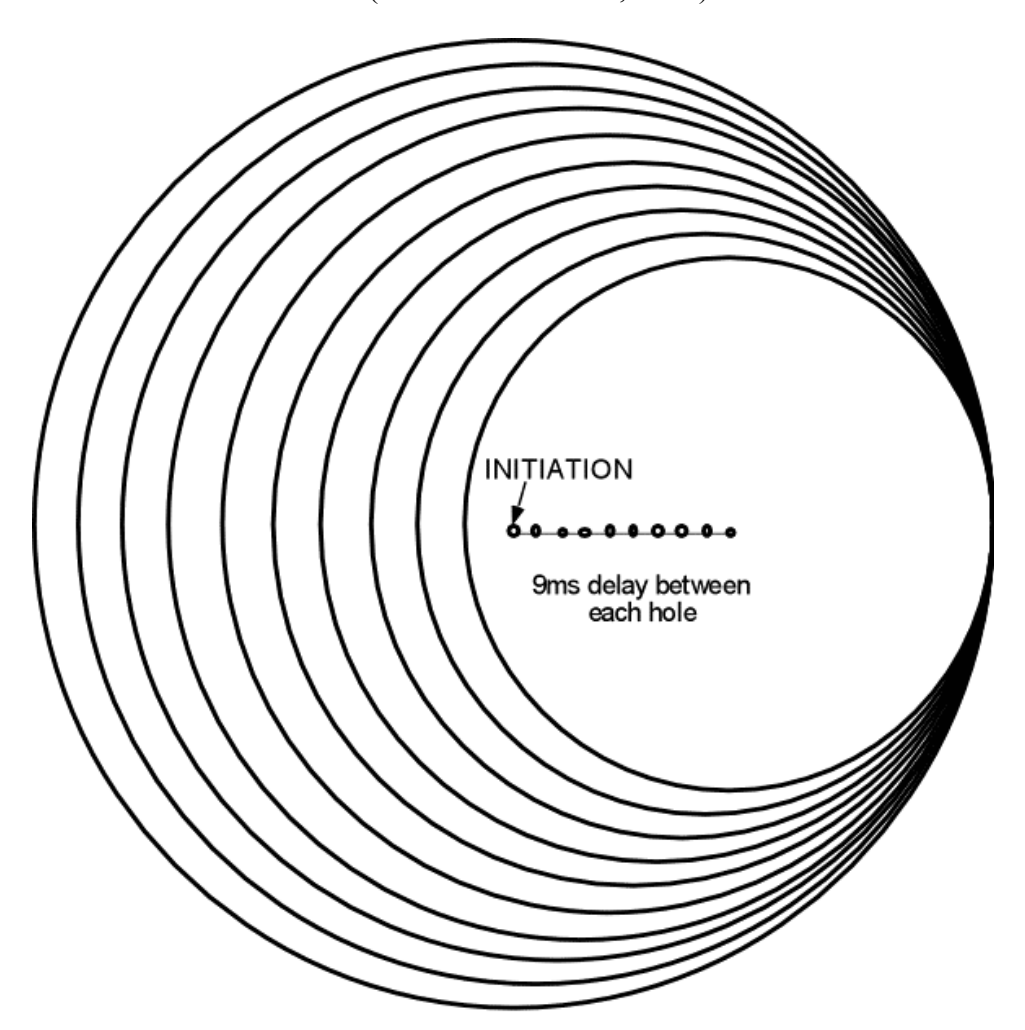


Figure 2.6 resulting air overpressure wave front pattern [spacing 3 metres, spacing delay 9 ms & velocity 340 m/s]

2.4.7 Meteorological conditions

The effect of meteorology on air overpressure levels at close (100 metres) distances is limited to the effect of surface winds, which will cause an increase of up to 2 dB(Lin) downwind from the blast.

The effect of meteorology at distances greater than 500 metres can result in greater increases due to inversions and changes in wind velocity at heights well above the surface. When a blast is fired, the air vibration travels as a wave front outwards from the blast at the speed of sound in all directions. The speed of the wave front is then affected by wind (speed and direction) and by atmospheric temperature. The effect of wind velocity and air temperature can be demonstrated if the wave front is considered as a series of sound "rays" radiating out from the blast and perpendicular to the wave front. Reinforcement occurs when the sound rays are deflected by wind or air temperature variation and are concentrated at the surface as shown in Figure 2.7 below

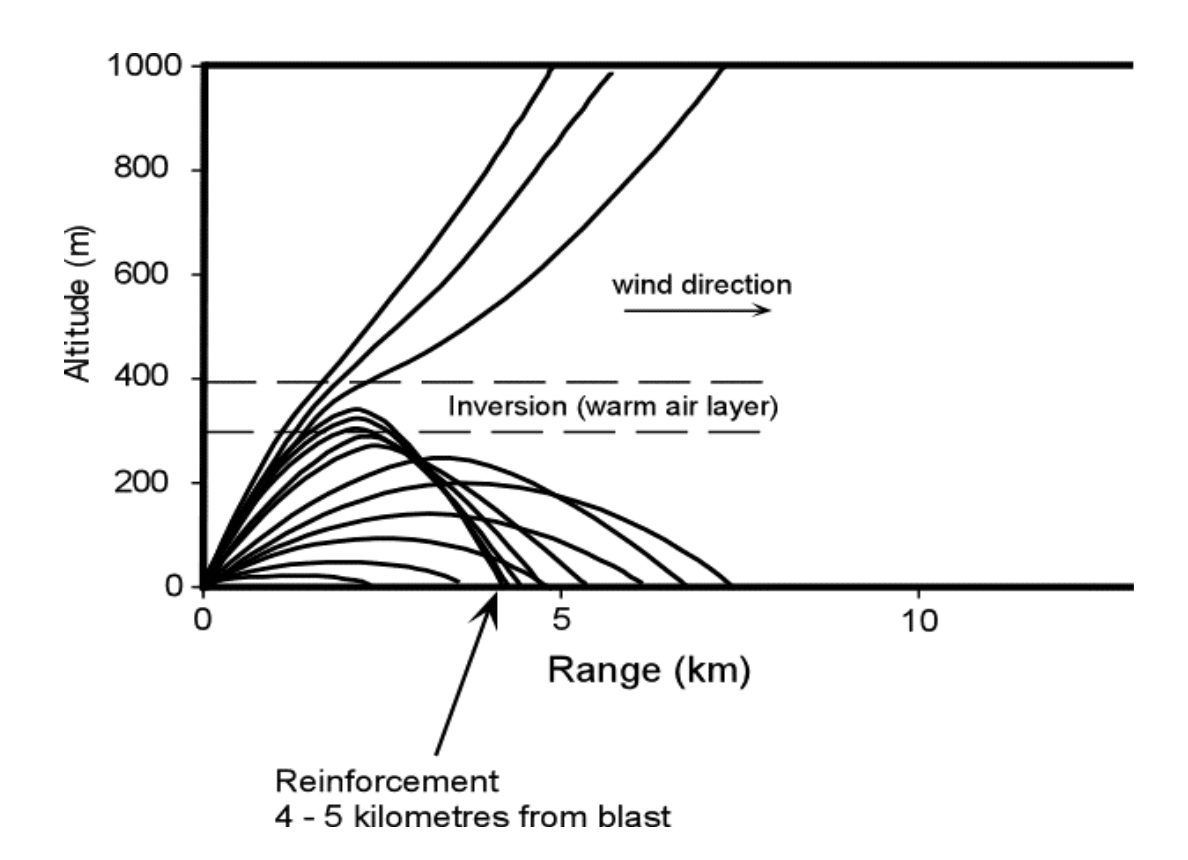


Figure 2.7 example of air overpressure reinforcement due to atmospheric conditions

This results in a higher air vibration level than that resulting from the normal decay rate. Increases of 10-20 dB(Lin) may result from this reinforcement at distances greater than 1 km from the blast site. The significance of this reinforcement for quarry blasts is that blasts which would normally not be noticed due to the reduction in air over-pressure with distance may on occasions result in complaints at distances greater than 1 km from the blast site. It must be borne in mind that this effect is generally restricted to large blasting events under unusual atmospheric conditions and is unlikely to occur as the result of small scale quarry blasting.

2.5 Review of models available for the prediction of air overpressure for initial quarry blast design

2.5.1 Effect of Charge Mass and Distance

Models commonly in use world-wide are cube root scaling models that calculate the effect of charge mass and distance on air overpressure levels.

An example of this model is show below:

$$P = C \left[\frac{D}{W^{1/3}} \right]^{-a}$$

where:

P = pressure (kPa)

W = explosives charge mass per delay (kg)

D = distance from charge (m)

C = site constant

a= site exponent

It is emphasised that air vibration is proportional to the cube root of the charge mass. This limits the effectiveness of charge mass reduction as a method of reducing vibration levels; other factors are often more important, especially for confined blast hole charges.

The site constant in the above formula incorporates the effect of all variables other than charge mass and distance. An improved level of prediction and control is

obtained by the use of empirical models developed by Terrock that in addition to charge mass and distance, make use of additional factors including:

- 1. Face height and orientation.
- 2. Topographic shielding.
- 3. Stemming height and type.
- 4. Blast hole diameter to burden ratio.
- 5. Burden, spacing, and sequential initiation timing.
- 6. Meteorological conditions.

2.5.1.1 Face Height and Orientation

The effect of face height and orientation has been recognised in Hong Kong, and may be quantified by the use of models such as the one described in the preceding section of this report.

2.5.1.2 Topographic Shielding

The effect of topographic and man-made noise barriers in reducing air overpressure is far less than the effect on higher frequency audible noise. The effect of noise barriers on air over-pressure may be determined from the graphical model shown in the preceding section.

The effect of barriers in situations where the incident angle is less than 15 degrees (which covers many United Kingdom blasting situations) is less than 2 dB(Lin).

2.5.1.3 Stemming Height and Type

In blasts where there is no vertical/sub-vertical free face or there is a free face but the stemming practice is inadequate to contain the gas pressure until the face moves, most of the energy of the gases of the explosion is projected through the collar region of the blast hole; they defined this situation as stemming controlled blasts. Stemming controlled blasts may result in cratering or stemming ejection but, in a well managed blast, may only result in general ground swell. All well designed Opencast coal buffer blasts are of this type as long as they only result in a controlled heave of the surface.

The contours of air blast levels from stemming controlled blasts are circular in form because the energy is directed equally in all directions. The air blast levels are a function of charge mass, distance, hole diameter and stemming height, according to the empirical formula:

$$D120 = \sqrt[3]{m.x.} \left[\frac{K_{s.}x.d}{SH} \right]^{2.5}$$

where:

D120 = distance in front of blast to the 120 dB(Lin) contour

d = hole diameter (mm)

SH = stemming height (mm)

m = charge mass/delay (kg)

 $K_s = a$ calibration factor typically varying from 80-180

Circular contours are then drawn based on the D120 calculated and the air blast attenuation rate. Use of the formula requires local calibration by site measurement and serves as an indicator of the effectiveness of the stemming practice and the ability of the shotfiring crew to achieve consistent loading. The limitation of the formula is that as the stemming height is reduced approximately 8 hole diameters for good quality crushed aggregate stemming, the explosion performs as an unconfined charge and the air blast levels are as predicted by Formula 1.

2.5.1.4 Blast hole Diameter to Burden Ratio

Burden controlled blasting occurs when there is a vertical/sub-vertical free face available and the stemming practice (stemming height, stemming material, specification and placement) is adequate to contain the gases of the explosion until the free face begins to move forward. All well designed quarry blasts should be of this type. In these circumstances, most of the energy is emitted through the face and higher air blast levels result in front of the face than in other directions.

Contours of air blast levels from burden controlled blasts are elliptical with air blast commonly measured 6 dB(Lin) to 10 dB(Lin) higher in front of the face than

behind the face. From analysis of field measurements over many years, we have found that the air blast levels in front of the face are a function of charge mass, distance, hole diameter and burden, according to the empirical formula:

$$D120 = \sqrt[3]{m.x.} \left[\frac{K_{b.}x.d}{B} \right]^{2.5}$$

where:

D120 = distance in front of blast to the 120 dB(Lin) contour

d = hole diameter (mm)

B = burden (mm) actual burden for analysis or design burden for prediction

m = charge mass/delay (kg)

 $K_b = a$ calibration factor typically varying between 150-250

The formula requires local calibration by site measurement and serves as an indicator of the ability of the shotfiring/survey crew to measure burden and compensate for under-burdening during loading. The highest k value of 250 gives a more conservative prediction for 'average' face control. Elliptical contours are then drawn based on the D120 calculated and the air blast attenuation rate.

This formula has been proven useful for back calculating effective burdens from blasts where face burst was observed and high air blast levels measured. The limitation of the formula is that, as the actual burden is reduced to approximately 17 hole diameters, the explosion acts as an unconfined charge and the air blast levels can be predicted from Formula 1.

2.5.1.5 Burden, Spacing, and Sequential Initiation Timing

The combined effect of burden, spacing, and sequential initiation timing may be determined by wave front models that produce outputs of the type shown in the preceding section.

2.5.1.6 Meteorological Conditions

In most United Kingdom quarry blasting situations, the effect of meteorological conditions is limited to an increase in air overpressure levels of 1-2 dB(Lin) downwind, and the use of meteorological atmospheric refraction models is not warranted.

2.6 Good Practice for minimising air overpressure

Overpressure can be minimised at source, but the debate continues amongst experts as to whether it is practicable to use planning controls to monitor and enforce limits in view of the fluctuations caused by varying weather conditions. Good quarry.com has defined a number of actions that can be taken at the blast planning stage that can be used to help minimise the air overpressure at source and these are listed below.

Avoid using surface detonating cord and, if it has to be used, cover it adequately.

Avoid using plaster blasting; this is not prohibited by the Health & Safety Executive but is discouraged due to the unacceptable risk of flyrock. Secondary blasting has now largely been replaced by mechanical methods.

Reduce the surface area subject to heave.

Reduce the degree of surface heave by minimising the total charge and using a low charge weight per delay.

Use an appropriate sequence of detonation and consider the orientation of the working face in relation to sensitive areas; if the direction of blast initiation is away from or at right angles to, rather than towards a sensitive location, then reductions of 10- 15dB and 6dB respectively may be possible

Avoid gas venting through local rock weaknesses (also a cause of flyrock) by accurate drilling and placement, and regular face surveys, ensuring that the trace velocity between holes is significantly less than the speed of sound, i.e. the delay between holes is more than 5 ms/m; this will avoid air-blasts from individual holes reinforcing each other.

Avoid resonance with floors, which can increase the acoustic response (shaking and rattling) of nearby buildings, by using delays of less than 25-40ms.

Avoid blasting in adverse weather conditions which include:

- significant temperature inversions,
- moderate to strong winds towards sensitive areas,
- · foggy, hazy or smoky conditions with little or no wind,
- a still cloudy days with a low cloud ceiling,
- periods when the surface temperature is falling in the middle of the day,
- periods when strong winds accompany the passage of a cold front,
- before mid-morning or after sunset on clear calm days.

Clearly it would be advantageous to be able to predict the effects of the weather on overpressure in a quantified way. The Meteorological Office has a computer programme which can predict the propagation of overpressure but sufficient local weather information to use it is unlikely to be available; to use the programme effectively needs the use of radio-sonde balloons.

2.7 Measurement of air overpressure

Air overpressure can be measured in any unit which measures pressure. The commonest and preferred unit are Pascals (Pa), which is the derived international SI unit of pressure (N/m² or SI base unit = $m^{-1} \cdot kg \cdot s^{-2}$). It is also reported as decibels (dB), which strictly speaking is not a direct measurement of pressure but is a logarithmic scale using the ratio of the recorded pressure to a reference pressure. This has a reference value of ($P_0 = 2 \times 10^{-5} P_0$) and is given as dB (Lin) = 20 $\log_{10}(P/P_0)$ where P is the pressure in Pascals. Unlike noise measurements, there is no weighting applied to the value in decibels and so the unit is sometimes given as dB (Lin) although this is often abbreviated to dB. A strictly definition should also give the frequency above which it is linear (e.g. 2Hz). In the interest of standardisation it recommended that all overpressure measurements should be in Pascals and reported in Pascals

2.8 Conclusions

Moore & Richards have built on earlier work by the U.S. Bureaux of Mines to derive a series of relationships between Maximum Instantaneous Charge Weight, Distance and Burden to predict likely Air Overpressure levels from quarry type blasts.

They have also indicated that the directionality of the borehole initiation sequence in combination with the inter-hole delay period could be important, as it may result in constructive interference between successive holes being fired such as to significantly increase the resulting maximum air overpressure values.

Meteorological conditions can be important, but it must be borne in mind that effect of "focusing of air overpressure pulses" is generally restricted to large blasting events under unusual atmospheric conditions and is unlikely to occur as the result of small scale quarry blasting.

Many instances of high air overpressure readings from a blast can be attributed to poor blasting practice. Goodquarry.com has defined a number of actions that can be taken at the blast planning stage that can be used to help minimise the air overpressure at source.

In the interest of standardisation it recommended that all overpressure measurements should be in Pascals and reported in Pascals.

Chapter 3

Preliminary Investigation into the relationship between air overpressure and face velocity at Newbridge Quarry

3.1 Introduction

The aim of this investigation is to provide an insight into the origins of air overpressure and to establish whether it has a direct relationship with the face velocities produced from a quarry blast. In order to determine whether a relationship between the two exists, twelve quarry blasts were conducted at two limestone quarries in England, UK. These quarries were Newbridge Quarry in North Yorkshire and Whitwell Quarry in Derbyshire.

The air overpressure produced from each blast was monitored at several locations, and video footage of every blast was recorded. The video recordings of each blast were then analysed by using a computer software program - "Front Calc" which measures the velocities of the rock as it is blasted from the face.

Blasts conducted at two limestone quarries in the United Kingdom were monitored for air overpressure and at the same time a video recording was made of each of the blasts. The blasts monitored at Newbridge Quarry, North Yorkshire, varied in size. The number a number of holes per blast ranging from 10 - 15, all of which were triple decked. At Whitwell Quarry, Derbyshire, the blasts had either 6 or 7 holes which were all single decked.

Seismographs were set up around the blast; these were each equipped with a low frequency microphone in order for them to accurately record the pressure waves produced from the blast. For each blast, at least one seismograph was placed directly in front of the face and one behind the blast. On some occasions an extra seismograph was placed in front, behind or to the side of the blast. It was important to record the air overpressure levels at different locations in relation to the blast so that the nature of the air overpressure pulse produced can be analysed more effectively. This allowed for comparison of pressure levels recorded in front and behind the blast and to determine why they differed. Figure 2 shows a seismograph equipped with a low frequency microphone in position and ready to record the air

overpressure in front of a blast at Whitwell Quarry. Throughout the investigation, proprietary seismographs from a leading equipment manufacturer were used.

It is important for the microphone to be in direct view of the blast, so that the peak air overpressure level is recorded. If it is not in direct view, then the pressure waves that are recorded will have become attenuated as they bend or refract around obstacles.

In order to be able to calculate the face velocities produced during a blast, the blast was recorded by a video camera. Once a blast is recorded, the video footage allows for the face velocities to be calculated using the "Front Calc" computer software program. The camera must be in a position where its angle to the face does not exceed 45° otherwise the accuracy of face velocity calculations is severely reduced.

The recorded footage of the blasts also allows for any atypical occurrences during a blast to be critically analysed so as to ascertain whether they have an impact on either the air overpressure produced or the face velocities. Such occurrences can be gas venting through the face or venting through the stemming.

The air overpressure levels recorded are stored in the seismographs and the data can then be downloaded onto a computer where it can be accessed by the Seismograph Data Analysis (SDA) software program. Each set of air overpressure data recorded by each of the seismographs located around the blasts were exported from SDA to Microsoft Excel where the air overpressure values and traces were analysed in more detail.

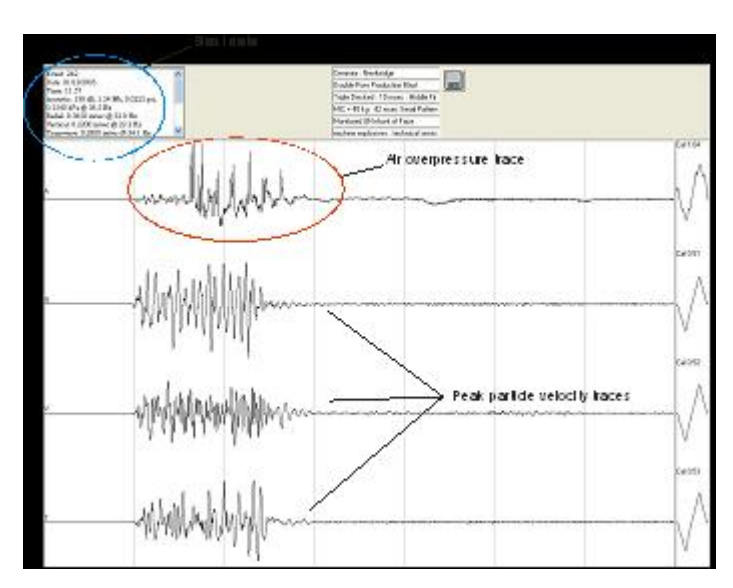


Figure 3.1 Data processed in SDA

Figure 3.1 is a screen shot of the SDA program once a .dtb file has been opened. The traces of the air overpressure can be previewed in the program along with all three peak particle velocity traces. Information of the blast can also be accessed. This includes; the peak values of each of the traces, trigger levels and duration of the recorded data [in this case three seconds].

The data can then be exported into Microsoft Excel. The air overpressure data was exported in four units; decibels (dB), millibars (Mb), pounds per square inch (psi) and kilopascals (kPa). Throughout this investigation, the air overpressure levels were analysed in kilopascals. The sample time is also included in the exported data. This represents the time intervals at which the pressure values are recorded once the seismograph has been triggered.

Once in Microsoft Excel, the data was plotted to produce a trace of the air overpressure similar to that seen in SDA (shown in Figure 3.2).

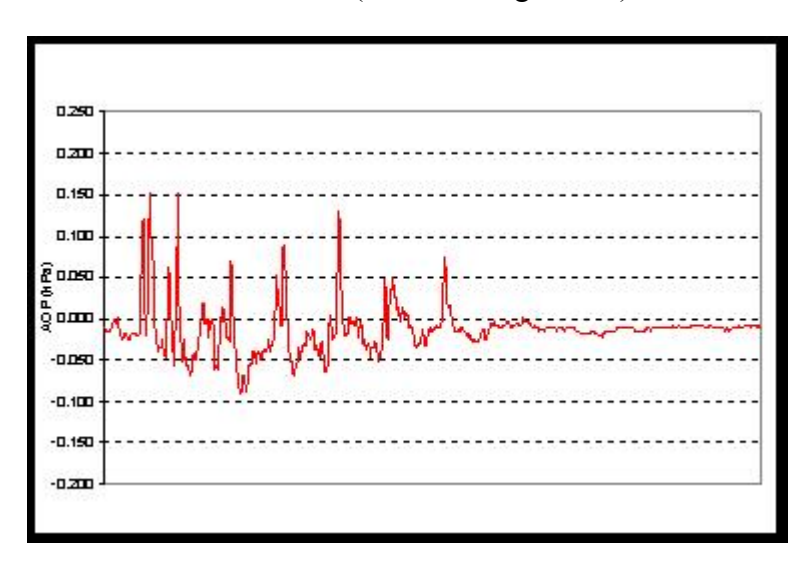


Figure 3.2 Air overpressure trace plotted in Microsoft Excel

3.2 Front Calc Software

Front Calc measures the face velocities of specific points on the face which are defined by the user, so for example if the user was interested in the face velocities produced from a particular hole in a blast, then a vertical line of points can be added to the video or photo clips over the quarry face in front of the blast hole. The points are individually attached to a specific section of the face. Figure 3.3 shows an

example of a line of points that have been inserted on the quarry face in front of the first hole of a blast.



Figure 3.3 Inserting points to monitor face velocities from a particular hole.

Once the points are inserted and the video/picture sequence is played, Front Calc tracks the movement of the face, by tracking the movement of the points which are of interest. This is illustrated in Figure 3.4. The white lines extending from each point, trace the movement of the face with respect to time of a number of particular points.

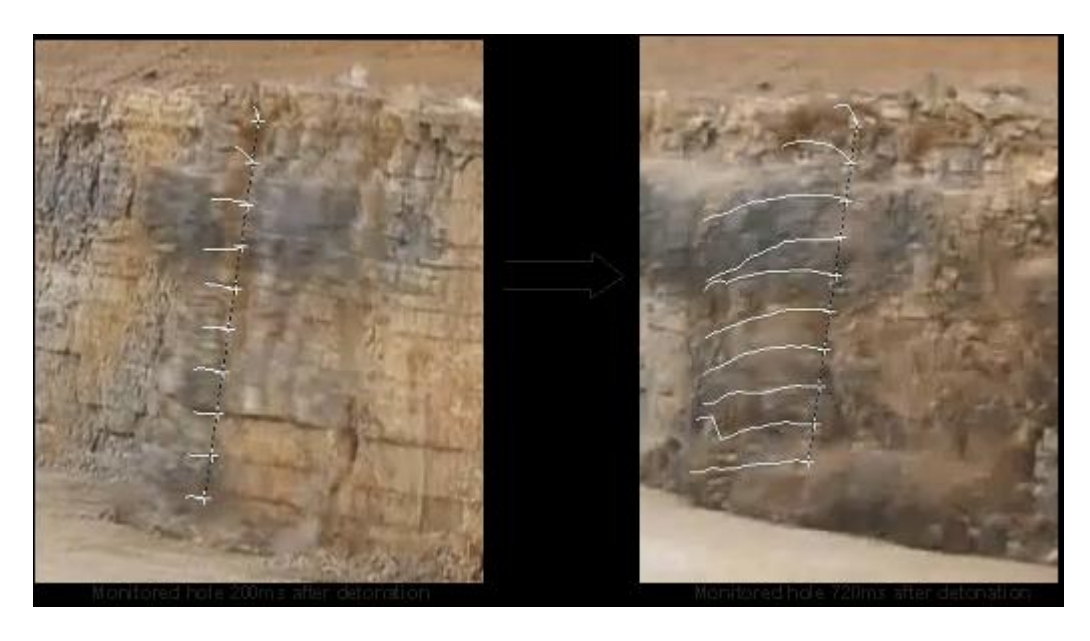


Figure 3.4 Tracing of points in Front Calc.

To collect the velocities produced from the blast, the global movement data with values recorded in (m/s) were exported in a text file and then opened up within Microsoft Excel. The results provide the velocities measured at each assigned point of every frame in the video, [i.e. in this case velocities values every 40 milliseconds]. To ensure an accurate velocity is acquired which reflects the action that the blast has on the rock, velocities at each point were recorded for the first five frames after the initial movement of the rock. By experimentation it was found that the initial movement of the rock has a greater significance in its relation with the peak air overpressure recorded. Velocities after that were reflecting the loss momentum of the rock as it is in free fall.

Using the velocities derived from the first five frames of the video, their maximum and average velocities were calculated, along with the maximum and average velocities for all the points along the whole face. For any given blast hole, this will provide the maximum face velocity and also the average face velocity. This was then compared with the peak air overpressure from that hole. For the triple deck blasts, the peak air overpressures of each deck were compared to the maximum and average face velocities of each deck.

3.3 Results

Peak air overpressure recordings from in front and behind each blast were then correlated with average and maximum face velocities. The recorded video footage was used to identify the causes for any anomalous results such as gas venting through the face. Where these anomalous results occurred and the cause of them was able to identified, it was considered justifiable to remove them from all statistical analysis.

The air overpressure data for each blast was analysed in the form of an air overpressure trace (as shown in Figure 3.5). This enabled easier analysis of the air overpressure results as each air overpressure level from each blast hole can be seen and in many cases the air overpressure from each deck within a blast hole was also visible.

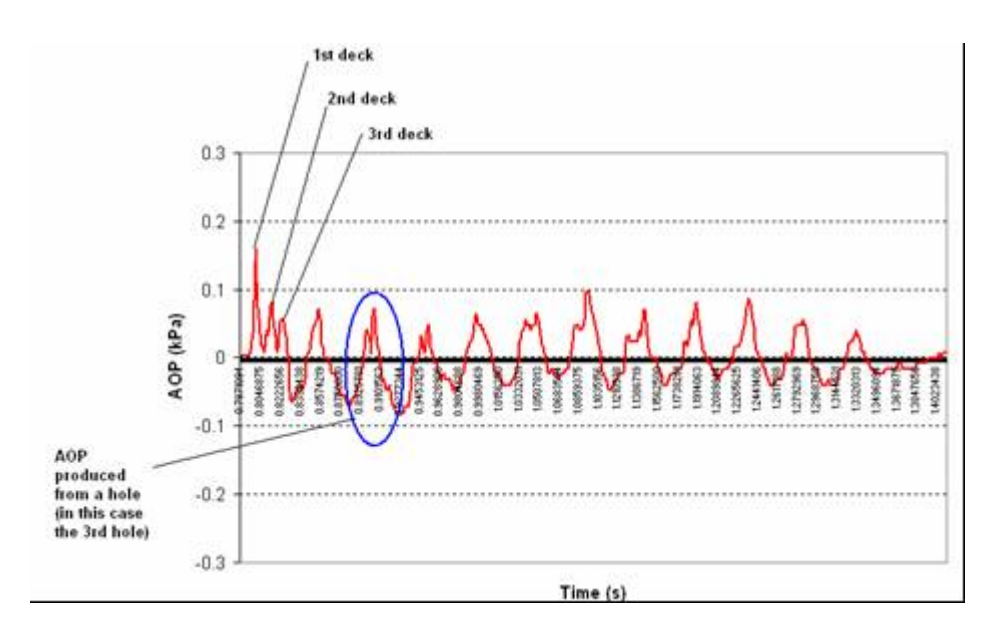


Figure 3.5 Example air overpressure trace

Figure 3.5 shows a typical air overpressure trace, each peak, like the one highlighted by the blue ring, represents the air overpressure produced from a single hole. In some cases, individual peaks can be distinguished within one of these peaks, as shown in the beginning of the trace. Each of these peaks represents an individual deck within that hole. Therefore by examining the Figure 3.5 in detail, we know that the blast consisted of twelve holes and that each hole consists of three decks. The air overpressure is measured in kilopascals and is plotted against time. The time distance between each peak represents a combination of the delay time between each hole and the travel time from the quarry face in front of a given blast hole to the monitoring location.

3.3.1 Relationship between Air Overpressure & Face Velocities

A large quantity of data has been correlated in order to determine whether a relationship exists between the peak air overpressure and face velocities (maximum and average).

Statistical analysis has been conducted on the air overpressure and face velocity of;

- 1. Each blast hole of every blast monitored
- 2. The first blast hole of every monitored blast

Data from three blasts at Whitwell Quarry have been excluded from the analysis due to inaccurate face velocity results. Unfortunately, the video camera at

these blasts had been positioned at angles greater than 70° to the quarry face, which as explained earlier, was found to greatly affect the accuracy of the calculated velocity of the rock which were being tracked by the "Front Calc" software programme.

The peak air overpressure and the face velocity of each hole in every monitored blast (excluding three blasts at Whitwell as explained above) was then correlated and the data indicated that no correlation exists with either maximum or average face velocity (see Figure 3.6).

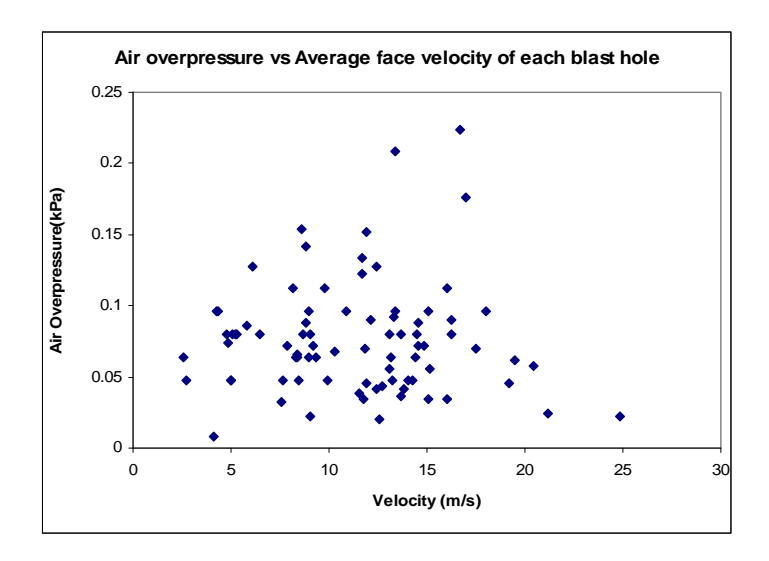
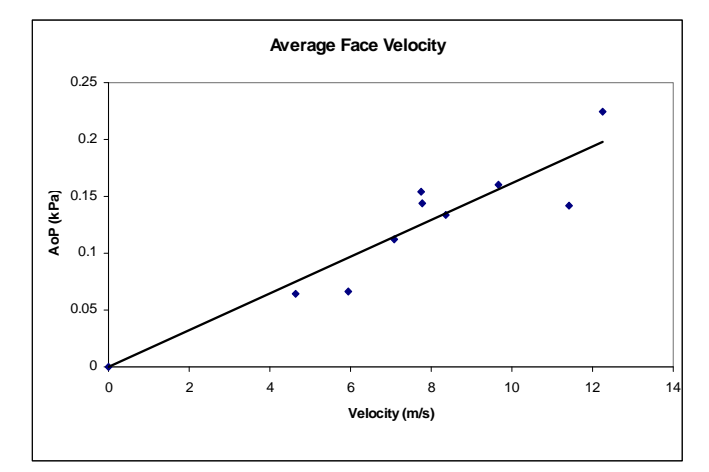


Figure 3.6 Correlation of peak air overpressure and average face velocity of each blast hole monitored.

In Figure 3.6 the average face velocity for each hole is plotted against the air overpressure. From inspection it appears that there is no causal relationship, which was also confirmed by an indicative statistical assessment as being poor. [The limited amount of space precludes the presentation of a data table for this graph]. The reason for this is considered to be the successive superimposition of the pressure waves from adjacent holes. As explained earlier, a pressure wave consists of a positive and a negative phase, with the negative phase lasting up to three times longer than the positive phase. For blast holes which are detonated later in the blasting sequence, the positive phase of their pressure wave is superimpose onto the negative phase of the previous hole(s) and so reducing the amplitude of the wave. As a result of this, the magnitude of the air overpressure with respects to the ambient air pressure appears to be lower.

Due to this 'interaction' between the blast holes, it was decided to correlate the peak air overpressure and face velocities only of the first blast hole of each blast so that none of the air overpressures values recorded could be affected by the air overpressure of an adjacent blast hole. The face velocities were then recalculated for each of the first holes. To gain more accurate velocities along the whole length of the hole, the "Front Calc" software programme was used in such a way that all ten points were placed along the quarry face in front of the first hole so that velocities at ten different points on the line of the hole were calculated. Thus a more accurate average face velocity was able to be determined.

Figure 3.7 below, shows the correlation of the peak air overpressure against average face velocities for only the first hole in each blast.



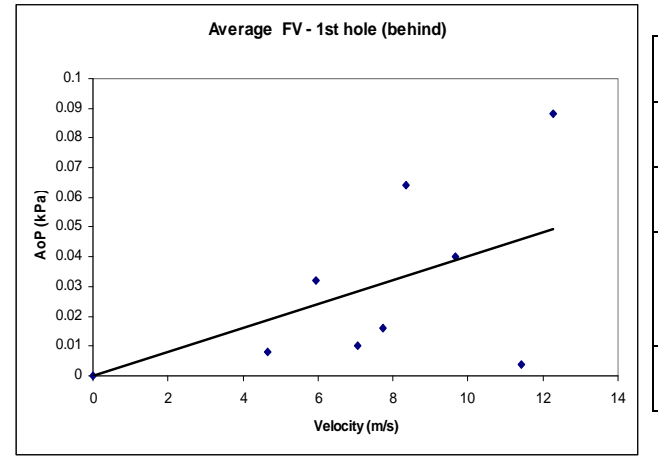
Regression Statistics			
Multiple R	0.9319518		
	0.86853415		
R Square	8		
Adjusted R	0.85210092		
Square	7		
Observations	10		

Figure 3.7 Peak air overpressure (in front of the blast) plotted against average face velocity (1st hole only).

The average face velocities provide a closer correlation with the air overpressure when compared to the maximum face velocities. This was found to be so for both the first blast holes in un-decked holes and the first deck in multi-decked. The reason for this is thought to be that the maximum face velocities values derived may have originated from limitations inherent in the "Front Calc" program. For example, the program may have lost track of the face where venting occurred which can result in dust obscuring the face and so the program may have inadvertently begun tracking the dust which will lead to a higher velocity. Ultimately, the maximum velocities are the result of one point in a line of ten points along the hole and so an error from Front Calc that results in an abnormally high velocity will

provide inconsistent results. However calculating the average velocities used data from all points being tracked. This means that if the program began tracing a cloud of dust, the effect will be minimised by the other nine points and therefore a more accurate representation of the face velocity due the detonation of the blast hole may be attained.

From the statistical analysis in Figure 3.7, it is clear that the peak air overpressure of the first blast hole has a positive linear relationship with average face velocity. However it is not known whether the face velocities will be a contributable factor to the air overpressure produced behind the blast. Figure 3.8 shows the correlation of average face velocity and peak air overpressure of each first hole of every blast.



Regression Statistics			
Multiple R	0.5736		
R Square	0.3290		
Adjusted R			
Square	0.2331		
Observations	9		

Figure 3.8 Peak air overpressure (at the rear of the Blast) plotted against average face velocity (1st hole only).

With the R square value as low as 0.329, it can then be concluded that the face velocities (average and maximum) does not directly affect the air overpressure that is produced behind a blast and that there is no clearly definable relationship between the two. The reason for this may well be that the energy created from the detonation of the explosives is utilised in fragmenting the rock and 'throwing' the rock out of the face at a given velocity. Therefore the velocity at which the rock is thrown is the face velocity. The displacement of air that results from the movement of a large volume of rock creates the air overpressure which travels almost perpendicularly away from the face. This forms the air overpressure that is monitored in front of

- 58 -

each blast. Therefore, the air overpressure which is recorded behind the blast is a result of the movement of rock on the top surface of the face and hence the velocity

of the rock from the face has little bearing on it.

Up to this point, the air overpressure has not been analysed in relation to the distance at which they were recorded from the blast. In light of this it was thought logical that the peak air overpressures levels should be related to the distance from the blast to the monitoring location. This was then carried out on the peak air overpressures monitored from the first blast holes only, as it had already been established that a relationship between face velocities and peak air overpressure values existed. The "scaled air overpressure" was then correlated with the face velocities of the first blast holes. This was carried out for air overpressures measured

The scaled air overpressure in front of the blast has been calculated by using the equation below. In this case the source of air overpressure in front of the face is

considered to be a line source.

both in front and behind each blast.

Air overpressure / Distance

The scaled air overpressure behind the blasts is calculated differently as the source of the air overpressure is the top of the blast holes and as such is treated as a point source. The equation below is used when assuming a point source.

Air overpressure / Distance²

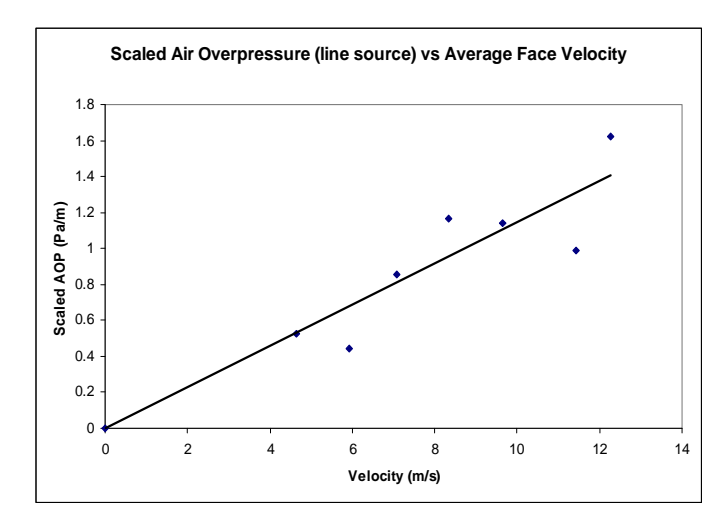
The distance of the seismograph from the face is used in these calculations.

Table 3.1 below lists the peak air overpressure and face velocities of each blast monitored along with the distance at which the air overpressure was recorded and the scaled air overpressure.

	Peak Air Overpressure (Pascals)	Peak Face Velocity - m/s	Average Face Velocity - m/s	Distance (metres)	Scaled Air Overpressure
Blast	(Lbs/sq.foot)	(feet/sec)	(feet/sec)	(feet)	(Pa/m)
Newbridge					
	160	12.131	9.66	140	1.1429
09/09/2005	(3.34)	(40.00)	(31.69)	(459)	
	66	15.176	5.936	148	0.4459
22/09/2005	(1.38)	(49.79)	(19.48)	(486)	
	224	27.54	12.26	138	1.6232
22/11/2005	(4.68)	(90.34)	(40.22)	(453)	
	134	15.845	8.35	115	1.1652
05/07/2005	(2.80)	(51.98)	(27.40)	(377)	
	142	12.621	11.42	144	0.9861
16/02/2006	(2.96)	(41.41)	(37.47)	(472)	
	112	10.106	7.07	131	0.8550
16/08/2005	(2.34)	(33.16)	(23.20)	(430)	
	64	6.413	4.647	121	0.5289
25/08/2005	(1.34)	(21.04)	(15.25)	(397)	
	154	22.377	7.74	38	4.0526
01/12/2005	(3.22)	(73.42)	(25.39)	(125)	
Whitwell					
	144	11.834	7.79	60.2	2.3920
15/11/2006	(3.01)	(38.79)	(25.56)	(197)	
	207	6.46	4.77	54.3	3.8122
29/11/2006	(4.32)	(21.19)	(15.65)	(178)	
	200	5.297	3.22	49.6	4.0323
05/01/2007	(4.18)	(17.38)	(10.56)	(163)	

Table 3.1 Measured data from each blast including the scaled air overpressure

The scaled air overpressures from the Whitwell blasts are much higher than the scaled air overpressure from the Newbridge blasts. The reason for this is that, although the seismographs were positioned much closer to the blast at Whitwell than when monitoring at Newbridge, the air overpressure levels recorded were approximately the same if not slightly higher than the average Newbridge blast. Due to the difficulty in correctly locating the camera and thus the resulting inaccurate face velocities calculated from the blasts at Whitwell Quarry, they have been excluded from the analysis.



Regression Statistics			
	0.92705		
Multiple R	7161		
	0.85943		
R Square	4979		
Adjusted R	0.83600		
Square	7476		
Observations	8		

Figure 3.9 Scaled air overpressure vs. average face velocity in front of the blast

The R Square value of 0.859 shows that the scaled air overpressure appears to correlates well with the average face velocity. This indicates that the velocity of the rock as it leaves the face appears to greatly influence the air overpressure. Figure 3.9 illustrates that the greater the face velocity, the greater the air overpressure produced per metre which will ultimately result in larger air overpressure levels at longer distances from the blast.

The scaled air overpressure was also calculated behind the blasts however, only the blasts at Newbridge Quarry have been used because the air overpressure monitoring behind the blasts at Whitwell Quarry was not possible due to site constraints. Table 3.2 lists the data measured at the blasts at Newbridge Quarry. The scaled air overpressure is also included.

Blast	Air Overpressure (Pa) (Lbs/sq/foot)	Peak Face Velocity (m/s)	Average Face Velocity (m/s)	Distance (m)	Scaled Air Overpressure (Pa/m²)
	42	12.131	9.66	62	0.0109
09/09/2005	(0.88)	(40.00)	(31.69)	(203)	
	40	15.176	5.936	35	0.0327
22/09/2005	(0.84)	(49.79)	(19.48)	(115)	
	88	27.54	12.26	58	0.0262
22/11/2005	(1.84)	(90.34)	(40.22)	(190)	
	80	15.845	8.35	12.8	0.4883
05/07/2005	(1.67)	(51.98)	(27.40)	(50)	
	16	12.621	11.42	30	0.0178
16/02/2006	(0.33)	(41.41)	(37.47)	(98)	
	20	10.106	7.07	48	0.0087
16/08/2005	(0.42)	(33.16)	(23.20)	(157)	
	12	6.413	4.647	154	0.0005
25/08/2005	(0.25)	(21.04)	(15.25)	(505)	

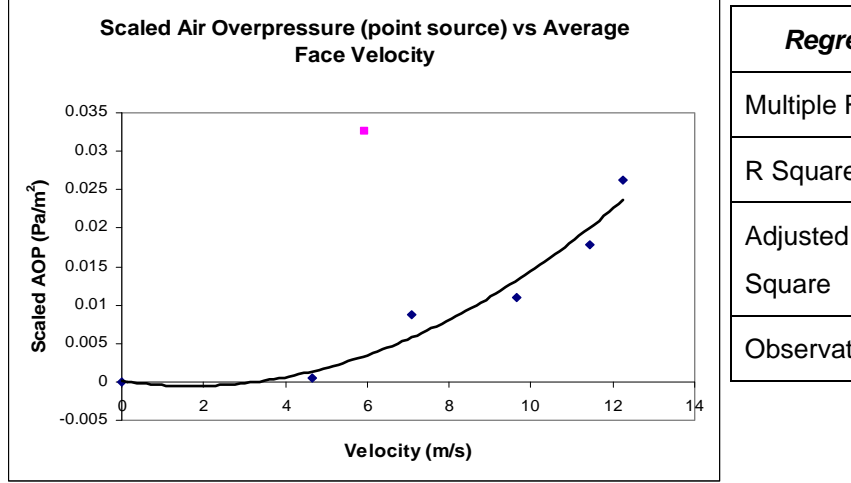
Table 3.2 Air overpressure recorded behind each blast and the corresponding scaled

The air overpressure monitored behind the blast at Newbridge Quarry, 05/07/05 was recorded only 12.8m from the blast. This distance is extremely close to the blast but does not record an abnormally high air overpressure level. As a result of this, the scaled air overpressure is very high in contrast to scaled air overpressures from the other blasts monitored. Therefore the blast has been excluded from the analysis as it is not known why the air overpressure is so low considering the short distance from the blast. There may have been an error when recording the G.P.S. co-

ordinates of the seismograph or the low frequency microphone attached, may have been obstructed from the blast.

Figure 3.10 appears to show that a good correlation exists between the average face velocity and the scaled air overpressure behind the blasts when treating this as a point source. Clearly the data set was in reality too small to allow any significant conclusions to be drawn. However, it does indicate that this could well be a profitable area for future research. The pink data point represents the blast conducted on 22/09/05 which produced a very low level of air overpressure at a very short distance which for reason stated above has not been included within the regression analysis.

It must however be borne in mind that this is only a pilot study and that the number of observation points considered unfortunately was very small. Thus the apparent relationship between air overpressure and face velocity should be considered as indicative rather than definitive. Therefore whilst a trend is apparent, it is too soon to attempt to derive a relationship that directly relates: the face velocity of the first hole/charge, distance (source to monitoring location) and air overpressure, in terms of magnitude. This hypothesis can only be validated or rejected by a further in depth study.



Regression Statistics			
Multiple R	0.905072678		
R Square	0.819156552		
Adjusted R Square	0.77394569		
Observations	6		

Figure 3.10 Scaled air overpressure behind the blast vs. average face velocity

3.3.2 Recommended Protocol

During the monitoring of the blasts for this investigation, there have been a number of factors which have may have contributed towards the collection of anomalous results. Also in this preliminary study, subtle changes in the monitoring methods used, were made as the project evolved. These may well have also contributed to variances in the results which if known before hand may have lead to a more consistent data set being collected with fewer exclusions. All of these factors have been taken into account when developing the following recommended protocol for monitoring and collating data relating to face velocities and air overpressures from quarry blasting operations.

- 1. For every blast at least two seismograph equipped with a low frequency microphone should be used, one placed in front and the other behind the blast.
- 2. In front of the blast, the seismograph should be placed at a slight angle to the perpendicular so that the blasting sequence progresses towards the seismograph in order to register the highest air overpressure possible. This will then aid in formulating a method of prediction of air overpressure so that the highest possible air overpressures are taken into account. This would mean that the predicted air overpressure is most likely to be the highest actual level produced. If possible try to keep the distance of the seismographs from the face the same throughout all blasts so that air overpressures from other blasts may be compared with one another more critically.
- 3. The video camera should also be positioned so that the blast progresses towards it. This will enhance the calculation of the face velocities as each hole can be traced without dust or rock from the adjacent hole obscuring it. This will also allow for more consistent face velocity results whilst avoiding dust produced from the previous blast hole.
- 4. Most importantly, the camera should be positioned no greater than an angle of 45° from the face. This is extremely important in enabling the Front Calc software program to accurately calculate the velocities from the traces of the face. Any angle that is greater than this will make it much more difficult to calculate the true velocity. Once at a quarry, this may prove difficult to accomplish as good judgement is required. Also, the placement of the position

of camera may be restricted due to physical constraints, as was the case when monitoring the blasts at Whitwell Quarry during this investigation. Indeed, if an angle less than 45° from the face cannot be achieved then it is not advisable to monitor the blast as the true velocities of the face cannot be calculated with any degree of certainty.

3.4 Conclusion

It can be concluded that there is a relationship between the face velocities and the air overpressures of the first blast holes when monitoring in front of the quarry face being blasted. This shows that the velocity of the rock as it is projected from the face has a large influence on the level of air overpressure that will be produced from a blast.

With respect to the relationship between average face velocities and the peak air overpressure monitored behind a blast, although results in terms of "scaled air overpressure" [that attempted to take into account distance] look promising, a more detailed study is required to establish if such a relationship does indeed exist.

With regard to collecting the data required for future investigations, it is strongly recommended that monitoring of blasts for face velocities should only be carried out by following the recommended protocol. It is the judgement of the authors that failure to do so will result in inaccurate data and poor results.

This clearly is a pilot study in that only 12 blasts were monitored. To fully define the relationship between the face velocity and air overpressure and to be able to predict values, a much more extensive study is required.

Chapter 4

Blast air overpressure instrumentation

Blast monitoring was performed at several quarries across the United Kingdom. The quarries ranged from a soft rock, chalk quarry at Melton Ross to limestone quarries at Whitwell, Thrislington, Dowlow and Wath to three hard rock quarries at Cragmill, Howick and Mountsorrel.

The instrumentation described in this chapter was used extensively during monitoring throughout this investigation.

4.1 Seismographs

In order to monitor the air overpressure at multiple locations from a blast, seismographs equipped with low frequency air overpressure microphones were extensively used. The ease of setup and the fact that they are 'stand alone' units, not requiring any external power, means that they are ideal for the purpose of recording data at a multitude of distances away from the blast in a working quarry. Two different seismograph models had been used; these are the White Mini-Seis II seismograph and the Instantel Minimate Plus Series III seismograph.

4.1.1 White Mini-Seis II seismograph

The White Mini-Seis II (pictured in plate 4.1) like a number of other commercial seismographs consists of a tri-axial array which records the ground vibration in the longitudinal, vertical and transverse plane as well as a low frequency microphone to record air overpressure. The devices used are capable of recording at a variety of sample rates, ranging from 32 to 1024 samples per second (sps). The maximum limit to which the device can record air pressure levels is 148dBL and the range of vibration levels that can be recorded is 0.127 to 63mm/s. In reality the fastest sampling rate of 1024 sample per second was barely adequate to perform the experiments required

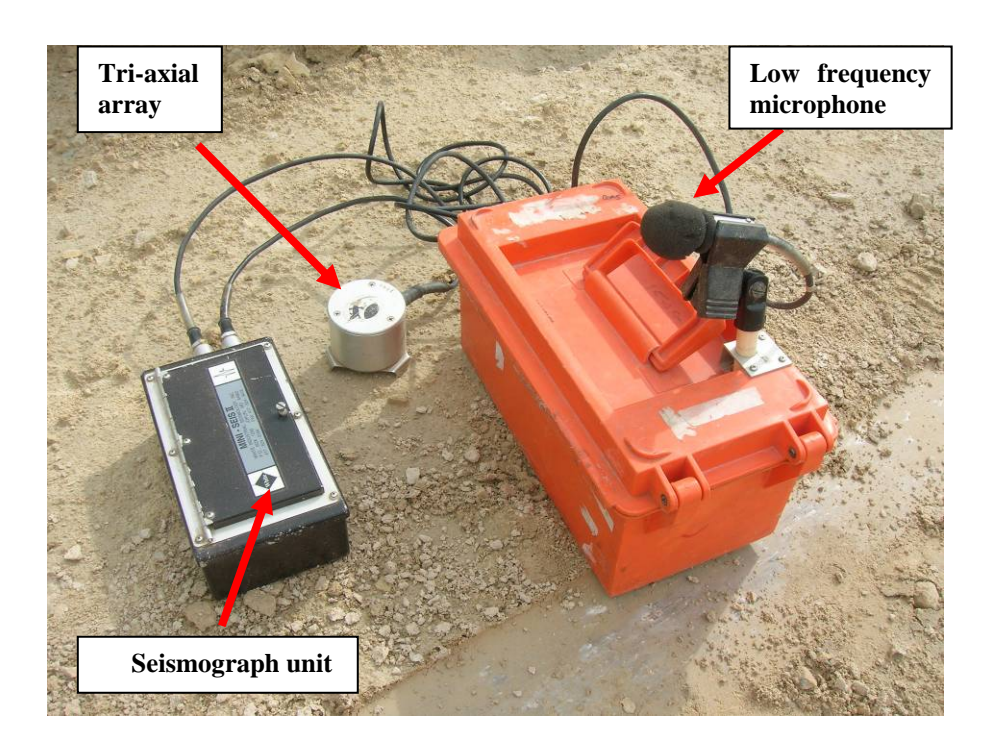


Plate 4.1 White Mini-Seis II seismograph deployed and ready to monitor

Triggering the seismograph into recording mode is achieved by setting the unit to start recording once a ground vibration wave or air pressure wave arrives at the unit which exceeds the threshold or trigger level. For the use of recording air overpressure generated from a quarry blast, the seismographs were set to trigger on ground vibration. Triggering the seismographs on ground vibration allows for the whole vibration waveform to be recorded as well as the full air overpressure waveform. This also reduces the possibility of false triggering which can be the case when programming the seismograph to trigger on air overpressure for a blast during windy conditions.

An additional feature to the White Mini-Seis II seismograph is the ability to connect one or more units together allowing for all of the connected units to record on the same time basis. One seismograph (closest to the blast) acts as the master unit and once triggered, the connected slave unit(s) also begin recording. These slave units cannot trigger by themselves. This allows for the speed of sound in air and in rock to be calculated. However on occasions spurious timings were obtained which can only have been due to a difference in the initial time between the Master Seismograph and the Slave Seismograph.

4.1.2 Instantel Minimate Plus Series III seismograph

Instantel Minimate seismographs were also deployed to record data from the quarry blasts.

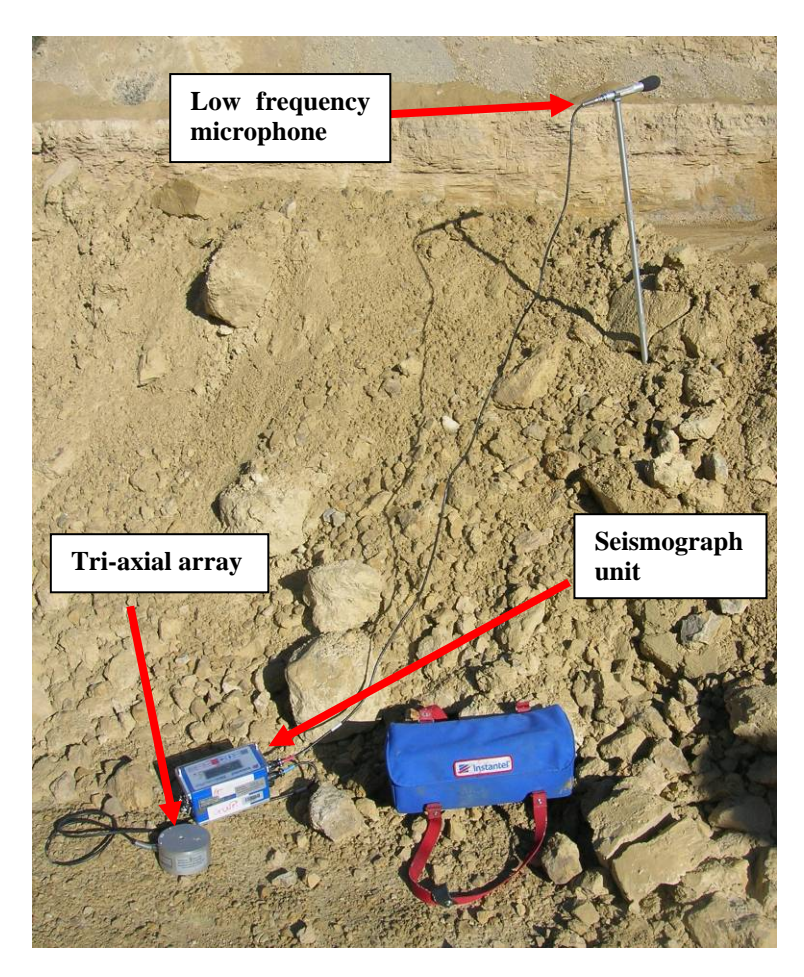


Plate 4.2 Instantel Minimate Plus Series III seismograph

These units are capable of recording at a sample rate of 4096sps. This increase in sample rate compared to the White Mini-Seis II seismographs provides a higher resolution wave trace which allows for an increase in accuracy in the analysis of the recorded waveform. Throughout blast monitoring, a sample rate of 4096sps was used.

The Minimate Plus Series III is capable of recording air overpressure from 88 to 148dBL (0.5 to 500 Pa) with trigger levels ranging from 100 to 148 dBL and 0.127 to 254mm/s with regards to ground vibration.

As explained earlier, the seismograph was programmed to trigger on ground vibrations.

4.2 Instrumentation used to establish the origin of air overpressure

An extensive monitoring system was implemented in order to establish whether the vibrations along the face caused by the arrival of the shockwave, are the source of the air overpressure in front of a blast or whether it is the initial face movement.

4.2.1 Piezoelectric sensor

A sensor was lowered down the blast face, directly in front of the first hole at the corresponding height of the primer charge. The sensor is designed to record the exact time at which the shockwave arrives at the face and then the first movement of the face.



Plate 4.3 Face sensor is encased in a rubber ball, positioned in front of the face

The sensor consists of a piezoelectric wafer encased in plaster within a rubber ball (in this case, a yellow ball) to protect it from the abrasive surface of the face as it is lowered into position (plate 4.3).

The application of force or stress results in the development of a charge in the wafer's material, this is known as the direct piezoelectric effect. The initial movement of the rock as it leaves the face imposes a force on the ball and thus the sensor, creating a voltage which is then recorded by the data logger. The plaster surrounding the piezoelectric wafer provides an effective medium to transmit the force imposed by the moving rock to the wafer, allowing for a clear signal to be recorded. Figure 4.1 is an example of a piezoelectric sensor output.

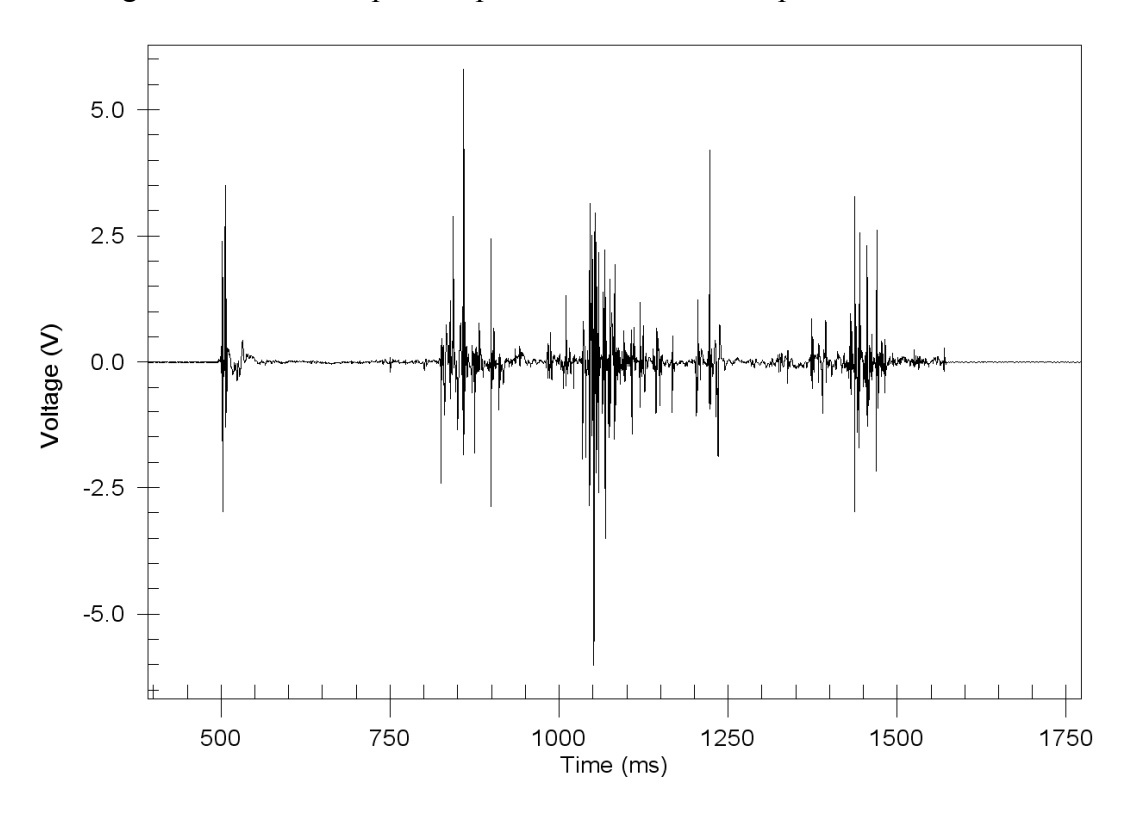


Figure 4.1 An example of a recording from a piezoelectric sensor

The pulses shown in the recording indicate the movement of the face as the rock is projected outwards from behind the sensor. One slight problem was that the "wafers" only vibrated in one direction. Thus there might be a slight delay if the "wafer" was not orientated so that its mode of vibration was aligned to the blast face.

4.2.2 Borehole microphone

During the initial stages of the investigation, a miniature microphone was placed down a blast hole further along in the blasting pattern with the intention of recording the arrival of the shockwave from the first hole and therefore providing a basis to calculate the velocity of vibration in the rock. This was to be used to confirm the exact arrival of the shockwave at the free face. The sensor was taped to an air bag which provides excellent coupling to the inside wall of the blast hole to ensure that the exact arrival time of the shockwave was recorded and to also record a 'cleaner' signal with the intention of further analysis. The air bag is placed above the charge and below the stemming. After many trials, the results from the borehole microphones proved to be erroneous and did not measure the shockwave arrival time from the subsequent blast holes in the firing pattern.

It was not clear what exactly the borehole microphone recorded and so the use for calculating the speed of sound in the rock was replaced by linking two White Mini-Seis II seismographs together so that they each recorded the arrival time of the ground vibration wave at each location at a known distance apart, as explained earlier.

4.2.3 Low frequency air overpressure microphones

As well as seismographs, two additional low frequency air overpressure microphones were deployed in front of every blast. These were set up in a straight line perpendicular to the face, in line with the first blast hole to be fired. The distances from the face were typically 50m and 100m, however these distances varied depending on the nature of rock being blast. At Melton Ross chalk quarry, the microphones were positioned at distances of 40 and 80m and at hard rock quarries, for example Cragmill quarry where the rock being blasted was basalt, microphones were positioned at greater distances to avoid potential damage to the equipment.



Plate 4.4 Air overpressure microphones positioned directly in front of the first blast hole

4.2.4 MREL MicrotrapTM data logger

Each of the monitoring components were connected to a high speed data logger, MREL's MicrotrapTM. This resulted in all of the components listed above being recorded on the same time basis. This allowed for the speed of the air overpressure pulse to be calculated and then back calculated to determine when the pressure wave left the face. Once this is known it is possible to determine the source of the air overpressure (see chapter 10).

The data logger is capable of recording on all four channels at 1 million samples per second.



Plate 4.5 MREL MicrotrapTM deployed and armed.

The data logger relies on either VOD cable or a break wire to trigger it into recording. Initially, standard speaker cable was used to trigger the system. The break wire was prepared by removing the insulation around each of the two wires and connecting the ends of the wires together so that the circuit is closed. As soon as the circuit is broken the Microtrap should begin to record. To ensure that the box starts recording at the exact moment the first hole is detonated, the end of the break wire was strapped to the primer before being loaded into the first blast hole. In theory this was a failsafe method of triggering the Microtrap, however on many occasions the cable did not break at the exact moment the first blast hole was detonated or a break in the cable occurred once the blast had happened and therefore did not trigger at the moment the time of the first hole detonation. This then resulted in no data being recorded. Thus a more reliable triggering method was required to be developed.

4.2.5 Optic fibre triggering system

A new triggering method using optic fibre cable was designed and implemented with excellent results. The optic cable ends was inserted into a 10 x 100mm transparent glass tube and then attached to the primer before being loaded down the blast hole. The light produced from the detonation propagates up the cable (before its destroyed down the hole) and is received at the optical unit interface which in turn is connected to the internal trigger channel of the Microtrap. The optic fibre triggering system has successfully triggered the Microtrap for every blast when used.

This system and its use for recording inter hole delay times in non-electric blasts is explained in detail in chapter 5.

4.3. Conclusions

A variety of blast monitoring equipment was deployed.

The development of the optic fibre system for triggering the MREL data trap has been very successful.

The system using the two low frequency microphones connected to the MREL data trap via two separate amplifiers was also very successful.

The deployment of the piezoelectric wafer encased in plaster within a rubber ball was satisfactory as a low cost solution, but in reality to obtain 100% reliable data, a disposable geophone would have been needed that could have been fixed to the quarry face to be blasted. Needless to say this would have been extremely difficult to accomplish in a safe manner.

The deployment of the Instantel Minimate plus series III seismographs utilising there higher sampling rate was very successful, however the inability to connect two such units together was a disadvantage.

The deployment of the white seismographs was satisfactory, however a higher sampling rate would have been very beneficial. The ability to connect two such seismographs together on the same time base was a very useful facility, however on a few limited occasion, some spurious readings were obtained in terms of timing of the first arrival of an air overpressure pulse.

Chapter 5

Development and application of a low cost optic fibre system to monitor blast performance.

5.1 Introduction

For many years, the accepted method of Measuring the Velocity of Detonation (VOD) in blast holes has been to use an electric cable of a constant resistance per metre. Thus as the wire is consumed by the explosive in the blast hole, the change in resistance is monitored and when this data is plotted against the time period of the in-hole explosion, the VOD can be calculated.

The velocity of detonation (VoD) is defined as the velocity at which the detonation wave travels through an explosive charge. The detonation wave travels at speeds above the normal sound speed of the unreacted explosive. Typical detonation velocities for commercial explosives range from 2500 to 7000 metres per second. The detonation velocity is amongst the most important property of the explosive and can be easily and accurately measured. Once determined, it can be used for the calculation of the detonation and borehole pressures which are of importance in explosive applications. The velocity of detonation of a particular explosive depends on factors such as

- 1. charge diameter
- 2. confinement
- 3. density
- 4. particle size

This can be done under test conditions to quality assure manufacturing. A number of different methods our outlined in a paper by Katsabanis (1990).

However, of more interest to Blasting engineers is the ability to determine VoD by monitoring explosives within blast boreholes at a mine or quarry. This is most commonly done using the "Continuous Probe Method". The system consists of the explosive charge, to which is attached a uniform resistance wire. The wire typically is deployed so as to be in contact for the total length of the explosive

charge in one or more blast holes. The wire is then attached to a data logger which has a constant current source and is able to be triggered by detecting a change in electrical resistance. The resistance wire is usually a "NiChrome" wire having an accurately known linear resistance. At the detonation front created by the explosive, the wire is consumed. This usually results in the circuit remaining closed due to the fact that the detonation wave is sufficiently ionized (although not always). The circuit follows Ohm's law. Therefore, since current is constant, the voltage change with time recorded in the data logger will be proportional to the resistance. Knowing the full voltage drop and the length of the wire, the voltage drop can be converted to distance along the charge. Therefore the velocity of detonation can be calculated by interpreting the voltage drop - time record provided by outputting the recorded data to a graph.

An alternative method of monitoring in-hole VoD is the VODR-1 method. The concepts involved in the operation of the VODR-1 are similar to that of RADAR where a pulse of radio waves is sent out and an echo or reflected pulse is returned to give ranging information. The VODR-1 uses a coaxial cable to carry a fast rise time electrical pulse back and forth. The time between the sending of the pulse and its return is accurately measured. Knowing how the time changes from pulse to pulse gives an accurate picture of the length of the cable in time. This method was developed to produce one of the earliest portable multi-channel continuous velocity of detonation recorders (Chiappetta, Vandenberg & Pressley (1992)

A fuller explanation of the basic technique used to monitor VOD in blast boreholes can be found in a paper by Chiappetta & Vandenberg (1990). In addition a fuller explanation of various options to monitor VOD within blast holes is given in paper by Moxon et al (1991).

The use of optic fibre cable to monitor VoD is not in itself new. Indeed Chiappetta, Vandenberg & Pressley (1997) discuss the efficacy of a number of different methods of determining VoD. They separate methods to measure VoD into two different systems

- 1. Point to point VoD systems
- 2. Continuous VoD systems

The point to point VoD methods compared three different sensing techniques. These were Fibre Optic cable, Blasting wire (two wires) and Ribbon Wire (two wires). The Continuous VoD method also compared three different sensing systems. Resistance wire (two wires measuring voltage drop), Inductance wire (single coaxial cable measuring changes in frequency) and Time Domain Reflectometry (TDR - single coaxial cable measures two way transit time of pulse similar to RADAR). The paper is an excellent summary of all the advantages and disadvantages of the methods available to measure VoD in blast holes, in terms of issues related to the physical deployment, cost of monitoring and usefulness of the results likely to be obtained.

5.2 Optic Fibre Instrumentation

5.2.1 Optical Interface Unit

The principle of operation of this novel detector is to record each instance of optical impulse detected at each of the discrete sensing locations within the blast medium. In order to harness the optical energy generated by the blast into an electrical signal compatible with the MicrotrapTM VOD/Data Recorder, a custom optical receiver unit was developed (plate 5.1). As the standard VoD input on the unit was used, the signal had to present a varying electrical resistance in response to the optical input rather than a more typical voltage or current source attributed to standard optical detectors. Moreover, the interface unit was required to stay within the resistance boundaries expected by the MicrotrapTM VOD/Data Recorder in order to trigger and record in a reliable and consistent manner.

To determine the blast dynamics, multiple discrete optical couplings are used, each using its own low cost 1000µm plastic optical fibre. The interface unit was therefore developed using an array of high-speed electrically coupled photo-detector elements. The detectors all accept the input fibre using a simple screw locking mechanism, thus eliminating the need to terminate the fibre in the field.

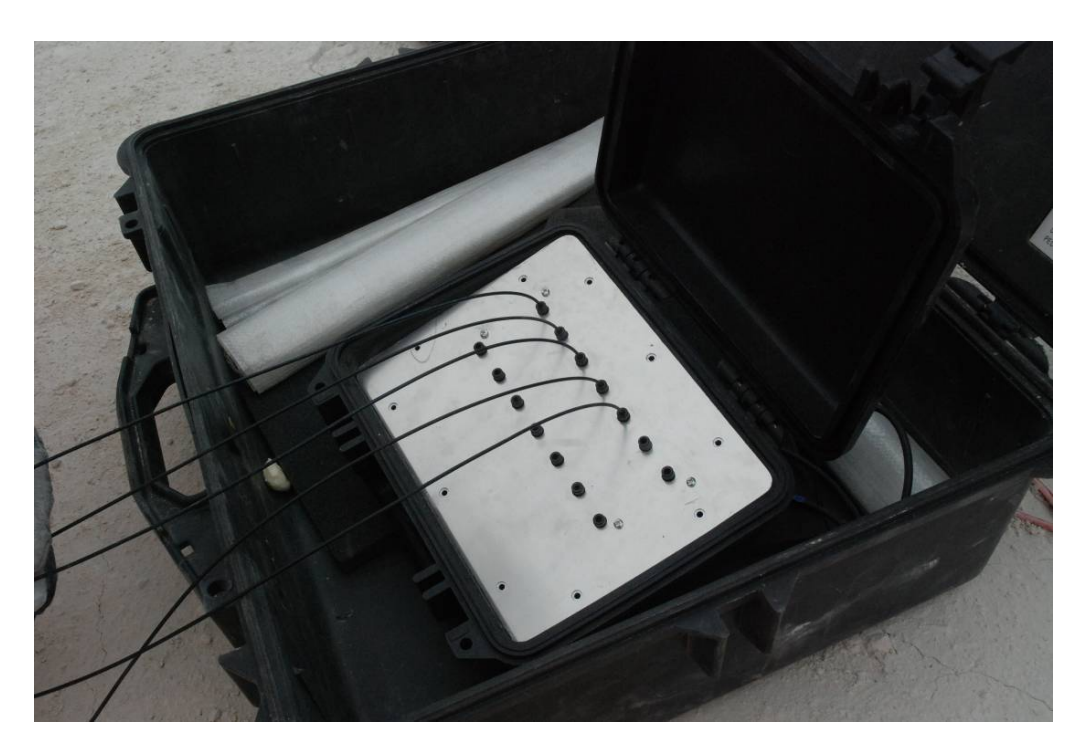


Plate 5.1 Optical Interface Unit

The polarity and voltage level supplied by the MicrotrapTM VOD/Data Recorder input connector are sufficient to bias the photo-detectors into their operating region. Upon receipt of each short duration optical impulse, the apparent DC resistance of the array experiences a rapid negative pulse which is detected and recorded by the VOD channel. The response time of the detector array is sufficient to clearly identify impulses from each discrete location, providing precise timings as the detonation wave-front extends through the blast medium.

5.2.2 Data logging

The MREL MicrotrapTM VOD/Data Recorder (plate 5.2) was use to log the data that was being continuously collected by the Optic Fibre Interface unit. This is directly connected to the VOD channel and thus can be used to control the other four scope channels (which were used in an air overpressure monitoring experiment). The unit has 14 bits resolution (i.e. 1 part in 16,384), can store 4 million data points and is capable of operating at a range of 1 Hz to 2 Mhz.



Plate 5.2. MREL MicrotrapTM VOD/Data Recorder

5.2.3 Deployment of the equipment.

Initially the optic fibre cable was simply put directly adjacent to the shock tube detonator, which in turn was inserted into the primer cartridge prior to lowering it down the blast hole. Whilst this did give a response, the magnitude of the response in terms of the voltage output into the MicrotrapTM VOD/Data Recorder was disappointingly low. It was thought that this was because the explosive itself was totally opaque and that the optic fibre cable was being destroyed at the same precise time that the "light" from the detonation front was arriving at the core of the cable. It was therefore decided that what was needed was to allow a very small faction of time, such that the light from the detonation of the explosive would be detected just prior to the sensor being destroyed. To achieve this, the optic fibre cable was inserted into a 10 mm (0.4 in) diameter x 10 cm (3.9 in) length of laboratory glass tubing (Plate 5.3).



Plate 5.3 10 mm (0.4 in) diameter x 10 cm (3.9 in) length of laboratory glass tubing with Optic Fibre Cable



Plate 5.4 attaching Glass tubing with Optic fibre Cable to down hole Shock Tube

This was then subsequently strapped to the shock tube down lines just above the primer cartridge, (see Plate 5.4). and lowered down the blast hole (Plate 5.5).



Plate 5.5. Lowering primer cartridge with Shock tube detonators and Optic fibre cable down the blast hole



Plate 5.6 Yellow shock tube to In-hole Detonators connected to red surface Delay Relay Detonators. Green shock tube links one detonating relay to the next. Black optic fibre cable connected to the Optical Interface Unit

The blast holes were then filled to the appropriate level with explosive and then stemmed to the surface of the blasting bench. The shock tube to the in-hole detonators were then linked up to the surface delay relay detonators (plate 5.6).

Each of the Optic fibre cables from the individual blast holes were then connected to the Optic Fibre Interface Unit, which in turn was connected to the MREL MicrotrapTM VOD/Data Recorder.

5.3 Determinations of timing scatter in shock tube Detonators and Delay Relay Detonators.

The optic fibre VoD method has been routinely used to trigger the MicrotrapTM VOD/Data Recorder during the field experiments designed to examine the origins of Air Overpressure from quarry blasting. It must be borne in mind that when examining the output data from the optic interface unit that is then captured by the MicrotrapTM VOD/Data Recorder and then processed using MREL bespoke software, the y axis in this case does not show "distance", but is merely an indicator of the brightness of the light

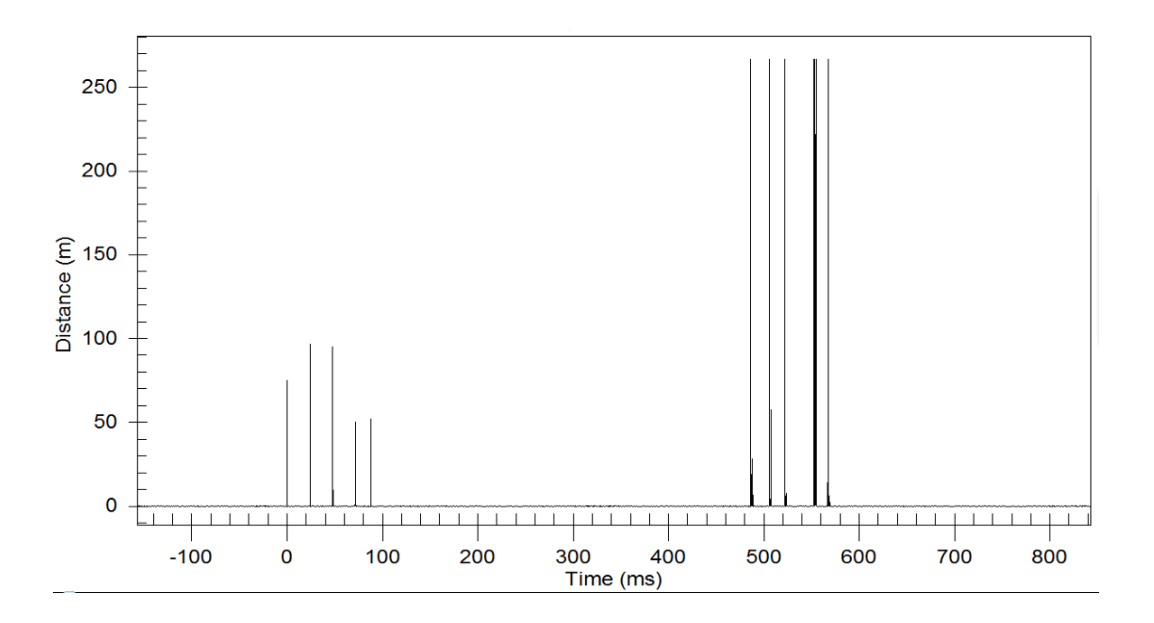


Figure 5.1 Output from MicrotrapTM VOD/Data Recorder

The results routinely collected (See Figure 5.1) show not only the time that the in-hole detonators fired, but also the time at which the flame in the shock tube passed the glass tube attached to the optic fibre cable.

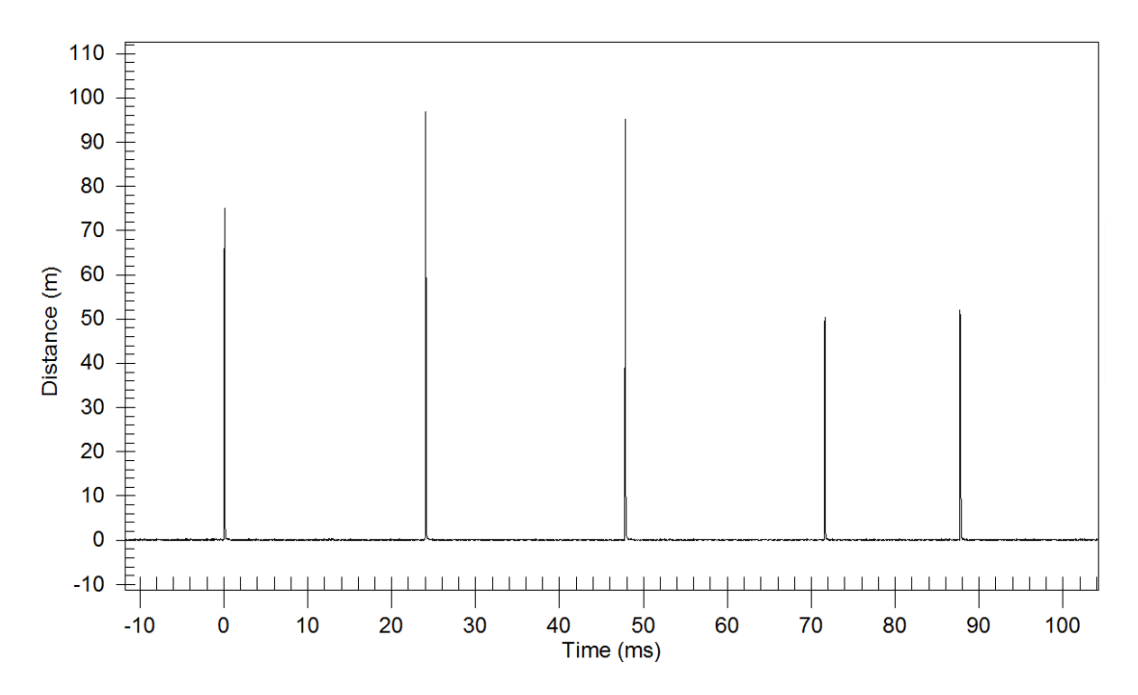


Figure 5.2 Close up surface Delay Relay Detonator firing section of Figure 5.1

A more detailed examination of the earlier time period of the graph clearly (see Figure 5.2) shows the time at which the delay relay detonators fired and shows that whilst they are all nominally 25 milliseconds apart, the four time period intervals area where 24, 24, 24 & 16 milliseconds apart respectively.

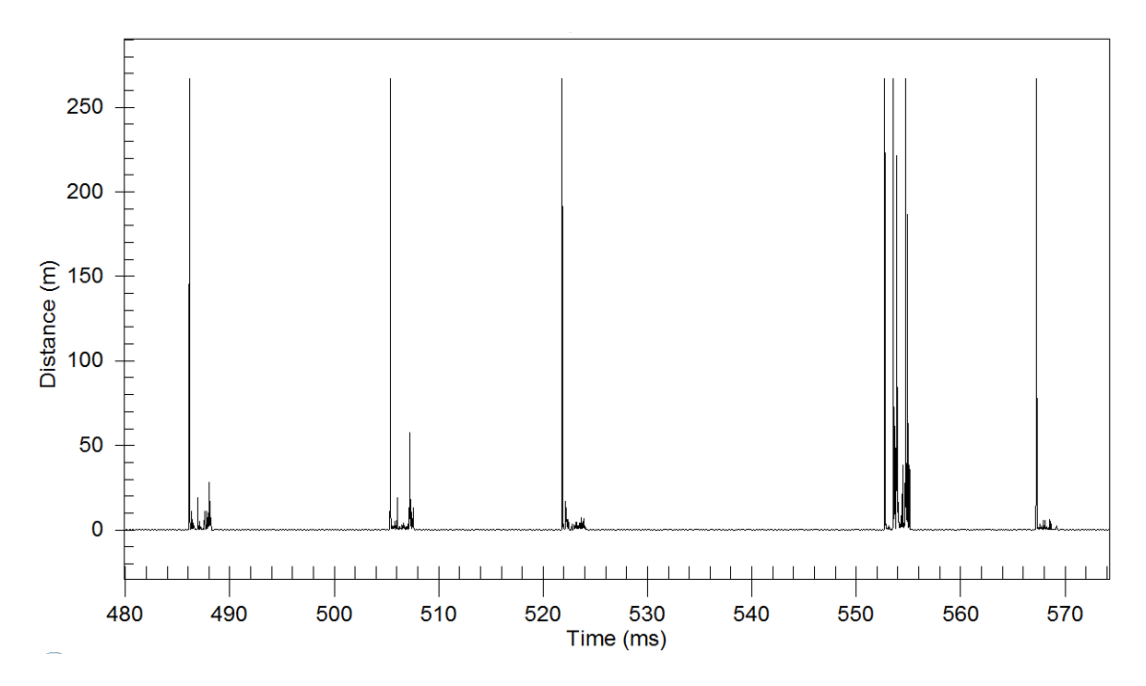


Figure 5.3 Close up In-hole Detonator firing section of Figure 5.1

Similarly a more detailed examination of the later time period of the graph clearly (see Figure 5.3) illustrates the time at which the in-hole detonators fired. This shows that, whilst they are all nominally 475 millisecond delay detonators that should (due to the action of the surface detonating relays) have fired 25 milliseconds apart, the four time period intervals area where 19, 17, 30 & 15 milliseconds apart respectively. What also can be clearly seen is the burn time of the actual boreholes. Whilst the "signal to noise" ratio is excellent at identifying the start of the explosion, it is somewhat poorer at identifying the end of the explosion. The "highs and lows" of the trace during the burn period of the explosive has no real meaning and is simply where there existed a very short period of time when the optic fibre could clearly see the light of the explosion prior to that section being destroyed.

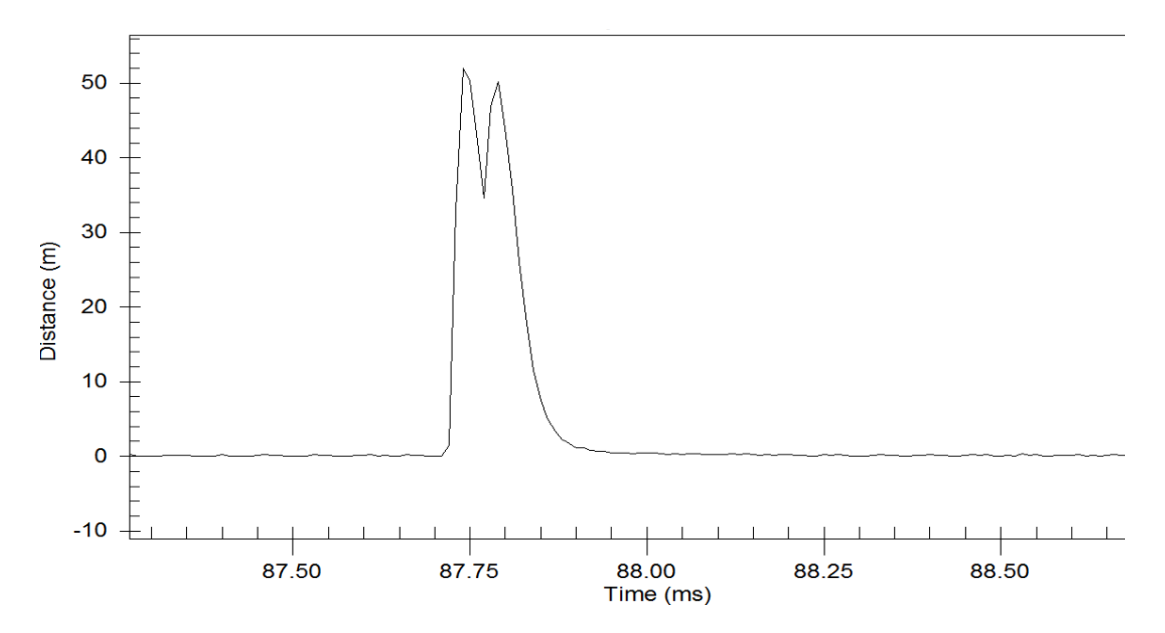


Figure 5.4 Close up of Figure 8 - Flame in Twin Shock tubes passing In-hole optic sensor

If the last peak in Figure 5.3 is examined in more detail, then two peaks appear some 0.1 milliseconds apart. This is because UK legislation requires that each hole must have two in hole detonators so that if the first one fails, the second one will fire, thus reducing the chances of a misfire. The fact that there is a separation of 0.1 milliseconds is due to small variations in the burn time of the shock tubes, which will most likely be due to a small difference in length of the two shock tubes from the surface detonating relay to the in-hole glass tube on the optic fibre cable.

The main purpose of developing the technique was to be able to determine the exact firing time of a shock tube initiated blast so that this could be used in the study of the origins of air overpressure. This section of the study was carried out at a small chalk quarry in the north of England [UK]. Only small single row shock tube blasts are carried out (maximum 8 holes per blast). The reason for this being that the blasted rock deteriorates rapidly during adverse weather if left in a rock pile at the blast face. The relationship between the various components used in the blast design can be seen in Figure 5.5.

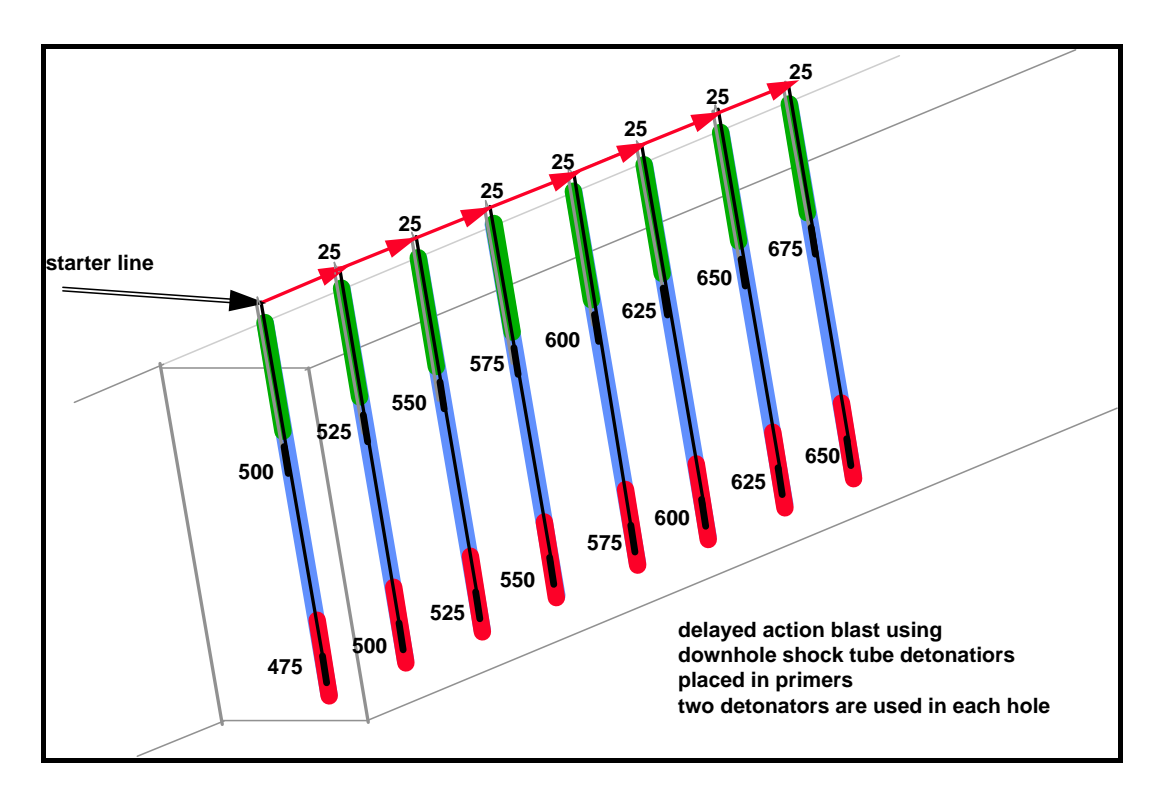


Figure 5.5 Interaction between surface delay relay detonators relays and long period in hole detonators to create advanced initiation in a quarry blast.

From a brief study of six small blasts, the incidental data collected on the variation in detonating times for both delay relay detonators, the in-hole detonators and then the combination of both to give the actual inter hole delays can be seen in the table below.

	Delay Relay	In-Hole Detonator	Total Inter hole
	Detonators	timing	delays
	[millisecs.]	[millisecs]	[millisecs]
Min	16.16	446.78	13.90
Max	36.60	486.07	45.10
Average	22.83	476.88	23.28
St. Dev.	4.73	8.06	6.89

Table 5.1 Statistical analysis of detonator performance

The nominal delay relay detonator timing and hence inter hole timing was 25 millisecs. and the nominal in-hole detonator timing was 475 millisecs. The results obtained (see table 5.1) clearly demonstrate that the technique can very accurately

determine both surface and in hole delay components as well as how they interact to give the actual time that one hole detonated with respect to all the other holes in that particular blast.

5.4 Comparison of VOD Measurements

An experiment was carried out to compare the point to point system of calculating VoD using the optic fibre method with the currently accepted industrial standard of using the continuous system of calculating VoD using the resistance wire method. The first hole in a blast was instrumented such that four optic fibre cables were attached at 1.5 metres spacing to the twin shock tube down hole lines and connected via the optical interface unit to the MicrotrapTM VOD/Data Recorder. The results obtained can be seen in Figure 5.6.

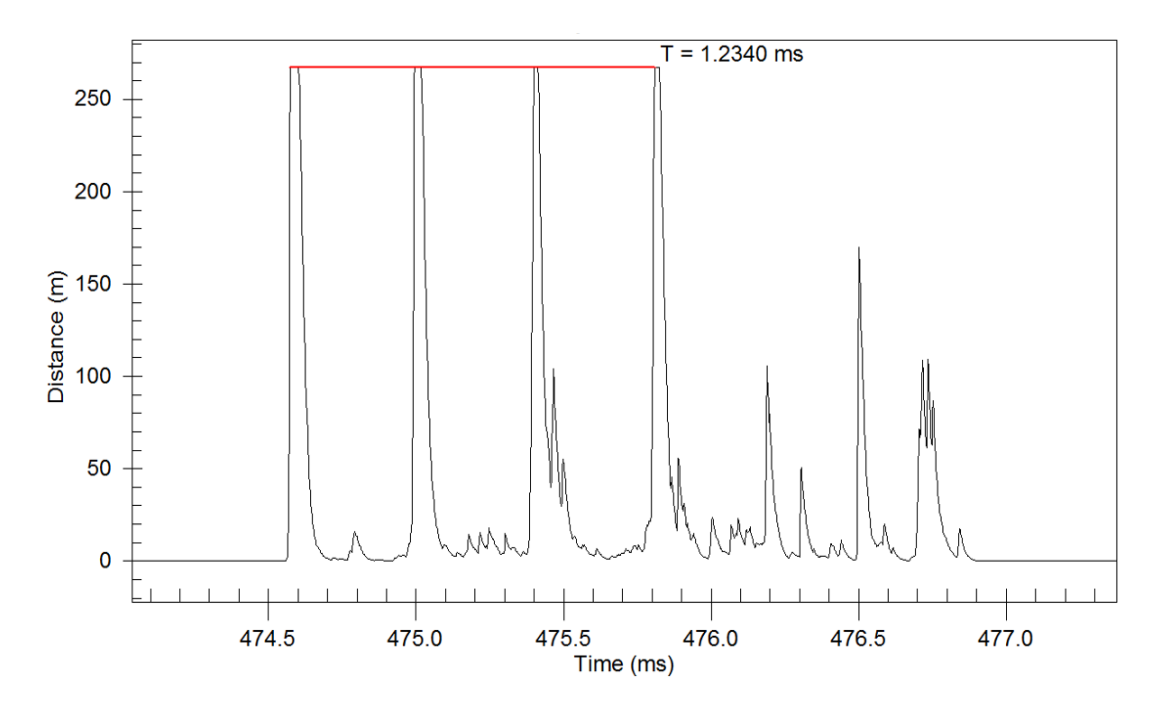


Figure 5.6 Output from Optic Fibre system showing time of 1.230 ms for 4.5 metres travel as the detonation front proceeded through the Anfo explosive

At the same time standard VoD resistance wire was attached to the same down hole lines and then connected to a MREL Handitrap VoD recorder. The results obtained can be seen in Figure 5.7.

The calculated VoD from the four in hole optic fibre sensors gave individual readings of 3554, 3712, and 3676 metres per second as the detonation front proceeded up the blast hole with a total average VoD of 3646 metres per second.

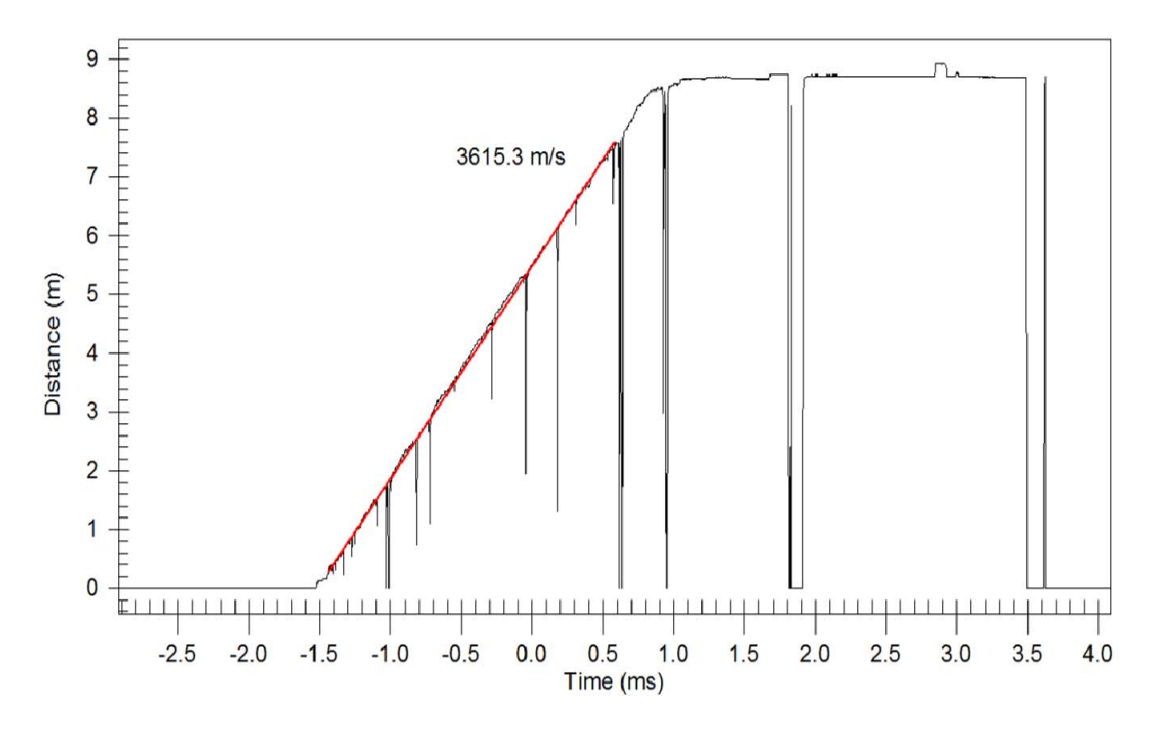


Figure 5.7 Output from MREL Handitrap showing VoD of 3615 m/s in site mixed Anfo

The average VoD reading from the MREL Handitrap using the resistance wire method was 3615 metres per second, thus showing a very good agreement between the two systems.

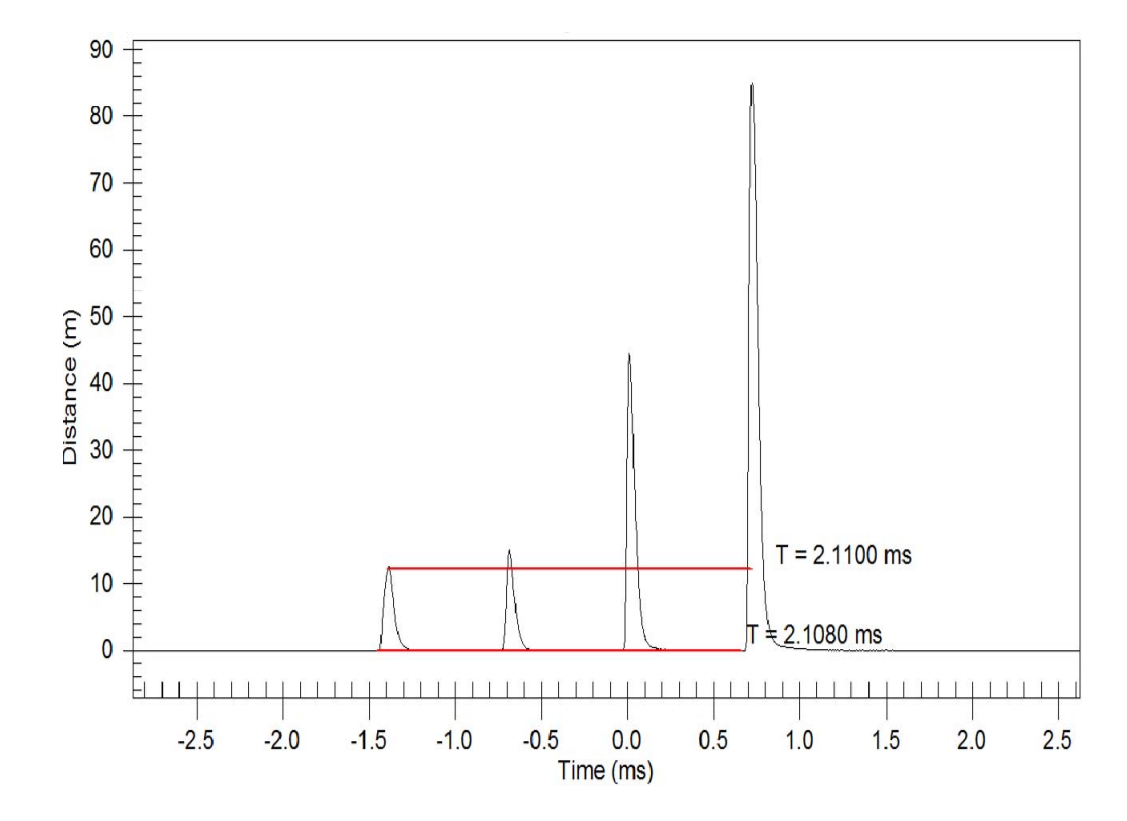


Figure 5.8 Output from Optic Fibre system showing time of 2.100 ms and 2.108 ms for 4.5 metres travel as the flame front proceeded down the shock tube.

Using the optic Fibre system it was also possible to determine the velocity of the flame front within the shock tube (see Figure 5.8). This was calculated by two different methods. The first method relied on being able to determine the first point at the base of the first peak to the first point at the base of the last peak. The second method was simply from the maximum value of the first peak to the maximum value of the last peak. The values determine were 2132 and 2134 m/s respectively. Thus showing very good agreement between the methods. The results obtained also are in quite close agreement with laboratory based shock tube measurements carried out by R. Farnfield, W. Birch, G. Rangel-Sharp & C. Adcock (2009). As a result of 55 test firings, they determined the mean velocity of the flame front to be 2045 m/s with a standard deviation of 11.2 m/s.

5.5 Conclusions

The optic fibre system developed allows the firing times of the various shock tube pyro-technique delay detonators (both surface delay relay detonators and in hole long period delays) to be accurately and precisely determined.

When deployed using the "point to point" method it can used to determine, both the VoD of the explosive used in a blast as well as the velocity of the flame front within the shock tube immediately prior to detonation, to a high level of accuracy and precision.

Chapter 6

Air overpressure data collection and analysis

6.1 Introduction

An extensive monitoring campaign was carried out at several quarries in the United Kingdom. This has resulted in a large data set of air overpressure levels that have been recorded from production and single hole blasts where the rock in question has varied greatly from soft chalk to granite and basalt.

Data analysis has been implemented by statistical means and air overpressure data has been analysed on a site by site basis.

6.2 Statistical Analysis Techniques

6.2.1 Scaled distance regression

Regression analysis is a statistical methodology that is used to relate a dependent variable, in this case air overpressure to an independent variable, the scaled distance. The objective of this regression analysis is to provide an equation such that peak air overpressure levels can be predicted from future blasts. The accuracy of the predictions will inevitably depend upon the quality of the data set. The correlation coefficient and standard error of the data set will be used as an indicator of quality.

Scaled distance modelling is commonly used to model and predict the expected levels of air overpressure produced by a blast at a specific distance in relation to the mass of the maximum instantaneous charge (MIC) per delay. As discussed in Chapter 2, when applied to air overpressure modelling, the scaled distance is derived by the following formula

$$SD = \left[\frac{D}{\sqrt[3]{MIC}} \right]$$

Where:

 $SD = \text{scaled distance (m.kg}^{-1/3})$

d = the distance of the desired location from the blast (m)

MIC = maximum instantaneous charge mass (kg)

The cubed root scaling is applied to explosions of differing magnitudes in a constant medium. As air overpressure travels through the air which is considered a constant medium, the cube root scaling law applies. This differs when applied to ground vibrations where on occasion the square root of the MIC can also be used. This use of cube root scaling is more common when dealing with air overpressure as this provides less scatter in the regression model compared to using the square root scaling method.

The expected level of air overpressure from a free face blast can be determined by equating the air overpressure with a scaled distance into a bivariate expression. The expression assumes the form:

$$AOP = A.SD^B$$

Where:

AOP = maximum air overpressure (Pa)

A and B are the site constants.

The site factors A and B allow for the influence of geology and local micro climate (temperature and pressure) as well as pressure wave attenuation to be taken into account. The values of the site factors can be derived by least square regression analysis of a logarithmic plot of peak air overpressure against logarithmic scaled distance. A mathematical line of best fit is applied to the plot (y = mx + c). Site factor A is the air overpressure intercept at the point where the scaled distance is at unity (c) (x = 0) and site factor B is the gradient of the line of best fit (m).

Scaled Distance Regression Model Example

1000

100

100

100

100

Scaled distance (m.kg^{-1/3})

An example of a scaled distance regression model is illustrated in Figure 6.1

Figure 6.1 Example of a scaled distance regression model applied to air overpressure

Power (Pred. AOP (95%))

Statistical Summary	
Data Count	28
Standard Error	0.36
Correlation Coefficient	-0.84

AOP

Site Factors	
Α	4376.9
В	-1.15
A (95%)	7962.7

Power (Pred. AOP (50%))

The above regression model displays 28 data points that have been plotted on a logarithmic scaled. Once plotted, a line of best fit is calculated. This line plots the mean value of air overpressure at a given scaled distance. From this, the site factors can be derived. A negative value for site factor B indicates the direction the line of best fit and that maximum air overpressure is inversely proportional to Scaled Distance.

This can be used to predict the air overpressure at a given scaled distance where there's a 50% probability that the pressure level will not exceed the predicted value. For the purpose of complying with planning restrictions, this is not consider a sufficient safe guard and so a 95% prediction level is more commonly used. This

then determines the 1 in 20 chance of the actual air overpressure level exceeding the predicted value.

The accuracy of these predictions depends entirely on the quality of the dataset. If there is a large degree of scatter, the predictions will become less accurate. The standard error and the correlation coefficient provide a numerical assessment of the quality of the dataset.

6.2.2 Standard Error

The standard error statistic is used to determine the degree of scatter of a specific data set. It is generally used to examine the error in a derived model. It is calculated directly from the standard deviation of the data about the least squares mean trend line i.e. the line of best fit as shown in Figure 6.1. As it a measure of the degree of scatter of the data in question, it is therefore closely linked to the correlation. The greater the correlation, then in general, the smaller the standard error which means a tighter fit of the data around the line of best fit (50% line). The standard error value can range from 0 to 1. The closer the value is to 0, the less scatter there is amongst the data points and thus a value of 0 indicates a perfect data set. From the example in Figure 6.1, the standard error is 0.36 which is indicates a moderate level scatter about the mean regression line.

An example of a data set with a high standard error is given in Figure 6.2.

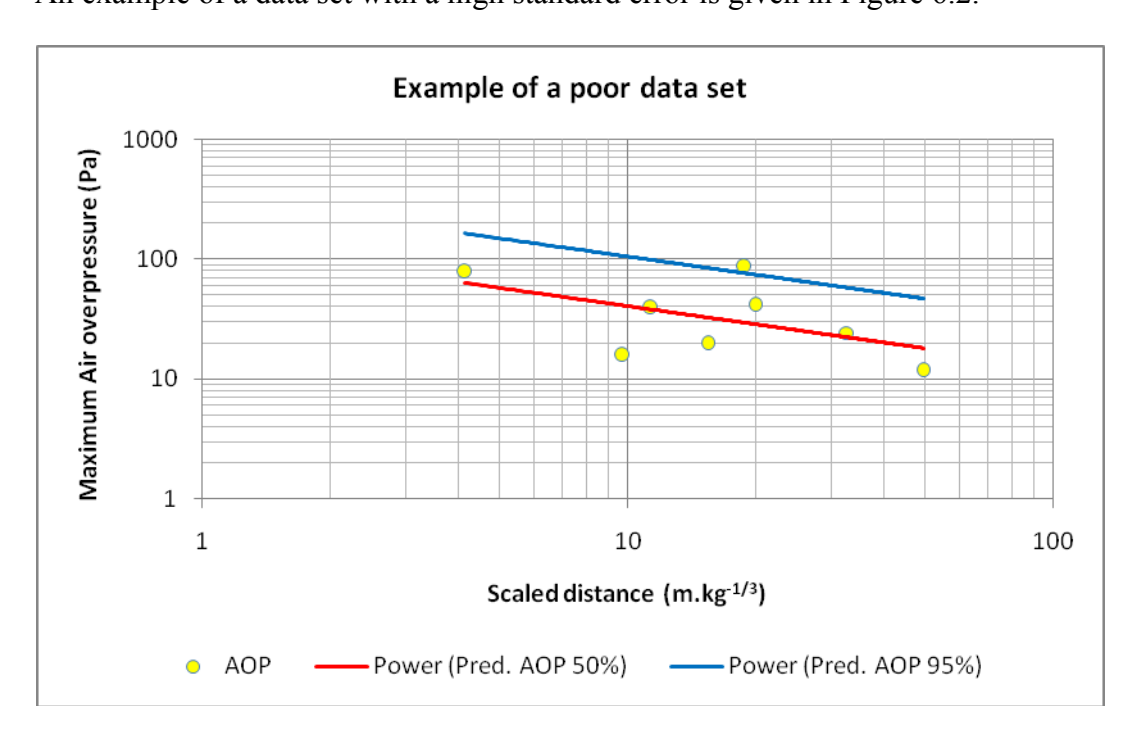


Figure 6.2 Example of a data set with a high standard error

Statistical Summary	
Data Count	8
Standard Error	0.58
Correlation Coefficient	-0.53

Site Factors	
Α	128.98
В	-0.5
A (95%)	334.4

The high degree of scatter around the mean regression line is clearly evident in Figure 6.2 and is reflected with a high standard error value of 0.58. As a result of the high level of scatter, it would not be prudent to make a 95% prediction using this data. To illustrate, at a scaled distance of 10m.kg^{-1/3}, the mean air overpressure level expected would be 40 Pascals whilst using the 95% confidence line would result in a prediction of 100 Pascals. This is a very large difference.

Figure 6.3 provides an example of a data set with a very low standard of error.

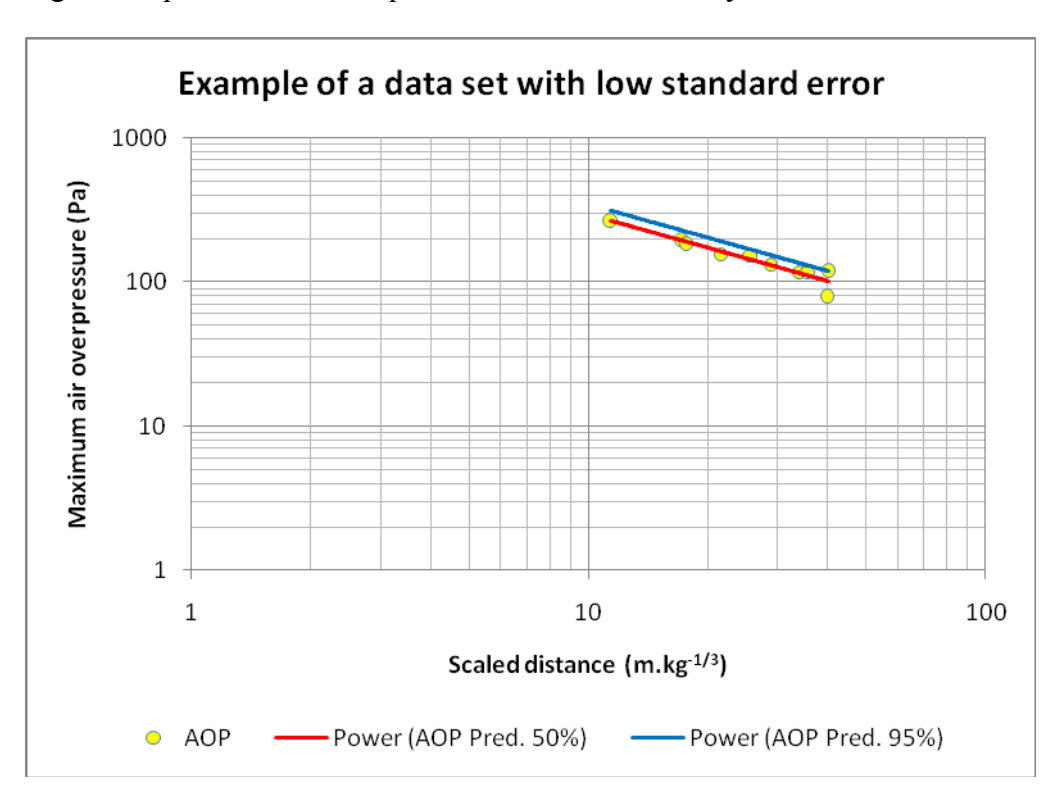


Figure 6.3 Example of scaled distance regression model with a low standard error

Statistical Summary	
Data Count	10
Standard Error	0.098
Correlation Coefficient	-0.95

Site Factors		
Α	1707.84	
В	-0.7654	
A (95%)	2006.15	

The data presented in Figure 7.3 shows a very tight fit around the mean regression line. With a standard error of 0.098, a more accurate prediction of air overpressure can be made.

6.2.3 Correlation Coefficient

The correlation coefficient is the proportion of the dependent variable (in this case, the maximum air overpressure level) that is explained by the mean regression equation. Like the standard error value, the correlation coefficient value (r^2) ranges from 0 to 1. A value of 1 would mean that the equation explains 100% of the variation in the dependent variable. A value of 0 would mean that none of the variations can be explained.

The example in Figure 6.3 shows a very high r^2 value and suggests that the equation explains that the level of air overpressure is very closely related to the charge mass and scaled distance. Conversely, Figure 6.2 shows an r^2 value of 0.53 which indicates that the mean regression equation only explains 53% of the variation in air overpressure and that there are other factors affecting air overpressure levels, which are unexplained in this model.

It should be noted that the correlation coefficient value is purely statistical and cannot be regarded as evidence for cause and effect (Pegden 2005).

6.2.4 Criticism of the scaled distance regression method for predicting air overpressure

The equations introduced by the United States Bureau of Mines which is commonly used for air overpressure prediction suggests that peak levels are primarily controlled by the explosive charge mass per delay and distance from the blast to the sensitive/monitoring location. McKenzie et al 1990 states that using the mean regression line equation does not provide an indication of the degree of scatter and then demonstrates that using the equation to predict air overpressure levels from the data set presented in the paper is inadequate as the total scatter exceeds 20dB at any value of scaled distance.

It can be said that scaled distance analysis of air overpressure can be used to determine the magnitude of the scatter within a data set but depending on the severity of the scatter, a reliable prediction on future air overpressure levels may not be accurate. It is evidenced further in this chapter that the scaled distance regression model does not fully explain variations in air overpressure levels. This can be explained by the many addition variables which can influence the magnitude of air overpressure that are not guaranteed to occur during every blast. This includes events such as; gas ejection from the face, stemming ejection, which are dependent on burden and stemming heights as well as stemming material. Also of importance are spacing distances between blast holes in combination with the detonator firing times.

6.3 Data Collection

Data collected from 69 blasts have been used for analysis in this investigation. From these 69 blasts, 289 Air overpressure blasting events have been recorded. These blasts were monitored at 8 sites around the United Kingdom which are listed in the table 6.1 below, along with the type of rock that was blasted.

Site Name	Rock Type	Number of Blasts	Number of data points
Newbridge	Limestone	9	20
Whitwell	Limestone	32	103
Melton Ross	Chalk	16	115
Thrislington	Limestone	5	18
Wath	Limestone	2	13
Cragmill	Basalt	2	11
Howick	Whinstone	3	32
Ffos-y-fran	Coal	2	10
Dowlow	Limestone	2	5
-	Γotal	73	327

Table 6.1 Summary for all data collected

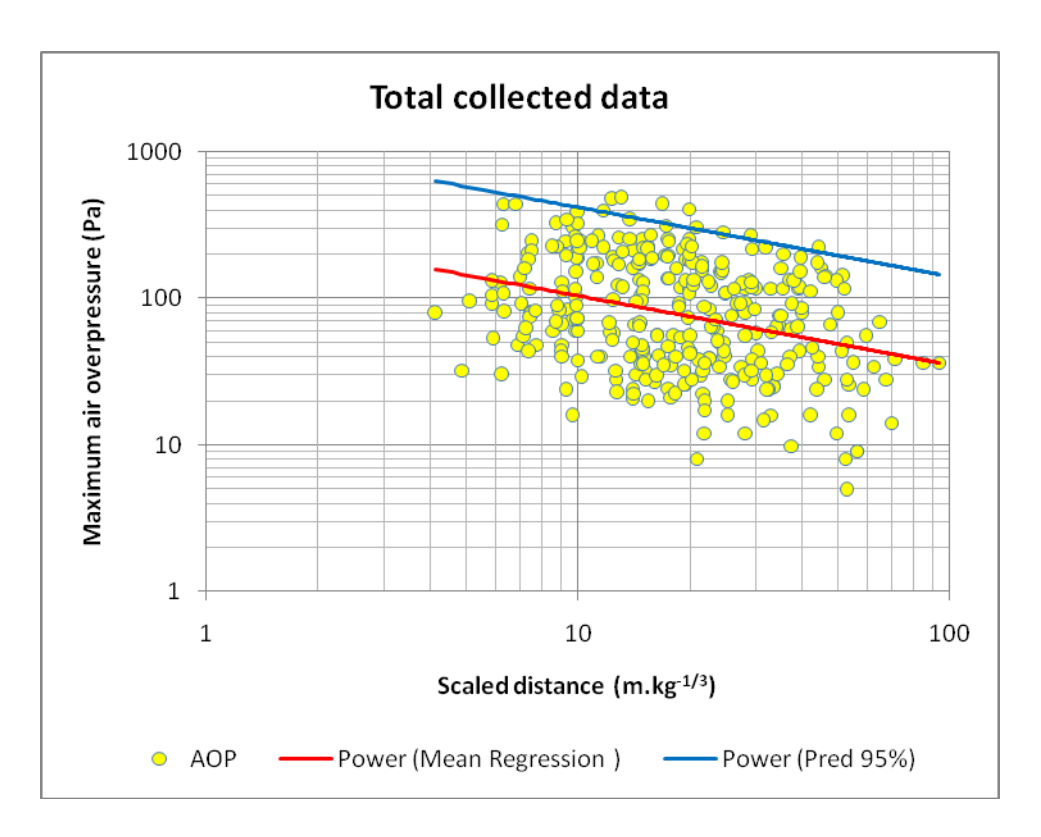


Figure 6.4 All air overpressure data recorded

Statistical Summary	
Data Count	327
Standard Error	0.847
Correlation Coefficient	-0.32

Site Factors		
Α	307.5	
В	-0.47	
A (95%)	1233	

Figure 6.4 displays the entire data collected which was used for the purpose of this investigation. It is clearly evident that there is a very high level of scatter within the data set, which makes it unusable for predictive purposes. As each site varies geologically, the data is subsequently analysed in the following sections of this chapter on a site by site basis.

6.4 Whitwell quarry

A total of 32 blasts have been monitored at Whitwell quarry. The vast majority of these were production blasts which consisted of between 7 to 15 blast holes arranged in one or two rows. All of these blasts were initiated with electronic detonators. Three single hole blasts were also recorded at Whitwell.

Seismographs were positioned at various distances from the blast throughout the monitoring of the blasts, in front and to the rear of the blast. In total, 103 air overpressure levels were recorded, 61 in front of the blast and 41 to the rear of the blast.

The accumulated data from all the blasts are presented in relation to scaled distance in Figure 6.5.

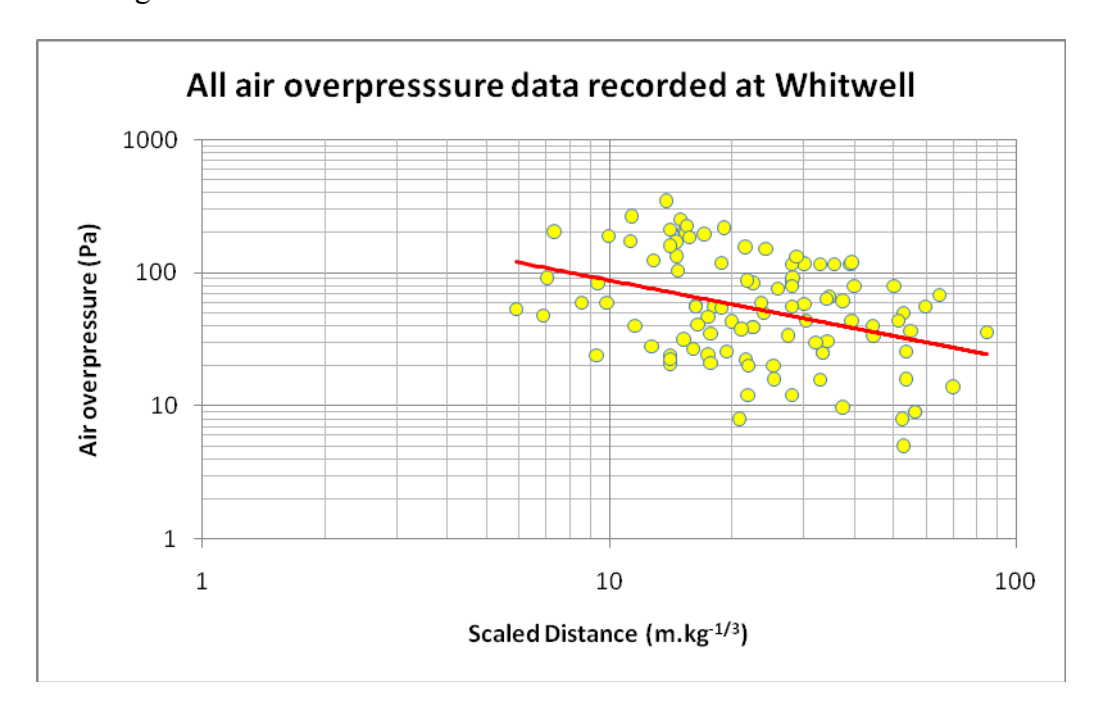


Figure 6.5 Regression curve for the entire data set accumulated at Whitwell quarry

Statistical Summary	
Data Count	103
Standard Error	0.85
Correlation Coefficient	-0.37

Site Factors		
Α	349.5	
В	-0.599	
A (95%)	1410.2	

The data shows a large degree of scatter with a standard error value of 0.85 and a very low correlation coefficient (r^2) value of 0.37 which shows that the maximum air overpressure level recorded for each of the blasts has a poor correlation with the scaled distance. This suggests that the regression equation ($y = 349.5x^{-0.599}$) does not explain the variation in air overpressure in relation to both the charge mass and distance (components of scaled distance).

To improve the regression model, the data recorded in front of the blast has been separated from the data recorded behind the blast and a plot against scaled distance is shown in Figure 6.6.

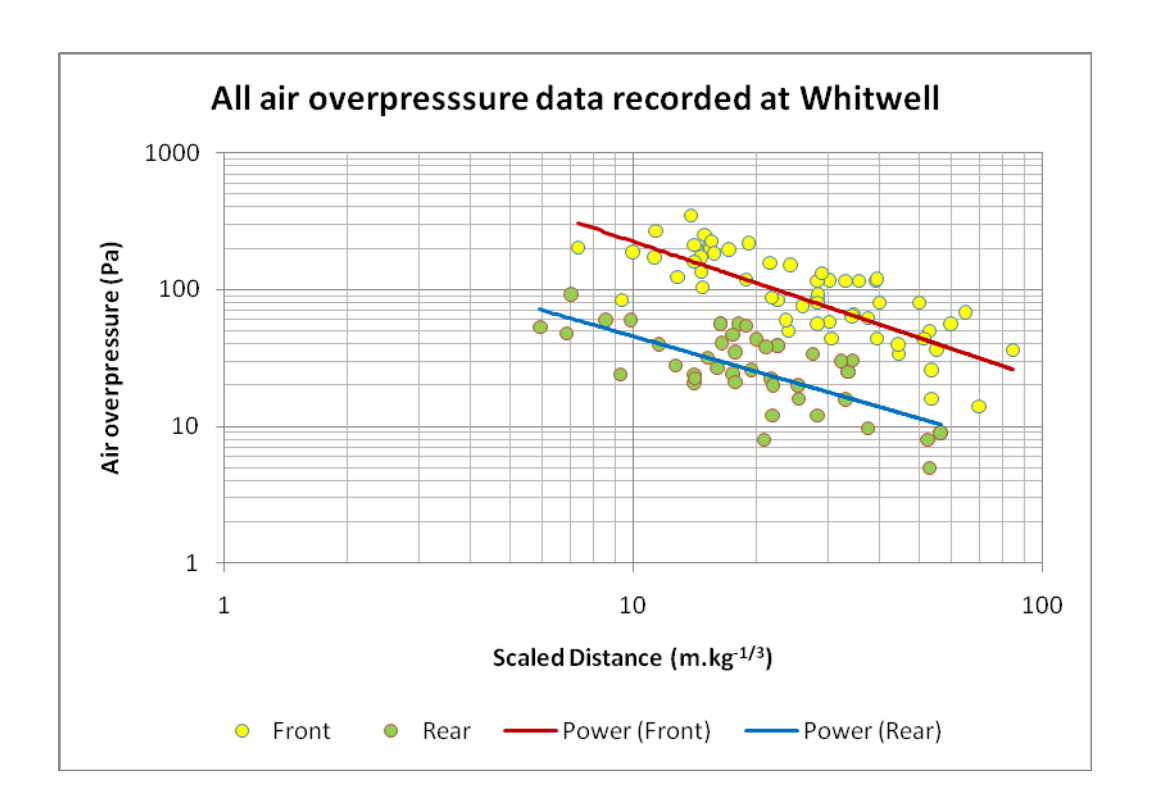


Figure 6.6 Regression model depicting the location of recorded air overpressure levels

Statistical Summary	
Data Count	62
Standard Error	0.507
Correlation Coefficient	-0.74

Site Factors		
Α	2277.76	
В	-1.007	
A (95%)	5231.25	

Statistical Summary		
Data Count	41	
Standard Error	0.45	
Correlation Coefficient	-0.705	

Site Factors			
Α	327.69		
В	-0.857		
A (95%)	688.6		

It is clear from the regression model above (Figure 6.6) that the magnitude of the air overpressure differs greatly in front of the blast when compared to the readings obtained behind a blast. This is primarily due to quarry blasts being designed so that the energy generated by the detonation of the explosive charge is directed towards the free face so that the rock can be sufficiently fragmented and 'thrown' from the face to allow for ease of excavation. The free face provides a shielding effect to the air overpressure travelling behind a blast as explained by Moore et al, 2003.

The equation of the mean regression lines for both the data recorded in front and behind the blast highlights the difference in magnitude of air overpressure in the two directions. The equations, shown below, define the site factors, *A* and *B*.

The mean regression line equation for the air overpressure data recorded in front of the blast is

$$y = 2277.76x^{-1.007}$$

The mean regression line equation for the air overpressure data recorded behind the blast is

$$y = 327.69x^{-0.057}$$

The difference of *A* from the two equations above illustrates statistically the difference in the mean levels of air overpressure produced in front and behind the blasts at Whitwell quarry. This indicates that the initial air overpressure pulse in front of the blast is of the order 7 times larger than the equivalent initial air overpressure pulse generated behind the blast.

The value of B in the front of blast line of best fit equation is -1.007 which indicates that on average, the level of air overpressure generated in front of the blast attenuates a faster rate (some 15% faster) than the air overpressure behind the blast (B value of -0.857).

The data collected at Whitwell quarry clearly shows the difference in propagation of air blast waves in relation to the direction from a blast. It has confirmed previous researchers findings that levels of air overpressure generated in front of the blast are much higher than those generated behind the equivalent blast.

6.5 Melton Ross quarry

A total of 16 blasts were monitored at Melton Ross quarry in a similar manner to the monitoring carried out at Whitwell quarry. Seismograph units were positioned at various distances in front of the blast and to the rear, along the surface of the bench. 115 air overpressure levels were recorded from the 16 blasts, 61 in front and 54 to the rear and on the surface of the bench.

From the 16 blasts, 3 were single hole blasts and the rest were production blasts of a small design. The production blasts consisted of a single row of 5 blast holes, apart one blast which consisted of only four blast holes and one which was made up of two rows with three blast holes in each row.

The data recorded in front of the blasts are displayed in Figure 6.7 and the maximum air overpressure levels recorded by each seismograph have been plotted against scaled distance.

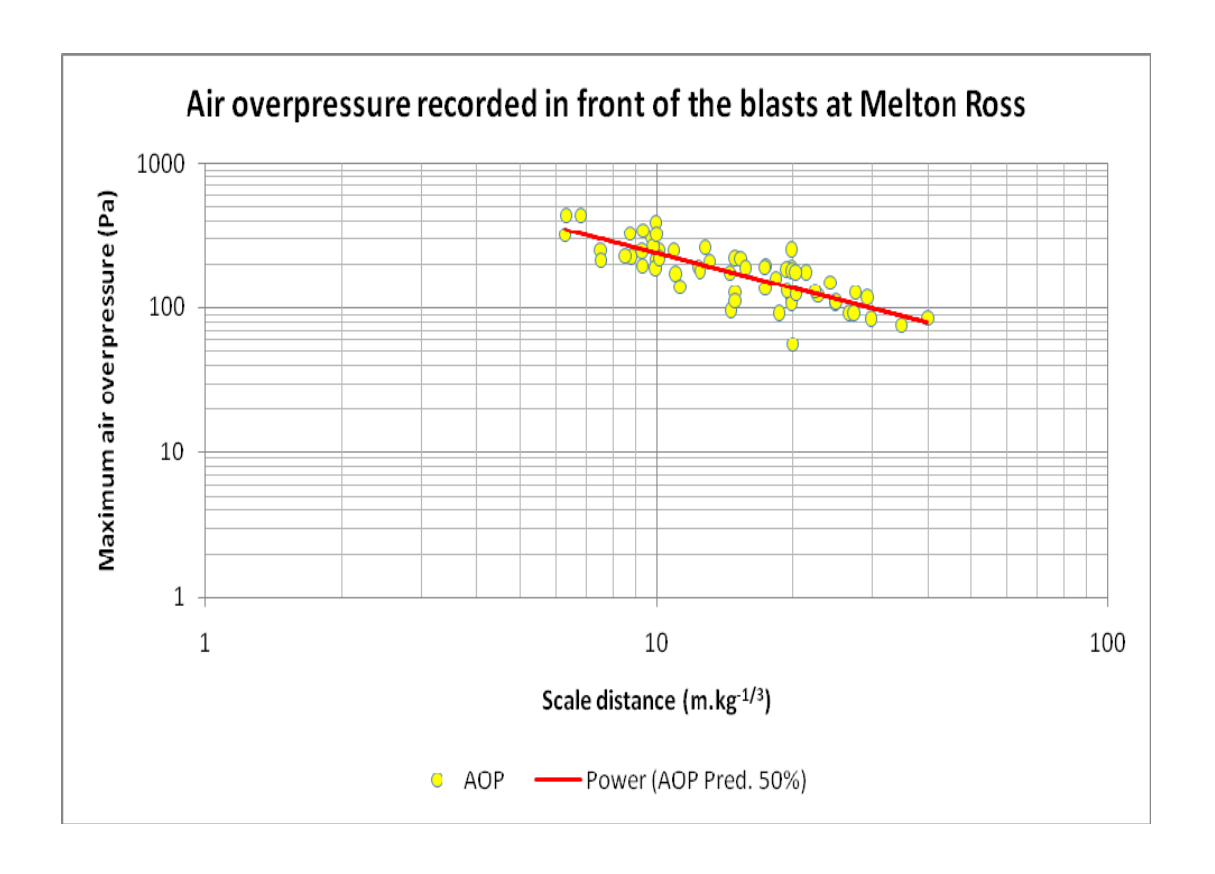


Figure 6.7 Regression model of air overpressure levels in front of the blasts at Melton Ross quarry

Statistical Summary		
Data Count	61	
Standard Error	0.269	
Correlation Coefficient	-0.79	

Site Factors		
Α	1489	
В	-0.796	
A (95%)	2316	

The data recorded in front of the blasts at Melton Ross show a relative tight fit around the mean regression line where the r^2 returned value is 0.79. This suggests that 21% of the variation in the data has not been explained.

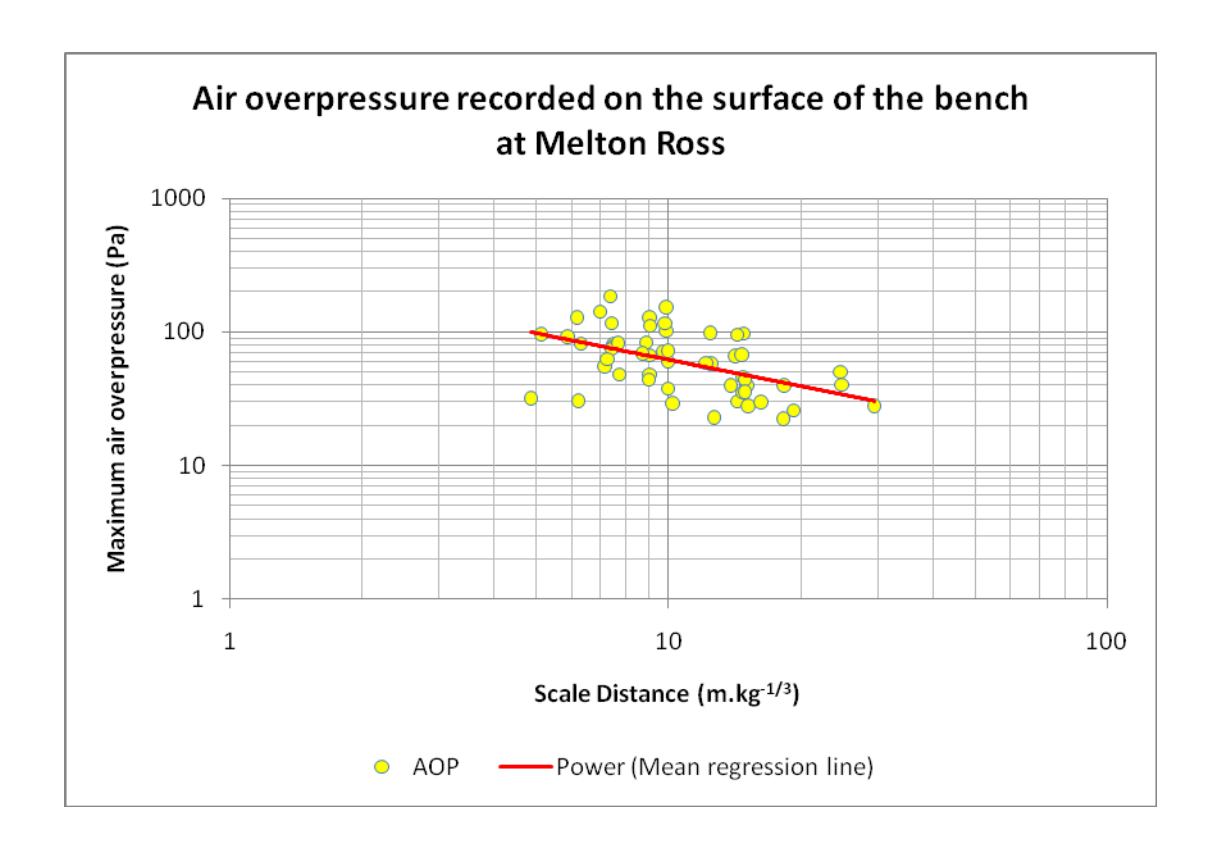


Figure 6.8 Regression model of air overpressure levels recorded on the surface of the bench at Melton Ross quarry

Statistical Summary		
Data Count	54	
Standard Error	0.459	
Correlation Coefficient	-0.5	

Site Factors		
Α	280.05	
В	-0.655	
A (95%)	594.3	

The air overpressure data recorded on top of the blasting bench for each of the blasts show a poorer correlation with scaled distance compared to the data recorded in front of the blasts. The scatter around the mean regression line is also much greater as seen in the standard error value.

In front of the blasts, the seismographs were deployed in a straight line leading from the first blast hole and perpendicular to the face, whereas on the bench surface, seismographs were positioned in three different ways; a straight perpendicular line with respect to the face leading from the first blast hole and also in a line parallel with to the face, on either side of the blasting pattern where possible (see Figure 6.9). The degree of scatter in the data shown in Figure 6.8 can be attributed to the monitoring locations differing in orientation to the blast. To examine the effect that

directionality of the blast has on emitted air overpressure levels, the data in Figure 6.8 has been separated by orientation to the blast (Figure 6.10). The data has been separated into three groups as shown below

- •data recorded at locations perpendicular to the face, directly behind the blast
- •data recorded at locations parallel to the face, in line with the blast holes where the firing sequence progresses towards the locations (AOP towards)
- •data recorded at locations parallel to the face, in line with the firing pattern where the firing sequence progresses away from the locations (AOP away)

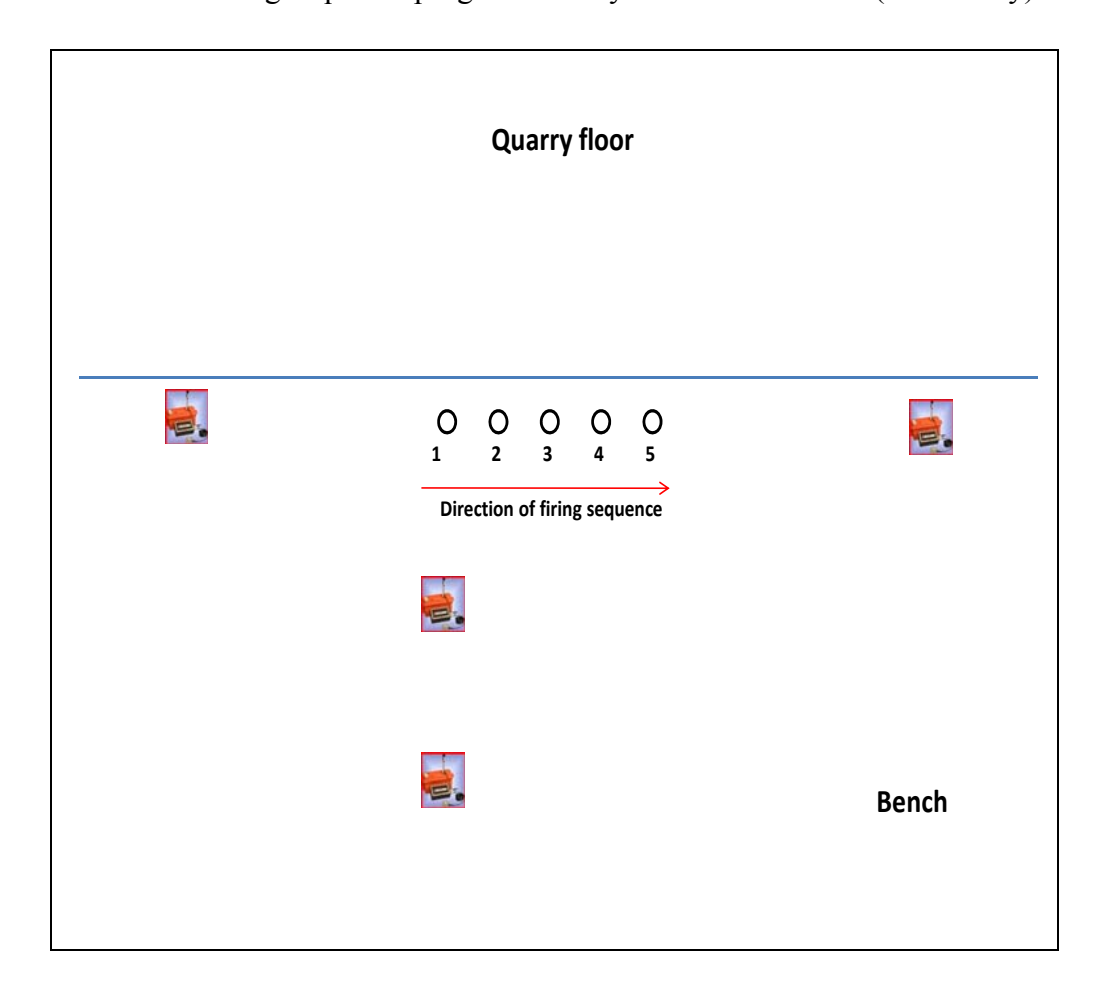


Figure 6.9 Example of monitoring locations on bench surface in relation to directionality of a blast

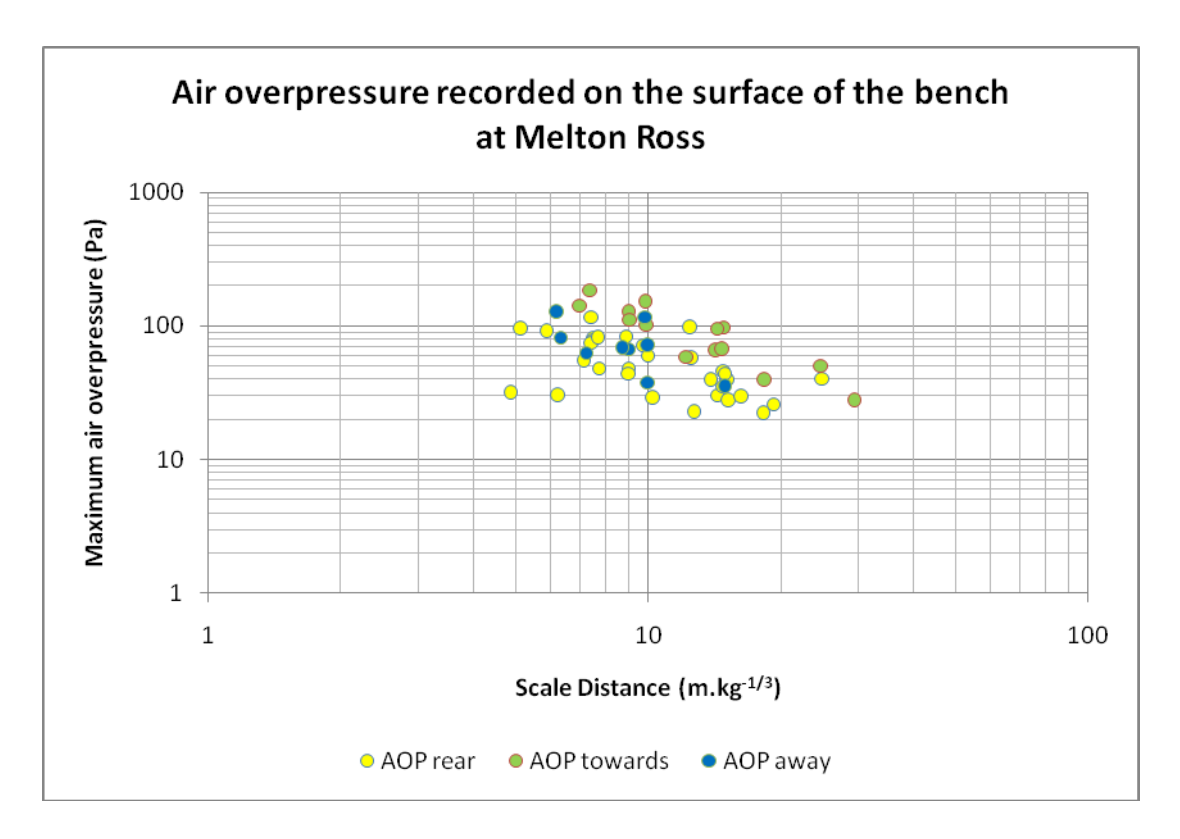


Figure 6.10 Regression model showing variations in air overpressure levels due to directionality in relation to the blasting pattern and firing sequence

There is a clear difference in maximum air overpressure values recorded in line with the blast as the blast progresses towards it compared to those recorded elsewhere on the bench. This is due to the construction interference of each blast wave per hole which results in wave front reinforcement (see section 2.4.6.).

Monitoring location in				Site f	Site factors	
relation to firing pattern	Data count	Standard Error	Correlation Coefficient	Α	В	
AOP behind blast	31	0.39	-0.54	211.5	-0.63	
AOP towards	14	0.224	-0.9	1559	-1.15	
AOP away	9	0.3	-0.66	658	-1.037	

Table 6.2 Statistical table comparing Air Overpressure levels on the top of the blast bench, behind the blast.

The statistics for each data set presented in Figure 6.10 have been tabulated above in Table 6.2. The statistics shows that on average that air overpressure levels are highest in the same direction as the hole firing order. This is shown by the site factor A value of 1559 whereas the air blast travelling directly to the rear of the blast is the lowest in magnitude of the directions.

The air overpressure travelling in the opposite direction from the hole firing sequence produces lower magnitudes in pressure due to the lack of interaction between each of the individual pressure pulses.

Figures 6.111, 6.12 and 6.13 are three air overpressure traces which have been recorded from a blast at Melton Ross. Each of the traces have been recorded at monitoring locations situated in different orientations to the blast hole pattern and firing sequence. The differences in the recorded pressure waves demonstrate the effect that wave interaction has on the overall air overpressure, depending the directionality from the blast. These three waveforms have been recorded from a five hole blast.

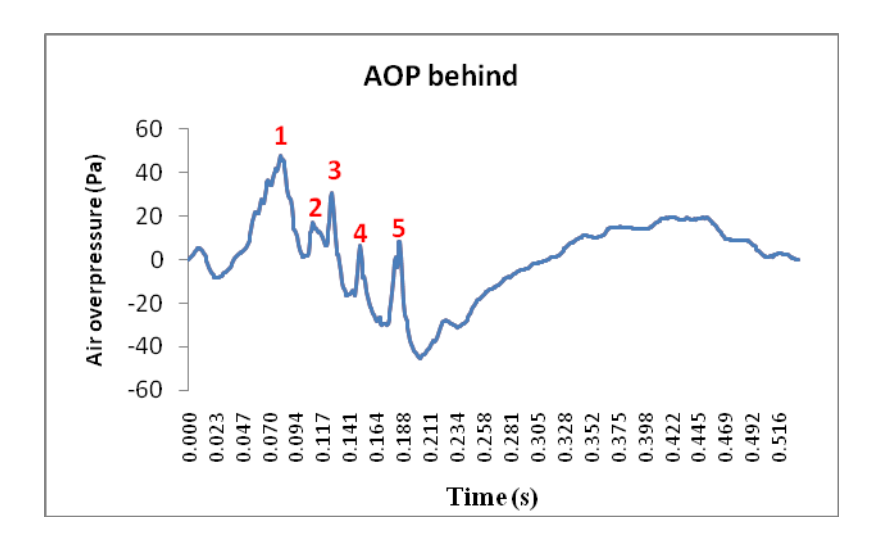


Figure 6.11 Air overpressure waveform on the blast bench perpendicular to blast pattern

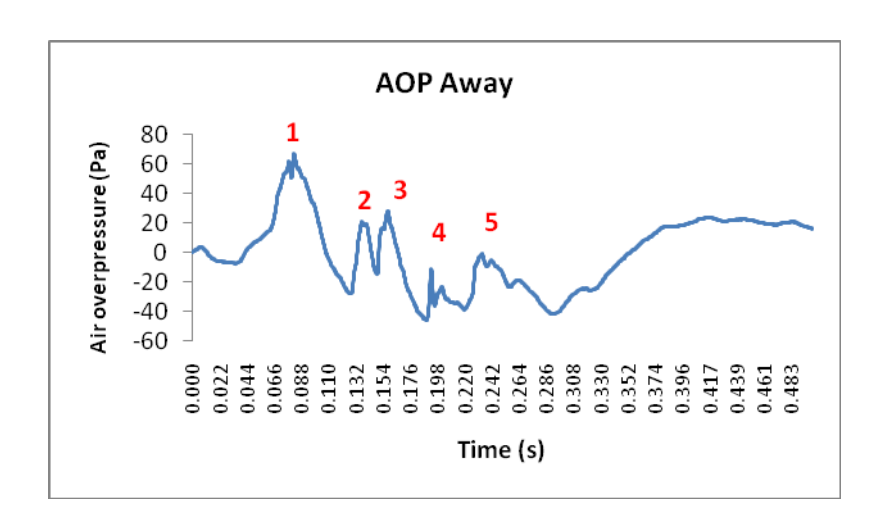


Figure 6.12 air overpressure waveform on the blast bench in line with the blast pattern and the timing sequence between holes going away from the monitoring point.

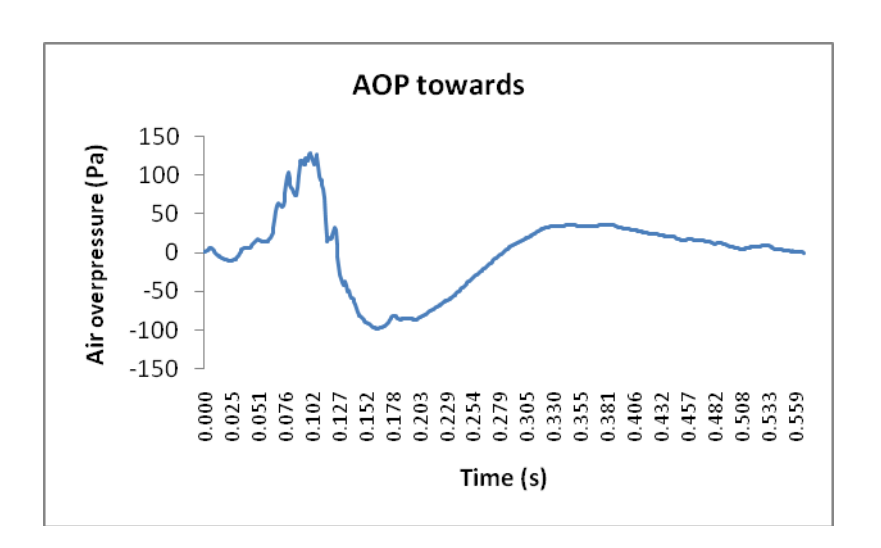


Figure 6.13 air overpressure waveform on the blast bench in line with the blast pattern and the timing sequence between holes going towards the monitoring point.

Where the firing sequence is progressing away from the monitoring location, the individual air overpressure pulses from each blast hole detonation are clearly evident. The same can also be said about the waveform recorded directly behind the blast. Due to the delay times between each of the blast holes and the direction in which the delay sequence is designed, minimal wave interaction occurs and when it does, it has a negative interaction effect i.e. the positive phase of the air overpressure

pulse interacts with the negative phase of the previous pressure pulse(s) and thereby reducing the amplitude of the pulse.

However, at a location where the blasting sequence is progressing towards a location, the opposite effect happens and the waves reinforce one another resulting in constructive reinforcement. This is where the positive phase of pulse interacts with a positive phase of another pressure pulse that is produced from a blast hole further along in the sequence. If a monitor is located along the same line as the blast holes, the time delay period separating the pressure pulses is reduced. As a result, the positive phase of the pulse superimposes itself on the positive phase of another pulse whereas in the two other locations as mentioned earlier, any pulse interactions occur with the positive phase superimposing onto a negative phase of another pulse. The extent of the reinforcement is dependent of the spacing dimension between the blast holes and the inter-hole delay times. The following formula can be used to determine the arrival times between each pulse.

$$\delta T = t_{th} \pm \frac{S}{V_{oto}}$$

Where:

 t_{ih} = inter hole delay time (ms)

S = hole spacing (m)

 V_{air} = is the velocity of sound in air (approximately 340m/s)

For example, if the inter hole delay is 17ms and the spacing between each of the holes is 4m, the arrival time between each pulse will be 28ms at a location in line with the blast. For the same scenario the arrival time between each pulse will be 6ms at a location in line with the blast where the delay sequence are firing towards it.

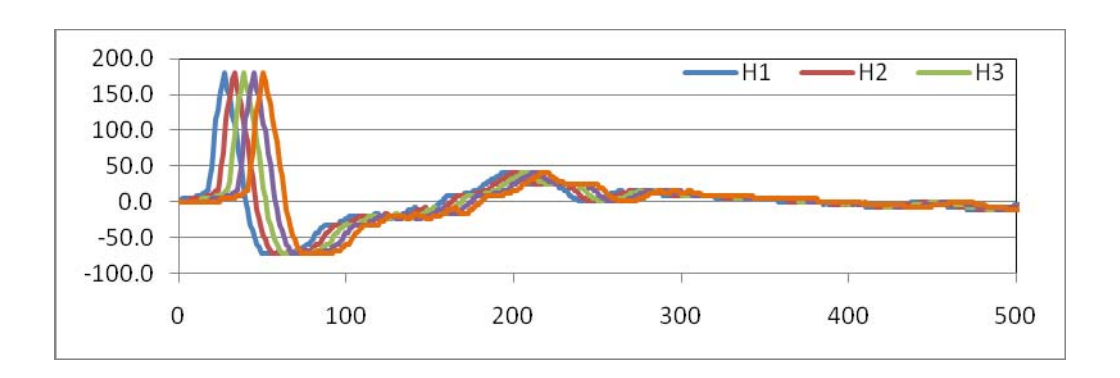


Figure 6.14 Example of the effects of wave front reinforcement - 5 single holes detonating so as to arrive at a monitoring location @ 6 milli second intervals.

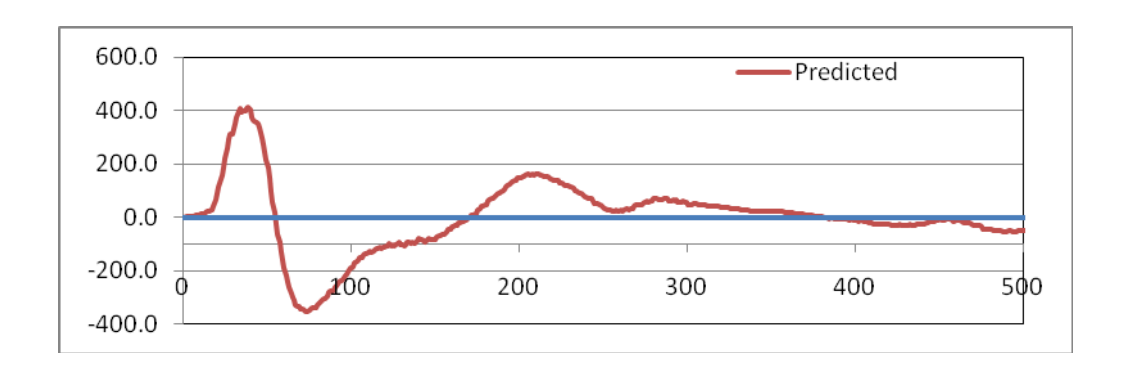


Figure 6.15 Example of the effects of wave front reinforcement - Resulting Air overpressure pulse from the combine effect of the 5 separate holes

In Figure 6.14 a waveform recorded from a single hole blast has been used to create a model of an air overpressure wave fitting to the example shown in Figure 6.15. The time between each arrival is 6ms. From elemental waveforms it can be seen that each hole creates an air overpressure level of 188Pa but due to the interaction with each hole, the resulting peak pressure level is 400Pa.

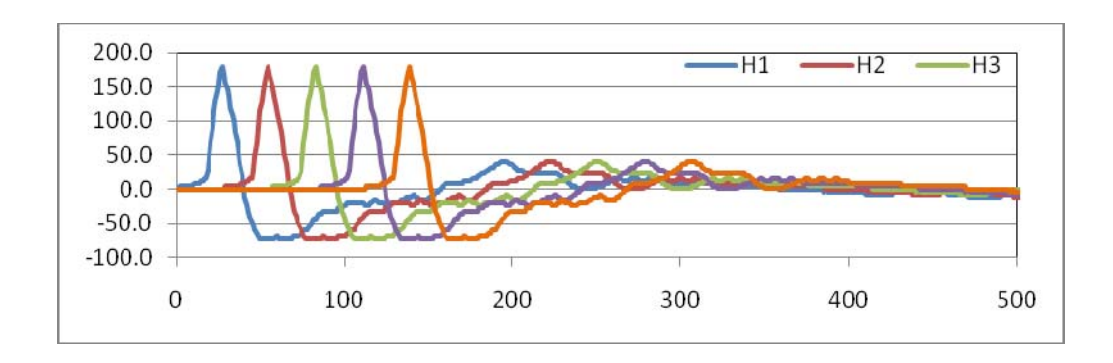


Figure 6.16 Example of the effects of wave front reinforcement - 5 single holes detonating so as to arrive at a monitoring location @ 28 milli second intervals.

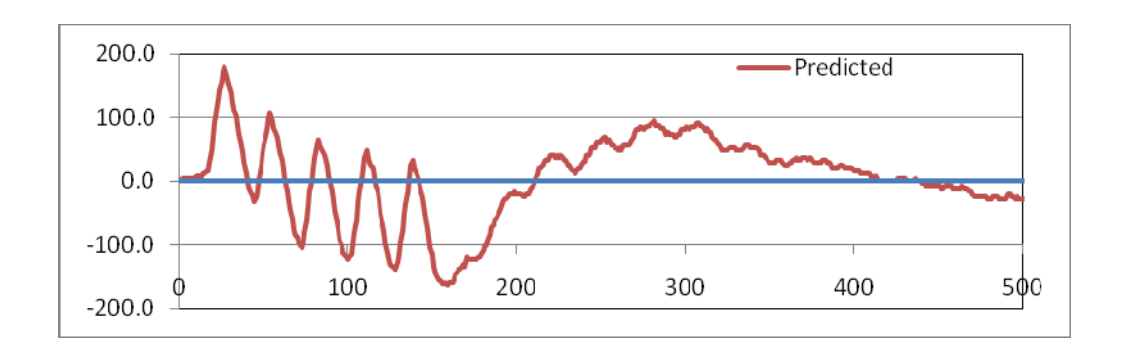


Figure 6.17 Example of the effects of wave front cancellation - Resulting Air overpressure pulse from the combine effect of the 5 separate holes

Five individual peaks can be seen, representing the pressure pulse from each detonated hole (Figure 6.16). Due to the time between the arrivals of each pulse being 28ms, the positive phase of each pulse interacts with the negative phase of the previous pulse and so the amplitude of the pressure pulses are reduced resulting in lower pressure levels. The model in Figure 6.17 is an example of what the pressure wave will appear when monitoring away from the blasting sequence. In this case it should noted that due to air overpressure pulse interaction the maximum air overpressure is associated with the first hole to fire. This is typical of most of the small scale blasts monitored at Melton Ross Quarry.

6.6 Comparisons of air overpressure levels between conventional bench blasting and fully confined 'buffer' blasting

Typical blasting operations at quarries employ a bench blasting method, where it is designed so that the rock will be fragmented and then projected from a free face into a 'working area' on a quarry floor where it can then be excavated. In the case of the blasts monitored during this investigation, the level of confinement ranged from 3 to 4 metre burdens and spacings. These can be termed as 'semi confined blasts'.

In contrast to this, a few blasts have been monitored at an opencast coal mine that carried out buffer blasts. The explosives are totally confined and are designed to fragment the rock sufficient for excavation and not to project the rock from a free face..

Two blasts have been monitored at Ffos-y-fran, on top of the bench and in front of the blast. The air overpressure was monitored at five locations for each blast, three seismographs were deployed on the bench and two in front of the blast. The recorded data is presented in Figure 6.13

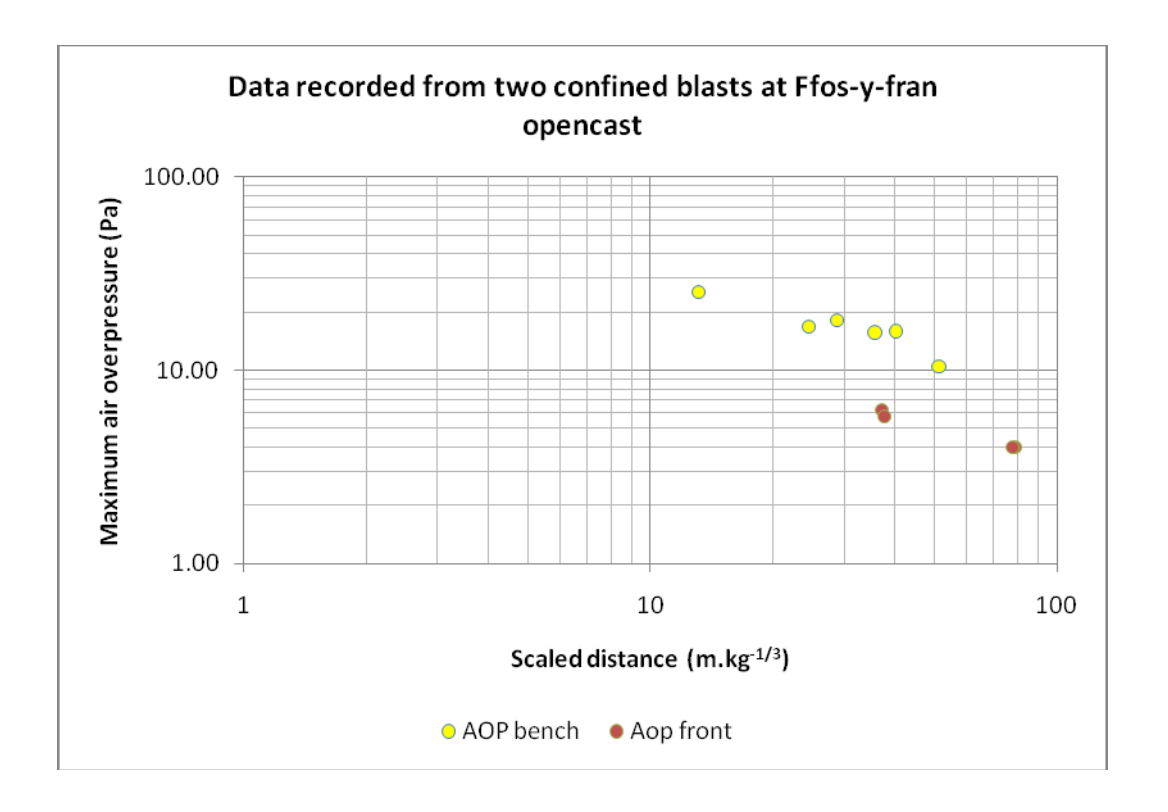


Figure 6.18 Regression model of air overpressure recorded from confined blasts

Interestingly the air overpressure recorded on the bench surface produced higher values in comparison to those recorded in front of the blasts. Due to the extent of the blast design, the blast holes were at a greater distance from the free face than the blast hole collar and so a large proportion of the explosive energy travelled up towards the bench surface, whereas in conventional bench blasting, the explosive energy is directed towards the free face. The magnitude of air overpressure generated was significantly lower than those produced from quarry bench blasting.

6.7 The influence of rock type on levels of air overpressure produced from blasting

If air overpressure originates from the face movement or from a shockwave arriving at the face, they are both influenced by the nature of the rock. The shockwave associated with a hard rock will generally propagate from the face at a faster rate than a soft rock and the speed of sound through rock and the magnitude of the disturbance arriving at the face will also be greater. To establish whether rock type has any influence on the resulting air overpressure produced from blasting, data recorded at various sites listed earlier in the chapter have been collated and input into a regression model (Figure 6.19).

The 'hard rock' data has been collected from Howick and Cragmill quarries where the rock blasted was basalt and whinstone. The data collected at Whitwell quarry has been used to represent the 'medium rock'. At this site, limestone was blasted. Representing the 'soft rock' is the data recorded at Melton Ross whose main production is from blasting chalk.

For the purpose of comparison all air overpressure data included in this analysis has been recorded in front of the blasts.

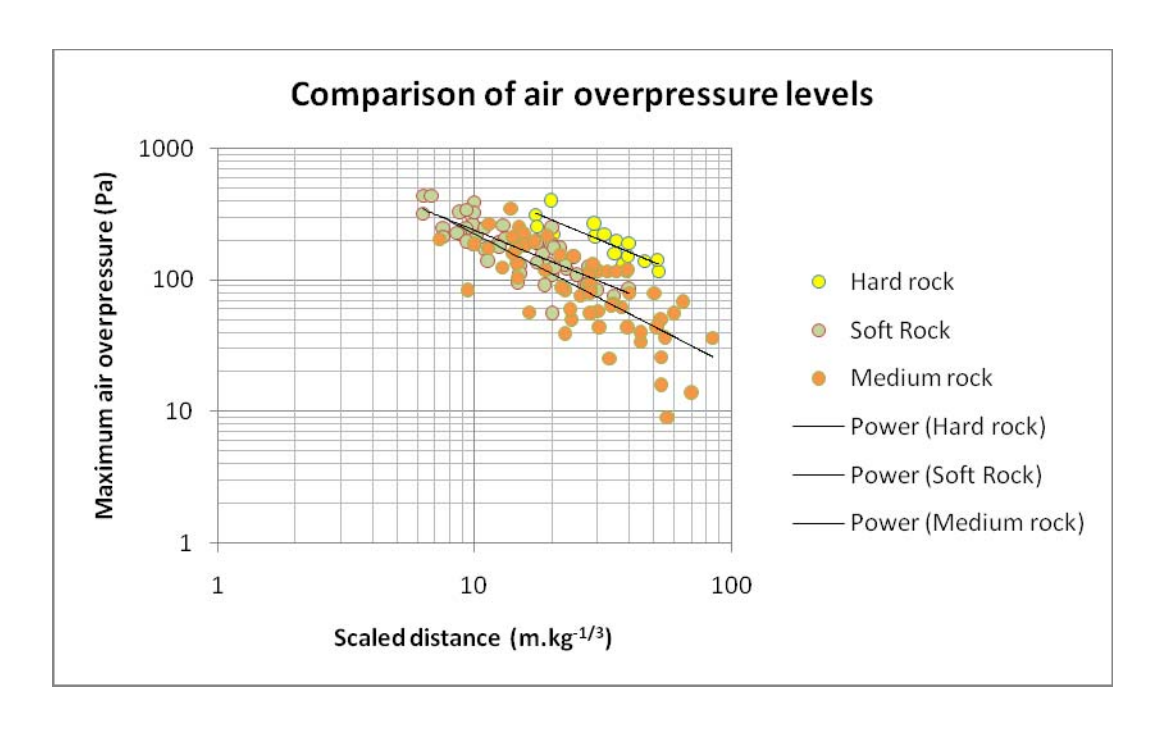


Figure 6.19 Regression model comparing air overpressure levels from various rock types

It is clear from the regression model (Figure 6.19) that the average air overpressure originating from hard rock blasting is of a higher magnitude than softer rock types. Interestingly, on average, air overpressure produced at Melton Ross is greater than that produced at Whitwell where the rock is harder (limestone compared to chalk at Melton Ross). However there is a very large degree of scatter amongst the 'medium rock' data set.

The equations for each mean regression line are as follows;

Hard rock: $y = 3224[M/Kg^{1/3}]^{-0.809}$

Medium rock: $y = 2278[M/Kg^{1/3}]^{-1.077}$

Soft rock $y = 1489[M/Kg^{1/3}]^{-0.796}$

These equations indicate that at unity, blasting harder rocks produces a higher air overpressure, however the rate of attenuation as indicated by the gradient of the mean regression line, does not follow the same trend. To provide a more accurate conclusion to how rock types influence the level of air overpressure and its

attenuation, a more balanced data set is required. In addition, the blast design at each site varied in terms of burdens, charge mass per delay, number of decks and face heights.

6.8 Conclusion

The collection of data relating only air overpressure values to distance and explosive charge weight in the form of a scaled distance relationship is insufficient for environmental control purposes as the resulting scatter of the data [standard error] will be too great and the correlation too poor.

A significant improvement in both the standard error and the correlation coefficient can be made if the AOP data set is divided into two unique sub sets. The two sub sets should be

- 1. all the data from observation locations in front of the line of permanent displacement (i.e. in front of the quarry face to be blasted).
- 2. all the data from observation locations behind the line of permanent displacement (i.e. behind the quarry face to be blasted)

The analysis has shown that the directionality of blasting is a very important factor when trying to avoid air overpressure disturbances outside the quarry boundary. If this is known to be a problem, it is imperative to take note of the direction in which the blast holes are fired within the delay sequence and the delay times between the blast holes so that positive interaction between the pressure pulses are reduced or if possible, avoided.

To determine whether the rock type has an influence on the magnitude of air overpressure produced during blasting, a more controlled comparison is required where blast designs do not vary from site to site.

Chapter 7

Field investigation, with respect to orientation and distance from an explosive source, into the interaction of multiple short delay detonations in free air

7.1 Introduction

The aim of this field investigation was to determine how blast waves interact with each other as they attenuate. Firstly by examining how the blast waves produced from a single surface initiation attenuate by monitoring the waves in different orientations. Then by examining how multiple explosive initiations in "free air", with different delays, interact and attenuate in different orientations. This is then compared to how blast waves attenuate in different directions when they are produced from confined holes, such as those typically used in quarry blasting.

The air overpressure from all of the trial shots were recorded by several seismographs located at surveyed distances, at pre determined orientations from the line of initiation (see Figure 7.1). A base line was established (0 degrees) together with three additional lines; perpendicular (90 degrees), 60 degrees, and 30 degrees. The seismographs were set up at know distances from one another, 2 pairs of seismographs were connected with one another, one pair of seismographs was set up parallel to the line of initiation and one pair of seismographs was set up perpendicular to the line. The closest unit to the point of initiation of the paired seismographs triggered both units to record in order that the speed of the air overpressure pulse could be determined. This is done by examining the time difference between the units recording the arrival of the air overpressure pulse across the known distance. All other seismographs were triggered to record the air overpressure levels to determine how the magnitude of the pulse attenuated with both distance and orientation.

There were 6 tests conducted, including three single points of initiation and three, 5 point initiation on delay timings. The firing points consisted of 1m lengths of 12g/m detonation cord suspended from bamboo poles positioned 4m apart, initiated by electronic detonators.

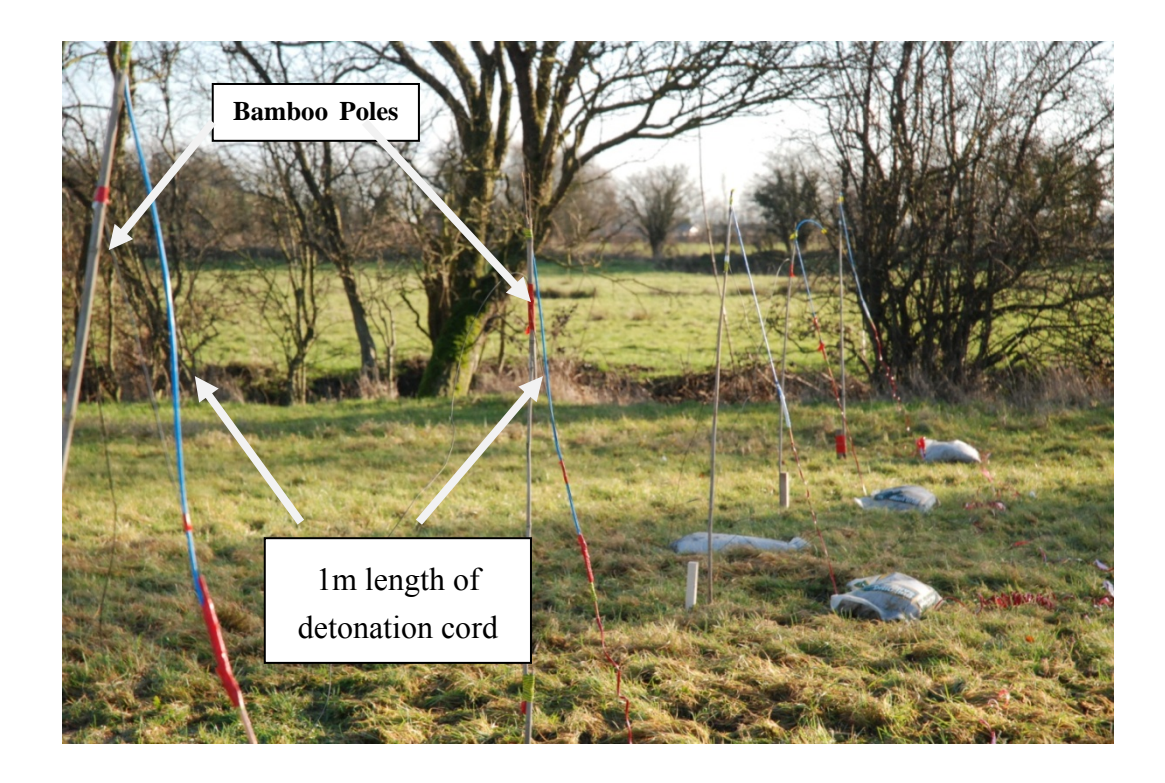


Plate 7.1 Setup of five 1m lengths of detonation cord suspended on bamboo poles, spaced 4m apart

The delay timings between each of the firing points for the three multi point detonations consisting of 5 point initiations were 25ms between firing points, 8ms between firing points and 12ms between firing points except for the last (5th) point which was fired 1ms after the 4th. These tests were all fired such that the imitation propagated towards the seismographs that had been placed on the base line. The distance between each firing point was chosen so as to simulate typical spacing between drill holes commonly used in quarry blasting.

Optical fibre cable was used to trigger the MREL Microtrap to start recording the air overpressure from the two connected microphones. The low frequency air overpressure microphones were set out on tripods and positioned at alongside seismograph units 4227 and 11705 (see Figure 7.1). The ends of the optical fibre cable were inserted into a 120 x 10mm glass tube and strapped to the detonation cord, adjacent to the detonator as shown in plate 7.2. The optic fibre cable was then connected to the optical interface unit which triggers the Microtrap to record once the emitted light from the detonation travels along the optic fibre cable. The use of the optic fibre triggering system is fully explained in chapter 5.

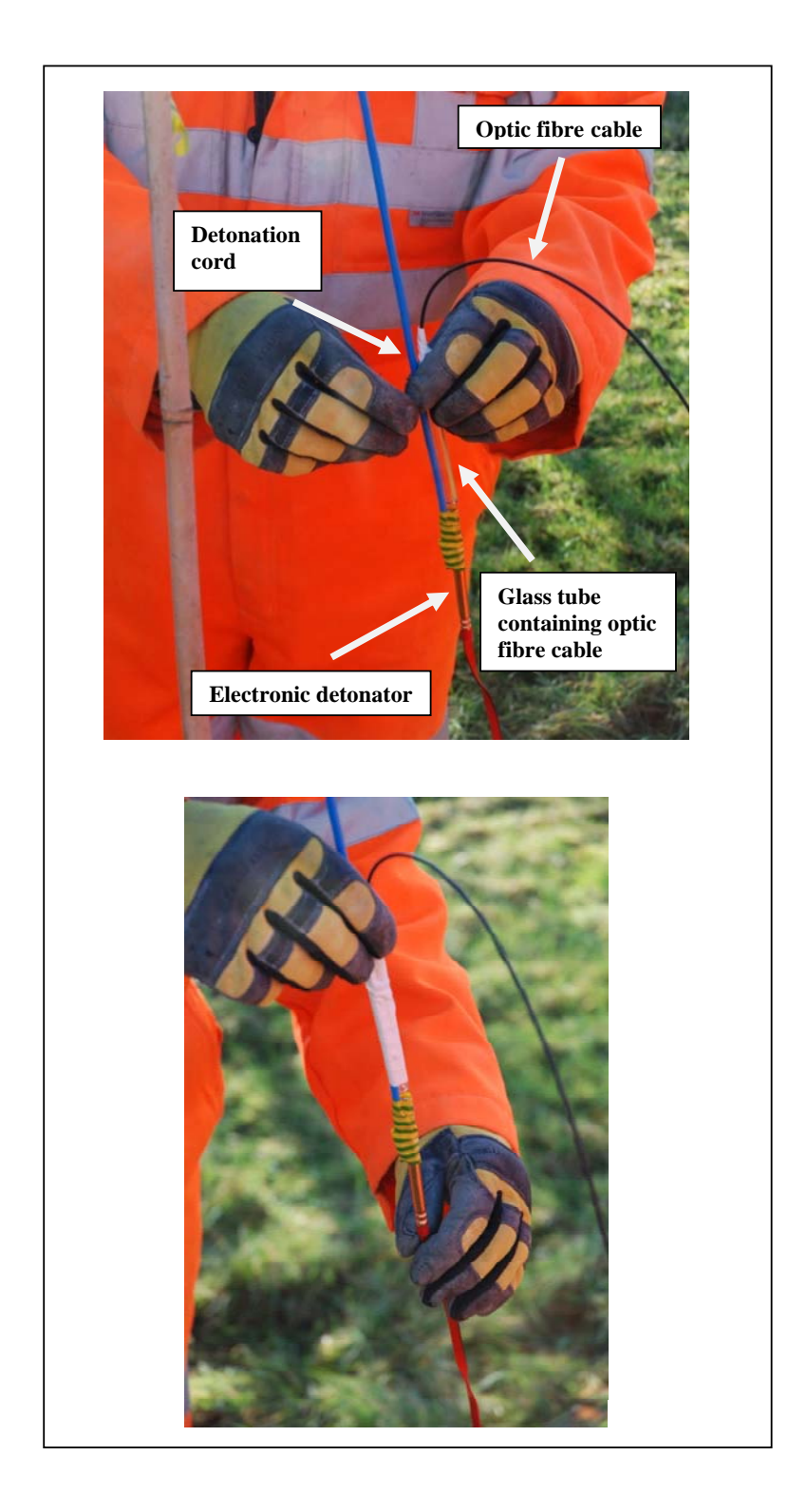


Plate 7.2 Close up of the electronic detonator connected to the detonator cord which in turn is strapped to the glass tube with the optic fibre cable in it.

The monitoring equipment was positioned in such a manner as to be able to examine how air overpressure pulses interact with each other during a simulated quarry blast. Below is a diagram (fig 7.1) showing the locations of the seismographs

in relation to the firing locations. The serial unit numbers of each seismograph have also been included.

The surface firing points were initiated from the left to the right (with respect to the plan in Fig 7.1) with all the monitoring equipment positioned to the front and right of the simulated blast. If the simulated blast was initiated in a sequence away from the monitoring locations, right to left in this case, then there would be very little or no interaction. This is due to the fact that the air overpressure pulse of the first point of firing would 'outrun' the pulses of the following points of firing.

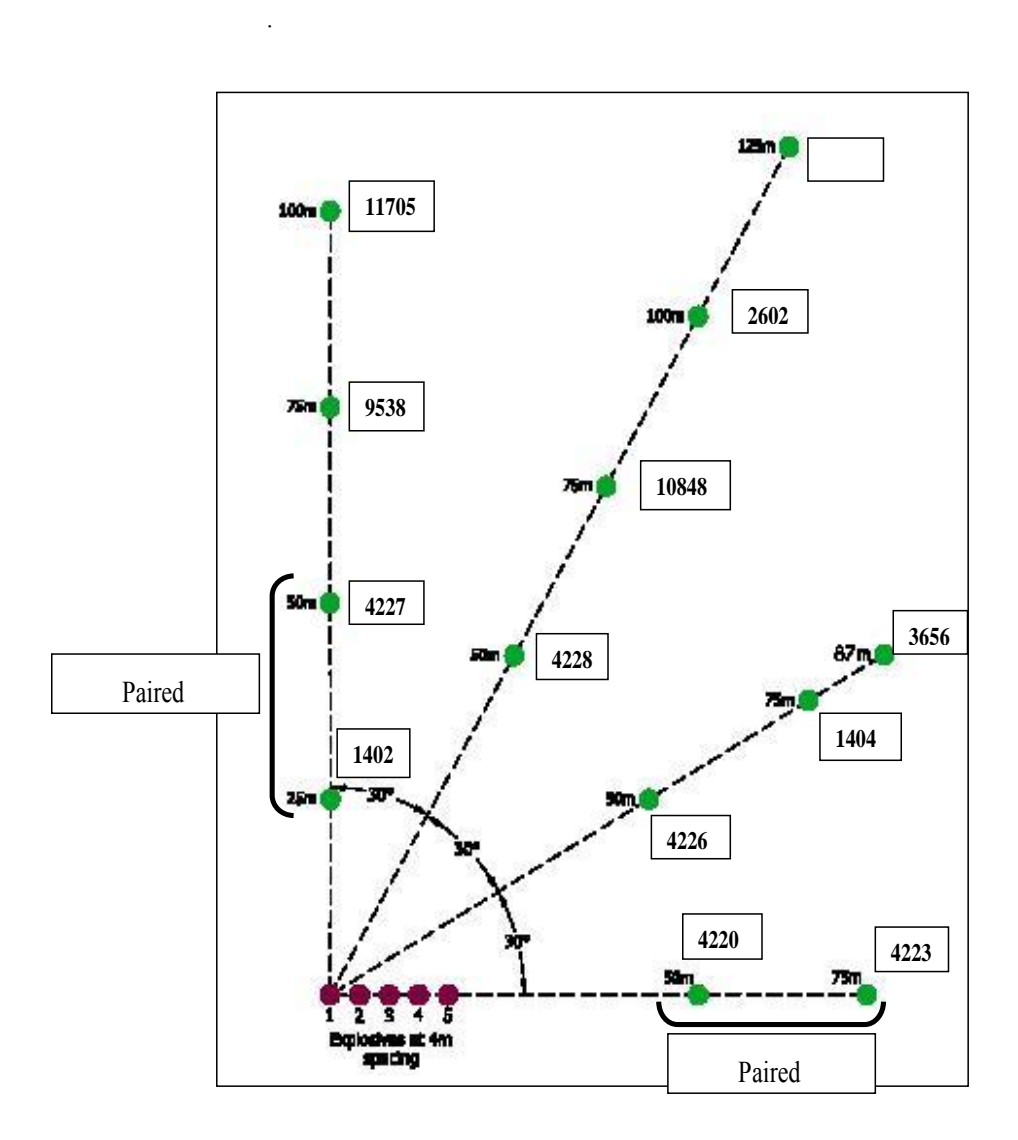


Figure 7.1 Plan of the monitoring locations

7.2 Results

The results from the field investigation have been sub divided into the individual tests. It should be noted that seismograph units 4223 and 3656 did not trigger during any of the tests. The reason for this is unknown.

As the charge weights used in the field trials were constant, throughout this section, air overpressure (measured in Pascals) has been plotted against distance instead of scaled distance.

7.2.1 First Test – single charge

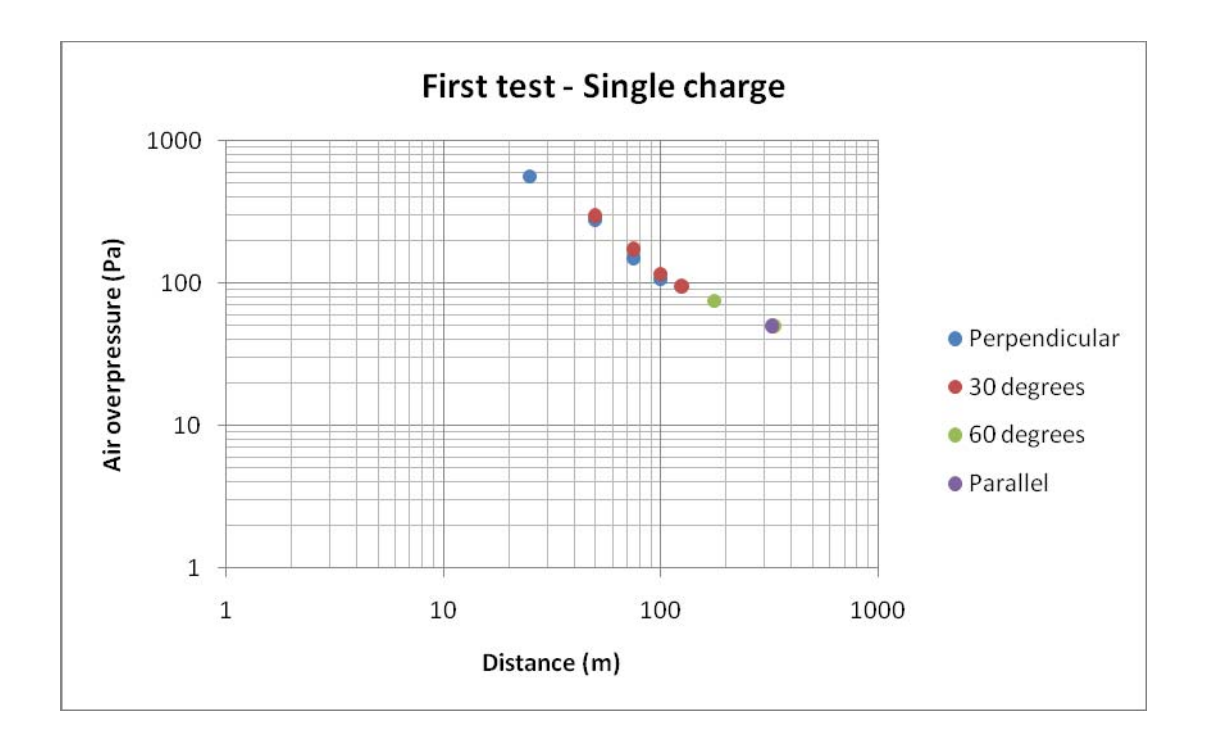


Figure 7.2 Results from the first single charge test

From the results of this test, it is clearly demonstrated that the directionality or orientation of the monitoring locations in relation to the single charge shows no variation in air overpressure magnitudes. This is expected due to the pressure wave produced upon detonation of the explosive expands and travels spherically without any interaction of pressure waves from additional explosive charges.

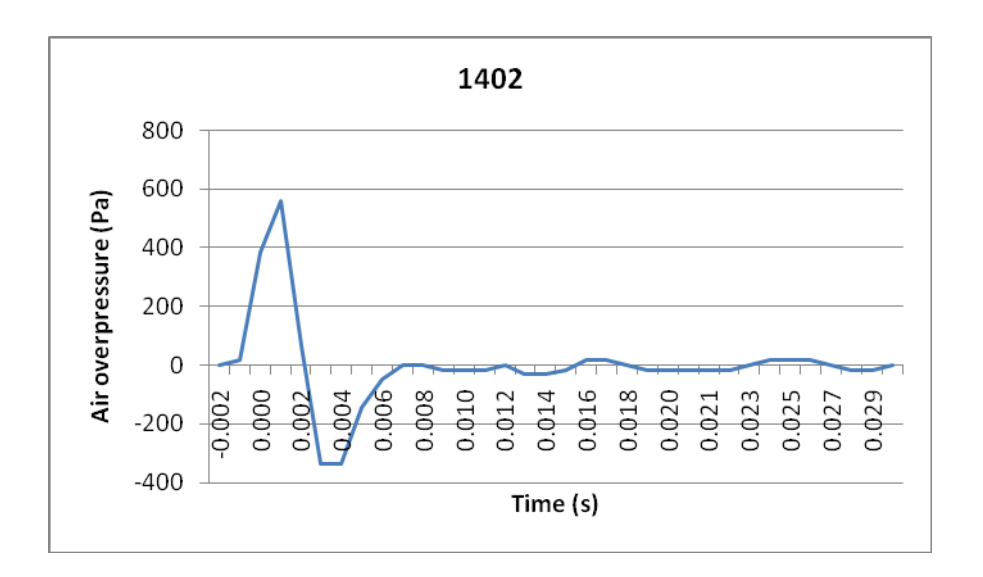


Figure 7.3 Air overpressure waveform recorded from the first test

The waveform in Figure 8.3 shows a very fast rise and fall of the initial pulse (positive phase of the wave). The time duration of this phase is an indicator to the VOD of the explosive and length of explosive column whilst the amplitude of the pressure pulse is a reflection of the explosive mass.

Due to the high VOD of the explosive and the limited sample rate of this seismograph (1024sps), the positive phase of the trace only consists of four samples thus making it impossible to record a smooth curve. This will inevitably place a limit on the effectiveness of using the waveform for modelling theoretical unconfined blasts with the linear superposition model as described later in chapter 9. It may therefore be necessary to use the signature waveforms recorded by Instantel Minimate II seismographs, which have a higher sample rate of 4096sps. The improvement of the waveform with contains four times as many samples is evident in Figure 7.4.

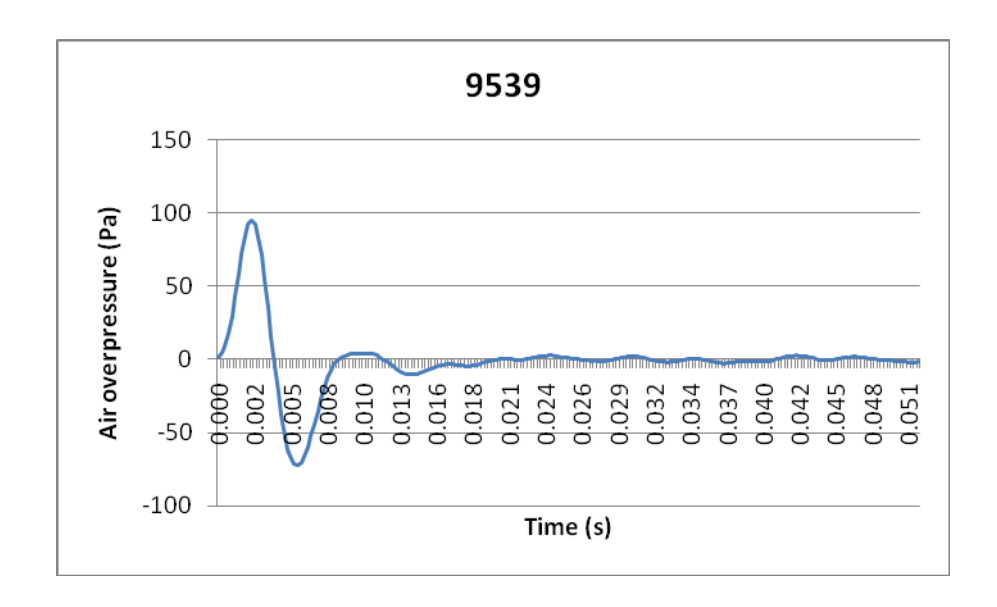


Figure 7.4 Air overpressure waveform recorded at 4096sps

7.2.2 Second test – single charge

The results from the second test are similar to the first test, showing very little scatter in the data set, as shown in Figure 7.5.

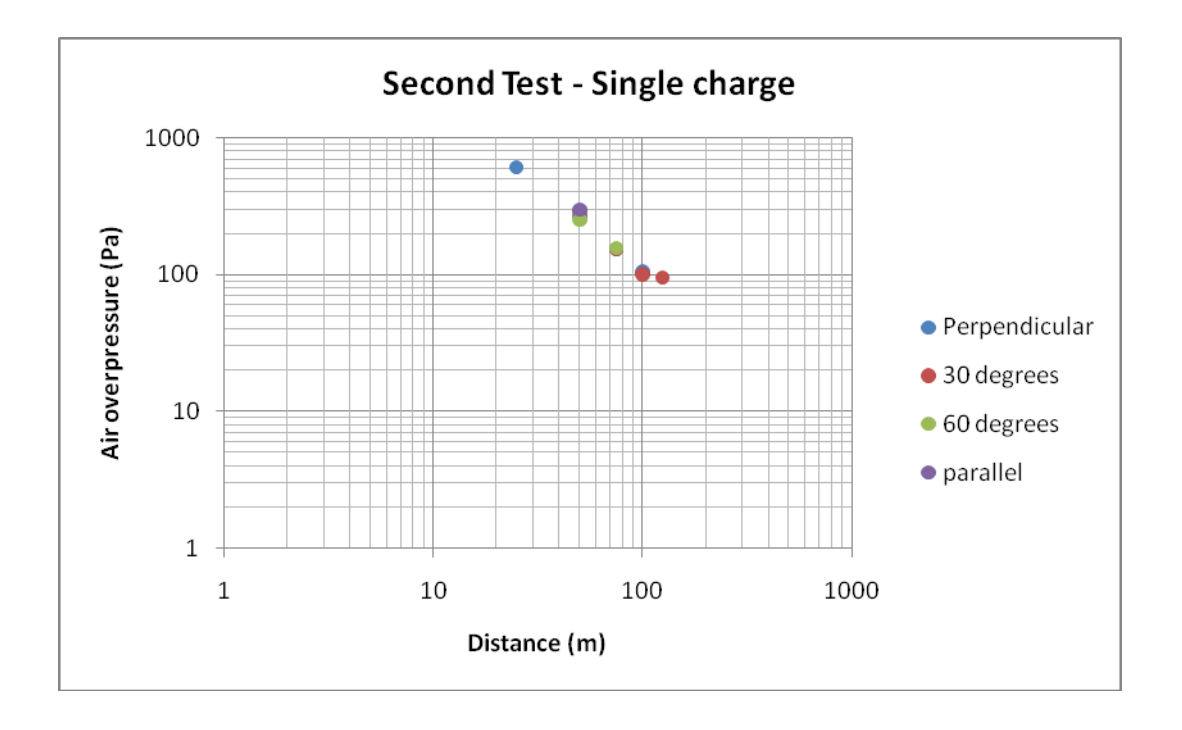


Figure 7.5 results from the second single charge test

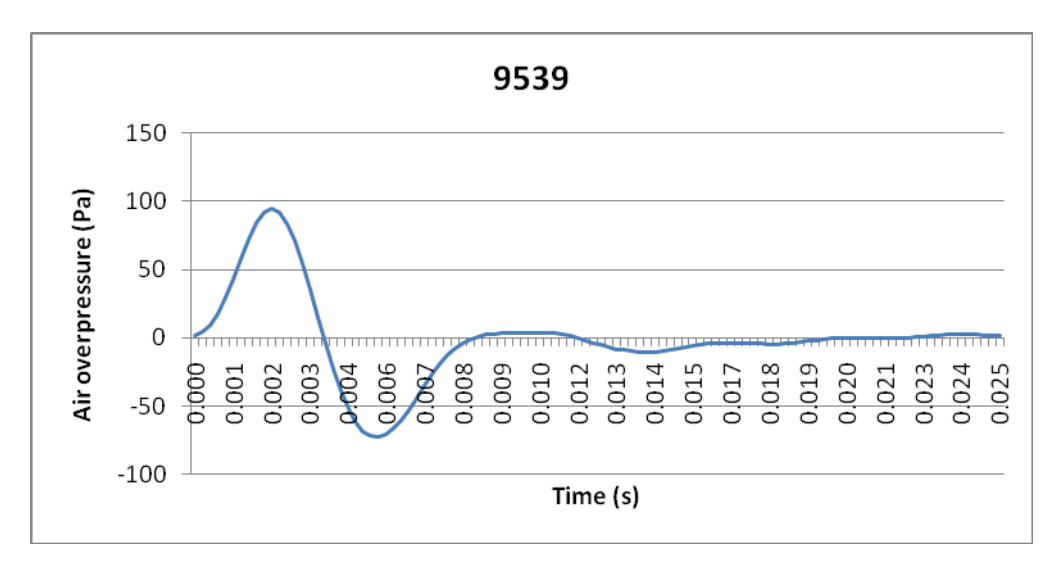


Figure 7.6 Air overpressure waveform recorded from the second single charge test

Figure 7.6 is the output from Instantel seismograph 9539 (sampling at 4096 sample per second) and shows a much smoother wave form than would be possible from a seismograph that can only sample at 1024 samples per second.

7.2.3 Third test – 5 charges with a 25ms delay

The third test consisted of 5 lengths of shock tube, positioned 4m apart and was detonated with a 25ms between each of the charges with the result that the time duration for the blast was 100ms. The results illustrated in Figure 8.7 show a small degree of scatter amongst the data points.

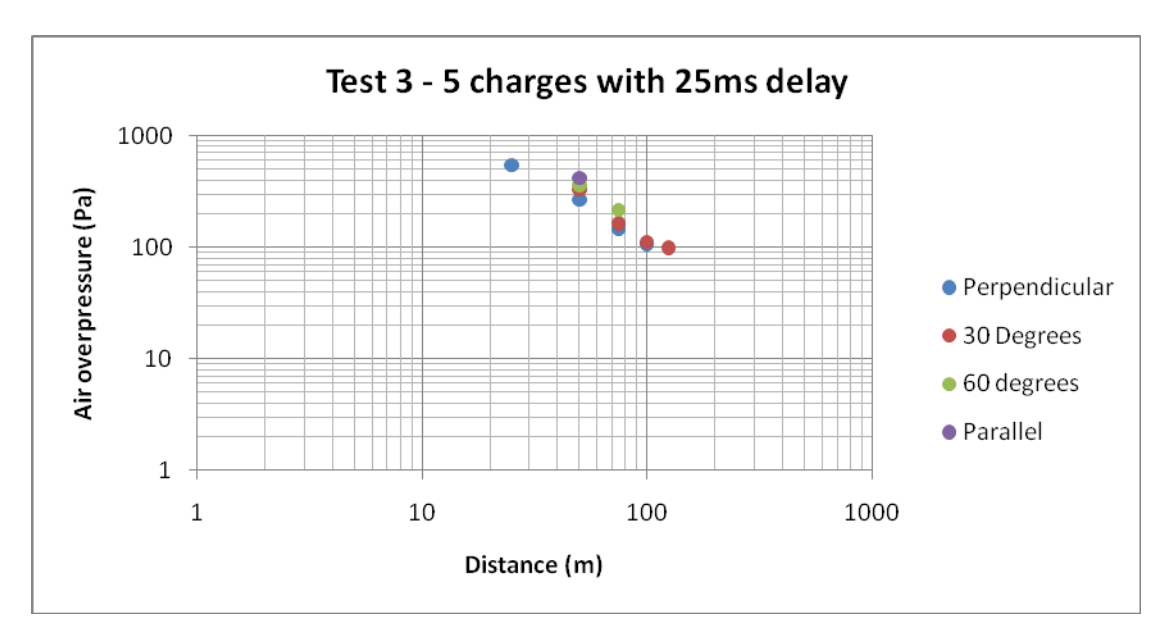


Figure 7.7 Results from the third test

It is evident from the plot that as the angle from the first charge increases (i.e. from 0 towards 90 degrees) so the magnitude in air overpressure decreases. Thus the

highest air overpressure level is recorded on the base line in line with the five charges, showing a pressure level of 416Pa at a distance of 50m whereas directly in front of the first charge, at a distance of 50m, a maximum value of 268Pa was recorded (see figure 7.1).

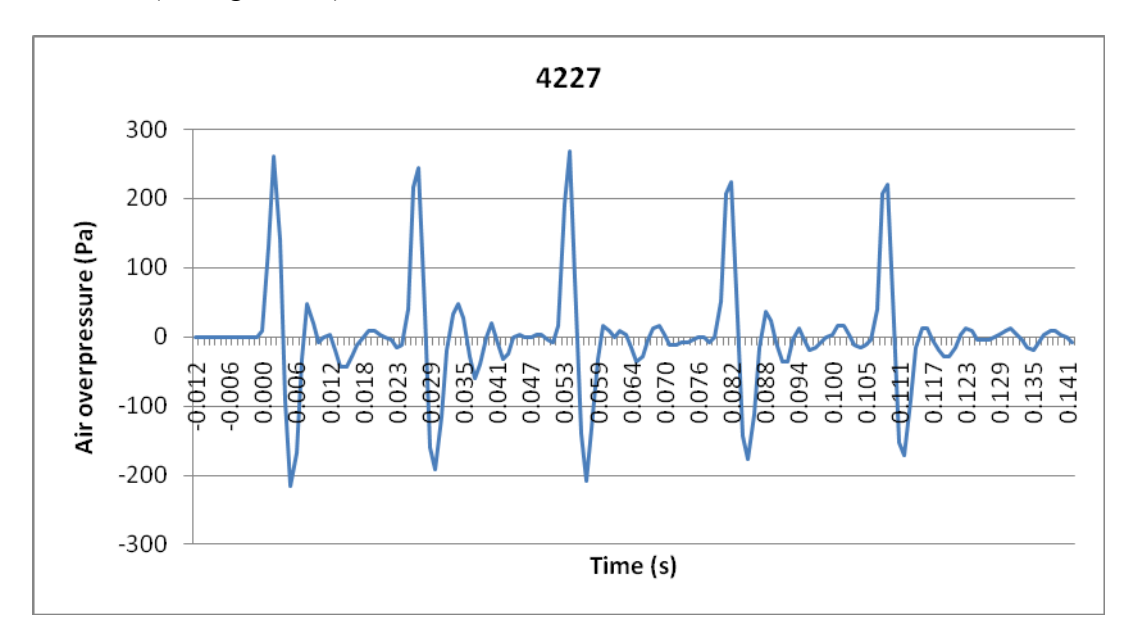


Figure 7.8 Air overpressure traces between locations perpendicular to the charges at a distance of 50m

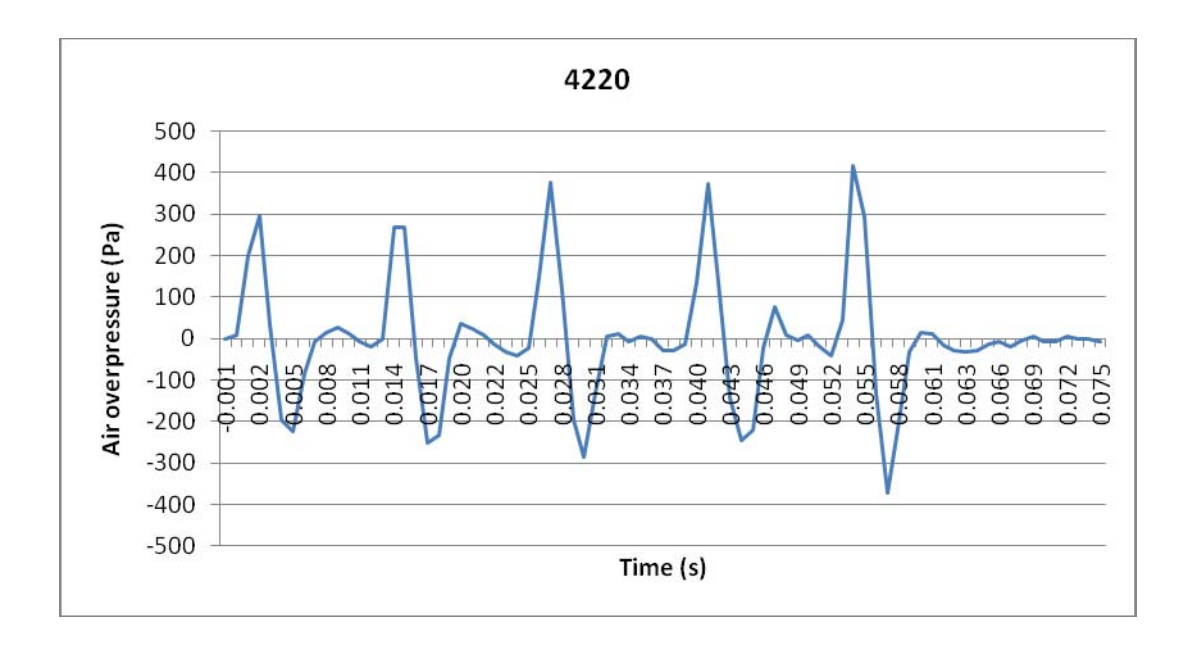


Figure 7.9 Air overpressure traces between locations parallel to the charges at a distance of 50m with the firing sequence towards the monitoring location.

The reason for the increase level of air overpressure along the base line in the direction that is parallel with the five charges is not due to wave interaction but because of the incremental decrease in distance of 4m for each successive explosive initiation.

It is evident from the single waveform in Figure 7.6 that the duration of the entire wave is approximately 8ms and thus with a delay time of 25ms between each explosive being detonated in combination with the speed of sound in air on the day (336m/s), the pressure pulse from each explosive would be unable to interact together. Seismograph unit 4220 is located 50m from the first explosive, as is the case with seismograph unit 4227, however 4220 is located only 38m from the fifth explosive and this significant decrease in distance (some 30%) explains the rise of amplitude of each pressure pulse in the air overpressure trace (Figure 7.9) as the explosive initiations progress towards seismograph 4220.

7.2.4 Fourth test – 5 charges with a 8ms delay

The fourth test again consisted of 5 explosives but with a significant reduction in delay period (delay of 8ms between each initiation). Seismograph units 9539 and 2602 also did not trigger during this test. It is not known why unit 2602 did not trigger however the battery of unit 9539 became depleted and was not able to be used in the later tests.

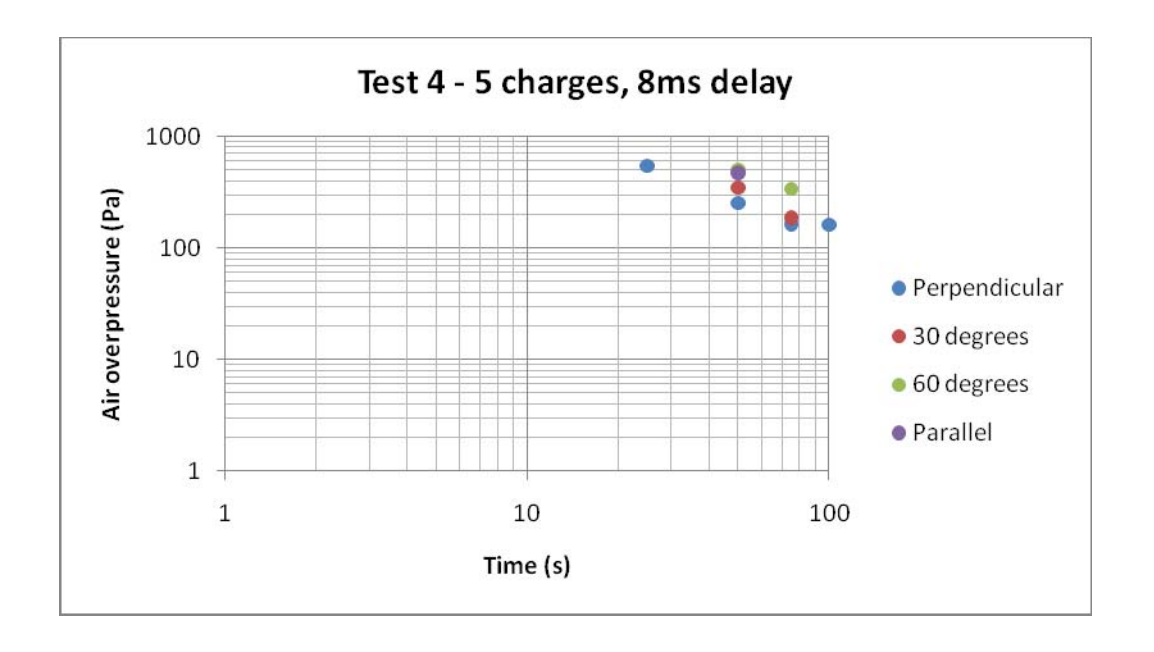


Figure 7.10 Results from the fourth test

Once again it is evident from the plot that as the angle from the first charge increases (i.e. from 0 towards 90 degrees) so the magnitude in air overpressure decreases. Thus the highest air overpressure level is recorded on the base line in line with the five charges.

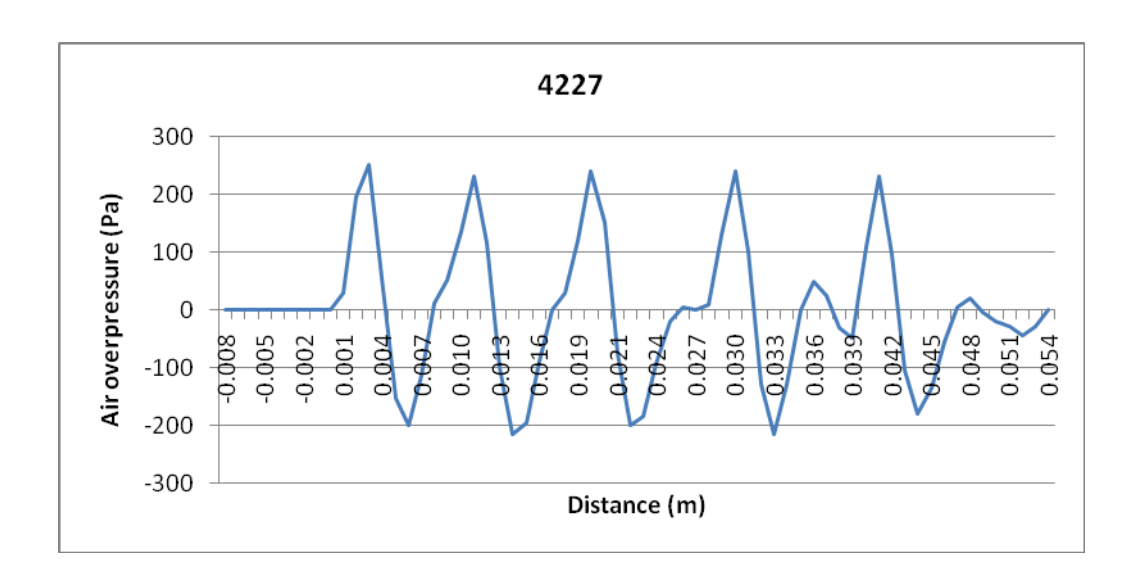


Figure 7.11 Air overpressure traces between locations perpendicular to the charges with 8ms delay times.

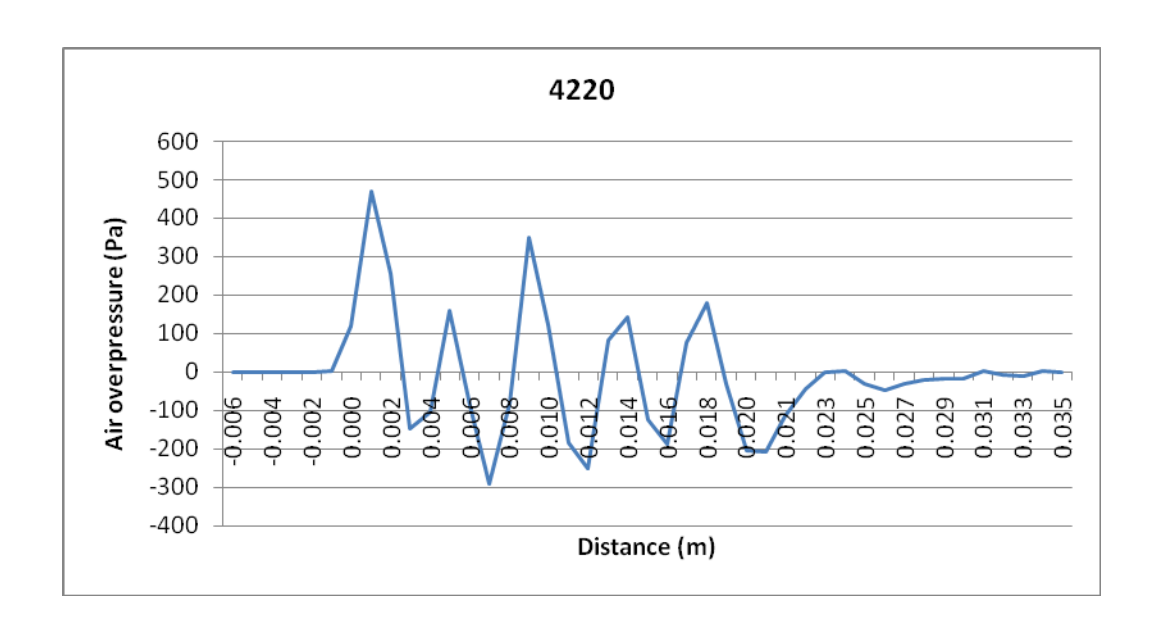


Figure 7.12 Air overpressure traces between locations parallel to the charges with the firing sequence towards the monitoring location 8ms delay times.

Here the data recorded by seismograph unit 4227 displays five individual peaks with consistent amplitudes (figure 7.11). The data recorded by seismograph unit 4220 (figure 7.12), shows the five individual peaks but with varying amplitudes. This is an effect of the interaction between pressure pulses from each explosive.

The time difference between the creation of a pressure wave and the arrival of the pressure wave generated by the previous detonation is given below.

$$\partial t = t_d \pm \frac{S}{V_{ode}}$$

Where:

 T_d = delay time (ms)

S = Spacing (m)

 V_{air} = velocity of sound in air (m/s)

A separation time of 3.76ms shows that the pressure pulse of the previous detonation (approximately 8ms) interacts with the adjacent pulse. The negative phase of pulse one arrives as the positive phase of pulse two is created which leads to deconstructive interference resulting in a reduction in the amplitude of pulse 2 as can be seen in Figure 7.12. This has a chain reaction effect on subsequent pressure waves in the blast.

7.2.5 Fifth test – 5 charges with a delay of 12ms & 1ms

The fifth test consisted of five explosives with a 12ms delay time between explosives one to four and a 1ms delay between the fourth and fifth explosive. [it should be noted that for some in explicable reason, Seismograph unit 4226 did not trigger during this test}.

The results from the test show a similar trend to the third and fourth test (see Figure 8.11).

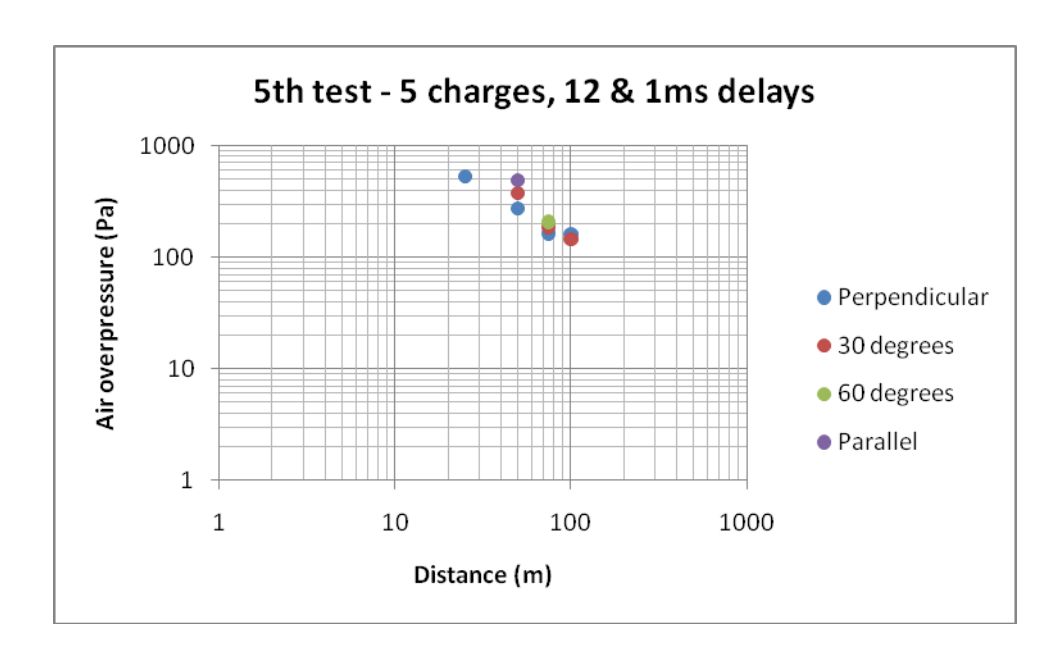


Figure 7.13 Results from the fifth test

Figure 7.14 and Fig 7.15 show the comparison of air overpressure traces recorded perpendicular and parallel to the blast. It is clear from the traces that the 1ms delay between the fourth and fifth explosive has a great effect on the amplitude of air overpressure at the end of the trace. Perpendicular to the blast, the pressure pulse from the fifth charge interacts with the negative phase of the previous pressure pulse resulting in a much lower pressure value (fig 7.14).

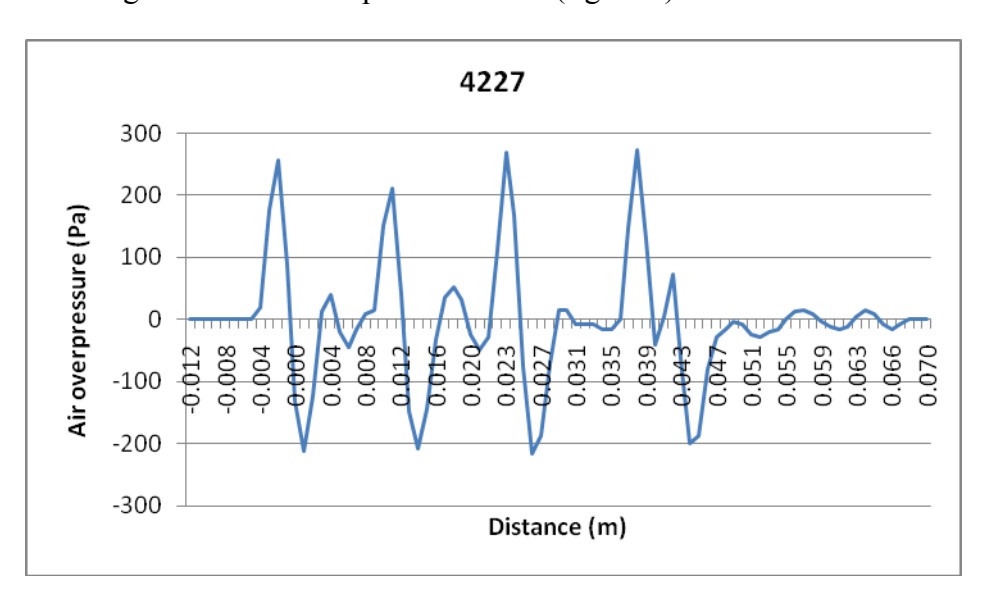


Figure 7.14 Air overpressure traces between locations perpendicular to the charges with detonations 1 to 4 @ 12ms & detonation 5 @ 1ms delay times.

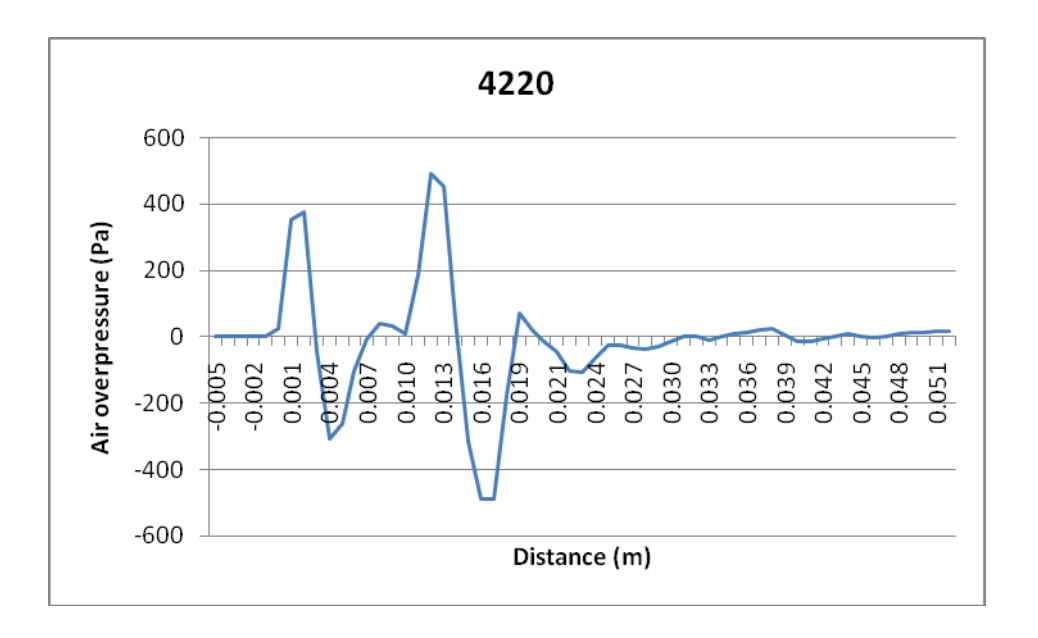


Figure 7.15 Air overpressure traces between locations parallel to the charges with detonations 1 to 4 @ 12ms & detonation 5 @ 1ms delay times.

Interestingly, the data recorded by seismograph unit 4220 shows only two distinct peaks. From the calculation in 7.2.4, the time taken for the pressure pulse to travel to the location of the next explosive is 11.76ms. This means that the pulse has arrived 0.24ms before the adjacent explosive has detonated and therefore the two pressure pulse superimpose onto one another. As a result of such close interaction in the direction towards 4220, the magnitude of the air overpressure is vastly increased and becomes more difficult to determine the peak values produced by each detonated explosive.

7.2.6 Sixth test -3^{rd} single charge

The sixth and final test involved a single charge.

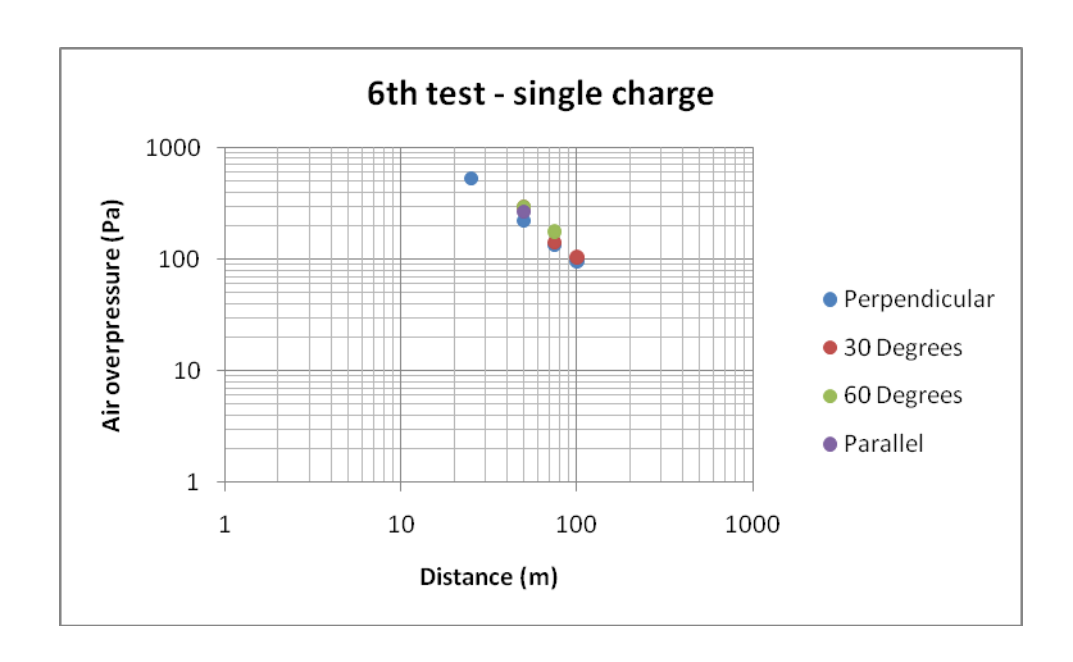


Figure 7.16 Results from the sixth test

The results show a small degree of scatter which is not present during the previous single charge tests. This may be due to windy conditions which had developed later that day and so the pressure waves were carried further in the direction of the 60 degrees line of seismographs, resulting in a lower rate of attenuation.

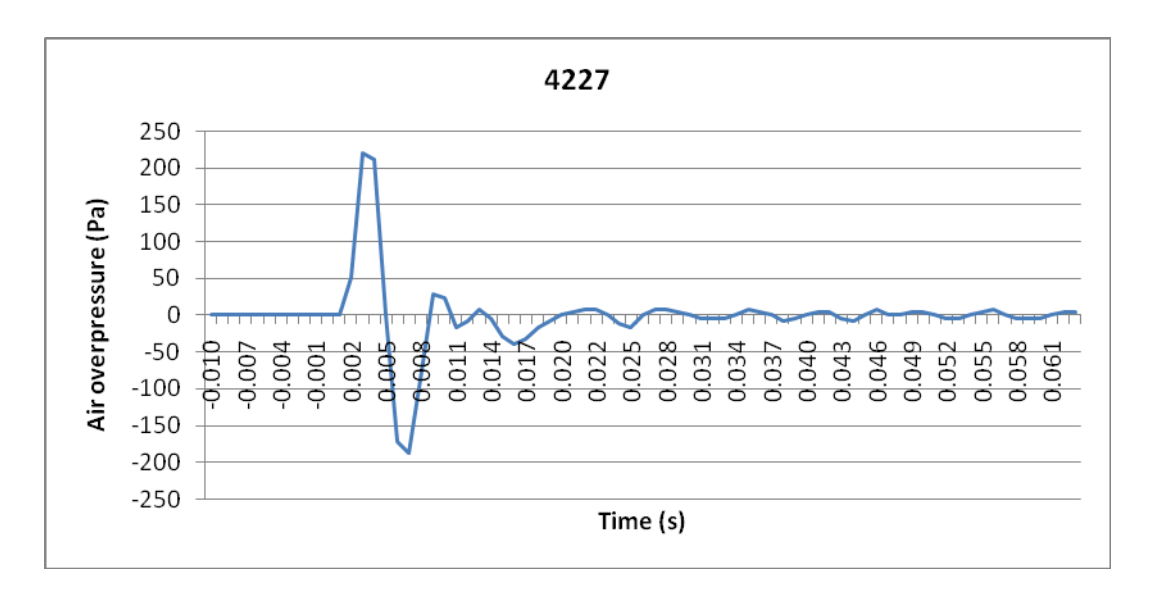


Figure 7.17 Use of single charge waveform to model an unconfined quarry blast

7.3 Theoretical single hole wave form modelling

The waveform recorded from the single charge tests can be used to recreate a theoretical model of an unconfined quarry production blast by using the linear superposition programme from chapter 9. The differences in wave shape between the recorded air overpressure traces from production blasts at Melton Ross and the modelled wave can be attributed to the burden and from this, the extent of the burden's influence on air overpressure can be determine.

Below is an air overpressure waveform recorded from a single hole blast at Melton Ross quarry.

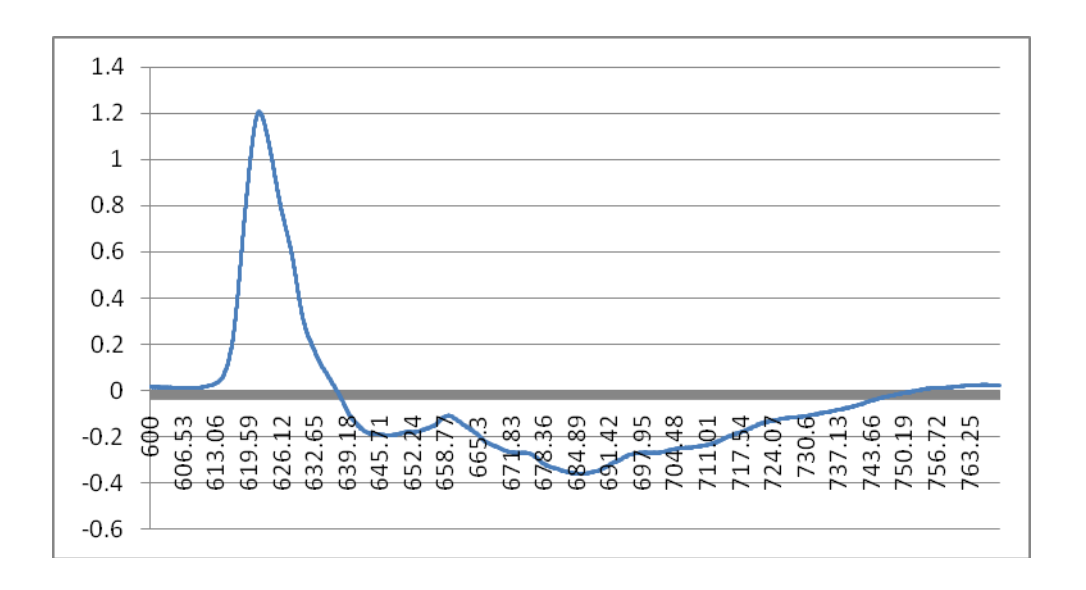


Figure 7.18 air overpressure waveform recorded from the 1st single hole blast at Melton Ross quarry.

The air overpressure wave consists of a positive and negative phase. The positive phase experiences a rapid increase and decrease in pressure and has a time duration of 25.46ms which is much shorter than the time duration of the negative phase. This lasts for 115.33ms but the peak magnitude is much lower than the positive phase.

The second single hole blast also shows that the positive phase of the wave consists of a rapid increase and decrease in pressure whilst the negative phase experiences a more gradual decrease to its minimum amplitude and a gradual rise to unity.

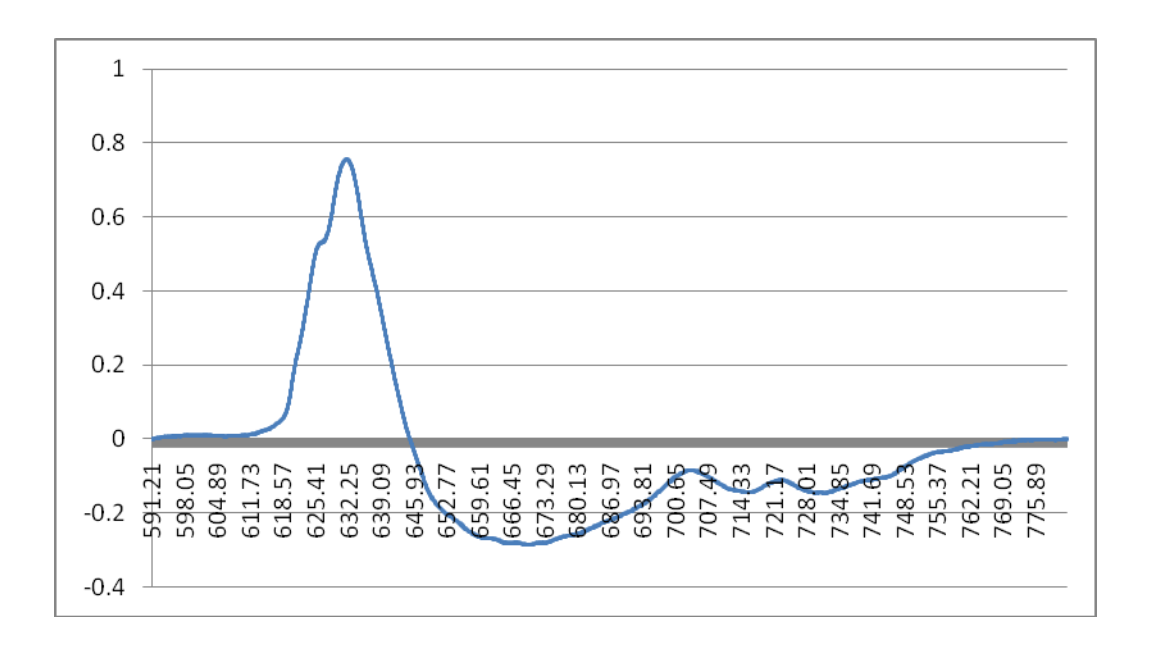


Figure 7.19 air overpressure waveform recorded from the 2nd single hole blast at Melton Ross quarry.

The time period of the positive phase is 32.46ms and for the negative phase, is 137.44ms. Richards and Moore (2002) indicate that the time period of the positive phase can be related to the weight of explosive in that blast hole. The following equation shows how the charge weight relates to the time period of the positive phase.

$$T_{\bullet} = 7 \times \sqrt[4]{Wt}$$

Where

Wt =the charge weight per delay (kg)

The equation however does not take into account the velocity of detonation of the explosive or the length of explosive column. If an explosive with a higher VOD is detonated whilst the charge column is shorter, the time duration of the positive phase and the negative phase must be shorter. To illustrate this, the air overpressure recorded from the sixth test which consisted of a single 1m length of detonation cord being fired is presented in Figure 7.20.

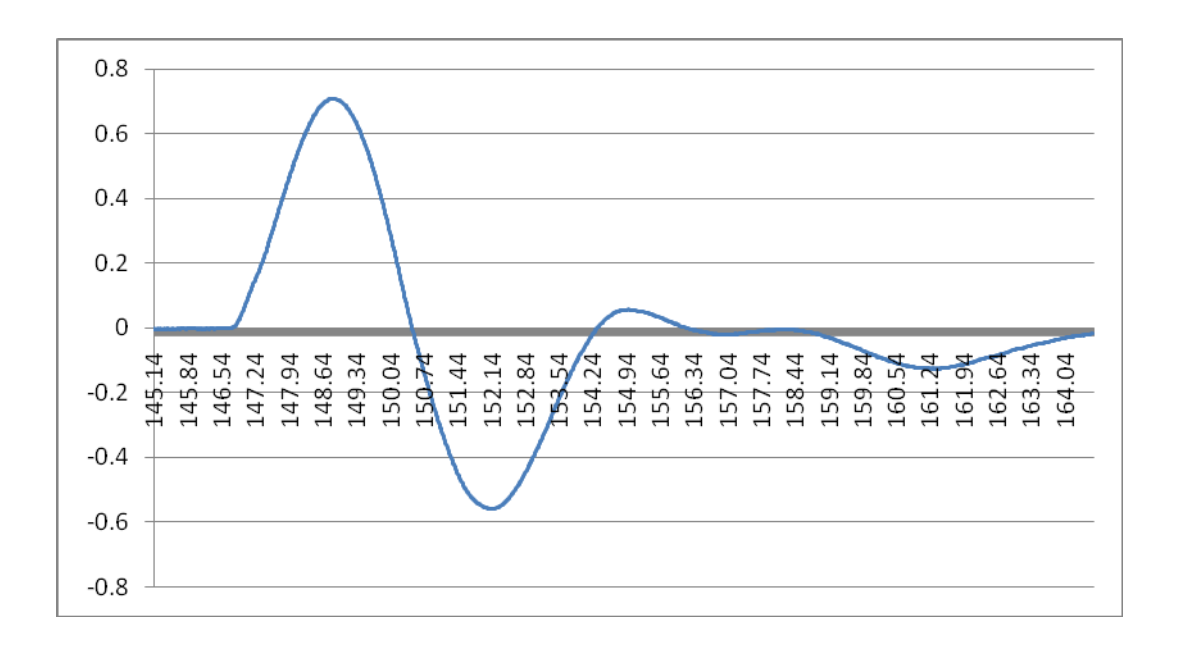


Figure 7.20 air overpressure recorded from a single 1m length of detonation cord being fired in "free air"

The VOD of the detonation cord is 7000m/s whereas the VOD of the ANFO loaded in the single blast hole at Melton Ross is 3500m/s. The length of the detonating cord was 1 metre, whilst the height of the explosive column at Melton Ross was 9.5m.

The time period of the positive phase of the wave from the unconfined detonation is 3.9ms and the negative phase lasted for 3.8ms.

The amplitude of the wave is related to the weight of explosive, the gradient of the rise and fall related to the VOD and the time period of the phase related to column length of explosive.

Using the equation by Richards and Moore (2002), the time period of the positive phase of the two single hole blasts at Melton Ross is 28.15ms and the time period for the unconfined detonation is 1.6ms. Compared to the time periods shown in the respective Figures above, the duration of the positive phases vary from the durations derived by the equation.

In order to scale the unconfined pressure wave so that it represents a pressure wavelet produced at Melton Ross quarry, the time period of the wave must be adjusted to factor in a slower VOD of the explosive used (3500m/s) and the increase in charge length which is approximately 9.5m in length. The sample rate of the recorded pressure wave must also be reduced to 1024sps so that it can be used to

model a Melton Ross blast using the linear superposition program as described in chapter 9. The air overpressure recorded by the MREL Microtrap contains 100,000 samples per second of recording and therefore requires down sampling by a factor of 100.

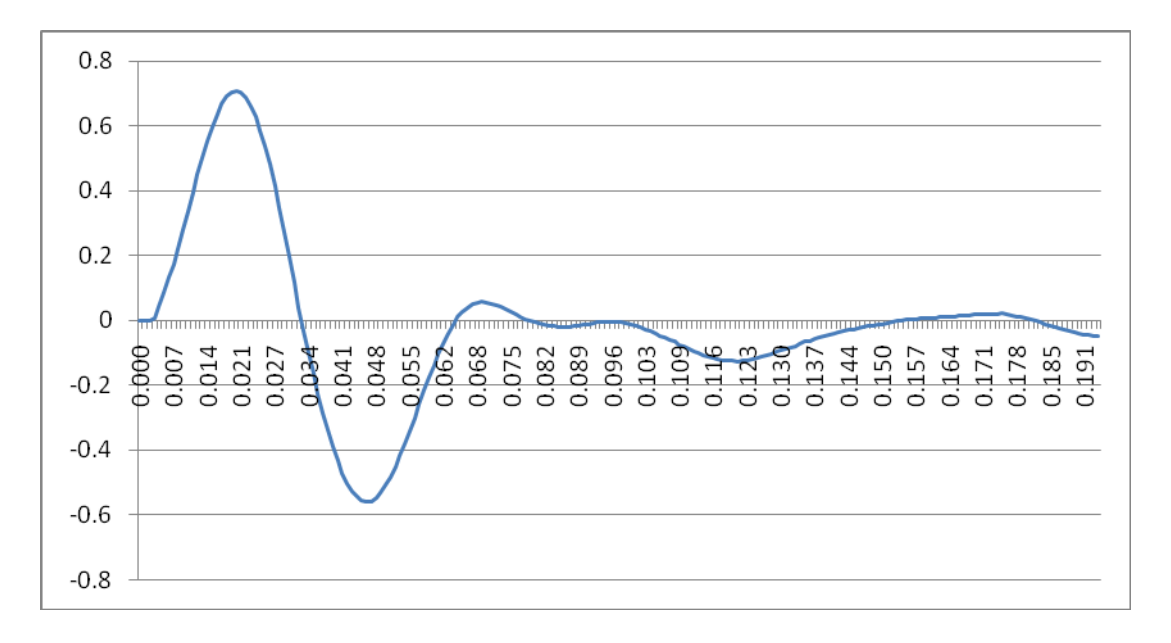


Figure 7.21 Pressure wave down sampled to 1024sps

The time period of the positive phase of the wave has been increased from 3.9ms as seen in figure 8.17 to 31.25ms, as shown in figure 8.18. The negative phase of the wave has also increased to 31.25ms. The time duration of the positive phases from these blasts were 25.46 and 32.46ms respectively.

A direct comparison of the modelled wave has been compared to a single hole wave in figure 7.22.

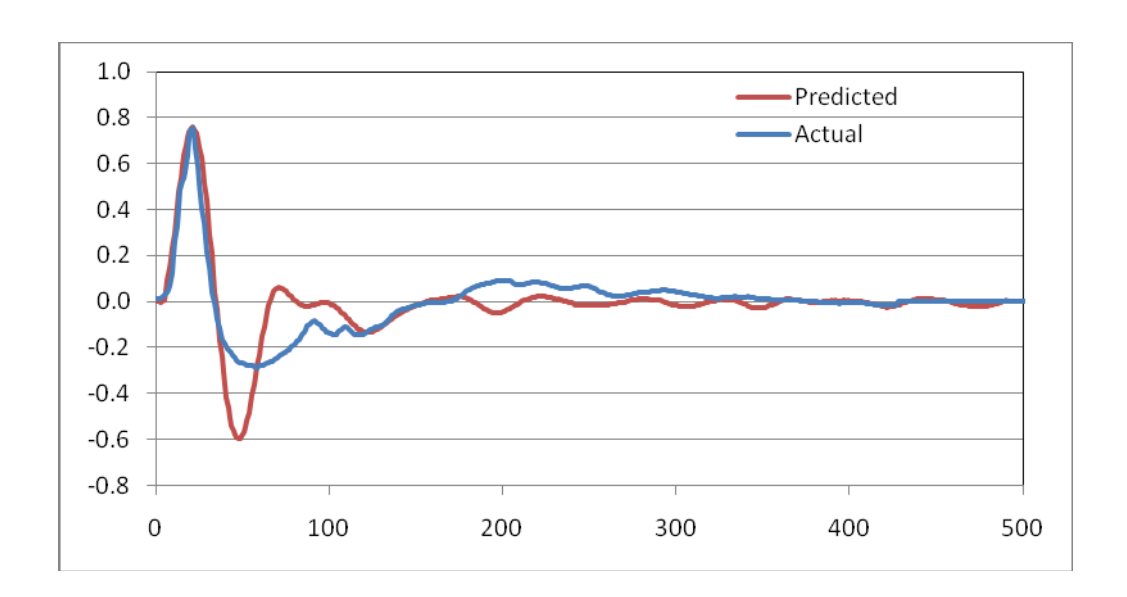


Figure 7.22 Comparison between a confined and unconfined single hole blast

The two waves show a close comparison with one another. The distinct difference between the two waveforms are the shape and duration of the negative phases. The negative phase of the pressure wave produced from the unconfined explosion has a much shorter duration as noted earlier and experiences a greater rate of fall and rise from and to ambient pressure level.

This clearly shows the effect of confinement on an air overpressure wave produced from a typical quarry blast. The pressure emanating from a blast assumes the form of a compression wave. This acts like a piston, pushing and compressing the surrounding medium in the direction of travel. The front of the wave transfers energy to the atmosphere and generates a steep fronted wave which is shown by the rapid rise and fall of pressure in an air overpressure trace. The time period of the negative phases for the two waves in figure 8.19 differs due to the level of confinement. In regards to the quarry blast, the pressure wave pushes the rock from the face exhibiting a piston effect. In contrast the detonation of an unconfined charge causes the a sharp rise in overpressure and also a sharp decline into the negative phase and a rapid increase back to ambient pressure, resulting in a shorter time period of pressure wave's negative phase. This is due to the air reacting elastically to the unconfined detonation and so once the peak pressure is reached, the wave is then reflected at the same rate as the rise, resulting in a rapid fall decline in pressure to a negative phase which is of the same time duration as the positive phase, whereas in a quarry blast, the gas pressure from the explosives pushes the rock out from the bench

which then reduces the magnitude of the wave reflection into the negative phase, resulting in a longer, more gradual rise back to ambient pressure levels.

7.3.1 Creating a model of an unconfined blast at Melton Ross

Now that a model of a pressure wave that is expected to be generated from an unconfined single hole ANFO blast, typical to Melton Ross quarry, a model of an unconfined production blast can be modelled. This is shown in figure 7.23 where the actual inter hole delay times of a production blast at Melton Ross were used. A comparison between the predicted unconfined air overpressure trace and the production blast has been made.

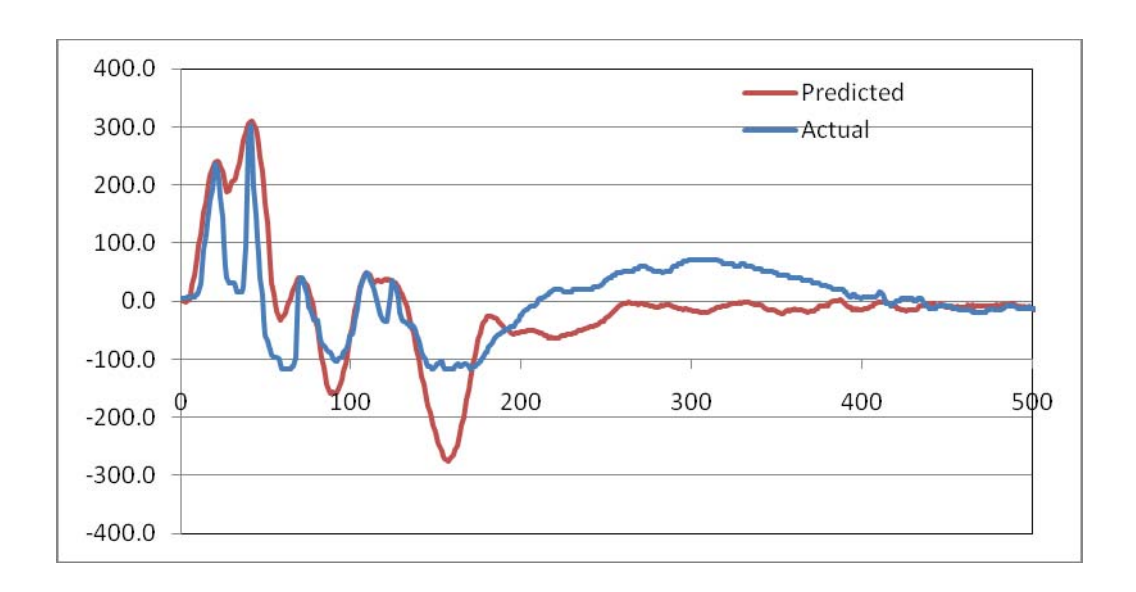


Figure 7.23 Comparison in air overpressure of a semi confined and unconfined blast at Melton Ross

The peaks of each pressure pulse become much less distinguished due to the faster pressure rise, fall and magnitude of the unconfined negative phase which results in greater interactions between pressure pulses.

7.4 Conclusions

The test undertaken using 1 metre lengths of Detonating Cord in air were shown to be very consistent. The test where the explosives were fired at 25 millisecond intervals showed no inter action. The test fired at 8 millisecond intervals showed some interaction with respect to the direction of firing, however this was such that the positive negative phase of the previous hole interacted with the positive phase of the hole firing to reduced the air overpressure from the explosive charge in question due to negative interference of the two wave forms. The test will 4th and 5th hole firing 1 millisecond apart did show positive interference that gave rise to an enhanced air overpressure values

There is a fundamental difference in the wave form of the air overpressure pulse between a detonation in free air and a confined detonation in a quarry blast. The difference mainly relates to time duration of the negative phase of the pulse in that in a "free air" detonation the positive phase of the pulse is approximately equal to the negative phase in terms of time. However in a confined quarry blast detonation the negative phase can be between 3 to 5 times longer in duration that the positive phase.

Chapter 8

Single hole air overpressure test blasts at Melton Ross Quarry

8.1 Introduction

As part of the experimentation, two single hole signature test blasts were carried out at Melton Ross Quarry. This is a small chalk quarry that produces chemical grade feed for the lime kilns of Singleton Birch.

8.2 The experiment

Two blast holes were drilled on the lower bench of the chalk quarry. Seven seismographs were set out in front of the quarry face and four seismographs were set out on the blasting bench behind the blast. Seismographs 4228 and 4227 as well as 1404 and 3656 were linked together so that the speed of sound at the moment of the blasting events might be determined. In addition two overpressure microphones were set out in front of the quarry face. These were connected to an MREL high speed data acquisitions system that in turn was triggered using an optic fibre cable from each of the two blast holes in turn. The spatial relationship between the blast holes and the monitoring points was as indicated in Figure 1.

8.3 Results of the experiment

a number of different parameters were able to be determined as a result of the two tests

- 1. The value of the air overpressure wave as it decayed with distance
- 2. The shape of the air overpressure time history trace as it decayed with distance
- 3. The speed of sound in air on the day of the experiment.

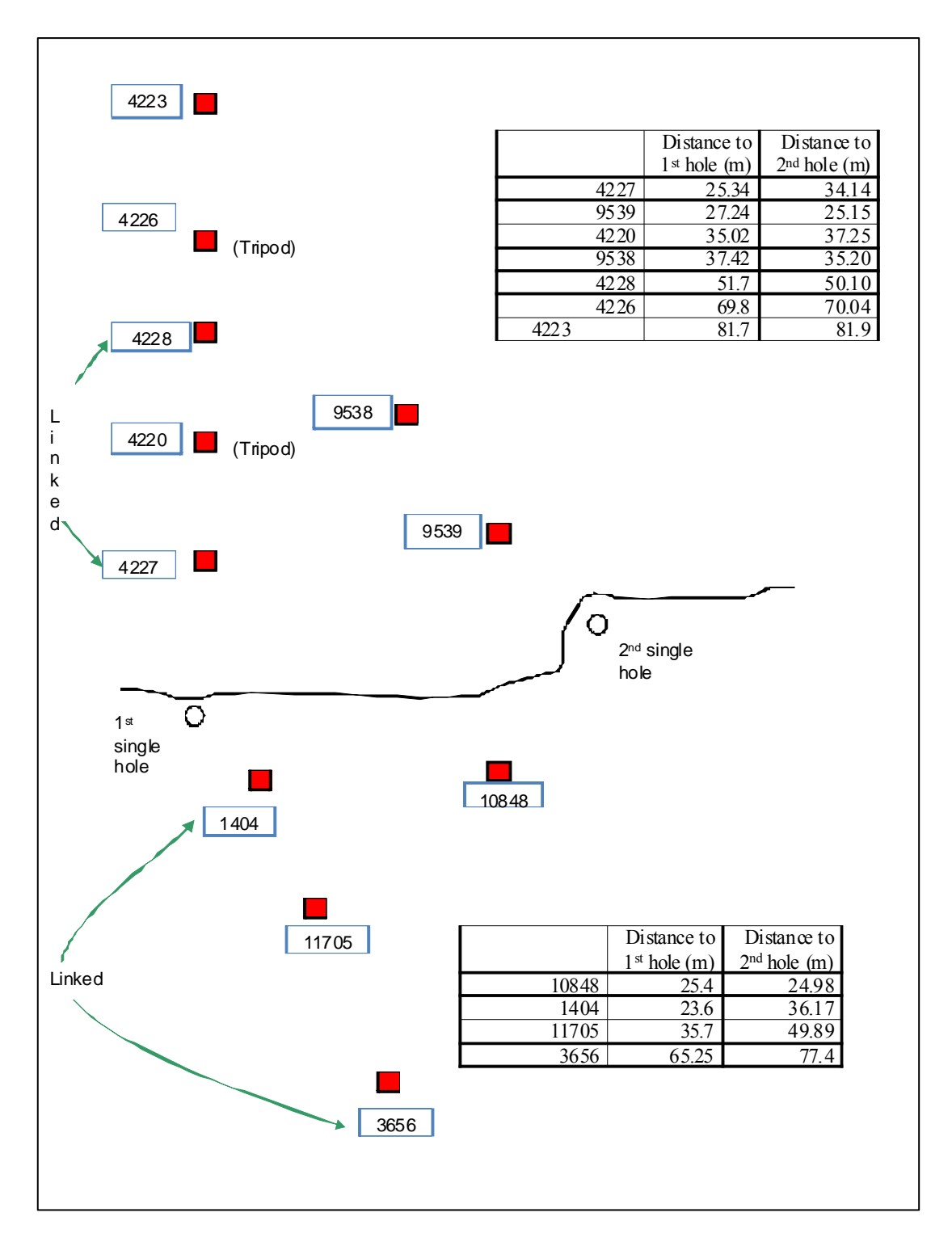


Figure 8.1 location of the air overpressure monitors with respect to the two single hole blasts.

8.3.1 The value of the air overpressure wave as it decayed with distance

As previously discussed, the accepted formula that relates air overpressure values to charge weight and distance is the cube root scaling formula:

$$P = C \left[\frac{D}{W^{1/3}} \right]^{-a}$$

where:

P = pressure (kPa)

W = explosives charge mass per delay (kg)

D = distance from charge (m)

C = site constant

a= site exponent

	Seismograph	4227	4220	4228	4226	4223	9539	9538
	Distance	25.3	35.0	51.7	69.8	81.7	27.2	37.4
	Average	4.8	4.8	4.8	4.8	4.8	4.8	4.8
Burden	Median	4.3	4.3	4.3	4.3	4.3	4.3	4.3
	Toe	6.2	6.2	6.2	6.2	6.2	6.2	6.2
	Face Height	12.4	12.4	12.4	12.4	12.4	12.4	12.4
	MIC	65.0	65.0	65.0	65.0	65.0	65.0	65.0
	D/e ^{^0.333}	6.31	8.72	12.88	17.38	20.35	6.78	9.32
	Max AOP	436	328	260	192	176	438	325

Table 8.1 The relationship between air overpressure, distance charge weight and burden for blast 1.

	Seismograph	9539	9538	4228	4227	4220	4226	4223
	Distance	25.2	35.2	50.1	34.1	37.25	70.0	81.9
	Average	6.53	6.53	6.53	6.53	6.53	6.53	6.53
Burden	Median	6.7	6.7	6.7	6.7	6.7	6.7	6.7
	Toe	7.4	7.4	7.4	7.4	7.4	7.4	7.4
	Face Height	12.7	12.7	12.7	12.7	12.7	12.7	12.7
	MIC	65.0	65.0	65.0	65.0	65.0	65.0	65.0
	D/e ^{^0.333}	6.26	8.77	12.48	8.50	9.28	17.44	20.40
	Max AOP	317	226	180	228	196	136	124

Table 8.2 The relationship between air overpressure, distance charge weight and burden for blast 2.

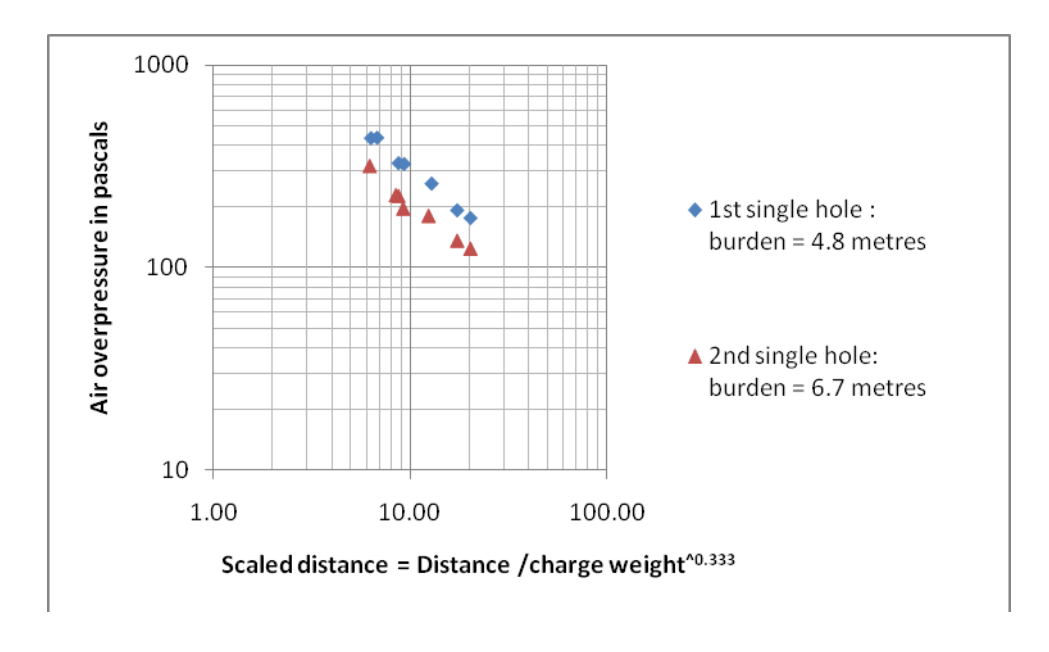


Figure 8.2 Plot of the two single hole tests

The results of the two test blasts show two parallel lines with the blast with the lower burden giving rise to higher air overpressure readings at the equivalent scaled distance. If the data is then analysed using a trivariate regression, with air overpressure as the dependant variable and scaled distance (in the form of $D/e^{^{0.333}}$) and the Median Burden being the two independent variables, then the relationship becomes as given below

$$\log AoP = \log a + \alpha \log[D/E^{0.333}] + \beta \log[B]$$

Thus

$$AoP = a[D/E^{0.333}]^{-\alpha} x[B]^{-\beta}$$

As a result of carrying out the trivariate analysis the following values were derived

a = 6719

 $\alpha = 0.777$

 $\beta = 0.890$

mean squared error = 0.0025

standard error = 0.0502

Total variance = 91.688

Explained variance = total variance - unexplained variance = 91.661

Thus the trivariate model can be said to explain 99.97% of the variability within the system. [i.e. 91.661/91.688]. This is a remarkable result even given the fact that both tests were carried out on the same day.

Whilst caution needs to be exercised in that the data set contains only 14 results from two blast, it does show that there is a very strong relationship between resulting values of air overpressure from distance combined with burden at least for single hole blasts. However as the two single hole blasts were identical charge weights, it is not possible to determine in this experiment the relationship between charge weight and distance in the form of Scaled Distance as it is conventionally used.

8.3.2 The shape of the air overpressure time history trace as it decayed with distance

The changing values of air overpressure were recorded against time as the air blast effect passed the monitors. The resulting traces can be seen in Figure 8.3. As can be seen, the traces are very similar in shape and only vary in amplitude.

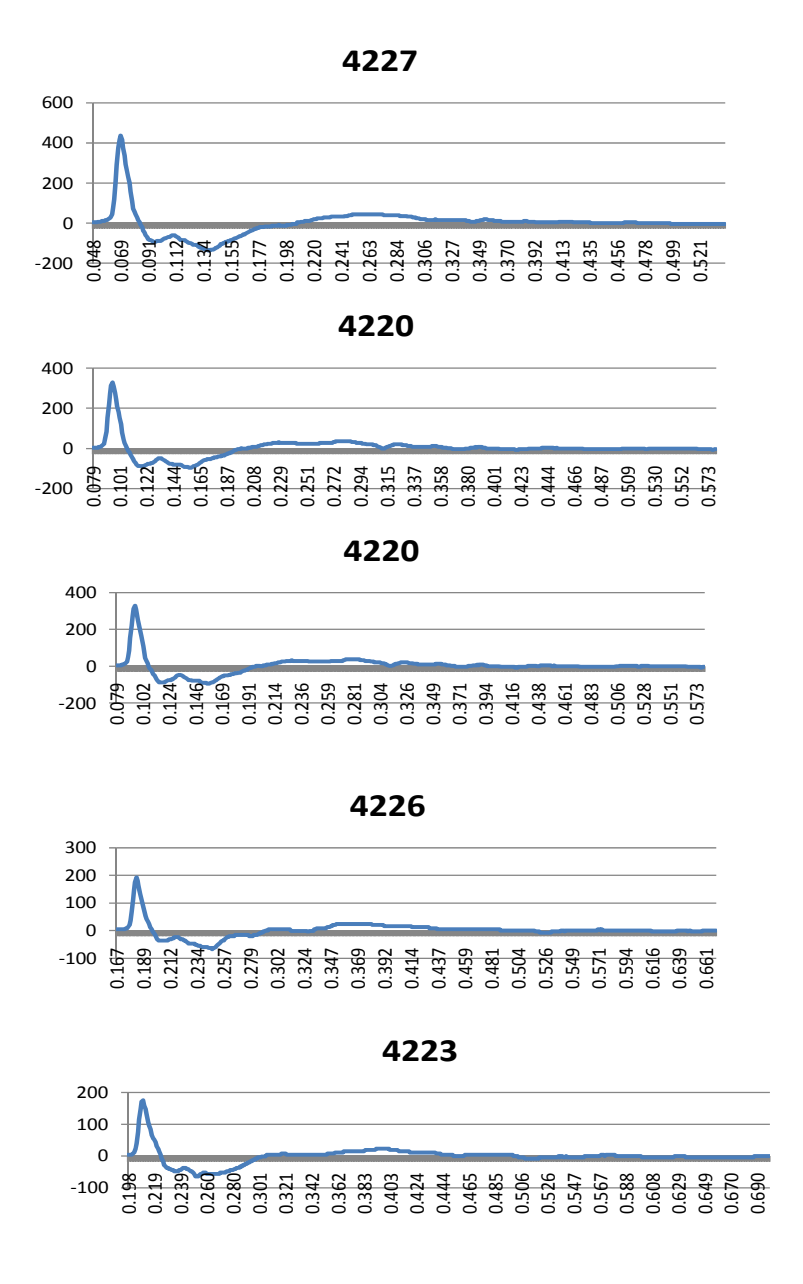


Figure 8.3 Consistent shape of the air overpressure wave form even as the amplitude decays with increasing distance from the blast site

It is this consistence in shape that makes it possible to use this basic form to model a multi-hole air overpressure event from a single hole wave form. This will be discussed more in Chapter 9.

8.3 Conclusions & Summary

The experiment carried out does show that there is a very strong relationship between resulting values of air overpressure with respect to variations in distance combined with burden at least for single hole blasts. However as the two single hole blasts were identical charge weights, it is not possible to determine in this experiment the relationship between charge weight and distance in the form of Scaled Distance as it is conventionally used.

The constant shape of the wave form of the single hole as it attenuates with distance makes it possible to use this as the basic form to model a multi-hole air overpressure event from a single hole wave form

Chapter 9

Application of statistical analysis in combination with a linear superposition technique using a signature acoustic wave form to create a model of the air overpressure produced from a full scale production blast at Melton Ross Quarry

9.1 The Application of linear Superposition techniques to the air overpressure generated by quarry blasting

Whilst the use of linear superposition techniques has been used for many years for the simulation of ground vibration generated by quarry blasting operations, there appears to be no published information on the application of this technique to the generation of air overpressure by such blasting operations.

9.1.1 Linear Superposition

The technique of linear superposition is a simulation algorithm that combines timing information from a blast or proposed blast with a recording previously made of the ground vibration resulting from a single-hole blast. The single-hole blast is essentially a seed for the simulation process. The other parameter required for the simulation is the firing time of each blast hole.

It is worth noting that the linear superposition technique relies on a number of assumptions for each of the input parameters and it is vital that consideration is given to these when applying the technique in a practical application.

For the single-hole seed waveform it is assumed that each hole in a blast will produce the same ground vibration transient. For this reason a basic requirement of the technique is that the single-hole trial carried out before the simulation should closely resemble a hole in a typical production blast in terms of explosive type, charge weight, burden, and face height. It is also important that the single-hole trial takes place close to the existing area of production blasting. Experience has shown that in operations employing multiple benches it is wise to repeat the entire process for each excavation horizon. It is also important that the vibration monitoring point is close to the location of interest and that, if there are multiple points of interest, monitoring is carried out at each location. It should also be expected that the nature

of the vibration produced by each hole will vary with the transmission distance and can also be significantly altered by the intervening geology. Even at relatively short distances it is also the case that the vibration arriving at any monitoring location is a combination of at least three vibration wave types; compression, shear and Rayleigh and Love waves. Given that these four wave types all travel at different velocities, another layer of complication is added to the process.

The primary assumption made relating to blast-hole timing is that the explosive charges initiate in accordance with the nominal blast design. It is widely recognised that this assumption is completely invalid when employing detonators including delay elements that rely on the burning time of a pyrotechnic compound. For this reason the linear superposition technique is only employed in conjunction with accurate electronic initiation systems. It possible to use linear superposition in combination with a Monte-Carlo simulation to simulate blasts employing pyrotechnic detonators but it has been demonstrated that each time the simulation is run a different result will be obtained. To be absolutely correct the initiation time employed in the simulation process should also take into account the relative positions of the blast holes and monitoring locations. Given the relatively high propagation velocities of vibration through rock it is normally considered that this type of correction does not need to be undertaken.

9.2 Optimisation with Linear Superposition

The most common application of the linear superposition technique is in determining the optimum delay time for blasting to minimise the resulting ground vibration. In this application the simulation is run multiple times with a series of differing detonator delay increments. Typically this is done with a series of delays ranging from 0 to 100 milliseconds. Each increment of delay time will produce a simulated peak vibration level and this is normally plotted on a graph against delay time. From this graph an optimum delay time can be chosen. It is worth noting that this process has to be repeated for each location of interest and that, for ground vibration, this has to also be repeated for each component of the ground vibration (vertical, transverse and longitudinal). Experience shows that the optimum delay value may vary between both monitoring locations and vibration component – in such cases the final delay time chosen will actually be the least-worst delay rather than the optimum.

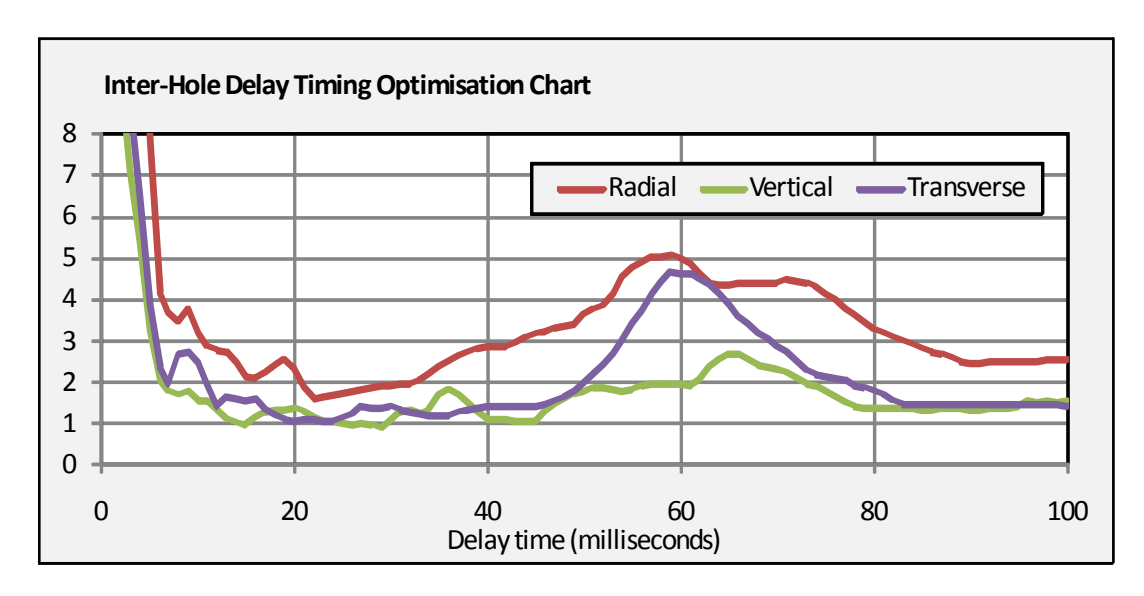


Figure 9.1 Example of a blast vibration optimisation chart for a single row blast

It can be seen in example Figure 9.1 above that in this case an inter-hole delay time between 50 and 80 milliseconds should be avoided but that 15 to 40 milliseconds is reasonable with an optimum delay time of 22 milliseconds. It is also interesting to note that, as the delay time reduces below 8 milliseconds, the predicted vibration level increases rapidly.

9.3 Application of Linear Superposition Techniques to Air Overpressure

As previously noted there appears to have been little work carried out on the application of linear superposition to the air overpressure generated by quarry blasting. This shortcoming has been partially addressed in this project by the development of simulation software suitable for use with air overpressure data.

The input parameters for this version of the simulation model include, once again, a single-hole air overpressure transient and initiation timing for the blast. In the case of air overpressure only a single component is required and there is only a single wave type – compressive. However, matters can be complicated by the presence of reflecting surfaces such as nearby quarry faces. It is to be expected that the nature of the single hole air overpressure transient will vary with distance but that this will be more predictable as the intervening transmission medium is air and not rock. The requirement for initiation timing information remains the same but it should be noted that it is considered sensible to correct for the relative travel times

between each hole and the monitoring point as the speed of sound through air is relatively low.

The developed model also includes the possibility to change the amplification factor applied to each hole in a blast. The relationship of this factor to other parameters such as burden, face area, and face velocity have been addressed elsewhere in this report.

The Figure 9.2 and Figure 9.3 below shows an example output from the software relating to a five hole single-row blast in which the hole firing times were monitored and therefore precisely known. The predicted waveform is compared to the actually monitored waveform from that blast. The seed waveform is as monitored on the same bench in the same quarry and at the same approximate distance. In this example the amplification factors for each hole are set as x1.

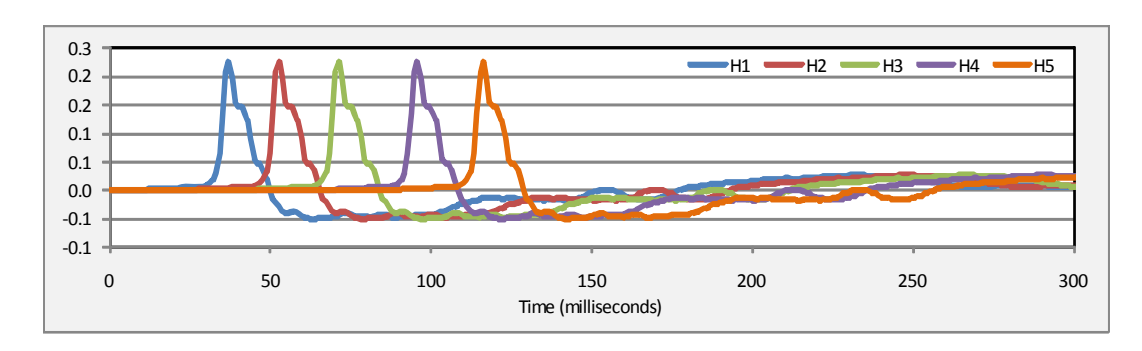


Figure 9.2 Air overpressure trace from individual holes firing at different designated times.

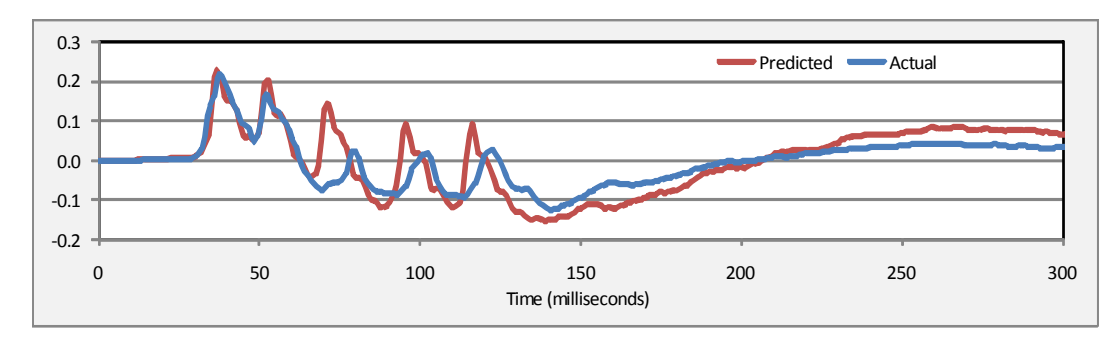


Figure 9.3 Combined effect of the traces from the individual holes into a single trace in comparison with an actual air overpressure trace from a 5 hole blast.

The Figure 9.2 shows the individual holes firing at the monitored hole initiation times. Whereas Figure 9.3 shows the result of combining the individual traces into a single trace. The combined trace is also compared to the actual recording.

Figure 9.4 below shows the result of modifying the individual amplification factors for each hole to best match the actual recorded air overpressure.

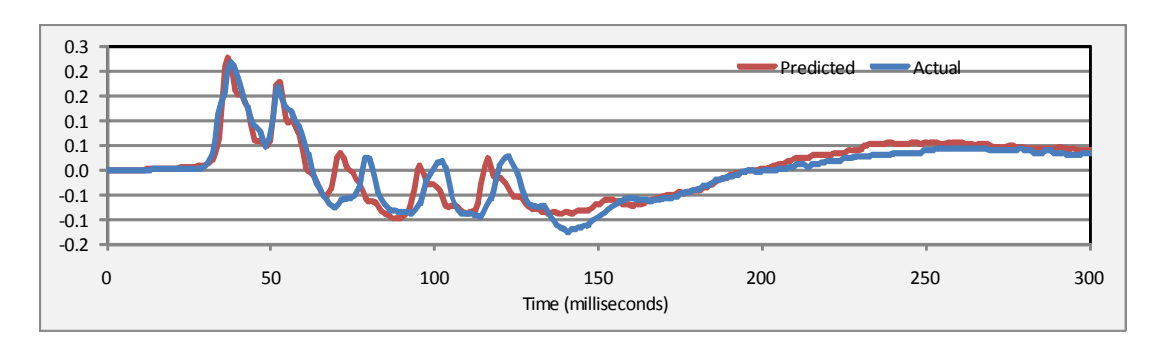


Figure 9.4 Modification of the amplitude of the individual holes to match an actual air overpressure trace from a 5 hole blast.

Once again this process can be extended to allow for an optimisation process to be undertaken. An example optimisation chart is given below. It can be seen that this chart is simplistic in nature to that given in the previous example for ground vibration.

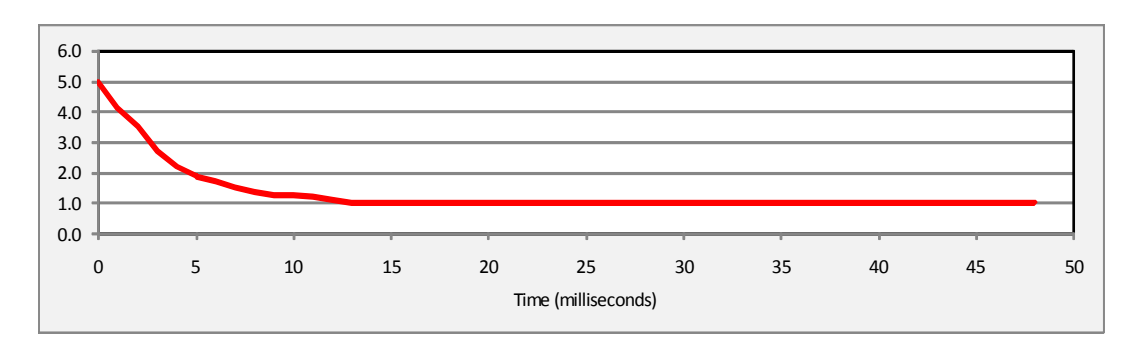


Figure 9.5 Air overpressure optimisation chart demonstrating how the initiation interval between successive holes in a multi hole blast pattern would interact.

It can be seen from the example optimisation chart above (Figure 9.5) that effectively the positive interaction air overpressure level remains constant at delays above an inter-hole delay of 10 milliseconds. This effect is caused by the fact that at these relatively long delays the air overpressure pulses from each hole have become separated. However, it can be seen that the predicted levels of air overpressure at short delays can be seen to increase rapidly. This is typical of such optimisation charts and gives credence to the widely held view that the use of very short delays across a quarry blast face result in a very high air overpressure level. Such short delays are commonly the aim of the application of electronic detonators.

On the other hand, it is known that once the positive phase of the air overpressure pulse is completed, there is a negative phase of the air overpressure pulse. On the basis of conservation of energy, the total energy of this negative phase should equal the total energy of the positive phase (less any minor frictional loss due to the inter action of air molecules as the air overpressure waves is transmitted onwards). As previously noted in Chapter 2, whilst typically this phase is some 1/3 lower in amplitude, it is approximately 3 times longer in duration. This then presents the possibility that successive holes can be made to destructively interfere. The boundary between constructive and destructive interference from one blast hole to another will be dependent on the actual form of the air overpressure pulse from the blast hole in combination with the speed of sound in air on the day and the spacing between successive blast holes. Whilst this will almost certainly vary from blast to blast, all of these three parameters can be easily derived or measured.

9.4 Air overpressure monitoring at Melton Ross Quarry.

A series of five hole blasts were carried out at Melton Ross Quarry. This is a chalk quarry that provides "quick lime" and "Slaked lime" as a finished product. The small scaled blasts were ideal for the research study undertaken, as they provided the opportunity to consider a very simple scenario where only a single row of holes were fired and not more than five holes in any one blast.

Due to the economic down turn, together with some problems with the recording system, only 10 blasts were able to be monitored. However these 10 blasts were monitored at 31 monitoring locations varying from 39.9 metres to 130.3 metres with charge weights varying from 35 kilograms to 70 kilograms and median burdens varying from 3.7 metres to 7.6 metres. If the number of identifiable air overpressure pulses is taken into account, then the number of observations rises to 157.

The air overpressure record for each observation pulse was recorded and the amplitude and wave form was visually correlated with the air overpressure pulse from a single hole in the manner previously described.

The example give is for the five hole blast recorded on 12th march 2010 at 44.5 metres from the quarry face of the blast.

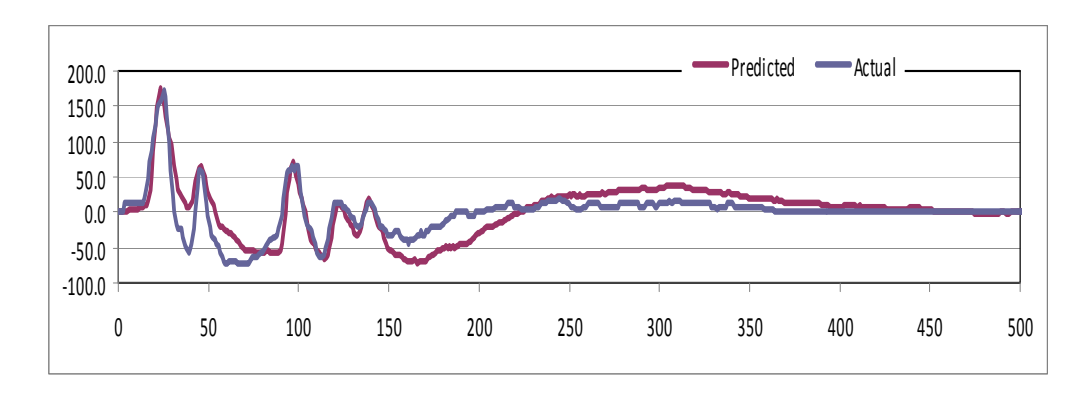


Figure 9.6 five hole blast recorded on 12th march 2010 at 44.5 metres from the quarry face of the blast.

Figure 9.6 shows the blast trace recorded at the observation point matched with the model of the same air overpressure trace. The model trace was created by combining the trace from the single signature hole at specific amplitudes and times. Figure 9.7 below indicates this process and table 9.1 indicates the magnitude and the arrival delay times used.

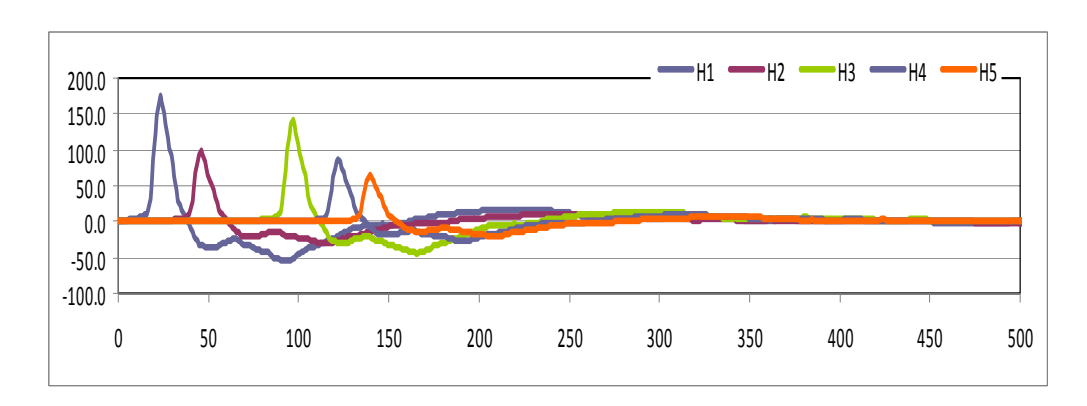


Figure 9.7 Model of 5 separate holes with varying magnitude and timings

Hole	1	2	3	4	5
Time					
(milliseconds)	0.0	23.0	74.0	99.0	117.0
Amplitude	0.8	0.5	0.7	0.4	0.3
		•			
Offset =	-91.0				
Scaler =	0.5				

Table 9.1 arrival times and magnitudes used to form the prediction model in Figure 9.6

This data was then combined with other measurements collated from the blast report to form table 9.2 below

sei	smograph	4228				
	Hole		2	3	4	5
	Distance					
Average		6.2	6.24	6.19	6.2	6.28
Burden	Median	6.5	6.9	7	6.2	6.3
	Toe	7.8	7.7	7.7	7.9	8.1
Face Height						
		12.48	12.48	12.54	12.6	12.59
	MIC	66.5	66.5	66.5	66.5	66.5
	Max					
	AOP	172	60	64	12	12
Derived						
	AOP	172	97	140	86	65

Table 9.2 relationship of blast parameters to maximum actual and derived air overpressure levels

This then gave rise to 157 such data sets. The derived air overpressure values were calculated by taking the first reading relating to the first hole to fire and scaling it using the derived relationship relating the amplitude of the first hole to the amplitude of the hole in question. In the example given above, the amplitude of the 4^{th} hole = $172 \times 0.4/0.8 = 86$ Pascals.

9.5 Statistical comparison of the original air overpressure data with the derived data.

9.5.1 Statistical comparison using a trivariate relationship

Using all 157 data sets, a statistical comparison was made between the original air overpressure values related to each hole and the derived values using a trivariate

statistical method to relate air overpressure in Pascals as the dependant variable to distance and explosive charge weight as two separate independent variables.

$$AoP = C.E^aD^{-b}$$

$$AOP = 11.317 * [Distance]^{-0.691} * [MIC]^{-1.095}$$

The above equation relates to the original peak air overpressure data for each hole in any given blast. As a result of carrying out the trivariate analysis the following values were derived

C = 11.317

a = -1.095

b = -0.691

mean squared error = 1.1006

standard error = 1.0491

Total variance= 296.7001

Explained variance = total variance - unexplained variance = 127.201

Thus the trivariate model can be said to explain 42.87% of the variability within the system. [i.e. 127.201/296.7001]. Also the key feature is that both exponents a and b are negative. Whilst it is logical that the air overpressure will decrease with increasing distance, it is not logical that air overpressure should decrease with increasing charge weight.

The above equation relates to the derived peak air overpressure data for each hole in any given blast. As a result of carrying out the trivariate analysis the following values were derived

C = 5.983

a = 0.532

b = -0.848

mean squared error = 0.1645

standard error = 0.4056

Total variance= 194.2782

Explained variance = total variance - unexplained variance = 168.938

Thus the trivariate model can be said to explain 86.96% of the variability within the system. [i.e. 168.938/194.2782]. Also the key feature on this occasion is that the exponent a is positive, whilst the exponent b is negative. This entirely logical as the air overpressure should decrease with increasing distance, and increase with increasing charge weight.

If this relationship is then remodelled using the previously defined relationship given below

$$AoP = C.(D/E^{a/b})^{-b}$$

(where the term $D/E^{a/b}$ becomes the new "scaled distance" term)

Scaled Distance =
$$\left[\frac{D}{E^{0.63}}\right]$$

Thus the equation would become

$$AoP = 5.983.(D/E^{0.63})^{-0.848}$$

What is clear is that the relationship between distance and charge weight is not proportional to either the square root or cube root of the charge weight in this circumstance.

9.5.2 Statistical comparison using a quadrivarainte relationship

Having established that it is acceptable to use the derived air overpressure to examine the relationship between it as dependant variable and distance and charge weights as independent variables, the next stage was to examine how burden influenced the resulting air overpressure values.

Again using all 157 data sets, a statistical comparison was made between the derived air overpressure values related to each hole using a quadrivarainte method to relate air overpressure in Pascals as the dependant variable to distance, explosive charge weight and burden as three separate independent variables

To do this, three different burdens were derived from the quarry blast records, these burdens were calculated from the face profiles carried out by laser profiler prior to the blast being fired. This profile calculates the distance between the borehole and the quarry face. The three burdens calculated where

- 1. Average burden along the loaded borehole from the quarry floor to the base of the stemming
- 2. Median burden along the loaded borehole from the quarry floor to the base of the stemming
- 3. The toe burden located at the location of the primer explosive cartridge in the blast hole.

As previously stated, from analysis of field measurements over many years, Moore & Richards have found that the air blast levels in front of the face are a function of charge mass, distance, hole diameter and burden, according to the empirical formula:

$$D120 = \sqrt[3]{m.x.} \left\lceil \frac{K_{b.}x.d}{B} \right\rceil^{2.5}$$

where:

D120 = distance in front of blast to the 120 dB(Lin) contour

d = hole diameter (mm)

B = burden (mm) actual burden for analysis or design burden for prediction

m = charge mass/delay (kg)

 $K_b = a$ calibration factor typically varying between 150-250

It therefore follows that the relationship between the four parameters involved should take the generic form of

$$AoP = C * E^a * D^{-b} * B^{-d}$$

Where

C = a site constant

 \mathbf{E} = charge weight with \mathbf{a} its exponent

 \mathbf{D} = distance with \mathbf{b} its exponent

 \mathbf{B} = Burden with \mathbf{d} its exponent

thus

$$\log AoP = \log C + a\log E - b\log D - d\log B$$

9.5.2.1 Average burden

Using the Average Burden in the quadrivarainte expression, the following relationship was derived

AOP(Pascals) 5.611 * [Distance]^ -0.839 * [MIC]^ 0.758 * Burden^ -0.102

C = 5.611

a = 0.839

b = -0.758

d = -0.102

mean squared error = 0.1576

standard error = 0.3970

Total variance= 111.82279

Explained variance = total variance - unexplained variance = 87.557

Thus the quadrivarainte model can be said to explain 78.29% of the variability within the system. [i.e. 87.557/111.823].

9.5.2.2 Median burden

Using the Median Burden in the quadrivarainte expression, the following relationship was derived

AOP(Pascals) 5.300 * [Distance]^ -0.847 * [MIC]^ 0.814 * Burden^ -0.089

C = 5.983

a = 0.814

b = -0.847

d = -0.089

mean squared error = 0.1575

standard error = 0.3969

Total variance= 111.82279

Explained variance = total variance - unexplained variance = 87.565

Thus the quadrivarainte model can be said to explain 78.31% of the variability within the system. [i.e. 87.565/111.823].

9.5.2.3 Toe burden

Using the Median Burden in the quadrivarainte expression, the following relationship was derived

AOP(Pascals)	5.290	*	[Distance]^	-0.855	*	[MIC]^	0.935	*	Burden^	-0.144

C = 5.290

a = 0.855

b = -0.935

d = -0.144

mean squared error = 0.1462

standard error = 0.3823

Total variance= 111.82279

Explained variance = total variance - unexplained variance = 89.311

Thus the quadrivarainte model can be said to explain 79.87% of the variability within the system. [i.e. 89.311/111.823].

- 157 -

For all three different burdens used, the coefficients derived are logical, in that air overpressure is seen to decrease with increased distance and burden and increase with increased charge weight.

Whilst paradoxically the unexplained error appears to have increased with the introduction of burden into the quadrivarainte expression, the true test is that the standard error has decreased thus reducing the inherent scatter in the systems.

It is interesting to note that whilst it is only marginally better, the best correlation is to use was the Toe Burden.

9.5.2.4 Using the first hole in each blast

Using the Median Burden in the quadrivarainte expression, but this time only considering the air overpressure that relates to the first hole in each blast. The logic being that air overpressure for all subsequent holes, is subjected to either constructive or destructive interference from its immediate predecessor. On this occasion the following relationship was derived

AOP(Pascals) 7.477 * [Distance]^ -0.804 * [MIC]^ 0.476 * Burden^ -0.200

C = 7.477

a = 0.804

b = -0.476

d = -0.200

mean squared error = 0.0693

standard error = 0.2632

Total variance= 82.0843

Explained variance = total variance - unexplained variance = 80.145

Thus the trivariate model can be said to explain 97.64% of the variability within the system. [i.e. 80.145/82.0843]. This an excellent result, but again caution

should be exercised as this relates to only 31 individual monitoring points from 10 different blast. It should be noted that on this occasion, the median burden gave rise to a better standard error value that either the toe or average burdens.

9.6 Conclusion

Using the derived air overpressure values that result from the application of the linear superposition technique it was possible to derive a better understanding of the relationship between distance and charge weight as commonly combine in the form of "Scaled Distance." If this is examined using trivariate statistical approach, it becomes clear that the relationship between distance and charge weight is not proportional to either the square root or cube root of the charge weight in this circumstance.

Using a quadrivarainte approach to evaluate the relationship between peak air overpressure for the whole blast that resulted from variations in distance, charge weight of the explosive and burden, then the best correlations is achieved using the burden at the toe of the face to be blasted. Give the manner of the blasting at Melton Ross this is the closest point on the quarry face to be blast to the point of imitation of the individual blast hole.

Paradoxically, if the quadrivarainte technique is used to predict the air overpressure associated with the first hole rather than the peak air overpressure for the whole blast, then the median burden gives the best correlation. The results obtain show an unprecedented ability to be able to predict the likely air overpressure pulse generated. However caution should be exercised in that these were very small single row blasts with the variability of the detonator timings being incorporated in the original linear super position algorithm.

Chapter 10

Determination of the origins of air overpressure from blasting at Melton Ross Quarry

10.1 Previous research in determining the precise origin of air overpressure in surface blasting

There are two common theories of what phenomenon generates air overpressure produced from a typical quarry or opencast blast. These are whether ground vibration along the free face causes the pressure pulses seen in an air overpressure trace or whether it's attributed to the rock displacement.

The United States Bureau of Mines (USBM) conductive extensive research in the field of blasting induced air overpressure. The key research areas were; determining the source of air overpressure pulses from blasting and structural response and damage caused by overpressure produced from surface blasting.

The USBM Reports of Investigations (RI) 8485 by Siskind et al divines four mechanisms during a blast which is a root cause of air overpressure, these are;

- 1. Direct rock displacement at the face or collar of a blast hole. Known as Air pressure pulse (APP).
- 2. Vibrating ground, known as rock pressure pulse (RPP).
- 3. Escaping gas ejecting from the face through joints. Known as gas release pulse (GRP).
- 4. Ejected gases through the stemming, known as stemming release pulse (SRP).

The names given to these mechanisms were done so by Wiss and Linehan (1978). Siskind et al states in USBM RI 8485 that if a blast is properly designed and controlled, the air pressure pulse will be the dominant source, inferring that the rock displacement from the face is the main origin of air overpressure.

'The air pressure pulse (APP) will dominate in a properly designed blast, and will only be absent for cases of total confinement (that is, underground blasts).' Siskind et al. 1980.

The report also states that the rock pressure pulse provides the least amplitude in air overpressure out of the four mechanisms listed above whilst the gas release pulse and stemming release pulse if they occur, can produce very high pressure levels, greatly exceeding levels from air pressure pulse.

'RPP has the least amplitude of the air blast components; however, it is typically of higher frequency (identical to the Vv which spawns it), and enables us to predict the minimum air blast level expected (for example, 1.0 in/sec Vv will generate 0.0015 lb/in², or 144 dB-peak).'

A simple relationship between ground vibration and rock pressure pulse was found by Wiss and Linehan (1978);

$RPP = 0.0015 \, Vw$

Where Vv is the vertical component of the ground vibration and measured in inches per second (in/s) and RPP is measured in pounds per square inch (lb/in²).

McKenzie (1990) acknowledges previous research conducted by the USBM but suggests that in fact that the peak air overpressure levels are generated not by rock displacement from the face but by the vibrations along the face (excluding when gas venting occurs through the face or stemming area).

'The results of recent detailed studies suggest that after venting has been eliminated, the peak levels of overpressure are caused by ground vibration. The peak level is not generated by the ground vibration at the monitoring location, but instead by the peak vibration levels at the face.' McKenzie (1990).

This work describes an experiment which evaluates the relationship between air overpressure and ground vibration. To do this, a cement wall was struck with a sledgehammer and the vibrations along the wall were recorded by vibration gauges. These were bonded to the opposite side of the wall. The experiment was to simulate the ground vibrations along a blast face prior to the fragmentation of the rock and its projection from the bench. Over pressure gauges were positioned a various distances from the wall. The results showed a linear relationship between air overpressure and vibration levels at various distances.

It must be made clear that the ground vibration along the face is different to that which Wiss and Linehan refer to as 'rock pressure pulse'. The term rock pressure pulse is given to the piston-like affect the ground vibrations give which produces low amplitude pressure pulses at the monitoring location; whereas McKenzie is suggesting that the vibration along the face creates a high magnitude pulse which then produces the main overpressure pulse. Despite this, the results of their research provide conflicting conclusions.

Siskind and Stagg (1997) state that the overpressure amplitudes, created by the air pressure pulses are proportional to the initial face velocity. This has been reinforced by the work conducted by Birch et al (2008) which suggests that air overpressure, particularly in front of the blast, is related to the initial face velocities.

10.2 Air overpressure monitoring at Melton Ross Quarry

Extensive blast monitoring was carried out at Melton Ross chalk quarry. Typically each of the production blasts consisted of only five blast holes and initiated by non-electric detonators.

The optic fibre system as described in chapter 5 was used for all of the productions blasts to record the exact firing times of each of the blast holes. The face movement incurred by the blast was also recorded by lowering a piezoelectric sensor in front of the face and connected to the MREL MicrotrapTM along with the optic fibre system along with two low frequency microphones that were positioned at two known distances perpendicular to the face, directly in front of the first blast hole e.g. 50m and 100m from the first blast hole.

The data recorded by MREL's high speed data logger, MicrotrapT^M, provided the opportunity to calculate the exact moment the air overpressure is created during a typical quarry blast. The data logger recorded precisely the time the first blast hole was fired, initial face movement on the face and the time the air overpressure wave travels to two known points in front of the face, all on the same time basis. In addition to this, the speed of sound in the rock for each blast was attainable by connecting two seismographs together so that they also record of the same time basis as each other.

The acquisition of the data listed above allows for the precise time the air overpressure wave is created and to correlate with possible sources of its creation. i.e. the shockwave, created by the detonation of the charge in the hole or the initial face movement that occurs afterwards.

10.3 Example calculation

An example of how the source of the air overpressure for a given blast is calculated is provided below. The data in this example was recorded from a five hole blast at Melton Ross chalk quarry on 25/05/2010.

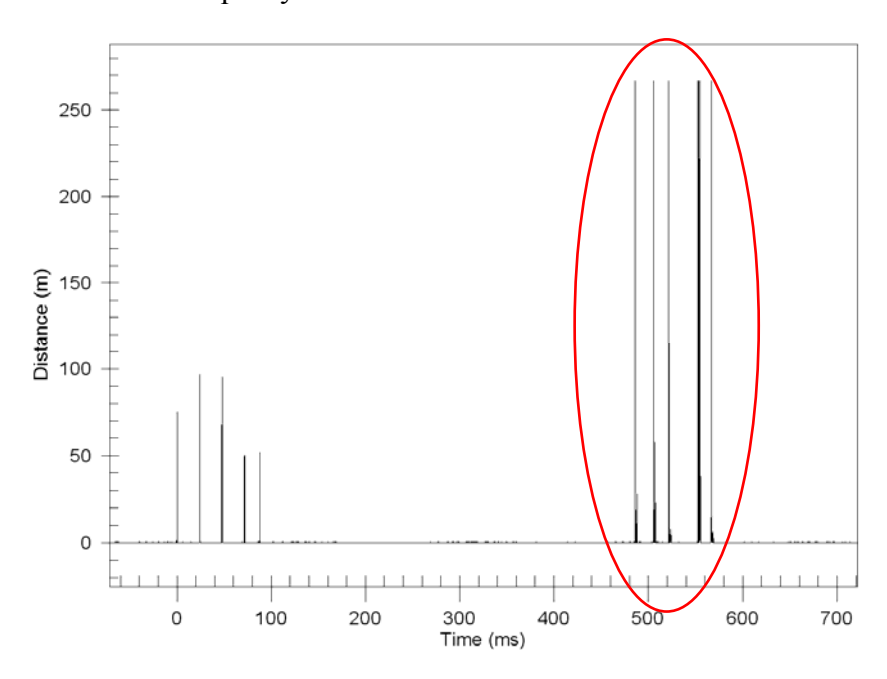


Figure 10.1 Typical trace showing the precise firing times of the surface delay relay detonators and then the long lead time in hole detonators for a 5 hole blast at Melton Ross Quarry.

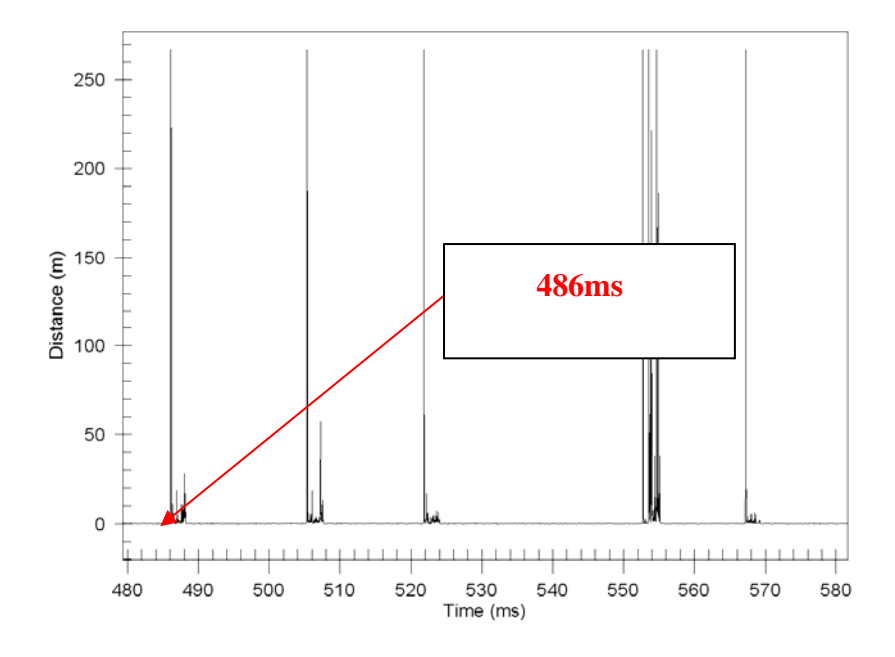


Figure 10.2 Optical fibre interface unit's output used to determine the precise time the first blast hole was fired

The optic fibre interface unit, as described in chapter 5 was used to trigger the monitoring system. The first group of readings in Figure 4.1 show the light impulse detected by the optic fibre sensors from the flame front proceeding along the shock tube, towards the detonators, attached to the primer, loaded at the bottom of the hole. The second group of readings (circled in red) show each of the five blast holes firing. To calculate the time at which the air overpressure wave is generated during a blast, the time at which the first blast hole detonated (486ms after the system triggered) must be set as t₀ and the time of the air overpressure traces must be relative to this point.

10.3.1 Calculating air overpressure velocity

As mentioned in chapter 2, two low frequency air overpressure microphones were positioned in a line, in front and perpendicular to the first blast hole. For the case of the blast monitored in this example, the microphones were deployed 40.17m and 80.17m from the first blast hole.

Each of the microphones was connected to the MREL MicrotrapTM data logger and so their output was recorded on the same time basis as the detonator firing times in Figure 4.1. As the pressure wave arrival times at each microphone is known, it is therefore possible to calculate the speed of sound in the air at the exact moment of the blast.

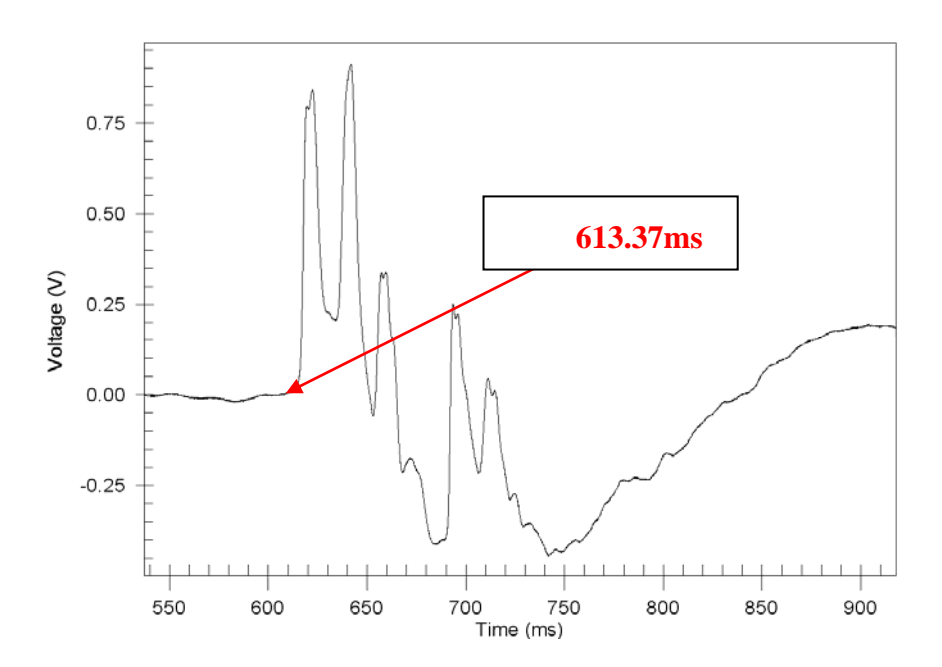


Figure 10.3 Air overpressure trace recorded by the first microphone at 40.17m

Figure 4.3 shows the air overpressure trace recorded by the first microphone. The time, at which the pressure level rises from zero, indicate the arrival of the pressure wave. For this blast the graph shows that the wave arrived 613.37ms after the data logger was triggered. However from Figure 9.1 it has been established that the first blast hole did not detonate until 486.0 ms after the data logger was triggered which, for the basis of this analysis, is deemed to be where time is Zero. This means that the blast wave arrives at the first microphone at 127.37ms (613.37-486.0).

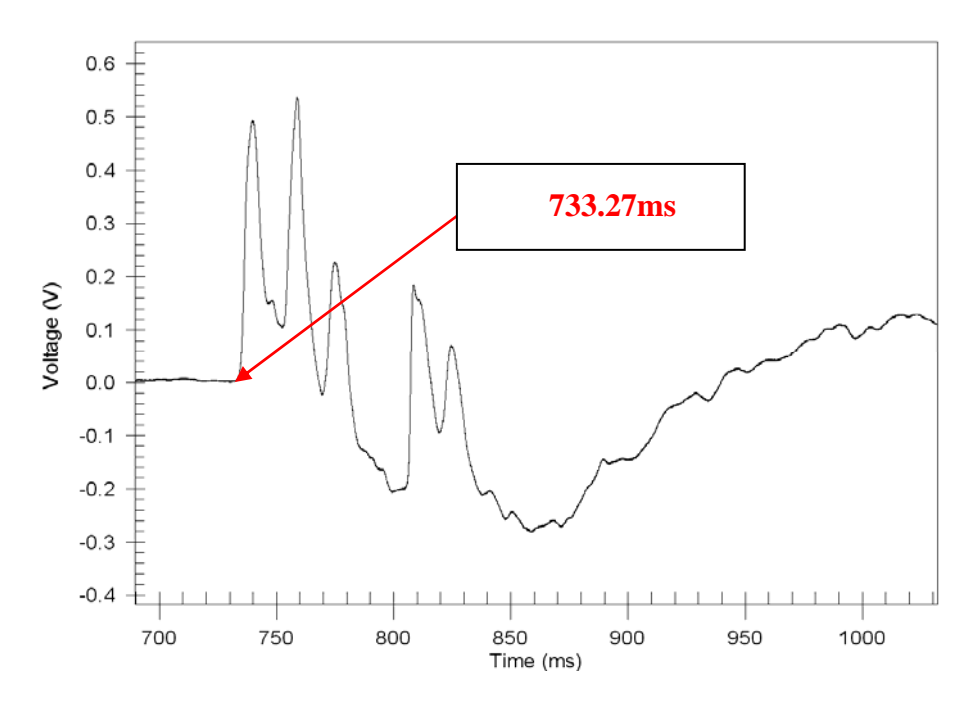


Figure 10.4 Air overpressure trace recorded by the second microphone at 80.17m

The arrival of the pressure wave at the second microphone, deployed at 40m from the first microphone and 80.17m from the first blast hole was recorded 247.27ms (733.27 - 486) after the blast was initiated.

Using the arrival times, the air overpressure velocity can now be calculated.

$$v = \frac{40}{(247.27 - 127.3) \times 10^{-8}}$$
$$v = 333.6 \frac{m}{s}$$

Knowing the velocity allows for the moment at which the air overpressure pulse emerges from the blast.

Air overpressure travel time from the face to the first microphone;

$$t = \frac{distance}{velocity}$$

$$t = \frac{40.17}{333.6}$$

t = 120.4ms

Therefore the time at which the air overpressure wave is generated is

$$127.3 - 120.4 = 6.9 ms$$

Now that the time at which the air overpressure leaves the face, has been calculated, it can be correlated to a possible source of its generation.

10.3.2 Determining the source of air overpressure

The determine the source of air overpressure from a typical bench blast, the time at which the shockwave from the blast arrives at the free face and also the time at which initial face movement occurs must be known. Seismographs were deployed in the field to calculate the speed of sound in the rock and hence the time at which the resulting shockwave from the hole detonation, arrives at the free face. A piezoelectric sensor was created to detect the movement of the face. This was lowered down the face, in front of the first blast hole whilst ensuring the sensor was in contact with the rock at all times.

A seismograph was deployed directly below each of the two air overpressure microphones and connected together so that they both recorded on the same time basis. Once the 'master' seismograph triggered, the 'slave' seismograph also triggers. The arrival time of shockwave in the rock recorded by each seismograph unit can be utilised to calculate the speed of sound in this particular rock for this given blast. The seismograph detects the vibration with a tri-axial array, therefore providing displacement along three axes, vertical, longitudinal and transverse. For the case of the blast in this example, the data recorded on the vertical channel of each seismograph was used in calculating the velocity. The first vibration recorded by each of the seismographs was in the vertical channel and so indicates the arrival of the shockwave.

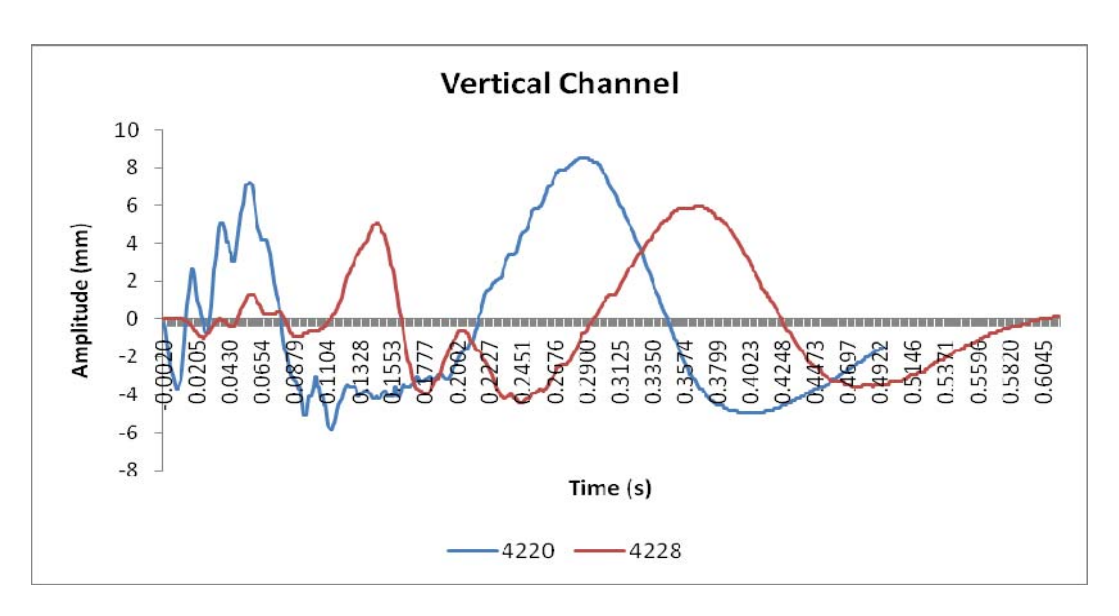


Figure 10.5 the recorded vibration on the vertical channel of both linked seismographs

Figure 9.5 shows the displacement in the vertical plane of both seismographs with unit '4220' being the closer to the blast.

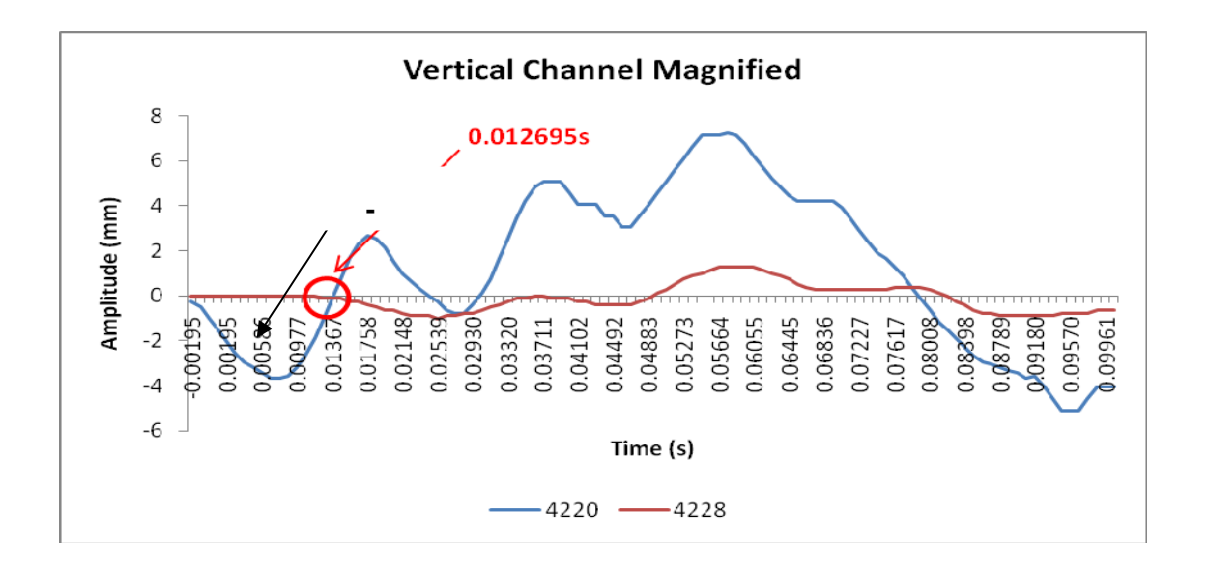


Figure 10.6 Figure 4.4 magnified to display the arrival of vibration to the slave seismograph.

The master unit (4220) began recording at -0.00195s which signifies the arrival of the shockwave through the rock. The initial reading was not of a sufficient magnitude to trigger the unit and so was recorded in the pre-trigger window of the seismograph. The wave arrival at the slave unit (4228) occurred at 0.012695s.

Figures 9.5 and 9.6 are graphical representations however analysis of the raw data was used to determine the arrival times as this can be performed more precisely.

The speed of sound in rock was therefore

$$v = \frac{40}{0.01465}$$

$$v = \frac{2740m}{0.01465}$$

Determining the speed of sound in the rock, allows for the time at which the shockwave from the blast hole arrives at the free face which in turn can be compared to the time at which the air overpressure leaves the face.

The burden for this particular blast was 4.5m.

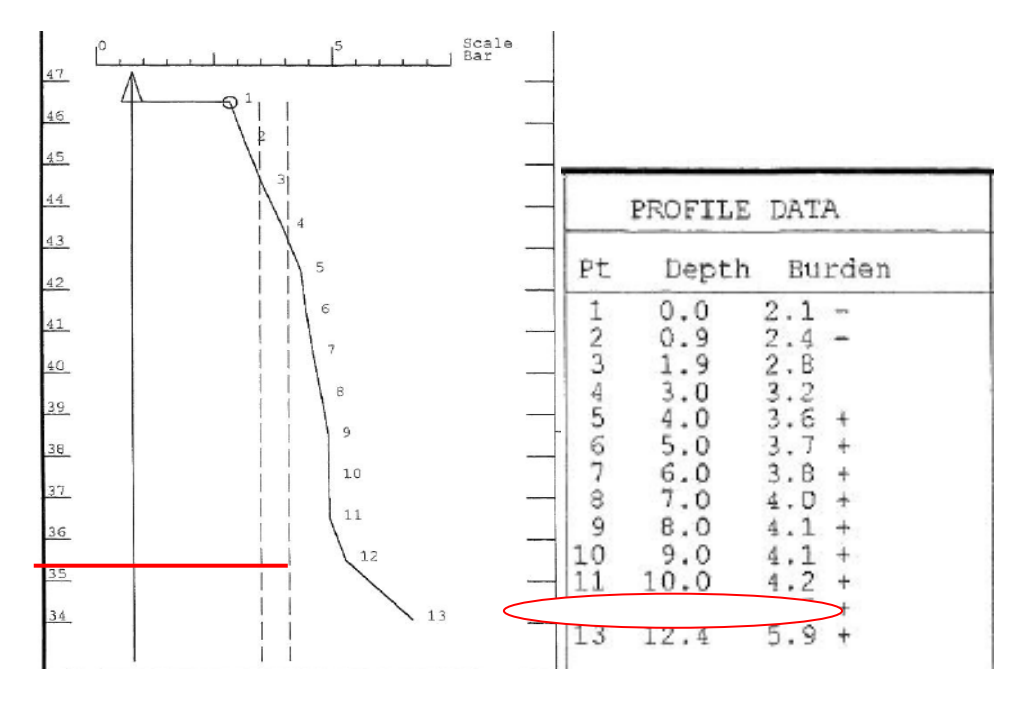


Figure 10.7 Face profile data of the first blast hole

The taken for the shockwave to travel from the blast hole to the free face

$$\varepsilon = \frac{4.5}{2740}$$

t = 1.64ms

The shockwave arrives at the face 2.6ms after the charge is detonated in the first blast hole.

The first movement along the face was monitored by a piezoelectric sensor lowered down the face in a position where the sensor is in line with the primer and detonators within the blast hole and also remaining in contact with the rock at all times.

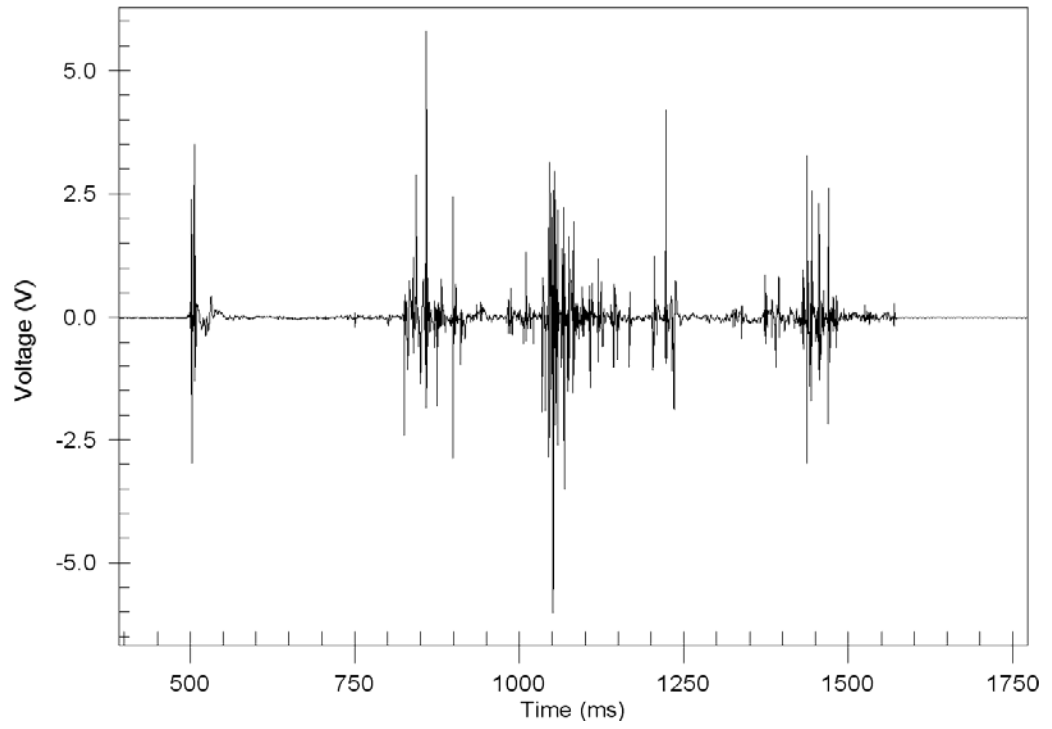


Figure 10.8 Output from the piezoelectric sensor in front the of face

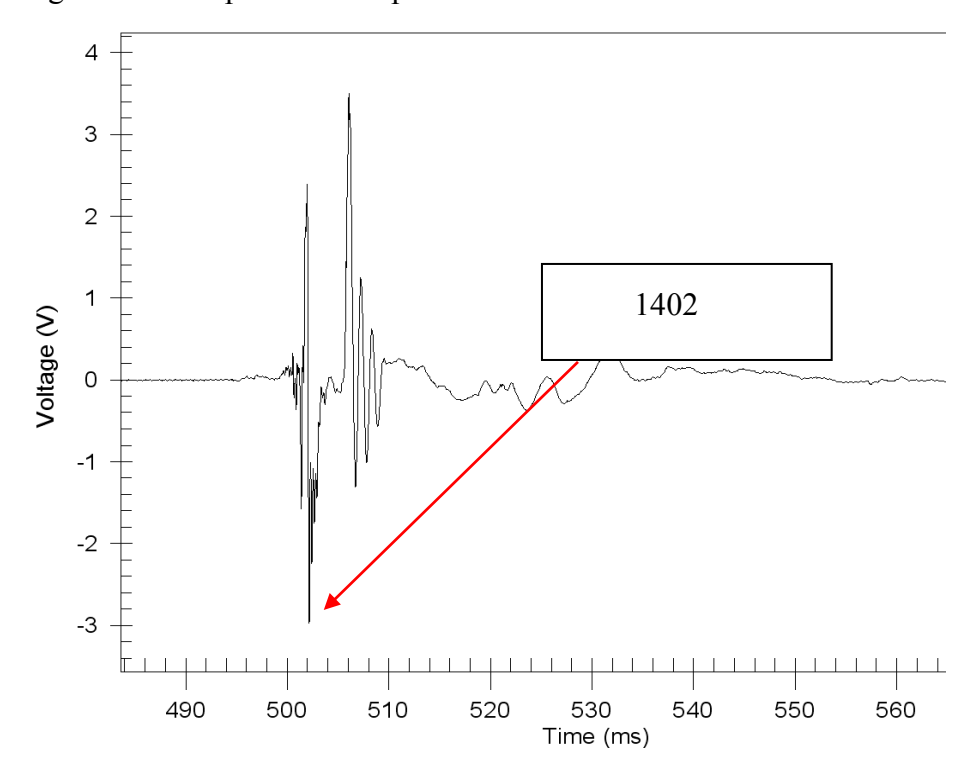


Figure 10.9 The first movement detected by the piezoelectric sensor

The first movement along the face was detected by the sensor 13.23ms (499.23 – 486) after the blast was initiated. As the safest method of placing the sensor in front of the face was by lowering it down from on top of the bench with a member of the monitoring team directing the positioning from the quarry floor at a safe distance from the face, meant that it was not always guaranteed that the sensor was in contact with the face due to undulations on the rock surface. In addition to this limitation, it is impossible to judge the level which to lower the sensor to so that it is in line with the base of the charge and the in-hole detonators where initial face movement will occur. These factors will lead to a delay between the actual initial face movement and the recorded initial face movement which will explain the short time difference between the time the air overpressure leaves the face and the initial face movement.

10.4 Origins of air overpressure at Melton Ross quarry

		Time AOP		Speed		
	АОР	leave	First Face	in	Shockwave	
Date	Velocity (m/s)	face (ms)	Movement (ms)	rock	Arrival at face (ms)	Burden
Date				(m/s)	iace (iiis)	(m)
25/05/2010	333.6	6.9	13.23	2740	1.64	4.5
12/03/2010	335.0	70	10.14	2719	2.76	7.5
			1.65			
07/05/2010	328.0	6.86	or 18.36	2574	2.70	7.0
04/06/2010	339.6	3.2	4.31	2547	2.50	6.4
14/05/2010	327.5	3.0	5.23	2734	2.85	7.8
18/05/2010	340.0	8.1	6.73	2731	2.05	5.6
30/09/2010	344.0	9.94	5.65	2181	3.70	8.1
19/10/2010	332.3	5.91	n/a	2728	1.90	5.3

Table 10.1 Air overpressure levels timings and associated velocities related to Burden

Table 10.1 lists the calculated times of the shockwave arrival at the face, the time at which the air overpressure wave is generated and the first face movement detected on the face by the piezoelectric sensor.

Date	Time difference between the shockwave arrival and AOP leaving the face (ms)	Time difference between the AOP leaving the face and initial face movement (ms)
25/05/2010	5.25	6.33
12/03/2010	4.24	3.14
07/05/2010	4.16	11.5
04/06/2010	0.7	1.11
14/05/2010	0.15	2.23
18/05/2010	6.05	-1.37
30/09/2010	6.24	-4.29
19/10/2010	4.01	No value

Table 10.2 Comparison of time differences between shock wave and face movement in relationship to air overpressure pulse leaving the quarry face

The methodology established has proved to be practical and effective in collecting the data required, however caution needs to be exercised for the following reasons

- only 8 measurements containing all the relevant data were possible
- the derived time for the point of origin on the blast face is subject to inaccuracies in the actual burden
- The speed of sound in rock is derived from the white seismograph data that can only sample at 1024 samples per second and there were clearly times when the slave seismograph did not respond in a fully synchronised manner to the master seismograph.
- Due to irregularities in the blast face, it was not always possible to position the face sensor precisely at the level of the primer cartridge.
- Measuring the exact height of the primer cartridge in the blast hole was not possible due to operational constraints.
- The orientation of the face sensor cannot be adjusted once it has been placed on the face and this may well affects its response time.

Nevertheless, it is evident from table 10.2 that the time the air overpressure wave leaves the face does not coincide with either of the shockwave's arrival at the face or the time of initial face movement. Also a closer inspection of table 10.1 indicates that the shock wave comes first, then the air overpressure pulse originates on the face and then the face moves. This implies that another mechanism is responsible for the timing of the appearance of the air overpressure pulse. Having reached this conclusion late in the project, it has not been possible to fully explore this phenomenon.

Whilst this is clearly speculation, the only other key driver that could be operating is the gas pressure pulse. It is known that 1 kg of AnFo (Ammonium Nitrate and fuel Oil mixture) gives rise to 3.78 mega joules of energy, a detonating pressure of 1.7 Giga Pascals (SME engineering Hand book) and this in turn produces 970 litres of gas (with the correct oxygen balance and under normal temperature and pressure). Thus a typical blast borehole containing 65 kilograms of AnFo will gives rise to 246 Giga Joules of energy and 63,050 litres of gas. By definition the gas pressure pulse cannot arrive at the blast face before the shock wave. Also as it is known to be responsible for heaving out the blast face into a rock pile, it cannot arrive after the face has commenced to move. Also of note is that in Figure 6.9 for the median value of Scaled Distance, the "hard rock" gives the highest value of air overpressure, the "medium rock" gives the lowest value and the "soft rock" gives the intermediate vale. In this case the hard rock was heavily jointed and fissured dolerite igneous rock,. The medium rock was finely laminated but poorly jointed Magnesian Limestone. The soft rock was Chalk which is very permeable but with no discernable joints. Thus a key factor that the study has not been able to address might well be the "gas permeability in the rock mass". Whilst this assessment is to an extent subjective and anecdotal in nature, it might be an indicator of where the next phase of the research should be targeted.

10.5 Conclusions

The experimental methodology to examine the origin of air overpressure has been developed and is available for other researchers to build upon.

The key finding is somewhat puzzling as the derived time at which the air overpressure pulse exited the blast face did not coincide with either the derived time

at which the shock wave exited the face nor indeed the measured first movement of the face.

The timing order indicates that the shock wave comes first, then the air overpressure pulse originates on the blast face and then the blast face moves.

Given the amount of energy and volume of Gas generated in the Gas Pressure Pulse and that by definition the gas pressure pulse cannot arrive at the blast face before the shock wave, nor can it arrive after the face has commenced to move, it is logical that this is where the next phase of the research should be targeted.

Chapter 11

Conclusions and further work

11.1 Summary of conclusions

Chapter one outlined the fundamentals of blasting as employed in quarries and opencast coal sites in the UK. It has explained the key ingredients that constitute an explosive and then continued to discuss the methodology required to design an effective blast. Finally it has defined the terms blast ratio and drill ratio. It has then outlined that in terms of environmental limitations, that there is no need for an experienced blast design engineer to compromise the intended Blast ratio required to efficiently carry out the set task, provided that consequential impact on the drill ratio is understood.

Chapter two discussed the basic physics of blast vibrations. Moore & Richards have built on earlier work by the U.S. Bureaux of Mines to derive a series of relationships between Maximum Instantaneous Charge Weight, Distance and Burden to predict likely air overpressure levels from quarry type blasts. They have also indicated that the directionality of the borehole initiation sequence in combination with the inter-hole delay period could be important, as it may result in constructive interference between successive holes being fired such as to significantly increase the resulting maximum air overpressure values. Meteorological conditions can be important, but it must be borne in mind that effect of "focusing of air overpressure pulses" is generally restricted to large blasting events under unusual atmospheric conditions and is unlikely to occur as the result of small scale quarry blasting. Many instances of high air overpressure readings from a blast can be attributed to poor blasting practice. Goodquarry.com has defined a number of actions that can be taken at the blast planning stage that can be used to help minimise the air overpressure at source. In the interest of standardisation it recommended that all overpressure measurements should be in Pascals and reported in Pascals

Chapter three considered a preliminary investigation into the relationship between air overpressure and face velocity at Newbridge Quarry. It concluded that there is a relationship between the face velocities and the air overpressures of the first blast holes when monitoring in front of the quarry face being blasted. This shows that the velocity of the rock as it is projected from the face has a large influence on the level of air overpressure that will be produced from a blast. With respect to the relationship between average face velocities and the peak air overpressure monitored behind a blast, although results in terms of "scaled air overpressure" [that attempted to take into account distance] look promising, a more detailed study is required to establish if such a relationship does indeed exist. With regard to collecting the data required for future investigations, it is strongly recommended that monitoring of blasts for face velocities should only be carried out by following the recommended protocol. It is the judgement of the authors that failure to do so will result in inaccurate data and poor results. This clearly is a pilot study in that only 12 blasts were monitored. To fully define the relationship between the face velocity and air overpressure and to be able to predict values, a much more extensive study is required.

Chapter four outlined the blast air overpressure instrumentation used on the project. It concluded that the monitoring system using the two low frequency microphones connected to the MREL data trap via two separate amplifiers was very successful. The deployment of the piezoelectric wafer encased in plaster within a rubber ball was satisfactory as a low cost solution, but in reality to obtain 100% reliable data, a disposable geophone would have been needed that could have been fixed to the quarry face to be blasted. Needless to say this would have been extremely difficult to accomplish in a safe manner. The deployment of the Instantel Minimate plus series III seismographs utilising there higher sampling rate was very successful, however the inability to connect two such units together was a disadvantage. The deployment of the white seismographs was satisfactory, however a higher sampling rate would have been very beneficial. The ability to connect two such seismographs together on the same time base was a very useful facility, however on a few limited occasion, some spurious readings were obtained in terms of timing of the first arrival of an air overpressure pulse.

Chapter five discussed the development and application of a novel low cost optic fibre system to monitor blast performance. The optic fibre system developed allowed the MREL data trap to be triggered both consistently and with a high degree of precision. It also allowed the firing times of the various shock tube pyrotechnique delay detonators (both surface delay relay detonators and in hole long

period delays) to be accurately and precisely determined. When deployed using the "point to point" method it can used to determine, both the VoD of the explosive used in a blast as well as the velocity of the flame front within the shock tube immediately prior to detonation, to a high level of accuracy and precision.

Chapter Six was considered collection and analysis of the air overpressure data. It concluded that the collection of data relating only air overpressure values to Distance and explosive charge weight in the form of a scaled distance relationship is insufficient for environmental control purposes as the resulting scatter of the data [standard error] will be too great and the correlation too poor. A significant improvement in both the standard error and the correlation coefficient can be made if the AOP data set is divided into two unique sub sets. The two sub sets should be

- all the data from observation locations in front of the line of permanent displacement (i.e. in front of the quarry face to be blasted).
- all the data from observation locations behind the line of permanent displacement (i.e. behind the quarry face to be blasted)

The analysis has shown that the directionality of blasting is a very important factor when trying to avoid air overpressure disturbances outside the quarry boundary. If this is known to be a problem, it is imperative to take note of the direction in which the blast holes are fired within the delay sequence and the delay times between the blast holes so that positive interaction between the pressure pulses are reduced or if possible, avoided. To determine whether the rock type has an influence on the magnitude of air overpressure produced during blasting, a more controlled comparison is required where blast designs do not vary from site to site.

Chapter Seven related to a field investigation, with respect to orientation and distance from an explosive source, into the interaction of multiple short delay detonations in free air. It concluded that the test undertaken using 1 metre lengths of Detonating Cord in air were shown to be very consistent. The test where the explosives were fired at 25 millisecond intervals showed no interaction. The test fired at 8 millisecond intervals showed some interaction with respect to the direction of firing, however this was such that the positive negative phase of the previous hole interacted with the positive phase of the hole firing to reduced the air overpressure from the explosive charge in question due to negative interference of the two wave

forms. The test will 4th and 5th hole firing 1 millisecond apart did show positive interference that gave rise to an enhanced air overpressure values. There is a fundamental difference in the wave form of the air overpressure pulse between a detonation in free air and a confined detonation in a quarry blast. The difference mainly relates to time duration of the negative phase of the pulse in that in a "free air" detonation the positive phase of the pulse is approximately equal to the negative phase in terms of time. However in a confined quarry blast detonation the negative phase can be between 3 to 5 times longer in duration that the positive phase.

Chapter eight related to the single hole air overpressure test blasts at Melton Ross Quarry. It concluded that the experiment carried out does show that there is a very strong relationship between resulting values of air overpressure with respect to variations in distance combined with burden at least for single hole blasts. However as the two single hole blasts were identical charge weights, it is not possible to determine in this experiment the relationship between charge weight and distance in the form of Scaled Distance as it is conventionally used. The constant shape of the wave form of the single hole as it attenuates with distance makes it possible to use this as the basic form to model a multi-hole air overpressure event from a single hole wave form

Chapter nine was a concerned with a novel method that sought to apply statistical analysis in combination with a linear superposition technique using a signature acoustic wave form to create a model of the air overpressure produced from a full scale production blast at Melton Ross Quarry. It concluded that by using the derived air overpressure values that result from the application of the linear superposition technique it was possible to derive a better understanding of the relationship between distance and charge weight as commonly combine in the form of "Scaled Distance." If this is examined using trivariate statistical approach, it becomes clear that the relationship between distance and charge weight is not proportional to either the square root or cube root of the charge weight in this circumstance. Using a quadrivarainte approach to evaluate the relationship between peak air overpressure for the whole blast that resulted from variations in distance, charge weight of the explosive and burden, then the best correlations is achieved using the burden at the toe of the face to be blasted. Give the manner of the blasting at Melton Ross this is the closest point on the quarry face to be blast to the point of imitation of the individual blast hole. Paradoxically, if the quadrivarainte technique

is used to predict the air overpressure associated with the first hole rather than the peak air overpressure for the whole blast, then the median burden gives the best correlation. The results obtain show an unprecedented ability to be able to predict the likely air overpressure pulse generated. However caution should be exercised in that these were very small single row blasts with the variability of the detonator timings being incorporated in the original Linear super position algorithm.

Chapter ten was concerned with determining the origins of air overpressure from blasting at Melton Ross Quarry. It concluded that the experimental methodology to examine the origin of air overpressure has been developed and is available for other researchers to build upon. The key finding was somewhat puzzling as the derived time at which the air overpressure pulse exited the blast face did not coincide with either the derived time at which the shock wave exited the face nor indeed the measured first movement of the face. The timing order indicates that the shock wave comes first, then the air overpressure pulse originates on the blast face and then the blast face moves.

11.2 Further work

The use of advanced statistical techniques to the prediction of air overpressure events as developed in this study needs to be verified by use by other practitioners or by a further study that only considers this problem.

Given the amount of energy and volume of gas generated in the gas pressure pulse and that by definition the gas pressure pulse cannot arrive at the blast face before the shock wave, nor can it arrive after the face has commenced to move, it is logical that this is where the next phase of the research should be targeted at developing the technology to be able to monitor the actual gas pressure pulse in full scale quarry blasts.

REFERENCES

Birch, W.J. and Chaffer, R. (1983)

Prediction of Ground Vibrations from Blasting at Quarries

Transactions of the Institutions of Mining and Metallurgy, (Sect: A Min. Technol.), 109, May-August, pp. 103-106

Birch, W.J. and Hosein, S., (2004)

The Application of Electronic Detonators in Controlling Blast Vibrations – A Trial Study

Proceedings of the Thirteenth Extractive Industry Geology Conference, University Of Leeds, Leeds, 2004, The Mineral Industry Research Organisation, Leeds, pp. 194-205

Birch W.J, Bermingham L & Farnfield R. (2008)

Relationship between Air Overpressure & Face Velocity

[ISEE] Proceedings of the thirty fourth annual conference on explosives and blasting techniques, New Orleans, Lousianna, USA, January 27-30

Birch, W.J., Hosein, S. and Faenfield, R. (2009)

Influence of distance in the effective use of electronic detonators to control blast induced ground vibrations.

Proceedings of the Thirty-fifth Annual Conference of Explosives and Blasting Techniques, Denver, Colorado, 2009 International Society of Explosives Engineers, Cleveland, Ohio, Volume 1

Chiappetta R.F & Vandenberg B (1990)

Interpreting Continuous Velocity Of Detonation Measurements.

Second High Tech Seminar Blasting Technology, Instrumentation, and Explosives Applications Orlando, Florida, USA June 10-15, 1990

Chiappetta R.F., Vandenberg B & Pressley J.R. (1992)

Portable, Multi-Channel And Continuous Velocity Of Detonation Recorders
Fourth High-Tech Seminar Blasting Technology, Instrumentation and Explosives
Applications Nashville, Tennessee, USA June 20-25, 1992

Chiappetta R.F, Vandenberg B & Pressley J.R. (1997)

Portable, Multi-Channel And Continuous Velocity Of Detonation Recorders
Seventh High-Tech Seminar Blasting Technology, Instrumentation and Explosives
Applications Orlando, Florida, USA July 28 - August 1, 1997

Farnfield R, Birch W.J, Rangel-Sharp G.D & Adcock C. (2009)

Accurate Delay Detonation With Shock Tube.

[ISEE] Proceedings of the thirty fifth annual conference on explosives and blasting techniques, Denver, Colorado, USA February 8 - 11 In most

International Society of Explosives Engineers [ISEE] (1998).

Blaster's Handbook.

ISEE, Cleveland, OH.

Katsabanis P.D (1990)

Explosives Properties A N D Characteristics

Second High Tech Seminar Blasting Technology, Instrumentation and Explosives Applications

Orlando, Florida, USA June 1 O-1 5, 1990

McKenzie C.K, Heilig J.H, Hickey S.M & LeJuge G.E (1990)

Ground Vibration and Overpressure Generation: How much do we really know? Institute of Quarrying (Australia Division) 34th Annual Conference, Hobart, November

Moore, A. J., Evans, R. and Richards, A. B. (1993).

An Elliptical Air blast Attenuation Model,

Proceedings of The Fourth International Symposium on Rock Fragmentation by Blasting - Fragblast - 4, Vienna, Austria, pp 247-252.

Moore A.J & Richards A.B (2004)

Environmental Blast Design on Effective Implementation.

Explo 2004, Perth W.A. July 2004.

Moxon N. T, Hopkins M.L, Dane R.E, Chiappetta R.F, Bowman A, & Pressley J.R (1991)

Portable Continuous Velocity Of Detonation Systems.

Third High-Tech Seminar Blasting Technology, Instrumentation and Explosives Applications San Diego, California, USA June 2 - 7, 1991

Pegden M (2005)

The analysis and Prediction of Vibrations through Rock using advanced statistical techniques

PhD, thesis. Energy & Resources Research Institute, University of Leeds.

Persson et al. (1994)

Rock Blasting and Explosives Engineering.

CRC Press, Inc

Richards, A. B. and Moore, A. J. (1995).

Blast Vibration Control by Wave front Reinforcement Techniques, presented at EXPLO 1995, Australian Institute of Mining and Metallurgy in association with International Society of Explosives Engineers, Brisbane, Australia, pp 323-327.

Richards A.B & Moore A.J. (2002)

Airblast Design Concepts in Open Pit Mines

Proceedings Fragblast 7 Conference, Beijing, August 2002 pp553 – 561.

Richards, A. B. (2008).

Prediction and control of air overpressure from blasting in Hong Kong Geo report No. 232 Geotechnical Engineering Office, Civil Engineering and Development Department, The Government of Hong Kong, Special Administrative Region.

Siskind D.E, Stachura V.J, Stagg M.S & Kopp J.W. (1980)

Structure response and damage produced by airblast from surface mining.

USBM Report of Investigations 8485.

Siskind D.E & Stagg M.S. (1997)

Environmental effects of blasting and their control.

[ISEE] Proceedings of the twenty third annual conference on explosives and blasting techniques, Las Vegas, Nevada, USA February 2-5 (ISEE).

Wiss, J.R & Linehan P, (1978)

Control of Vibration and Blast Noise from Surface Coal Mining.

United States Bureau of Mines, Open Files Report, 103(4)-79.